

Study on the efficient purification of recombinant proteins from the silkworm expression system

メタデータ	言語: en 出版者: Shizuoka University 公開日: 2020-06-11 キーワード (Ja): キーワード (En): 作成者: Minkner, Robert メールアドレス: 所属:
URL	https://doi.org/10.14945/00027509

THESIS

Study on the efficient purification of recombinant proteins from the silkworm expression system

Robert Minkner

Graduate School of
Science and Technology, Educational Division

Department of Bioscience

Shizuoka University

December 2019

THESIS

Study on the efficient purification of recombinant proteins from the silkworm expression system

カイコ発現系からの組換えタンパク質の効率的な精製に関する研究

ロバートミンクナー

静岡大学
大学院自然科学系教育部

バイオサイエンス専攻

2019年12月

The present work was carried out under the guidance of

Prof. Enoch Y. Park

in the time from

April 2017 to March 2020

and prepared at the Green Chemistry Research Division of

Research Institute of Green Science and Technology

at the

Shizuoka University, Japan

Declaration of Independence

I, Robert Minkner, hereby declare, that I have authored the present work independently and only used the indicated sources and tools.

Shizuoka, December 2019

Robert Minkner

I dedicate this work to two people who are important to me and who have always supported me in my striving to go to Japan and to do my doctorate there and who were always eager for news. Unfortunately, it will still take a long time until I can announce the news of the end of my promotion in Japan to them personally, since both have already passed away.

Firstly, I dedicate this work to my grandpa Harald Drogis, who was one of my lighthouse and role model for many years and to whom I owe a lot, even if it was not always easy. He was one of the loudest advocates and supporters of my interest in Japan, as well as in my attempts to come here. Unfortunately, he passed away on the very day I received the promise that I could go to Japan. I was never able to tell you about it, I'm sure you would have been happy, because you also enjoyed other countries and their cultures. I would like to thank you for everything and regret not having said everything that I should have said.

Second, I dedicate this work also to my great-grandmother Waltraud Kossack, who was also an important supporter of my plans, even if she sometimes doubted my adventurous spirit. Sadly, she passed away during my second half in Japan. I will painfully miss you and our long phone calls and regret not having met you again one more before.

Acknowledgments

I owe the fact that I was able to create this dissertation to quite a few people.

Above all, I would like to thank Prof. Enoch Y. Park for the opportunity to do my doctoral study in his research group and to expand my own small horizon here, not only in research, but also in cultural way. Equally sincerely I want to thank Prof. Hermann Wätzig that he made it possible for me to join the double degree program between the TU Braunschweig and the Shizuoka university and that he established the contact to Japan for me.

I also would like to thank Assoc. Prof. Tatsuya Kato and Dr. Jian Xu for their support and insights into research.

I would also like to thank all members of the Laboratory of Biotechnology for their kind welcome, hospitality and support. A helping hand was always near. Many helpful talks, discussions and funny moments have accompanied my work and enriched my days here.

A special thanks goes to my family and my closest friends. For all the motivation and support I received during my studies here in the fare away Japan, I really would like to thank you from the bottom of my heart. I am very grateful to be blessed with you.

Table of Contents

Declaration of Independence	4
Acknowledgments	6
Table of Contents	7
List of abbreviations	13
1. General Introduction	14
1.1. Virus like particles (VLPs)	14
1.2. Production of recombinant proteins	15
1.3. Production of recombinant VLPs in silkworm	16
1.4. Physiology of silkworm haemolymph and fat body	17
1.5. Purification	20
1.6. Pre-treatment.....	21
1.7. Purification using chromatography	22
1.8. Stability of VLPs	24
1.9. Quality Control	24
1.10. Magnetic nano particles	25
1.11. Objective.....	27
2. General Material and Methods	29
2.1. Silkworms	29
2.2. Components of buffers, media and solutions.....	29
2.2.1. Gel electrophoresis	29
2.2.2. SDS-PAGE	29
2.2.3. Western Blot	30
2.2.4. Luria-Bertani medium.....	30
2.2.5. Buffer for chromatography screening.....	30
2.2.6. Buffer for chromatography.....	31
2.2.7. Solutions for bacmid isolation	32
2.2.8. Buffers for FLAG-tag purification	32
2.2.9. Buffer for purification of His-tagged proteins using nickel MNPs	33
2.2.10. Other Buffer and solutions.....	33
2.3. Restriction enzymes, polymerases and ligase.....	34
2.4. Primer.....	34

2.5.	Kits.....	34
2.6.	Recombinant proteins.....	35
2.6.1.	Recombinant <i>Bombyx mori</i> nucleopolyhedrovirus (BmNPV) bacmid preparation for SpCaVp1 and EDIII	35
2.7.	Antibodies	36
2.8.	Other reagents and materials	36
2.9.	Equipment	37
2.9.1.	Columns	37
2.9.2.	Other Equipment.....	37
2.10.	Software.....	38
2.11.	Methods of biotechnology	39
2.11.1.	Caring of the silkworms.....	39
2.11.2.	Infection of the silkworm	39
2.11.3.	Harvesting of the haemolymph.....	39
2.11.4.	Harvesting of the fat body	39
2.11.5.	Polymerase chain reaction (PCR).....	40
2.11.6.	Quantitative PCR.....	40
2.11.7.	Pre-treatment centrifugation.....	41
2.11.8.	Pre-treatment precipitation	41
2.11.9.	Thermal treatment of haemolymph.....	42
2.11.10.	Strep tag affinity purification	42
2.11.11.	Fast performance liquid chromatography (FPLC).....	42
2.11.12.	Ultrafiltration.....	43
2.11.13.	Sodium dodecyl sulphate – polyacrylamide gel electrophoresis (SDS-PAGE)	43
2.11.14.	Coomassie-Brilliant-Blue staining (CBB staining)	44
2.11.15.	Relative Quantification from proteins after SDS-PAGE	44
2.11.16.	Fluorescence Imaging	44
2.11.17.	Western Blotting.....	45
2.11.18.	Protein Assay using Bradford principle.....	45
2.11.19.	Protein Assay using Bichinonic acid (BCA)	45
2.11.20.	DNA Assay	46
2.12.	Other analytical methods	46
2.12.1.	Transmission electron microscopy (TEM)	46
2.12.2.	Dynamic light scattering (DLS).....	47

2.12.3. Office processing and analysis.....	47
3. Purification investigations from the silkworm haemolymph.....	48
3.1. Introduction.....	48
3.2. Specific Material and Methods.....	48
3.2.1. GFPuv- β 1,3-N-acetylglucosaminyltransferase 2 (GFP- β 3GnT2)	48
3.2.2. ALEX chromatography screening	49
3.3. Results and Discussion	49
3.3.1. Separation by Centrifugation.....	49
3.3.2. Separation by NaCl Precipitation	51
3.3.3. Separation by (NH ₄) ₂ SO ₄ precipitation	52
3.3.4. Separation by Poly ethylene glycol (PEG) 6000 precipitation	52
3.3.5. Separation by PEI precipitation.....	53
3.3.6. Precipitation in general	55
3.3.7. Anion exchange screening	56
3.3.8. Chromatographic separation	57
3.3.9. Additional aspects regarding filtration.....	61
3.4. Conclusion	62
4. A systematic and methodical approach for efficient purification from silkworm haemolymph.....	63
4.1. Introduction.....	63
4.2. Specific Material and Methods.....	63
4.2.1. Recombinant <i>Bombyx mori</i> nucleopolyhedrovirus (BmNPV) bacmid preparation for mCherry	63
4.2.2. Capillary electrophoresis sodium dodecyl sulfate (CE-SDS).....	64
4.3. Results and Discussion	65
4.3.1. Centrifugation	65
4.3.2. Precipitation.....	66
4.3.3. Chromatography matrixes as 1 st or 2 nd purification steps	67
4.3.4. Further HIC and SEC investigations	71
4.3.5. Fine-tuning the first two chromatography steps and addition of a 3 rd step.....	73
4.3.6. Improved purification protocol with additional thermal treatment	78
4.3.7. Purity comparison using capillary electrophoresis	81
4.4. Conclusion	84
5. Purification of non-enveloped VLPs from silkworm fat body	86

5.1.	Introduction.....	86
5.2.	Specific Material and Methods.....	86
5.2.1.	Sucrose gradient centrifugation.....	86
5.2.2.	FLAG tag affinity purification	87
5.2.3.	Agarose gel electrophoresis for DNA analysis	87
5.3.	Results and Discussion	88
5.3.1.	Screening of Ion-exchange chromatography and reproducibility test	88
5.3.2.	Conditions for the CHT chromatography buffer and gradient analysis	90
5.3.3.	Three-stage column chromatography	93
5.3.3.1.	AEX GigaCap Q-650M column chromatography	93
5.3.3.2.	CHT column chromatography.....	94
5.3.3.3.	Heparin column chromatography	95
5.3.4.	Analysis of purified HPV L1	96
5.3.5.	Comparison with other purification methods	99
5.4.	Conclusion	100
6.	Standard purification investigations of modified non-enveloped norovirus VLPs from the silkworm fat body.....	102
6.1.	Introduction.....	102
6.2.	Results and Discussion	102
6.2.1.	Pre-treatment of SpCaVP1, EDIII and their complex	102
6.2.2.	Chromatography purification of the SpCaVP1 and EDIII complex.....	105
6.2.3.	Additional precipitation investigation before chromatography.....	109
6.3.	Conclusion	110
7.	Purification investigations of enveloped VLPs from silkworm haemolymph.....	111
7.1.	Introduction.....	111
7.2.	Specific Material and Methods.....	111
7.2.1.	RSV-LP construction	111
7.2.2.	Bare iron MNPs as protein depletion method.....	112
7.3.	Results and Discussion	113
7.3.1.	RSV-LP construct 1.....	113
7.3.2.	RSV-LP construct 2.....	114
7.4.	Conclusion	116
8.	Magnetic nano particles for the affinity purification of His-tagged proteins from complicated matrixes as a pre-treatment step	117

8.1.	Introduction.....	117
8.2.	Specific Material and Methods.....	117
8.2.1.	Nickel ²⁺ MNPs preparation	117
8.2.2.	Nickel ²⁺ MNPs and commercial magnetic beads for purification of His-tagged proteins	118
8.2.3.	Lysis of <i>E. coli</i> cells.....	119
8.3.	Results and Discussion	120
8.3.1.	Preliminary and purification comparison tests.....	120
8.3.2.	Highly dispersible magnetic nano particles	123
8.3.3.	Proof of concept for purification from a complex sample matrix using highly dispersible MNPs.....	124
8.3.4.	Binding study of the highly dispersible MNPs	126
8.4.	Conclusion	128
9.	Conclusion and Outlook.....	129
10.	Acknowledgment	132
11.	References.....	133
12.	Appendix	145
12.1.	Coexpression of MERS-S protein and <i>Rous sarcoma</i> virus GAG protein as self-assembling VLP in silkworm haemolymph	145
12.1.1.	Introduction.....	145
12.1.2.	Specific Material and Methods.....	145
12.1.2.1.	Bacmids	145
12.1.2.1.1.	RSV-GAG protein bacmid.....	145
12.1.2.1.2.	MERS-S protein bacmid	145
12.1.2.2.	Bacteria	146
12.1.2.2.1.	BmDH 10 Bac <i>E. coli</i> containing the bacmid for the <i>Rous sarcoma</i> virus-Gag protein.....	146
12.1.2.2.2.	BmDH 10 Bac <i>E. coli</i> containing the bacmid for the modified <i>Rous sarcoma</i> virus-Gag protein.....	146
12.1.2.2.3.	BmDH 10 Bac <i>E. coli</i> containing the bacmid for the MERS-S protein	146
12.1.2.2.4.	Viral nucleic acid Isolation	146
12.1.2.2.5.	Bacmid Isolation.....	147
12.1.3.	Results and Discussion	148
12.1.4.	Conclusion	148
12.2.	MNPs for His-, Flag-and Strep-tag-affinity purification.....	148

12.2.1.	Introduction.....	148
12.2.2.	Specific Methods	149
12.2.2.1.	MNP for purification of Flag-tagged proteins	149
12.2.2.2.	Preparation of MNPs for purification of Flag-tagged proteins	149
12.2.2.3.	Preparation of MNPs for purification of Strep-tagged protein.....	149
12.2.2.4.	Purification using MNPs.....	150
12.2.2.5.	Enzyme-linked immunosorbent assay (ELISA)	150
12.2.3.	Results and Discussion	151
12.2.4.	Conclusion	151
12.3.	Standard purification of VP26 and VP28	151
12.3.1.	Introduction.....	151
12.3.2.	Specific Methods	152
12.3.2.1.	Cell lysate containing VP26 or VP28	152
12.3.2.2.	Glycoprotein staining in SDS-PAGE gels.....	152
12.3.3.	Results and Discussion	152
12.3.4.	Conclusion	153

List of abbreviations

AIEX	- Anion exchange chromatography
CHT	- Ceramic hydroxyapatite
CIEX	- Cation exchange chromatography
FPLC	- Fast protein liquid chromatography
GFP- β 3GnT2	- GFPuv- β 1,3-N-acetylglucosaminyltransferase 2
HAC	- Hydroxyapatite chromatography
HPLC	- High performance liquid chromatography
HPV	- Human papillomavirus
IEX	- Ion exchange chromatography
MNP	- magnetic nano particle
LP	- like particles
NoV	- norovirus
PEG	- Polyethylene glycol
RSV	- <i>Rous sarcoma virus</i>
RT	- Room temperature
TEM	- Transmission electron microscopy
SEC	- Size exclusion chromatography (also called: Gel chromatography)
VLP	- Virus-like particle

1. General Introduction

The intention of this doctoral study was to improve the purification of recombinant proteins from the silkworm larval haemolymph (*Bombyx mori*). Especially the purification of virus-like particles (VLPs) was particularly sought after. The silkworm expression system is promising, but the purification process requires methods with high recovery ratio without degradation of the target recombinant proteins. Nevertheless, the purification from silkworm compounds is not an easy feat as it will be presented in the following.

1.1. Virus like particles (VLPs)

Virus-like particles (VLPs) have stimulated the interest of many researchers and are therefore an expanding topic in biotechnology. Some are already commercialized as vaccines, such as Engerix (hepatitis B virus) and Cervarix (human papillomavirus) from GlaxoSmithKline or Recombivax HB (hepatitis B virus) and Gardasil (human papillomavirus) from Merck. Interestingly VLPs seems to be able to be utilized as drug delivery system [1]. Compared to their origin virus VLPs miss the genetic material. However, VLPs characteristics are nearly similar to their viruses without the genetic information and are still able to self-assemble from one or more subunit proteins. Therefore, VLPs are simply empty vehicles and not infectious [2]. Because they can still enter target cells, their use *in vivo* seems promising.

VLPs are structural distinguished in enveloped and non-enveloped ones [3]. One or even multiple capsid proteins are structural possible and some have also an envelope, for example the human immunodeficiency virus (HIV) VLP. Their lipid bilayer is acquired during the budding from the cell membrane of their host cells. It is possible to include one or several novel proteins in the envelope during and after assembly [4–9]. The proteins are able to trigger an immunological response, because the immune system can recognize these as antigens [10–14]. With additional proteins-modified VLPs are also highly usable as vaccine candidates.

A cheap and effective way to prevent diseases is vaccination, but the production takes long time. Approximately 6 months are needed to cultivate the attenuated or inactivated wild-type viruses and then the batch has to be controlled by official authorities, which takes time as well. Therefore, the flexibility of influenza vaccines is greatly reduced by this long production time. Antigen switches from the predicted one to another variant can happen and are not rare, but this leads to a less effective or even useless produced vaccine. One the other hand, VLP preparation time is shorter and they were proven to elicit a strong immune

response. The production time is expression system depending, but it is approximately 1–4 weeks. It is approximately 1–2 weeks depending on the method for insect cell- and silkworm-based systems [15]. Shorter is the whole production time with approximately 5 days in bacteria [16] and 7 days in yeast [17].

Another option is to use them as drug delivery system if in the membrane or capsid particular recognition proteins or antibodies are imbedded [18–22], because the empty VLPs can be filled with different compounds such as contrast media or drugs. For example the hepatoma cell line HepG2 was targeted using lactobionic acid and, to the rotavirus VLPs bound anti-cancer drug doxorubicin was delivered [23]. Pharmaceutical drugs were also packed inside VLPs and then specific types of cells were targeted by other studies [1,24]. Moreover, nucleic acids such as siRNA could be also stored inside VLPs and then transported [25]. With the single-chain variable fragment of humanized CC49 antibody functionalized *Rous sarcoma virus* VLPs (RSV-LP), displayed on the surface, delivered an anti-cancer drug specifically to LS174T cells, an colon carcinoma cell strain [21]. Another way was to anchor a recombinant single chain fragment variable, which binds recombinant human Inter leucine-2 and the cancer-associated glycoprotein 72, in the lipid bilayer of RSV-LP [26]. Colon cancer cells were specifically targeted by this VLP and macrophages were attracted to them.

Interestingly, VLPs can be a unique approach for gene therapy, which shows that they have a broad application spectrum. Thymidine kinase transporting VLPs with imbedded HIV CD4-specific receptors could target and kill HIV infected cells with ganciclovir [27]. Moreover, modified HIV VLPs targeted resting CD4 T cells and could manipulate their genes through gene silencing [28]. These studies show that VLPs are highly modifiable [29].

Furthermore, some types of VLPs are stable to alkaline treatment, for example hepatitis B VLPs and this can be used in their preparation [30]. Unfortunately, the difficulties in preparing cost-effectively VLPs with high purity and without contamination by nucleic acids and viruses are still enormous, even with the progress in biotechnology.

1.2. Production of recombinant proteins

Different host expression systems can be used for the expression of recombinant proteins and should be carefully selected based on the purpose [23]. Bacterial systems, especially *E. coli*, cannot undertake post-translational modifications and have problems with protein solubility, but are well-known and widely used. In opposite, yeast strains, such as

Pichia, don't form inclusion bodies and can modify proteins with post-translational modifications. However, the production capacity can be lower, in some cases the assembly of multimers cannot be supported, can lack chaperonins for proper folding and they have inappropriate glycosylation patterns [23,31]. To avoid misunderstandings, their production capacity is not generally low and is for recombinant proteins normally better than that of insect or mammalian cell-based systems. Provided that this kind of systems is not necessary for the expression of the recombinant proteins.

Insect cell-based systems are another option, especially the *Spodoptera frugiperda* Sf9 or the High Five cell lines are widely used. Post-translational modifications are possible with these systems, they have a high growth rate and large-scale production is also possible with them. However, for infection a construction of a vector from the recombinant baculovirus encoding the gene of interest is required [32].

As a side note, plants may be also used to produce recombinant proteins. They can be a cost-efficient and scalable alternative, as for example two types of VLPs of the non-enveloped polyomavirus protein VP1 were produced in the infected the leaves of *Nicotiana benthamiana* and yielded up to 58 µg VLPs/ fresh weight tissues g or 81 µg VLPs/ fresh weight tissues g after gradient centrifugation, respectively [33].

Although from these methods *E. coli* and yeast are still the preferred platforms for some protein expression groups, mammalian recombinant proteins often require mammalian cells for optimum yields and activity.

Mammalian cell lines are of course also used. Their benefit is that they are fully capable of post-translational modification and of assembling multimers, even if it's more complex to construct and handling them. Moreover, cell-free systems are also useable for the production of VLPs as reviewed and this is especially beneficial for complicated cases, when the production of the proteins is toxic for the host cell [23].

1.3. Production of recombinant VLPs in silkworm

In opposite, the Bac-to-Bac system for insect cells, e.g. silkworm (*Bombyx mori*) larvae, is a comparably cheaper production method and can provide the same posttranslational modifications as insect cells and for some proteins even higher protein yields than for the aforementioned systems [15,34–38]. In brief, the recombinant shuttle virus infects the cells in

the larvae and they express then the proteins. Depending on the recombinant protein, they will be released into the haemolymph or remain inside the cells [15].

For the rearing of silkworms, in Asian countries the necessary infrastructure have been already established, and beyond that, the use of silkworms is also comparatively cheap and they require only an simple, artificial diet [15]. As already mentioned this system has a beneficial cost : production capacity ratio, because high productions from recombinant proteins were reported [34,38].

On the second day the *Bombyx mori* nucleopolyhedrovirus (BmNPV) bacmid is injected into the fifth instar silkworm and 4 to 6 days after injection the protein is collected from the haemolymph. It takes approximately 1–2 weeks for the entire process of protein expressing including the bacmid preparation [15]. Moreover, during purification the used baculovirus for infection can be hard to separate from the product, but is not infectious for mammalian cells and it was shown that it could be even an adjuvant for vaccines [39,40]. The following procedure is done; the desired gene is after PCR amplification introduced into a recombinant bacmid vector, which is then amplified in *E. coli* as a large plasmid. This is the BmNPV bacmid expression system and it speeded the isolation and purification of the recombinant bacmid up, compared with the conventional baculovirus expression vector system. The latter method took usually 3–6 months, because it required several rounds of amplification in *Bombyx mori* cells.

Related to the silkworm production system is the production in the silkworm *pupae*. Studies about the VLP production in this system have been also already published [41–43], but this system is still lacking in terms of production and purification. This silkworm system with its advantages/disadvantages has yet to be explored.

1.4. Physiology of silkworm haemolymph and fat body

A literature search using the Scopus databank [October 2019] with the key words “silkworm and physiology” and “silkworm and protein or haemolymph or fat body” revealed only a handful and mostly older reported studies about the proteome of the silkworm *Bombyx mori*. Moreover, it doesn't reflect well that similar literature searches in 2017 and 2018 yielded in a lower count of found papers, even if most of them were published before 2017. The published works from these studies had all different objectives and prerequisites, but it is possible to gather some information about the silkworm proteins. However, the function of

the majority of the silkworms proteins is still unknown [44,45]. As short explanation, insects don't have a blood and lymph system as most of the higher animals, but a body fluid called haemolymph. The haemolymph bathes all organs inside of the insect, contains the functional proteins of the insect and transports nutrients and hormones, and reacts to injuries and functions as an immune system [44].

If someone is to examine the silkworm proteome, of course it has to be considered the development stage of the silkworm and this doesn't mean only the larvae, pupae and moth stage, but also the instar stages as it was shown [46]. Specifically, the expression level of the proteins around 30 and 80 kDa were changing significantly during the different development stages. The 80 kDa proteins were detectable from the 1st day of the fifth instar phase and since the 3rd day their expression level increased until the wandering stage, at which the level decreased until it more or less disappeared in the pupae stage. In opposite, the 30 kDa proteins appeared in the haemolymph on the 4th day and increased steadily until they were the major compound during the pupae stage. They vanished almost completely at the end of the pupae stage. This led to the conclusion, that both protein groups are most likely storage proteins, which the silkworm needs as it shifts from one development stage to the next one [46].

Moreover, a study investigated the food and allergically potential of the silkworm pupae and was able to show that a different diet, here between an artificial diet and fresh mulberry leaves, resulted in different protein expression profiles [47]. Not only was shown, that male and female pupae have different energy value and protein amount depending on the diet type, but also there were unique proteins depending on the gender and the diet, respectively. Furthermore, even if a 2D-gel electrophoresis was done, for some cases the spot volume variation could not be determined, because proteins were overlapping. For proteins around 80 kDa the sex-specific storage protein 1 and 2 and arylphorin had the most coverage together with their isoforms. For 20–30 kDa proteins it was the glutathione S-transferase delta. It should be mentioned again, that the leaf quality was considered as very good and that the authors suspect a less or even non relevant outcome with lower quality leaves. The different diet led to a different protein expression, however, this did not lead to different physiological traits [47].

Another study determined also a storage protein at the size of around 87.3 kDa, the *Bombix mori* storage protein 1 (BmSP1) [48]. As previously mentioned, this storage protein was also found to increase and had his peak concentration in the fifth instar larvae. Moreover, investigation with recombinant BmSP1 coupled with EGFP revealed that the overexpressed protein also inhibited the haemolymph melanisation and that BmSP1 interacted with the 30 kDa lipoprotein PBMHP-6 (BmLP6) [48]. The potential binding partner BmLP6 shows that storage proteins have the ability to interact and affect other proteins in their physical behaviour and to drag them with them. It can be assumed, that other storage proteins have similar characteristics and can interact also with not only host cell proteins, but also with recombinant proteins. This can affect the following downstream process.

Many proteins are inside of the silkworm larva and pupae as the previous studies showed. So were 177 proteins in the fat body detected [45], 153–168 proteins in male or female pupae, also with different diets [47] and one study investigated only the 56 main spots of a 2D-gel electrophoresis [46]. To complicate this issue, the proteome of the *Bombix mori* is different for the different strains. For one study 163 different silkworm strains were screened to investigate the response on the *Autographa californica* multiple nucleopolyhedrovirus (AcMNPV), which is less effective as gene vector for the *B. mori* compared to the BmNPV. The result could be roughly divided in 3 groups; whereby 5 strains were high-permissive, 74 middle-permissive and 84 low-permissive [49]. Another study used AcMNPV to investigate the proteome differences of two previously found AcMNPV-resistant or -sensitive silkworm strains. In total 63 haemolymph proteins were found, whereby 6 and 4 were strain specific [50]. Again could be shown that storage proteins (BmSP1 and BmSP2) and 30 kDa lipoproteins varied between the different development stages [50]. Finally, a review elaborated the differences of the heat shock proteins and the thermal acclimation of different silkworm strains. The strains have a different heat tolerance as some strains are able to survive under tropical conditions, but not under milder conditions and vice versa [51]. Silkworms have also during their life cycle different preferred environment temperatures. So prefer young silkworms 28°C by a relative humidity of 80 %, but older silkworms 24°C by 65 % relative humidity. Moreover, this review shows impressively with SDS-PAGE gels the different protein expression patterns of the silkworm strains Nistari, P2D 1 and CSR 2. Furthermore is explained, that results obtained under laboratory conditions cannot be achieved under field conditions [51].

For understanding the proteome of the silkworm during the different development stages, the mass spectrometry (MS) was the most crucial part for the protein identification in the mentioned studies. That the MS plays nowadays a crucial in protein identification was also shown by a review with focus on the silkworm research [52]. In the end it can be said, that silkworm compounds are a very complex sample matrixes, whereby also the different strains need to be considered.

1.5. Purification

Protein purification from the silkworm is still a major issue for widening the application of this system, especially because of the already mentioned high amount of host cell proteins. Few studies tackled the general protein purification from the silkworm, and only some of them attempted to establish an up-scalable purification process. For purification, protein tags are usually used [34,38,53,54] or non-scalable processes such as sucrose gradient centrifugation [35,55]. Heparin affinity chromatography and sucrose gradient centrifugation as comparison showed stable human papilloma virus 6b L1 VLPs, but still contained a high amount of host proteins [6]. Although up-scalable processes were used, yield and purity improvements were not investigated. Recombinant hemagglutinin was investigated for the antigenicity and the receptor binding capacity, whereby the production und purification yield was 500 µg/30 silkworms using Fetuin-agarose and size exclusion chromatography (SEC), but the purification optimization was not part of this study and not necessary [55,55,56]. Also ignoring purification optimization, another study solely expressed, characterized and checked the hemagglutinin inhibition of rat α 2,6-sialyltransferase in silkworm haemolymph. Ammonium sulphate precipitation was done as pre-treatment, FLAG-tag affinity chromatography for further purification and this resulted in a yield of purified 2.2 mg /11 ml silkworm haemolymph with a recovery of around 64 % [57]. Sometimes for DNA digestion benzonase was used, but it is expensive and increases the cost of purification and for each case the possible benefit has to be calculated independently [58]. Purification of VLPs or even viruses is usually not different from the general purification procedure of recombinant proteins. However, the VLPs purification is more complicated, because they are large biomolecules that behave differently in standard chromatography material and salts or pH environment can be more critical for their stability compared to simpler proteins [59,60].

1.6. Pre-treatment

In the current downstream processing for biotechnological products, it is necessary to remove large aggregates and cell debris to avoid clogging and fouling of the column in later stages, before starting the chromatography purification procedure. Well pre-treated samples made the whole purification process also more efficient [61]. For this, centrifugation, precipitation and filtration are the commonly used pre-treatment methods, and the latter facilitates a defined cut-off for the particle size and is easy to scale up. Typically precipitation reagents, such as polyethylene glycol (PEG) [62] or ammonium sulphate [63] are a good pre-treatment, because these reduces usually the chromatography steps and are cost effective if the treatment doesn't damage the recombinant protein, virus or VLP. Ammonium sulphate is the classic reagent for protein precipitation [64,65] and was therefore, together with other reagents chosen for the precipitation experiments and they were investigated in several setups.

PEG precipitation is an alternative method and has only a slight tendency to interact with proteins, contrary to ethanol, [66]. Besides these two, polyethylene imine (PEI) is also useful for protein precipitation. Negatively charged DNA will be precipitated due to PEI, because it is a basic, positively charged polymer. Moreover, in lower salt concentrations (0.1 mol/l NaCl) acidic proteins will also precipitate and therefore, to prevent protein precipitation higher salt concentrations are used [64]. A Design of Experiments, a statistical approach, was undertaken to purify human influenza virus from mammalian cells for the investigation of the ideal PEI condition. 0.045 % (w/v) 2 kDa PEI with a high salt concentration was the optimum condition for precipitation, whereby DNA was to 15 % reduced and a virus recovery of 86 % achieved [67]. However, PEI is *in vivo* toxic and can disturb assays and therefore, a low molecular PEI is favoured, and it is recommended to separate it in later purification steps [67]. However, it is still an unusual method for the protein purification from the silkworm haemolymph, at least no study was found which utilized this method for purification from silkworm compartments.

Furthermore, a heat treatment up to 80°C followed by centrifugation is able to reduce the host cell protein amount significantly, presupposed the target protein is heat stable [68,69]. Therefore, this approach is also interesting for investigation of the protein purification and was used in some studies, because other methods were not sufficient in reducing the protein amount.

1.7. Purification using chromatography

After a successful pre-treatment, fast protein liquid chromatography (FPLC) steps are usually done for efficient purification. It is the method of choice after the protein amount was reduced. Even if FPLC is reliable and already established, product-specific method development and carefully selected separation techniques are still required. Furthermore, protein and VLP purification with chromatography methods were often reported for different expression systems, but only rarely for silkworm haemolymph [58,69–72].

An advantage is that VLPs have similar properties as their corresponding viruses and therefore, the virus purification protocols can often be used for VLP purification. Moreover, the main aim for virus purification is normally the increase in the purification yield [73–75] and this knowledge can be beneficial for VLP purification. Sadly, this aspect was only reported by few studies. So it was shown the core bead technology from GE Healthcare, a newer chromatography material, has potential for intermediate enveloped virus purification [76]. This system uses a cut-off SEC principle and the cut-off is 70 kDa. Theoretical all proteins larger than 70 kDa cannot enter the shell of the beads through the pores and therefore, are not able to interact with the core and will remain in the flow through. In this manner, a respiratory syncytial virus produced in a Vero cell line was purified from the supernatant with about 50–60 % yield.

Opposite to the newer principle, one of the most universally used principles, especially as the first step of capturing, is the ion exchange chromatography (IEX). IEX and hydrophobic chromatography were investigated if they are beneficial for the purification of enveloped measles virus (MeV) and mumps virus (MuV) [77]. With a large IEX channel monolith QA column (BIA Separations, Slovenia) and a 50 mmol/l phosphate buffer (pH 7.3) was the best result for MeV achieved. In opposite the MuV was not further investigated, because the recovery was very low. With 1.0 mol/l ammonium sulphate, 50 mmol/l HEPES (pH 7.3) as loading buffer in an OH column (BIA Separations, Slovenia), a recovery of approximately 60 % was achieved for both viruses. The ammonium sulphate amount influenced the infective virus recovery by the fact that a higher concentration caused less infective virus, but with lower concentration less virus was able to bind to the column.

Moreover, it is interesting to use the flow through mode instead of the bind and elute mode of the traditional chromatography approach and material [69,74,76,78]. Q anion exchange chromatography (AIEX) material was with the inert polymer polyoligoethylene

glycol methacrylate modified and used for a negative chromatography mode. The modification resulted in steric exclusion of hepatitis B core VLPs and an additional heat treatment was also introduced. This resulted in a purity of approximately 87.5 % [69]. Other studies also used this approach successfully [79]. A review article already described detailed the utilization of the negative chromatography mode [80]. Steric exclusion chromatography is also interesting, because PEG 6000 is unable to interact with macromolecules and induces at a higher concentration a thermodynamically unstable state. When the macromolecules bind to the surface of the column, the thermodynamically unfavourable situation is reduced. Larger molecules are more affected and therefore, smaller molecules are in the flow through. This is beneficial, because target proteins are often macromolecules, such as a VLPs, which can then be comparable pure recovered. Bound macromolecules can be easily eluted by decreasing the PEG concentration [81].

SEC or also called gel chromatography, is a common principle and usually the polishing step in a chromatography purification protocol. From this set up are just some exceptions, because a crude sample would only cloak the column and would lead to fouling. On another note, hydroxyapatite chromatography (HAC) can be beneficial for protein purification, because of its unique characteristics. Non-enveloped enterovirus 71 VLPs from insect cells was purified using both methods and tangential flow filtration. Around 100 % VLP recovery was achieved with the HAC alone, whereby 17 % protein removal was obtained. The SEC step removed 5 % of the total protein amount, but the VLP recovery was with 55 % the lowest in this protocol. 36 % total VLP recovery and a purity of 83 % could be achieved, nevertheless, this is still not practical for wider industrial application. Especially, that the sample was a clean cell supernatant instead of the host cell protein rich silkworm haemolymph, but to defend them, it is still an improvement [82]. Only a high recovery or in a high removal of host proteins was achieved when using two SEC columns in a row for the purification of the BmNPV from the silkworm larval haemolymph [83]. On another note, since HAC could purify dengue virus type 2 ThNH7/93 with approximately 60 % recovery from the supernatant of C6/36 cells, it should be also applicable for enveloped VLPs. Especially, the viruses retained their infectivity and that means that their membrane were most likely still intact [84].

Viruses and VLPs have limited interaction with classical chromatography material, because their size range from approximately 30 nm to 300 nm. Therefore, the pore size of the packed porous beds is smaller than the particles, so that diffusion into them is not possible.

This restricts the utilization of traditional materials, except the proteins are smaller. One way to solve this are monolith columns, which consist of a single block of modified polymethacrylate with resulted in a controlled larger pore size. The larger pore size improved resolution and recovery, increased the capacity, and faster flow rates were possibly. In recent years these materials are more and more used and show promising results [77,81,85,86].

1.8. Stability of VLPs

VLP stability is another black box. Non-enveloped VLPs should be more stable than enveloped VLPs as it is the same as for viruses. Optimum pH environment is approximately 7–8 and temperature range from 0° to 30°C for the enveloped viruses, because at a lower pH and/or higher temperature they are more likely to aggregate [87]. Ionic strength/salt concentration is also a major factor [88] and therefore, the stability ranges of the enveloped VLPs is smaller than the stability ranges from the non-enveloped VLPs. A lipid envelope is more fragile as a capsid and this has to be especially considered for precipitation. For non-enveloped viruses, PEG and ammonium sulphate can be utilized for precipitation and purification [89]. However, the lipid bilayer envelope can be destroyed by ammonium sulphate, but it seems to tolerate low concentrations from 5–10 % (w/v) or up to 2 mol/l ammonium sulphate without being destroyed [79,85,86].

1.9. Quality Control

Even after purification, cell-assembled VLPs most likely still contain host DNA or host proteins [90], which can disturb the structure of the VLP. Moreover, for pharmaceutical use it is disadvantageous, because the least possible contamination is required. In the following case, empty VLPs were from loaded VLPs separated by sucrose gradient centrifugation [90], because only non-enveloped VLPs can be disassembled and subsequently reassembled, as it is not yet possible to reconstruct the plasma membrane after destruction. DNA contamination was reduced [71], the stability and biophysical properties of the VLPs improved [91] and a stronger immune response was elicited from the VLPs [92].

VLP structure and purity have to be checked after purification. SDS-PAGE and CBB staining are one of the first choices, followed by Western blot or ELISA, if specific antibodies are available. Since these methods measure also destroyed VLPs, transmission electron microscopy (TEM) is necessary to obtain a visual confirmation. This is especially important for enveloped VLPs to see the integrity of the envelope. Additional to ELISA and TEM, dynamic

light scattering for size, circular dichroism, fluorescence spectroscopy and, if necessary, the haemolysis assay are other reliable methods for characterizing the VLPs [33,87,93,94]. Further analytical methods are of course also usable, but this is depending on the purpose of the purified VLPs. For medical use in humans or animal a high purity is important. High performance liquid chromatography (HPLC) is a good choice for purity analysis, alone or additional with other methods. Moreover, capillary zone electrophoresis can be utilised for the analysis of VLPs, which is very useful because of its excellent resolution and separation quality [95]. Mass spectrometry can be used for detection of the desired VLP surface modification [79,94]. Another challenge is the tracing of the target protein during the different purification steps. This data is needed for calculation of the final yield or overall loss of the purification protocol. It is usually not possible to acquire the separate concentration of the target protein at each purification step.

The ideal purification process should be apply-able to all recombinant proteins, viruses or VLPs, however this is challenging because of the unique particle properties. Most likely it should be easier to establish purification protocols for specific model particles and to purify similar particles based on these protocols with slight variations.

1.10. Magnetic nano particles

These days nano particles are a rising topic in many scientific fields and because of their nano size these nanomaterials display several advantages. They can be of inorganic or bioorganic nature and can have several different advantages due to their nano size of around 10–100 nm. They can be used in many fields such as magnetic resonance imaging, target drug delivery, targeted cancer destroying through hyperthermia, magnetic transfection, tissue engineering or in purification. Magnetic nano particles (MNPs) can be produced through different methods, for example grinding, thermal decomposition, microemulsion, chemical vapour deposition, co-precipitation, reactions in constrained environments, polyol method, flow-injection synthesis and sonolysis as it was already summarized in several reviews [96–99]. The MNPs undergo often further surface modifications to modulate solubility, stability, internalisation or toxicity [96,98–100]. Very often silica is used as coating material, because of its efficiency, reduced toxicity, aggregation prevention and hydrophilicity [96,100]. Toxicologically, it can be assumed that iron nanoparticles are non-cytotoxic and safe, so long the concentration is under 100 µg/ml. Moreover, it can be cleared by the endogenous iron

metabolic pathway and this leads to the incorporation into haemoglobin or removal from the human body [98]. This relatively non-toxicity makes them intriguing not only for medical, but also for the biotechnology down-streaming process.

Furthermore, inorganic and bioorganic nano materials also have to be seen as a mutual supplement in biotechnology, and not only as separate entities. MNPs are ideal candidates for the purification of recombinant proteins, such as the VLPs which are bioorganic nanoparticles. Two ways are possible for the purification, directly binding to the target protein or in opposite, binding of host cell proteins and therefore, decreasing the general protein amount. Among other things it was for the latter one shown, that this can be an effectively and safe way to remove haze-forming proteins from wines [101]. The surface of the MNPs was modified with amine, carboxyl or oxazoline functionalized groups. This study showed that for each different wine, different depletion results were obtained with the different MNP modifications, but that the carboxyl functionalized are the most effective ones. Moreover, the general metal content was low after using the MNPs and only the iron concentration slightly increased, but the concentration is low and similar to as to the standard treatment for wines with Vitiben or Pluxcompact bentonite [101]. The same approach to remove the abundant protein bovine hemoglobin from bovine blood was done by using Silica coated iron magnetic nanoparticles functionalized with a nickel shell [100]. Nickel has not only a high affinity to the His-tag, but also of course to proteins with high amount of histidine residues. They were successfully able to selectively reduce the bovine hemoglobin, but due to protein-protein interactions, the reduction in the diluted bovine blood sample was low compared to pure samples [100].

The other purification way is to use modified MNPs, which are able to specifically separate the target protein. Interestingly, these modifications can be also different ones than the classical antibodies, so was adamantane beta-cyclodextrin (β -CD) used to modify MNPs, which were then able to bind the target lectin [102]. Concanavalin A was successfully separated from a mix with peanut agglutinin. Mannose as competitive ligand was used for the elution [102]. Another study modified MNPs in a modular fashion and separated the targeted biomarker, even if they were displayed on whole eukaryotic cells [103]. This modularity also allows to switch easily the receptor on the MNPs, so that different biomarkers can be targeted [103].

Opposite to this, the protein can be designed to match the MNP. A six glutamates containing peptide tag was very effective to be bound on bare iron oxide nano particles (BIONs) [104]. The purification was even tested on a technical scale and the BIONs achieved a mean recovery of 81 % target protein [104]. And as already known, MNPs can be modified to match already existing protein tags. Fe₃O₄ nano particles were encapsulated in polystyrene nano particles from Jose et al. [105] and then functionalized with Ni²⁺-nitrilotriacetic (NTA) for the purification of His-tagged protein. The purification efficiency was higher than for already commercial available Ni²⁺-NTA-magnetic beads [105].

1.11. Objective

As illustrated, purification of recombinant proteins from silkworm is not an easy undertaking. In several studies, we aimed to establish an easy up-scalable purification protocols suitable for industrial use. As gold standard was affinity tag purification appointed, because of its purity and recovery rates. Sucrose gradient centrifugation was only once performed as comparison, because of its low purity. Investigations of the aforementioned pre-treatments and FPLC principles such as ion exchange, hydrophobic interaction, size exclusion and affinity were conducted and recombinant proteins were used as model proteins. One aim was to build a databank of the host cell proteins behaviour for each purification method. As main model proteins, modified GFP_{uv}-β1,3-*N*-acetylglucosaminyltransferase 2 (GFP-β3GnT2), mCherry, SpCaVP1+EDIII and human papillomavirus (HPV) VLPs were used. GFP-β3GnT2 is a GFP fusion protein, has a molecular mass of approximately 77 kDa and it displays green fluorescence (Ex. 395 nm, Em. 509 nm). On the other side mCherry's molecular mass is lower with approximately 34.5 kDa, and has a strong red fluorescence (ex. 540–590 nm, em. 550–650 nm) [106]. Their fluorescence's and mCherry's red colour make the tracing during the purification process significantly easier as model proteins.

As real target proteins were among others a VLPs based on Norovirus VLP (NoV-LP) with dengue 1 envelope protein EDIII (sizes: SpCaVP1 approximately 70 kDa; EDIII approximately 15 kDa; both together approximately 95 kDa) and human papillomavirus (HPV) 6b L1 VLP (size approximately 56 kDa) investigated. Whereby the latter project was later joined and mainly the finishing touch was done.

The development of a purification protocol with pre-treatment steps followed by as few as possible FPLC steps was sought. In the end three paper could be published, a review of VLP

purification from the silkworm, an HPV 6b L1 VLP a purification protocol based on AIEX, CHT and heparin chromatography and, moreover, the first up-scalable purification protocol for silkworm haemolymph using mCherry as model protein was obtained. This protocol includes centrifugation, PEG precipitation and a thermal treatment followed by HIC, SEC and heparin affinity chromatography steps. The thermal treatment makes this protocol only usable for partial thermal stable proteins. Nevertheless, this study was successful published. Additionally, during these studies the behaviour of the host impurities during each purification step was examined.

Furthermore, using multiple recombinant proteins such as mCherry or SpCaVP1+EDIII, a project to utilize MNPs for the purification of recombinant proteins, because the afford mentioned MNPs for purification have in most cases a disadvantage. They are not easily self-made or commercial MNPs are expensive and have only a limited application for small scale experiments. For this very reason on project focused on the use of cheap, easily in the laboratory self-made and disposable magnetic nano particles for the purification. Their use should be as a simple and easy pre-treatment step for the purification of His-tagged recombinant proteins. This work is close to completion, but will be most likely finished after publication of this dissertation.

2. General Material and Methods

2.1. Silkworms

The silkworms were ordered from Ehime Yosan Kabushiki company (Ehime, Japan). The silkworms belonged to the strain Kinshu × Showa (Japanese race × Chinese race) strain.

2.2. Components of buffers, media and solutions

2.2.1. Gel electrophoresis

50x TAE-buffer: 242 g Tris, 57.1 ml acetic acid, 18.6 mg EDTA, up to 1 l deionised water

2.2.2. SDS-PAGE

30 % Acrylamide solution: 116 g Acrylamide, 3.2 g N, N'-methylenebisacrylamide, up to 400 ml MilliQ

8, 10, 12 or 15 % Acrylamide solution: 26.6 ml, 33.3 ml, 40 ml or 50 ml 30 % Acrylamide, 25 ml Tris-HCl pH 8.8 1.5 mol/l, 1 ml SDS, 47.4 ml, 40.7 ml, 34 ml or 24 ml deionised water

10 % Running gel: 6 ml 10 % Acrylamide solution, 6 µl TEMED, 20 µl 25 % APS

4% Stacking gel: 2 ml 4 % Acrylamide solution, 2 µl TEMED, 20 µl 25 % APS

10x SDS-PAGE running buffer: 61 g Tris, 288.2 g glycine, 20 g SDS, up to 2 l deionised water

1x SDS-PAGE running buffer: 1 l 10x SDS-PAGE running buffer, 9 l deionised water

2 x Sample Buffer solution with 2-ME (pH 6.8): 25 ml 0.25 mol/l Tris-HCl (pH 6.8), 5 ml 2-Mercaptoethanol, 2 g SDS, 10 ml Glycerol, 5 mg Bromophenol blue, up to 50 ml deionised water

Staining solution I: 90 ml ethanol, 20 ml acetic acid, 90 ml deionised water, 0.5 g Coomassie Brilliant Blue R-250

Decolouring solution I: 300 ml methanol, 70 ml acetic acid, 630 ml deionised water

Staining solution II: 1 l deionised water, 80 mg Coomassie Brilliant Blue G-250

Decolouring solution II and III: deionised water

Staining solution III: 5 g Beta-Cyclodextrin, 15 g Citric acid monohydrate, 80 mg CBB R-250, 1 l MilliQ

2.2.3. Western Blot

Transfer Buffer: 58.1 g Tris, 29.3 g Glycine, 2 l methanol, up to 10 l deionised water

TBS-T: 1 l 10xTBS, 50 ml 20 % Tween 20, 8.95 l deionised water

2.2.4. Luria-Bertani medium

LB-Medium (Luria-Bertani): 950 ml deionised water, 10 g trypton, 5 g yeast extract, 10 g Sodium chloride, pH 7 adjusted with 5 mol/l NaOH (around 200 μ l), after that filling with deionised water to 1 l, autoclaved. For plates: Agar 15 g/l

2.2.5. Buffer for chromatography screening

ALEX screening (Elution buffer with additional 1 mol/l NaCl):

NaH₂PO₂ 0.1 mmol/l, pH 7: 3.5814 mg NaH₂PO₂x12 H₂O /100 ml, pH adjusted

NaH₂PO₂ 0.1 mmol/l, pH 8: 3.5814 mg NaH₂PO₂x12 H₂O /100 ml, pH adjusted

NaH₂PO₂ 20 mmol/l, pH 7: 0.7163 g NaH₂PO₂x12 H₂O /100 ml, pH adjusted

NaH₂PO₂ 20 mmol/l, pH 8: 0.7163 g NaH₂PO₂x12 H₂O /100 ml, pH adjusted

Tris 10 mmol/l, pH 7: 0.1211 g Tris /100 ml, pH adjusted

Tris 10 mmol/l, pH 8: 0.1211 g Tris /100 ml, pH adjusted

Tris 100 mmol/l, pH 7: 1.2114 g Tris /100 ml, pH adjusted

Tris 100 mmol/l, pH 8: 1.2114 g Tris /100 ml, pH adjusted

HEPES 1 mmol/l, pH 7: 0.0238 g HEPES /100 ml, pH adjusted

HEPES 1 mmol/l, pH 8: 0.0238 g HEPES /100 ml, pH adjusted

HEPES 25 mmol/l, pH 7: 0.5957 g HEPES /100 ml, pH adjusted

HEPES 25 mmol/l, pH 8: 0.5957 g HEPES /100 ml, pH adjusted

MOPS 25 mmol/l, pH 7: 0.5232 g MOPS / 100 ml, pH adjusted

MOPS 25 mmol/l, pH 8: 0.5232 g MOPS / 100 ml, pH adjusted

MOPS 45 mmol/l, pH 7: 0.9417 g MOPS / 100 ml, pH adjusted

MOPS 45 mmol/l, pH 8: 0.9417 g MOPS / 100 ml, pH adjusted

PBS, pH 7: 10 ml 10x PBS, 90 ml demineralized water, pH adjusted

PBS, pH 8: 10 ml 10x PBS, 90 ml demineralized water, pH adjusted

2.2.6. Buffer for chromatography

DEAE

Tris 50 mmol/l, pH 8: 12.114 g Tris /2 l, pH adjusted

Tris 50 mmol/l, 1 mol/l NaCl, pH 8: 58.44 g NaCl per 1 l Tris 50 mmol/l, pH 8

Tris 10 mmol/l, pH 8: 1.2114 g Tris /1 l, pH adjusted

Tris 10 mmol/l, 0.0641 mol/l NaCl, pH 8: 3.75 g NaCl per 1 l Tris 50 mmol/l, pH 8

Tris 10 mmol/l, 1 mol/l NaCl, pH 8: 29.22 g NaCl per 500 ml Tris 50 mmol/l, pH 8

HIC

Tris 10 mmol/l, 1.2 mol/l (NH₄)₂SO₄, pH 8: 1.2114 g Tris /1 l, 79.284 g (NH₄)₂SO₄ / 500 ml , pH adjusted

Tris 10 mmol/l, 3 mol/l NaCl, pH 8: 1.2114 g Tris /1 l, 87.66 g NaCl / 500 ml , pH adjusted

Tris 10 mmol/l, pH 8: 1.2114 g Tris /1 l, pH adjusted

Blue sepharose

NaH₂PO₄ 20 mmol/l, pH 7: 1.5601 g/500 ml, pH adjusted

NaH₂PO₄ 20 mmol/l, 2.5 mol/l NaCl pH 7: 1.5601 g NaH₂PO₄/500 ml, 36.525 g NaCl /250 ml, pH adjusted

CHT

NaH₂PO₄ 8 mmol/l, pH 8: 0.8114 g NaH₂PO₄ x 2 H₂O /500 ml, pH adjusted

NaH₂PO₄ 600 mmol/l, pH 8: 60.8579 g NaH₂PO₄ x 2 H₂O /500 ml, pH adjusted

KH₂PO₄ 8 mmol/l, pH 8: 0.54436 g KH₂PO₄ /500 ml, pH adjusted

KH₂PO₄ 600 mmol/l, pH 8: 40.827 g KH₂PO₄ /500 ml, pH adjusted

HisTrap

NaH₂PO₄ 20 mmol/l, 0.5 mol/l NaCl, 20 mmol/l Imidazole, pH 7.4: 3.527 g NaH₂PO₄ x 2 H₂O /1 l, 29.22 g NaCl /l, 0.6808 g Imidazole /500 ml, pH adjusted

NaH₂PO₄ 20 mmol/l, 0.5 mol/l NaCl, 500 mmol/l Imidazole, pH 7.4: 3.527 g NaH₂PO₄ x 2 H₂O /1 l, 29.22 g NaCl /l, 17.02 g Imidazole /500 ml, pH adjusted

SEC

Tris 10 mmol/l, 150 mmol/l NaCl: 1.454 g Tris /1.2 l, 10.5192 g NaCl /1.2 l pH adjusted

HiTrap Heparin

10 mmol/l NaH₂PO₄, pH 7: 1.7636 g NaH₂PO₄ x 2 H₂O /1 l, pH adjusted

10 mmol/l NaH₂PO₄, 2 mol/l NaCl, pH 7: 1.7636 g NaH₂PO₄ x 2 H₂O /1 l, 116.88 g NaCl /1 l, pH adjusted

Strep-Tactin

NP buffer: 50 mmol/l NaH₂PO₄, 300 mmol/l NaCl, pH 8: 10.1405 g NaH₂PO₄ x 2 H₂O /1 l, 17.53 g NaCl /l, pH manually adjusted

NPD buffer: 50 mmol/l NaH₂PO₄, 300 mmol/l NaCl, 2.5 mmol/l Desthiobiotin, pH 8: 500 ml NP buffer + 0.27 g Desthiobiotin, pH manually adjusted

10x Wash buffer: 1 mol/l Tris, 1.5 mol/l NaCl, 10 mmol/l EDTA, pH 8: 3.0285 g Tris /25 ml, 2.1915 g NaCl /25 ml, 0.0731 g EDTA /25 ml, pH manually adjusted

10x Elution buffer: 1 mol/l Tris, 1.5 mol/l NaCl, 10 mmol/l EDTA, 25 mmol/l Desthiobiotin, pH 8: 3.0285 g Tris /25 ml, 2.1915 g NaCl /25 ml, 0.0731 g EDTA /25 ml, 0.1339 g Desthiobiotin /25 ml, pH manually adjusted

10x Regeneration buffer: 1 mol/l Tris, 1.5 mol/l NaCl, 10 mmol/l EDTA, 10 mmol/l HABA, pH 8: 3.0285 g Tris /25 ml, 2.1915 g NaCl /25 ml, 0.0731 g EDTA /25 ml, 0.0606 g HABA /25 ml, pH manually adjusted

2.2.7. Solutions for bacmid isolation

Solution I: 25 mmol/l Tris-HCl and 10 mmol/l EDTA in dH₂O, pH 8.0

Solution II: 0.4 g NaOH or 2 ml 5 mol/l NaOH, 5 ml 10 % SDS, 45 ml dH₂O

Solution III: 58.9 g potassium acetate, 23 ml glacial acetic acid, dH₂O up to 200 ml

3M Sodium acetate: 20.4 g sodium acetate x 3 H₂O dissolving in 30 ml H₂O, 5.7 ml glacial acetic acid, dH₂O up to 50 ml, autoclaved

2.2.8. Buffers for FLAG-tag purification

Washing buffer (50 mmol/l Tris, 300 mmol/l NaCl, pH 7.5, 0.1 % Triton): 12.12 g Tris, 35.04 g NaCl, 10 ml 20 % Triton solution, dH₂O up to 2 l, pH with HCl adjusted

Elution buffer: 0.1 mg/ml DDDDK-tag peptide in Washing buffer

Regeneration buffer (0.17 mol/l Glycine, pH 2.3): 12.7619 mg Glycine in 100ml dH₂O, pH adjusted with HCl

20 % [v/v] Triton X -100 solution: 20 ml TritonX-100 20 ml, dH₂O up to 100 ml

2.2.9. Buffer for purification of His-tagged proteins using nickel MNPs

5x T-buffer: 100 mmol/l Tris-HCl, 2.5 mol/l NaCl, pH 7.5 manually adjusted

NaPO₄ wash buffer (20 mmol/l NaPO₄, 0.5 mol/l NaCl, 20 mmol/l imidazole, pH 7: 0.1622 g NaH₂PO₄ x 2H₂O, 1.1688 g NaCl, 0.054464 g imidazole, 40 ml MilliQ water

NaPO₄ elution buffer (500 mmol/l NaPO₄, 0.5 mol/l NaCl, 20 mmol/l imidazole, pH 7: 4.05618 g NaH₂PO₄ x 2H₂O, 1.1688 g NaCl, 0.054464 g imidazole, 40 ml MilliQ water

Wash T-buffer (20 mmol/l Tris-HCl, 0.5 mol/l NaCl, 20 mmol/l imidazole, pH 7.5): 0.03404 g imidazole, 5 ml 5x T-buffer, 20 ml MilliQ water

1 Elution T-buffer (300 mmol/l Tris-HCl, 0.5 mol/l NaCl, 20 mmol/l imidazole, pH 7.5): 0.5106 g imidazole, 5 ml 5x T-buffer, 20 ml MilliQ water

2 Elution T-buffer (1 mol/l Tris-HCl, 0.5 mol/l NaCl, 20 mmol/l imidazole, pH 7.5): 0.3404 g imidazole, 1 ml 5x T-buffer, 4 ml MilliQ water

MagneHis Wash buffer (100 mmol/l HEPES, 10 mmol/l imidazole, pH 7.5): 9.966 ml 100 mmol/l HEPES solution, 33.33 µl 3 mol/l imidazole solution

MagneHis elution buffer (100 mmol/l HEPES, 500 mmol/l imidazole, pH 7.5): 8.33 ml 100 mmol/l HEPES solution, 1.66 ml 3 mol/l imidazole solution

2.2.10. Other Buffer and solutions

10xTBS (pH 7.6) (200 mmol/l Tris-HCl, 1.34 mol/l NaCl): 80 g NaCl, 24.2 g Tris, conc. HCl to pH 7.6, demineralized water up to 1 l

1x TBS (pH 7.6) (200 mmol/l Tris-HCl, 1.34 mol/l NaCl): 10 ml 10x TBS, deionised water 90 ml

10x PBS (pH 7.4): 80 g NaCl, 2 g KCl, 11.5 Na₂HPO₄ or 29 g Na₂HPO₄*12 H₂O, 2 g KH₂PO₄, deionised water up to 1 l

1x PBS (pH 7.4): 10 ml 10x PBS, 90 ml deionised water

0.25 mol/l Tris-HCl (pH 6.8): 3.03 g Tris, 80 ml deionised water, pH adjusted to 6.8 with HCl, ad dem. water to 100 ml

TBS (pH7.6), 0.1 % IGEPAC®CA-630 (newer NP40) + PI (fat body lysis buffer): 50 ml 10x TBS, 0.5 ml IGEPAC®CA-630, 1 tablet cComplete Mini EDTA free protease inhibitor version 09, ad MilliQ to 500 ml

60 % Sucrose solution: 60 g Sucrose in 100 ml filtered PBS (pH 7.4)

50 % Sucrose solution: 25 ml 60 % Sucrose solution, 5 ml filtered PBS (pH 7.4)

40 % Sucrose solution: 20 ml 60 % Sucrose solution, 10 ml filtered PBS (pH 7.4)

30 % Sucrose solution: 15 ml 60 % Sucrose solution, 15 ml filtered PBS (pH 7.4)

20 % Sucrose solution: 10 ml 60 % Sucrose solution, 20 ml filtered PBS (pH 7.4)

TMBZ solution: 10 mg TMBZ, 1 ml DMSO

TEM working solution: 20 µl TMBZ solution, 0.5 µl 30 % H₂O₂, 1 ml acetic buffer

2.3. Restriction enzymes, polymerases and ligase

GoTaq® Green Master Mix (Promega, Tokyo, Japan), Thunderbird® SYBR® qPCR Mix (TOYOBO, Osaka, Japan)

2.4. Primer

Bacmid:

Forward primer M13Bac F (Fasmac, Kanagawa, Japan),

Reverse primer M13Bac R (Fasmac, Kanagawa, Japan)

qPCR Baculo virus:

Bm ie-1 Forward (Fasmac, Kanagawa, Japan) CCCGTAACGGACCTTGTGCTT

Bm ie-1 Reverse (Fasmac, Kanagawa, Japan) TTATCGAGATTTATTTACATAACAACAG

2.5. Kits

BioRad Protein-Assay (BioRad, Hercules, CA, USA), High Pure Viral Nucleic Acid Kit (Roche), Immobilon™ Western Chemifluorescence HRP Substrate (Merck Millipore, Tokyo, Japan), Pierce™ BCA Protein Assay Kit (Thermo Scientific, Waltham, USA), Qubit® dsDNA BR Assay Kit (Thermo Scientific, Waltham, USA),

2.6. Recombinant proteins

2.6.1. Recombinant *Bombyx mori* nucleopolyhedrovirus (BmNPV) bacmid preparation for SpCaVp1 and EDIII

The DNA fragment of the Norovirus VP1 was sub-cloned to pFastBac-SpyCatcher plasmid (Xu et al., 2019, under revision) from an available recombinant *Autographa californica* nucleopolyhedrovirus (AcMNPV), provided from Dr. Tian-Cheng Li (Department of Virology 2, National Institute of Infectious Diseases, Japan). The DNA sequence was then coding also for poly-tags (His-Strep-TEV-NoroVP1-SpyCatcher, MHHHHHHHHGGGSAWSHPQFEKGGGSENLYFQGGSSGSGGSGKMASNDANPSDGSAAANLVPEVNN EVMALPVPVGAIAAPVAGQQNVIDPWIRNNFVQAPGGFTVSPRNAPGEILWSAPLGPLNPLYSLHARMYNGYAGGFVQVILAGNAFTAGKIIFAAVPPNFPTEGLSPSQVTMFPHIIVDVRQLEPVLIPDVRNN FYHYNQSNSTIKLIAMLYTPLRANNAGEDVFTVSCRVLTRPSPDFDFIFLVPPTVESRTKPFTVPILTVEEM TNSRFPIPLEKLTGPSSAFVVQPQNGRCTTDGVLLGTTQLSPVNICTFRGDVTHIAGSRNYTMNLASLN WNNYDPTTEEIPAPLGTDFVGVKIQGVLTQTTKGDGSTRGHKATVYTGSAFPTPKLGSVQFSTDTENDFETHQDTKFTPVGVVIQDGGTTHRNEPQQWVLPSSYGRDVPNVHLAPAVAPTFFPGEQLLFFRSTMPGCSGYPNMDLDCLLPQEWVQHFYQEAAPAQSDVALLRFVNPDTGRVLFECKLHKSGYVTVAHGTQHDLVIPPNG YFRFDSWVNQFYTLAPMGNGTGRRRALGGGSVTLSGLSGEQGPSGDMTTEEDSATHIKFSKRDEDGR ELAGATMELRDSSGKTISTWISDGHVKDFYLYPGKYTFVETAAPDGYEVATAITFTVNEQQQVTVNGEAT KGDAHT) and consists of the a His-, StrepTag II-, tobacco etch virus (TEV) protease cleavage site and a SpyCatcher. The resulting plasmid was designated as pFastBac-HSSc-SpCaVP1 for expressing the SpCaVP1 protein.

The codon optimized DNA fragment of the EDIII was synthesised (Genewiz, Suzhou, China) based on the sequence of Dengue virus 1 (GenBank No. KM204119). The EDIII sequence was then amplified using primes (1DIII-Fw agttatggtatgtgcaccgg; 1DIII-Rv gcccaaatagccattcgcc) and further ligated to the pFastBac-cSpyTag (Xu et al., 2019, under revision). The DNA sequence was then coding also for poly-tags (EDIII-cSpyTag-TEV-Strep-Flag, MRSYVMCTGSFKLEKEVAETQHGTVLVQVKYEGTDAPCKIPFSTQDEKGVTONGLITANPIVTDKEKPV NIEAEPFGEYSYIVVGAGEKALKLSWFKKGGSSIGKMLEATARGARRMAILGPSQPGSSGSGGSGVPTIVM VDAYKRYKGGGSENLYFQGGGSAWSHPQFEKGGGSDYKDDDDK) and consists of the a SpyTag, tobacco etch virus (TEV) protease cleavage site, StrepTag and a FlagTag. The resulting plasmid was designated as pFastBac-FSS-EDIII for expressing the EDIII protein. Both were constructed

and then utilized for making of a recombinant BmNPV bacmid. Subsequently, the recombination baculovirus were generated in the cultured silkworm Bm5 cells according to our previous reports [107]. The cell culture supernatant was collected and used for serial infections to obtain high titer virus stocks, which were employed to infect silkworm larvae.

2.7. Antibodies

Anti-Gag polyclonal (Laboratory self-made from mouse serum), Anti c-Myc Monoclonal (Wako Pure Chemical Industries, Osaka, Japan), Anti-Flag monoclonal M185-3L (MBL, Nagoya, Japan), Anti-DDDDK-tag mAb polyclonal (MBL, Nagoya, Japan), Anti-IgG (H+L chain) (mouse) pAb HRP (Medical & Biological Laboratories, Nagoya, Japan), Anti-mouse IgG HRP-linked Antibody (Cell Signalling Technology Japan, Tokyo, Japan)

2.8. Other reagents and materials

Absorbant Paper CB-20A (Atto, Tokyo, Japan), Ammonium Peroxodisulfate (Nacalai Tesque, Tokyo, Japan), Desthiobiotin (IBA Lifesciences, Göttingen, Germany), BioRad Protein-Assay (BioRad, Hercules, Ca, USA), cOmplete Mini EDTA free Version protease inhibitor (Roche, Tokyo, Japan), DDDDDK-tag peptide (Medical & Biological Laboratories, Nagoya, Japan), DDDDDK-tagged Protein Purification gel (Medical & Biological Laboratories, Nagoya, Japan), Disodium Hydrogen phosphate Dodecahydrate (Wako Pure Chemical Industries, Osaka, Japan), Dimethyl sulfoxide (Wako Pure Chemical Industries, Osaka, Japan), Dithiothreitol (DTT) (Nacalai Tesque, Tokyo, Japan), 1-Ethyl-3(3-dimethylaminopropyl)carbodiimide (EDC) (Sigma Aldrich, Tokyo, Japan), Ethyl bromide Solution (Nippon Gene, Toyama, Japan), Glycine (Wako Pure Chemical Industries, Osaka, Japan), 30 % Hydrogen peroxide (Wako Pure Chemical Industries, Osaka, Japan), 2-(4-Hydroxyphenylazo)benzoic acid (HABA) (Sigma Aldrich, Tokyo, Japan), HEPES (Dojindo molecular technologies, Kumamoto, Japan), IGEPAC[®]CA-630 (MP Biomedicals, Tokyo, Japan), Immobilon[™]- P (Merck Millipore, Tokyo, Japan), MOPS (Dojindo molecular technologies, Kumamoto, Japan), MagneHis[™] (Promega, Tokyo, Japan), Nexus Western Precise Marker Westernblot (Cosmo Bio, Tokyo, Japan), N-hydroxy succinimide (NHS) (Sigma Aldrich, Tokyo, Japan), 3,3',5,5'-Tetramethylbenzidine (TMBZ) (Dojindo molecular technologies, Kumamoto, Japan), N,N,N',N'- Tetramethylethylenediamine (TEMED) (Nacalai Tesque, Tokyo, Japan), 1-phenyl-2-thiourea (Wako Pure Chemical Industries, Osaka, Japan), Phosphotungstic acid (TAAB Laboratories Equipment Ltd, Aldermaston, United Kingdom), Pierce Glycoprotein Staining Kit (Thermo Scientific, Waltham, USA), PM 1700 Excel

Band Marker (Smobio, Tokyo, Japan), Polyethylene glycol 6000 (Wako Pure Chemical Industries, Osaka, Japan), Polyethylenimine solution average Mw 7500 kDa (Sigma Aldrich, Tokyo, Japan), Precision Plus Protein Dual Color Standards (BioRad, Hercules, CA, USA), Protein MW Marker (Broad)(TaKaRa, Kusatsu, Japan), Protein MW Marker (Low)(TaKaRa, Kusatsu, Japan), Silkmate S2 (Nosan, Yokohama, Japan), Skim Milk powder (Wako Pure Chemical Industries, Osaka, Japan), Sodium chloride (Wako Pure Chemical Industries, Osaka, Japan), Sodium Hydroxide (Wako Pure Chemical Industries, Osaka, Japan), Sucrose (Wako Pure Chemical Industries, Osaka, Japan), Sulfuric acid (Wako Pure Chemical Industries, Osaka, Japan), Tris (hydroxymethyl) aminomethane (Star Chemical, Nanjing, China), Western Marker I WN 1000 YesBlot (Smobio, Tokyo, Japan), XL-Western Marker (Apro Science, Naruto, Japan)

2.9. Equipment

2.9.1. Columns

HiTrap DEAE Sepharose 5 ml (GE Healthcare, Tokyo, Japan)
HiTrap Butyl FF 5 ml (GE Healthcare, Tokyo, Japan)
HiTrap Phenyl FF 5 ml (GE Healthcare, Tokyo, Japan)
HiTrap Blue HP 1 ml (GE Healthcare, Tokyo, Japan)
HiTrap Q HP 5 ml (GE Healthcare, Tokyo, Japan)
Bio-Scale Mini CHT Type II Cartridge 5 ml (BioRad, Hercules, CA, USA)
HiTrap HP 5 ml (GE Healthcare, Tokyo, Japan)
HiTrap Heparin HP 5 ml (GE Healthcare, Tokyo, Japan)
HiTrap CptoCore 700 1 ml (GE Healthcare, Tokyo, Japan)
HiScreen CptoCore 400 4.7 ml (GE Healthcare, Tokyo, Japan)
Superdex Sephacryl S-200 120 ml (GE Healthcare, Tokyo, Japan)
Strep-Tactin® Superflow Plus Cartridge 1 ml (Qiagen, Tokyo, Japan)

2.9.2. Other Equipment

Amicon Ultra-0.5 ml 30 kDa centrifugal filter unit (Merck Millipore, Tokyo, Japan), Amicon Ultra-15ml 3 kDa centrifugal filter unit (Merck Millipore, Tokyo, Japan), Acrodis PSF Syringe with Versapor® Filter 10 µm (Pall Life Science, Tokyo, Japan), Advantec 0.8 filters (Advantec, Tokyo, Japan), Analytical Balances ML 204T (Mettler Toledo, Tokyo, Japan), Apeos Port IV (Fuji Xerox, Tokyo, Japan) (for SDS gels), Auto-Injector Valve AVR7-3 (BioRad, Hercules, CA, USA),

BioLogic DualFlow (BioRad, Hercules, CA, USA), BioFrac Fraction collector (BioRad, Hercules, CA, USA), Bio Shaker (Takasaki Scientific Instruments corp., Tokyo, Japan), Bio Shaker BR-3000LE (Taitec, Koshigaya, Japan), Chromato Chamber MC8EF (Nihon Freezer, Tokyo, Japan), Collection Plate 500 μ l deep well (GE Healthcare, Tokyo, Japan), Conductivity Meter RG.12 (Organo, Tokyo, Japan), DeltaMixer Se-08 (Taitec, Koshigaya, Japan), DryThermoUnit DTU-1CN (Taitec, Koshigaya, Japan), Eycla Micro Tube Pump MP-3 (Tokyo Rikakikai Co., Tokyo, Japan), Growth chamber MLR-351H (Sanyo, Osaka, Japan), himac CS 120 GX II Micro Ultracentrifuge (Hitachi, Tokyo, Japan), Infinite M200 (Tecan, Kawasaki, Japan), Infinite M Plex (Tecan, Kawasaki, Japan), Ion exchanger RT-523J0 (Organo, Tokyo, Japan), Magnetic Stirrer Rexim RS-1AN (AS One, Osaka, Japan), Microplate Reader Model 680 (BioRad, Hercules, CA, USA), Micro refrigerated centrifuge Kubota 3700 (Kubota, Tokyo, Japan), Millex – AA 0.8 μ m (Merck Millipore, Tokyo, Japan), Millex – HA 0.45 μ m (Merck Millipore, Tokyo, Japan), Millex – SV 5 μ m (Merck Millipore, Tokyo, Japan), Minisart NML Hydrophilie (Sartorius, Goettingen, Germany), Mupid-2x (Advance, Tokyo, Japan), Nanodrop (Thermo Scientific, Waltham, USA), PCR TP-240 (TaKaRa, Kusatsu, Japan), Pharos FX Plus (BioRad, Hercules, CA, USA), PowerPac Basic (BioRad, Hercules, CA, USA), Pureelite PRA-0015-0V0 (Organo, Tokyo, Japan), Puric-ZII (Organo, Tokyo, Japan), Japan PreDicator™ ALEX Screenign 20 μ l (GE Healthcare, Tokyo, Japan), JEM 1400-Plus (JEOL, Tokyo, Japan), Prowipe (elleair, Tokyo, Japan), SevenCompact pH/Ion (Mettler Toledo, Tokyo, Japan), SDS-PAGE chamber (BioRad, Hercules, CA, USA), Shake-XR invitro Shaker (Taitec, Koshigaya, Japan), Trans Blot SD Semi-Dry Transfer Cell (BioRad, Hercules, CA, USA), Wave-SI invitro Shaker (Taitec, Koshigaya, Japan), Whatman UniVac 3 Vacuum Manifold (now GE Healthcare, Tokyo, Japan), Versa Doc (BioRad, Hercules, CA, USA), Vibra BG-300 (Shinko, Nagano, Japan), Vibra Cell VC 130PB (Sonics & Materials Inc., CT, Newtown, USA), Vortex Genie 2 (Scientific Industries, NY, New York, USA), Zetasizer Nano-ZS ZEN3600 (Malvern Instrumental, Tokyo, Japan)

2.10. Software

BioLogic DualFlow V. 5.30 Build 6 (BioRad, Hercules, CA, USA), i-control 1.6 firmware V2.11_04/08 (Tecan, Kawasaki, Japan), Tecan i-control 2.0.10.0 (Tecan, Kawasaki, Japan), ImageJ 1.51j8 (Wayne Rasband, National Institute of health, USA), Microplate Manager V. 5.2 Build 103 (BioRad, Hercules, CA, USA), Microsoft Office Professional Plus 2019 (Microsoft Cooperation, Redmond, WA, USA), Quantity One 4.6.5 Build 094 (BioRad, Hercules, CA, USA),

TEM center ver. 1.5.5.4011 (JEOL, Tokyo, Japan), Zetasizer v 7.12 (Malvern Instrumental, Tokyo, Japan)

2.11. Methods of biotechnology

2.11.1. Caring of the silkworms

Fifth instar larvae of the silkworms were stored in plastic boxes with holes for fresh air. The boxes had different sizes, depending on the number of silkworms. The silkworms in the boxes were reared in an incubation cabinet (MLR-351H, Sanyo, Osaka, Japan) at 25°C and at a humidity from 52 %. The boxes were regularly cleaned with Ethanol 70 %, new tissue paper (elleair, Tokyo, Japan) and new artificial food (Silkmate S2, Nosan, Yokohama, Japan) was also added.

2.11.2. Infection of the silkworm

On the second day of 5th instar larvae, the silkworm larvae were injected with 50 µl of a PBS solution containing 250 µl/ml recombinant baculovirus (for mCherry) using a 1 ml syringe (26G×1/2, 0.45×13 mm). For the other recombinant viruses, a dilution of 10 µl/ml or 50 µl/ml PBS of haemolymph or virus solution was used. They were injected from the side, targeting their stomach under the skin, without hurting their inner organ.

2.11.3. Harvesting of the haemolymph

Four- or five-days post-injection (dpi), the haemolymph was collected with 50 µl of 200 mmol/l 1-phenyl-2-thiourea (1522 µg solved in 5 ml 99,99 % Ethanol) per silkworm as preservative and stored at -80°C until use. For harvesting, one of the abdominal legs was cut with a scissor and the bleeding haemolymph were collected in a vessel. After the GFP project, only 20 µl preservative per silkworm was used.

2.11.4. Harvesting of the fat body

For harvesting the fat body, the silkworm was dissected. It was sliced and the skin stretched. All internal organs were disposed and the fat body was scraped of the skin. To the collected fat body was 1 ml TBS + 0.1 % Triton X-200 per 100 mg fat body given. This solution was sonicated on ice for at least 5 min using following protocol. 20 s sonication and 10 s a break. These steps were repeated for 5 min. After this treatment the solution was centrifuged 8000 × g, 10 min at 4°C. The supernatant was separated from the pellet.

Derivate from this, for the norovirus project the fat body was handled with a different protocol. The fat body was collected in 5 ml Lysis buffer (0.2 mol/l Tris-HCl, pH 7.6, 0.1 % IGEPAC[®], protease inhibitor) per silkworm. This solution was as followed sonicated; 10 s. sonication with an amplitude of 60–80 and 30 s on ice. This cycle was 20-times repeated. The sonicated solution was 1 h on ice incubated and centrifuged at 4°C, 8000 × g, 15 min. The supernatant was filtered with a 0.2 µm filter and stored at -80°C.

2.11.5. Polymerase chain reaction (PCR)

The conditions of the PCR were set regarding the company manuals to the corresponding used polymerases. Used thermocycler was PCR TP-240 (TaKaRa, Kusatsu, Japan). The used GoTaq[®] Green Master Mix contains 400 µM dNTP, 3 mM MgCl₂, a Taq DNA-polymerase and a blue and yellow stain. The used primer stock solution had a concentration of 10 µM.

The content of the protocol was general like this:

2.5 µl GoTaq Green Master Mix, 0.25 µl Primer forward, 0.25 µl Primer reverse, 1 µl dH₂O and 1 µl sample. The double amount was also used.

The PCR program for the GoTaq-Polymerase was like the following schema. 95°C for 2 min; 30 cycles: 98°C for 30 s, Primer T_m-5°C (55°C) for 30 s, 72°C for 1 min/Kb (2 min); 72°C for 5 min; storage at 4°C.

2.11.6. Quantitative PCR

The conditions of the qPCR were set regarding the company manuals to the corresponding used polymerases. Used thermocycler was qPCR Mx3000P (Stratagene La Jolla, CA, USA).

The used Thunderbird[®] SYBR[®] qPCR Mix contains dNTP, MgCl₂ and a rTaq DNA-polymerase. The used primer stock solution had a concentration of 10 µM. The content of the was general like this:

10 µl Thunderbird[®] SYBR[®] qPCR Mix, 1 µl Primer forward, 1 µl Primer reverse, 5 µl dH₂O and 3 µl sample. The PCR program for the SYBR[®]-Polymerase was like the following 2-step schema. 95°C for 1 min; 60 cycles: 95°C for 15 s, 60°C for 1 min. 3 standards with different known concentrations were carried with and used for calibration.

The analysis was done from the associated program Mx Pro 3000.

For baculovirus concentration determination the standards contained DNA from known baculovirus titer (pfu/ml).

2.11.7. Pre-treatment centrifugation

The centrifugations were done using a Kubota 3700 (Kubota, Tokyo, Japan) equipped with an AF-2724A or AF-5004CH rotor. The setups were grouped in high, medium and low centrifugal forces. High centrifugation forces were: 20600 × g 360 min, 20400 × g, 60 min; 17800 × g, 10 min and 10000 × g, 30 min. Medium centrifugation forces were: 6000 × g, 30 min; 5000 × g, 15 min; 3000 × g, 5 min and 2000 × g, 10 min. Low centrifugation forces were: 1000 × g, 5 min; 500 × g, 5 min; 100 × g, 20 min and 100 × g, 5 min, 22.6 × g 5 min and 3.6 × g 20 min.

2.11.8. Pre-treatment precipitation

The setups were grouped in several main precipitation protocols as followed. If necessary, ultrapure water (named also MilliQ) (Puric-ZII, Organo, Tokyo, Japan) was added for concentration adjustments. NaCl was in concentrations of 2 mol/l, 3 mol/l, 4 mol/l or 5 mol/l added and samples were incubated 30 min on ice. After that they were centrifuged at 5000 × g for 10 min. (NH₄)₂SO₄ precipitation was done with a concentration of 0.34 mol/l, 1 mol/l, 2 mol/l, 3 mol/l, 4 mol/l and 5 mol/l. The incubation was done for 30 min on ice, except for 0.34 mol/l which was for 4 h. After that, the samples were centrifuged at 5000 × g for 20 min. PEG 6000 had concentrations of 2.5 %, 5 %, 10 %, 20 %, 25 % and 30 % (w/v), and was incubated on ice for 60 min, except for 5 % with 17 h on ice. The centrifugation was done at 4200 × g for 20 min. Polyethyleneimine (PEI) was used with the final concentrations of 0.1 %, 0.3 % or 0.5 % (w/v) and together with the NaCl concentrations of 0.1 mol/l, 0.5 mol/l or 1 mol/l. The solution was mixed for 5 min and then incubated on ice for 30 min. The centrifugation was done at 2300 × g for 5 min. For Dithiothreitol (DTT) precipitation 300 μl + 30 μl 0.5 mol/l DTT solution [108] was mixed, 60 min on ice incubated and centrifuged at 10000 × g, 20 min. A second try was divergent with 60 min incubation at 37°C and 13000 × g, 40 min. The polyvinyl pyrrolidone was added to 3 % (w/v), 4 h stirred and then centrifuged at 17800 × g, 10 min. The pellet was discarded.

2.11.9. Thermal treatment of haemolymph

The thermal treatment is based on publications which shows the significant reduction of host cell proteins if the target protein is heat stable [68,69]. The screening for RSV-LPs was done with 30 min heating, followed by 6000 x g, 10 min. The resulting supernatant was used for the next higher temperature. Two approaches were done, 60°C and 70°C steps and, 30°C, 40°C and 50°C steps.

mCherry samples were treated for 30 min at 50°C, 60°C and 70°C or 70°C for 20 min. After thermal treatment the solution was once again centrifuged at 17800 x g for 10 min. Final treatment was 70°C for 20 min with the followed centrifugation.

The SpCaVP1, EDIII and their linked coexpression were in the same way as the mCherry samples handled.

2.11.10. Strep tag affinity purification

The Strep tag purification for mCherry was done in two different ways using the StrepTactin column. The first attempt was using the Dual Flow (BioRad, Hercules, CA, USA) as mentioned later in Liquid chromatography (chapter 2.11.11). The used buffers were the NP buffer as Load and wash buffer and the NPD buffer was used for the elution.

Divergent from this, the purification using the Strep-Tactin column was also done using a manual peristaltic pump at a low flow rate (0.5 ml/min). The sample was centrifuged at 17800 x g, 5 min at 4°C and filtered through a 0.8 µm filter before the chromatography. The column was at first regenerated with the regeneration buffer and then equilibrated with the wash buffer. The sample could be diluted (e.g. 1-part sample + 4 parts of wash buffer) and then loaded. After loading, the column was again washed with the wash buffer. The elution fraction which had a reddish/purple colour was separately caught. All fractions were investigated if they still emitted red fluorescence.

2.11.11. Fast performance liquid chromatography (FPLC)

The chromatography was done/carried out using the BioLogic DualFlow (BioRad, Hercules, CA, USA) with the associated software BioLogic DualFlow V. 5.30 Build 6 (BioRad, Hercules, CA, USA) and equipped with a BioFrac Fraction collector (BioRad, Hercules, CA, USA) and an Auto-Injector Valve AVR7-3 (BioRad, Hercules, CA, USA). Several different columns were used and the chromatography protocol varied and step or linear gradients were done.

Fractions were collected in different volumes, with ranges from 1 to 5 ml. Generally, after the column was equilibrated with the starting buffer, the sample was loaded and washed with at least 5 column volumes (CVs). For a linear gradient elution, the elution was done with at least 10 CVs with an increasing elution buffer share. Before reequilibration, the column was washed with at least 5 CVs of elution buffer. The steps of step gradients were at least 5 CVs and were individually determined. The standard flow rate was 2 ml/min and for the size exclusion chromatography (SEC) 0.5 ml/min if not mentioned otherwise. The samples were at least filtered through 0.8 μm filters and if necessary adjusted to the binding buffer before loading to the column. If necessary, samples from a previous chromatography step could be also adjusted to the next binding buffer and also 0.45 μm filtered. The individual protocols are mentioned in the corresponding figure legends.

2.11.12. Ultrafiltration

If necessary, samples were concentrated using ultrafiltration with Amicon 30K or 10K (Merck Millipore, Tokyo, Japan) with a defined cut-off of 30 or 10 kDa. Before use, the filters were cleaned from the glycine storage buffer with 500 μl water, 14000 \times g for 20 min. The concentration factor varied, but was mostly around 23 (14000 \times g, 10 min) or 32 (14000 \times g, 30 min). This was also done in a bigger scale using an Amicon 3K (Merck Millipore, Tokyo, Japan) with 15 ml capacity and a defined cut-off of 3 kDa with a centrifugation speed of 5000 \times g, whereby the duration varied.

2.11.13. Sodium dodecyl sulphate – polyacrylamide gel electrophoresis (SDS-PAGE)

Samples were diluted with an equal amount of sample buffer (0.125 mol/l Tris-HCl, 4 % SDS, 20 % Glycerol, 0.01 % Mercaptoethanol, 0.15 mmol/l Bromophenol blue), mixed and were heated at 95°C for 5 min for staining. The classification of the size was done mainly with the also carried standard PM1700 ExcelBand (Smobio, Tokyo, Japan). The stacking gel was 4 % and in most cases acrylamide gel was 10 %. After running the gel was analysed via fluorescence imaging or a Coomassie staining. The constant voltage was set at 90 V for the stacking gel and 120 V for the running gel. Samples were analysed in the following different dilutions, 10 μl sample to 22 μl or 8 μl sample to 24 μl for Coomassie brilliant blue (CBB) staining and 12 μl sample to 24 μl or 10 μl sample to 24 μl for fluorescence imaging. Each time 15 μl of this dilution was loaded on the gel lane.

2.11.14. Coomassie-Brilliant-Blue staining (CBB staining)

For the Coomassie staining the gel was put in a box with staining solution and was incubated at least for 3 h on a shaker. The unstaining was done by changing to a used decolouring solution and incubation at least for 40 min on the shaker. After that the solution was changed to an unused decolouring solution and incubated at least for 3 h on a shaker. The finished gel was copied with a scanner.

Another CBB staining was tested with G-250 instead of R-250. This staining was then chosen, because it is more effective and less hazardous to health. For this protocol the gel was in the staining solution heated until boiling and then stained for at least 2 h. If the staining was not sufficient, a second boiling could be done. The destaining was done with deionised water until sufficient decolouration.

2.11.15. Relative Quantification from proteins after SDS-PAGE

For the relative Quantification of the main impurities in the haemolymph ImageJ 1.51j8 (Wayne Rasband, National Institute of Health, USA) was used. First, the program plotted the intensity of the images of the SDS-PAGE's automatically and the integration of the area under the curve of the signals was then done manually. It was focused on the area of the main impurities, around 20-30 and 60-80 kDa, and they were set in relation to each other. This was used as a more objective parameter to compare the purity before and after a specific kind of treatment compared to the visual confirmation.

For the relative recovery determination of the mCherry the same procedure was done, but only for the mCherry bands. With samples of known mCherry concentration (127.2, 63.6 and 31.8 $\mu\text{g/ml}$), a calibration was done. Furthermore, for the purity after the final purification step the mCherry band was set in relation to all bands. This was used as a more objective parameter to compare the recovery during and the purity after the purification protocol instead of the naked eye.

2.11.16. Fluorescence Imaging

For the fluorescence imaging, the samples were not heat denatured before the SDS-PAGE and images were taken with the Pharos FX Plus (BioRad, Hercules, CA, USA). The GFP- βGnT2 was detected using the FITC set up (Ex. 395 nm, Em. 509 nm). The mCherry was detected using the Texas red set up (Ex. 532 nm, Em. 640 nm).

2.11.17. Western Blotting

For western blotting, the proteins were subjected to SDS-PAGE and transferred to polyvinylidene fluoride (PVDF) (Immobilon-P, Merck, Tokyo, Japan) membranes using the Trans-Blot SD Semi Dry Transfer Cell (Bio-Rad, Tokyo, Japan). Blocking was performed for at least 1 h with 15 ml 5 % skim milk in TBS containing 0.1 % Tween 20. After three 5-min washes with TBS and incubation for at least 2 h with mouse anti-Strep-tag antibody (1:10000, QIAGEN, Tokyo, Japan), anti-gag polyclonal antibody (Self-made from mouse serum), anti-his antibody (MBL, Nagoya, Japan), the blots were again washed three times for 5 min each time with TBS and incubated with a secondary antibody (goat anti-mouse IgG-horseradish peroxidase (HRP), 1:10000, MBL, Nagoya, Japan) for at least 1 h. Immunoreactive bands were visualized using the Immobilon ECL Ultra Western HRP Substrate (Merck K. K., Tokyo, Japan) on the Versa-Doc 4000 MP (BioRad, Hercules, CA, USA).

2.11.18. Protein Assay using Bradford principle

For the determination of the overall protein concentration BioRad Protein-Assay (BioRad, Hercules, CA, USA) according to the manual was used. Briefly, this Kit use the colour reaction between Coomassie® Brilliant Blue G-250 and proteins which result in a different absorption maximum to determinate the concentration. The dye binds mainly to basic or aromatic amino acids residues, especially to arginine, and the maximum shifts from 465 nm to 595 nm in an acidic solution by binding to proteins. On a microtiter plate 10 µl sample or standard was mixed with 200 µl diluted and filtered (Whatman #1 filter or similar) dye reagent (1 part to 4 parts MilliQ water). Incubation was at RT for at least 5 min, but not longer than 1 hour. The absorbance was measured at 595 nm. The analysis was done with at least three also measured standards of known concentrations. The calculations were manually done with the program Excel (Office 2016 and Office 2019).

2.11.19. Protein Assay using Bichinonic acid (BCA)

For the determination of the overall protein concentration the Kit Pierce™ BCA Protein Assay Kit (Thermo Scientific, Waltham, USA) according to the manual was used. Briefly this Kit use the reaction between Cu^{2+} and proteins which result in Cu^{1+} . Cu^{1+} forms with BCA a 1:2 complex which results in a purple colour which can be measured at 562 nm (range 540 to 590 nm) to determinate the concentration. On a microtiter plate 25 µl or 10 µl sample or standard was mixed with 200 µl working reagent. Mixing for 5 min and incubation was at 37°C, 30 min.

The absorbance was measured at 570 nm. The analysis was done with nine also measured standards of known concentrations. The calculations were manually done with the program Excel (Office 2016 and Office 2019).

2.11.20. DNA Assay

For the determination of the DNA concentration the Kit Qubit® dsDNA BR Assay Kit (Thermo Scientific, Waltham, USA) according to the manual was used. Briefly this Kit use a fluorescence dye which bind specifically at non denatured DNA. The florescence was induced with a wavelength of 485 nm and the emission was at 530 nm. Deviant from the manual the Assay was done on a 96 well microtiter plate and the fluorescence measured on a microplate reader Infinite M Plex (Tecan, Kawasaki, Japan). 20 µl standard or up to 20 µl sample was mixed with working reagent up to 200 µl, mixed for 2-3 seconds and incubated at RT for 2 min before measuring. The analysis was done multiple times and with three also measured standards of known concentrations. The calculations were manually done with the program Excel (Office 2016).

2.12. Other analytical methods

2.12.1. Transmission electron microscopy (TEM)

The samples were one day prior prepared. A metal plate was covered with Parafilm®. On this were 20-30 µl sample dropped. On another place were 20 µl 2% Phosphotungstic acid (TAAB Laboratories Equipment Ltd, Aldermaston, United Kingdom) and 3 times 50 µl filtered and sterilized PBS dropped. The grid was with the intended side dropped on the sample drop for around 30 s. After that for around 30 s on the PTA drop. The washing was done with at least 10 s on each PBS drop. The grid was then turned and placed on the plate for drying overnight. The TEM images were done with JEM 1400-Plus (JEOL, Tokyo, Japan) and the used software was TEM center ver. 1.5.5.4011 (JEOL, Tokyo, Japan).

Divergent from this, the sample was also two days prior prepared and the washing was done with dripping the washing solution (PBS or MilliQ water) on the grid, which was hold. The grid was then dried over two days.

For the nickel MNPs the protocol was also divergent. In this case the sample was directly applied to the grid and the sample only with a tissue carefully removed without

washing. PTA was as well directly applied to the grid and removed with a tissue. The sample dried then for two days before the TEM imaging.

2.12.2. Dynamic light scattering (DLS)

DLS is a physical method for the determination of the size distribution of small particles in a solution. When light hits small particles, compared to the wavelength of the light, it will be scattered in all directions which when interfering with each other. This phenomenon is called Rayleigh scattering. This also true for macro molecules in a solution. When using a coherent and monochromatic laser, then there will be because of the Brownian motion fluctuations of this interference and these can be analysed concerning the time scale, which gives information about the particle speed. With this the diffusion coefficient can be calculated which allows to use the Einstein relation for the calculation of the hydrodynamic radius.

For the DLS measurement was Zetasizer Nano-ZS ZEN3600 (Malvern Instrumental, Tokyo, Japan) with the associated software Zetasizer (v 7.12) used. For preparation only 700 μl sample was transferred in the sample cell and then measured.

2.12.3. Office processing and analysis

The general calculations and analysis were done with Microsoft Office 2016 or Microsoft Office Professional Plus 2019.

3. Purification investigations from the silkworm haemolymph

3.1. Introduction

This study used the GFPuv- β 1,3-N-acetylglucosaminyltransferase 2 (GFP- β 3GnT2) as a model protein to explore the purification of recombinant proteins from the silkworm haemolymph and to establish a database of the host cell behaviour during the different purification methods. GFP- β 3GnT2 has a molecular mass of approximately 77 kDa and it displays green fluorescence (Ex. 395 nm, Em. 509 nm) which makes it easy to trace and a suitable candidate for a model protein. The aim was to establish an easy upscale-able and industrial usable protocol, by targeting also high purity and yield.

3.2. Specific Material and Methods

3.2.1. GFPuv- β 1,3-N-acetylglucosaminyltransferase 2 (GFP- β 3GnT2)

Haemolymph containing infective recombinant baculovirus for GFPuv- β 1,3-N-acetylglucosaminyltransferase 2 (GFP- β 3GnT2) was received from a previous study [109]. This haemolymph was used for infection of silkworms and new haemolymph was used for further infection cycles. The origin of GFP- β 3GnT2 constructed was separately reported [110]. Very shortly, the human β 3GnT2 was obtained by PCR from cDNA of Quick-Clone™ human fetal brain cDNA (Clontech, Palo Alto, CA, USA). The PCR product was inserted into a modified plasmid containing GFPuv to yield GFPuv- β 3GnT2. This GFPuv- β 3GnT2 fusion fragment was amplified by PCR and was, including new signal sequence, inserted into the entry vector pENTR/D-TOPO (Invitrogen). The resulting plasmid was named pENTR/D/GFPuv- β 3GnT2 and inserted into a pDEST8 donor vector by Gateway Cloning Technology (Invitrogen). Recombinant baculovirus was made according to the manual of the Bac-to-Bac Expression System (Invitrogen). In brief, the recombinant donor vector pDEST/GFPuv- β 3GnT2 was transformed into bacmid containing *Escherichia coli* DB10. Auto-transposition between the bacmid and the recombinant donor vector occurred, and a recombinant bacmid was produced. For virus production the recombinant bacmid was extracted from *E. coli*, transfected into Sf-9 cells and recombinant baculovirus was harvested from the cell culture supernatant.

3.2.2. AIEX chromatography screening

For AIEX material and buffer conditions screening was the PreDicator™ AIEX screening plate (GE Healthcare, Tokyo, Japan) used. Shortly, this are 96-well plates which contain chromatography stationary material and are permeably. The principle is the same as for a chromatography column, but in this case the applied solutions and samples will be incubated and mixed on a micro plate shaker, before the rest will be removed via centrifugation or vacuum. In this case the solutions were removed via a Whatman UniVac 3 vacuum manifold. The protocol was regarding the company. All buffers were applied with 200 µl and the samples with 300 µl, premixed with the corresponding buffer. The ratio was 150 µl sample and 200 µl designated buffer. Incubation time of the sample was 30 to 60 min. Incubation time of all other buffers was 1 min. Divergent from the protocol was at the end a further regeneration step with 3 x 200 µl 1 M NaOH added. The applied samples were before stepwise filtered with 10, 5 and 0.8 µm filters. Four buffers were investigated with a high or low pH (7 or 8) and a low or high buffer salt concentration. Used were sodium phosphate (0.1 or 20 mmol/l), Tris (10 or 100 mmol/l), HEPES (1 or 25 mmol/l) and MOPS (25 or 45 mmol/l). Moreover, PBS was also investigated with a pH of 7 or 8.

3.3. Results and Discussion

3.3.1. Separation by Centrifugation

For the GFP-β3GnT2 purification from the haemolymph several pre-treatments, such

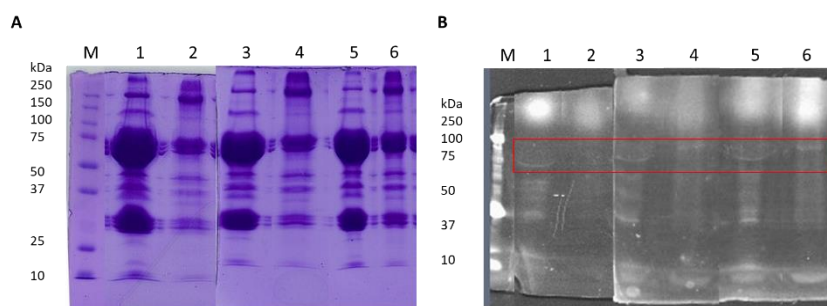


Fig. 1: Example centrifugation set ups for GFP-β3GnT2 (A) Coomassie blue staining SDS-gel and **(B)** fluorescence Images with example set ups for high, medium and low centrifugal forces. On each line 20 µl was loaded. On the SDS-PAGE it was a 1.2 to 10 dilution and on the fluorescence image it was a 1 to 2.5 dilution; Lane 1 and 2: supernatant and pellet 20380 × g, 60 min; Lane 3 and 4: supernatant and pellet 6000 × g, 30 min; Lane 5 and 6: supernatant and pellet 100 × g, 20 min; M is Marker

as centrifugation, precipitation and filtration were investigated to reduce the protein amount before chromatography. The haemolymph was subjected to centrifugation with different centrifugal forces, which were graduated into low, middle and high forces. SDS-PAGE results show that the main impurities at 20–30

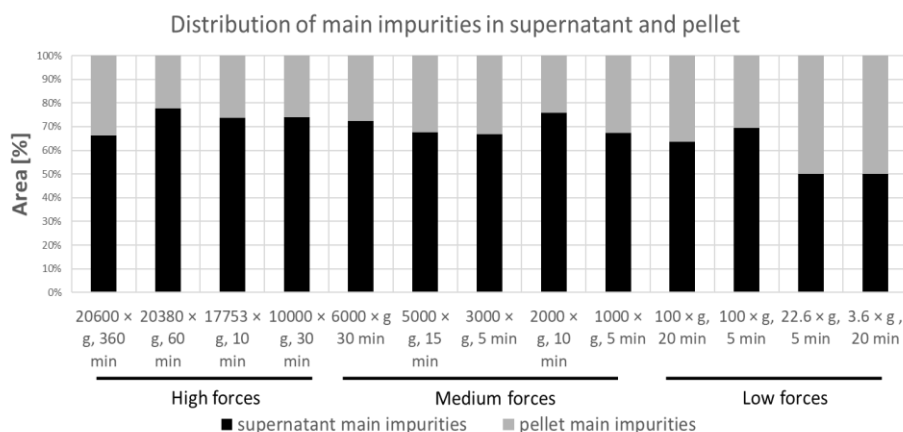


Fig. 2: A graphical overview of the distribution of the 2 main impurities in pellet or supernatant after centrifugation treatment. It's to see that the impurities at 20–30 and 60–80 kDa are mainly in the supernatant after the centrifugation.

and 60–80 kDa are mainly remain in the supernatant (Fig. 1A). Moreover, the fluorescence imaging revealed that the GFP-β3GnT2 is more or less evenly distributed in pellet and supernatant

(Fig. 1B). Using densitometry, the areas of the impurities were presented in proportion to each other which showed that these remain mainly in the supernatant (Fig. 2). This was supported by protein assay, whereby the higher protein amount was detected in the supernatant (data not shown).

For easier handling were the main impurities at 20–30 and 60–80 kDa are distributed, a ratio with the following formula was calculated (Table 1).

$$Ratio = \frac{supernatant (area)}{pellet (area)}$$

If the value is higher than 1, more of the impurities are in the supernatant than in the pellet. A graphical overview shows that the both main impurities behave similar, whereby the 20–30 kDa impurities are more likely to remain in the supernatant (Table 1). However, with increasing centrifugation force, more impurities remained in the supernatant which is paradox. This

Table 1: Ratio of the impurities from supernatant and pellet of the centrifugation methods.

A value is smaller than 1, means that more impurities are in the pellet than in the supernatant.

Category	sample	Ratio 60–80 kDa	Ratio 20–30 kDa
High centrifugation force	20600 × g, 360 min	1.545	3.020
	20380 × g, 60 min	3.140	4.175
	17753 × g, 10 min	2.610	3.266
	10000 × g, 30 min	2.659	3.203
Medium centrifugation force	6000 × g, 30 min	2.351	3.108
	5000 × g, 15 min	1.992	2.269
	3000 × g, 5 min	1.810	2.501
	2000 × g, 10 min	3.051	3.279
Low centrifugation force	1000 × g, 5 min	1.948	2.284
	100 × g, 20 min	1.745	1.756
	100 × g, 5 min	2.291	2.263
	22.6 × g, 5 min	1.010	0.976
3.6 × g, 20 min	0.964	1.081	

could be explained by the method. This calculation was done using densitometry of the CBB bands. With stronger force, the pellets were harder to resuspend and therefore, weaker bands appeared in CBB, because of protein loss. These results together indicate that centrifugation is not a good method for separation, especially if the GFP- β 3GnT2 is evenly distributed in both fractions which means loss of target protein. Nevertheless, a centrifugation force of $500 \times g$ 5 min was chosen, because the GFP- β 3GnT2 was only in low concentration in the pellet and the majority of the cell debris could be separated, which would disturb later filtration.

3.3.2. Separation by NaCl Precipitation

The analysis of the NaCl precipitation revealed that the main impurities are mainly in the supernatant and therefore, a good reduction of them in the pellet was archived (**Fig. 3A**). Furthermore, the fluorescence imaging of GFP- β 3GnT2 was observed in the pellet (**Fig. 3B**),

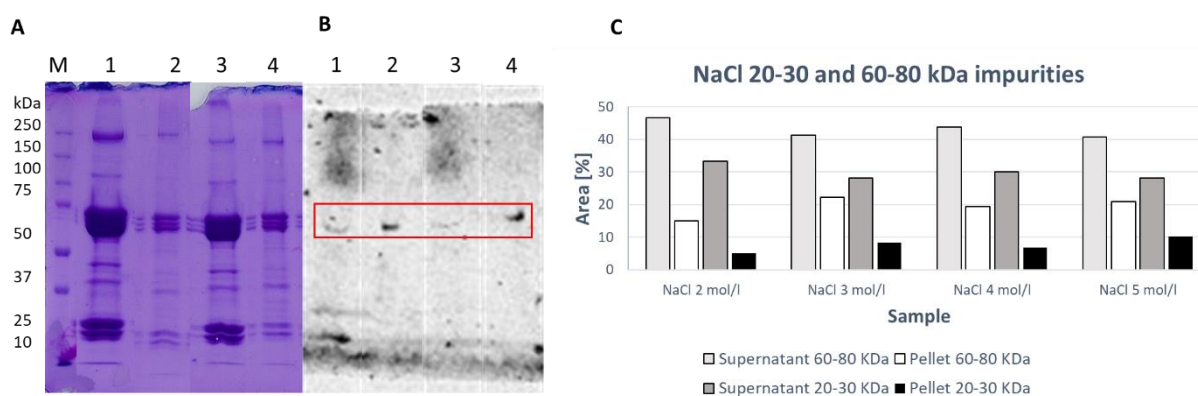


Fig. 3: Sodium chloride precipitation overview of GFP- β 3GnT2 (A) Coomassie blue staining SDS-gel with example set ups for NaCl in different concentrations compared with (B) fluorescence Image. On each line 20 μ l was loaded. On the SDS-PAGE it was a 1.2 to 10 dilution and on the Fluorescence image it was a 1 to 2.5 dilution. Lane 1 and 2: supernatant and pellet NaCl 2 mol/l; Lane 3 and 4: supernatant and pellet NaCl 4 mol/l; M is Marker; Red box indicates GFP (C) Distribution of the main impurities between the supernatant and pellet for the different concentrations of NaCl

but a non-negligible part is still in the supernatant. The analysis of the distribution of the main impurities showed also that the distribution of the impurities remains stable (**Fig. 3C**). On the other hand, compared to the centrifugation set ups, the GFP- β 3GnT2 is now mainly in the pellet due to the influence of the NaCl, despite the lower centrifugation force of $5000 \times g$, 10 min (**Fig. 3B**).

3.3.3. Separation by $(\text{NH}_4)_2\text{SO}_4$ precipitation

As expected, with increasing $(\text{NH}_4)_2\text{SO}_4$ concentration and centrifugation force, more proteins were mainly in the pellet and therefore, a separation of impurities couldn't be

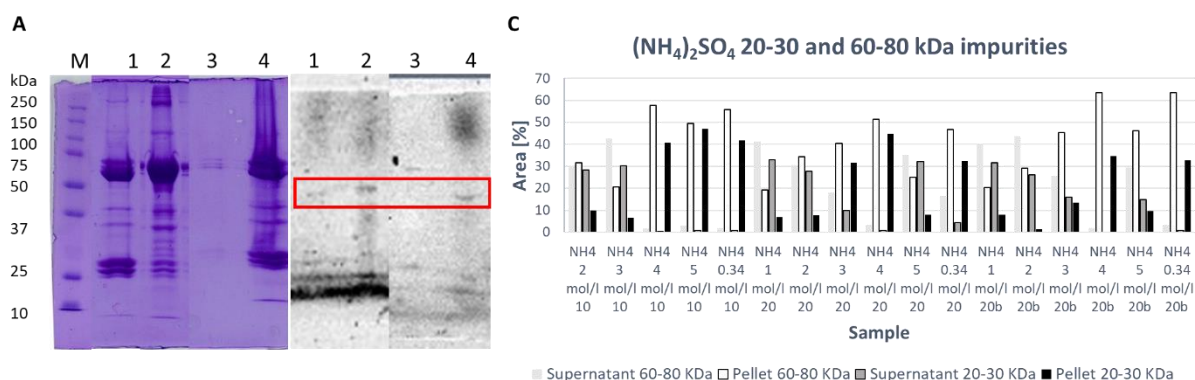


Fig. 4: Ammonium sulphate precipitation overview of GFP-β3GnT2 (A) Coomassie blue staining SDS-gel with example set ups for $(\text{NH}_4)_2\text{SO}_4$ in different concentrations and centrifugation forces compared with **(B)** fluorescence image. On each lane 20 μl was loaded. On the SDS-PAGE it was a 1.2 to 10 dilution and on the Fluorescence image it was a 1 to 2.5 dilution.

Lane 1 and 2: supernatant and pellet $(\text{NH}_4)_2\text{SO}_4$ 2 mol/l, 5000 × g 10 min; Lane 3 and 4: supernatant and pellet NaCl 4 mol/l, 5000 × g 10 min; M is Marker; Red box indicates GFP **(C)** Distribution of the main impurities between the supernatant and pellet for the different concentrations of $(\text{NH}_4)_2\text{SO}_4$ and centrifugation forces, 10: 10000 × g, 10 min; 20: 3000 × g, 20 min; 20b: 5000 × g, 20 min

archived (**Fig. 4**). Already with only 2 mol/l $(\text{NH}_4)_2\text{SO}_4$ GFP-β3GnT2 was mainly in the pellet together with the majority of the host proteins (**Fig. 4A + B**). As an additional side effect, the high salt concentrations affected the analysis via SDS-PAGEs visible and blurred the bands on the gels.

3.3.4. Separation by Poly ethylene glycol (PEG) 6000 precipitation

The analysis of the PEG 6000 precipitation revealed that the side impurities are more affected by this kind of precipitation, similar to the $(\text{NH}_4)_2\text{SO}_4$ precipitation, and are already at low PEG concentrations mainly in the pellet. In the opposite, the main impurities are evenly distributed with the tendency to the supernatant (**Fig. 5**). Furthermore, at PEG concentration of 10 % or higher, most of the proteins are already precipitated. Moreover, with GFP-β3GnT2 was also easily affected by PEG and was even at low PEG concentration mainly found in the pellet (**Fig. 5B**). The best separation was archived with 2.5 % PEG, where the bigger part of the main impurities was still in the supernatant only with just a very low amount of GFP-β3GnT2. With higher PEG concentration the bands of the SDS-PAGEs were very smeary. Higher

concentrations than 10 % aren't usable for haemolymph precipitation, because all proteins will be in the precipitate.

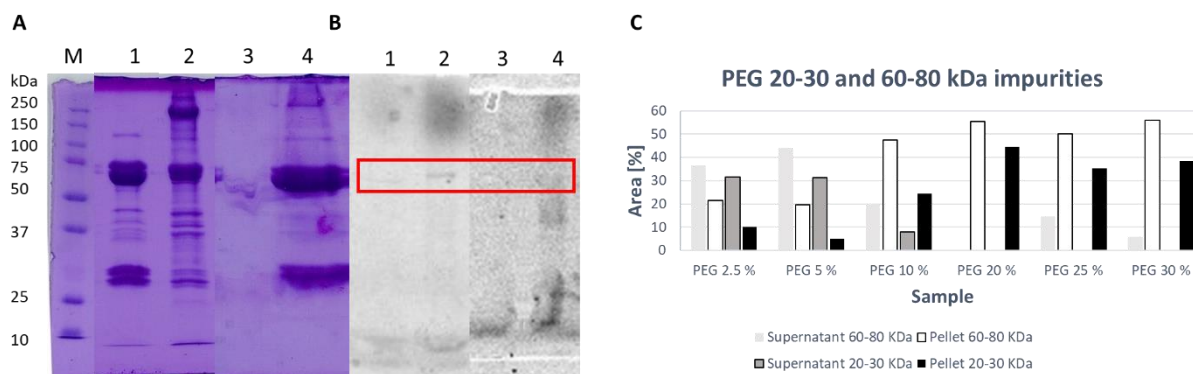


Fig. 5: Polyethylene glycol 6000 precipitation overview of GFP-β3GnT2 (A) Coomassie blue staining SDS-gel with example set ups for PEG 6000 in different concentrations compared with **(B)** fluorescence Image. On each line 20 μl was loaded. On the SDS-PAGE it was a 1.2 to 10 dilution and on the Fluorescence image it was a 1 to 2.5 dilution; Lane 1 and 2: supernatant and pellet PEG 2.5 %, 4200 × g 15 min; Lane 3 and 4: supernatant and pellet PEG 25 %, 4200 × g 15 min; M is Marker; Red box indicates GFP **(C)** Distribution of the main impurities between the supernatant and pellet for the different concentrations of PEG and centrifugation forces

3.3.5. Separation by PEI precipitation

During PEI precipitation most proteins bind with low NaCl concentration to the PEI and precipitated. This indicates that these proteins are mainly acid proteins. This effect was observed for all PEI concentrations and especially for the main impurities at 60–80 kDa (**Fig. 6**). With increasing concentration of NaCl, which disturbs the binding to the PEI, less proteins were in the precipitate (**Fig. 6**). The impurities at 20–30 kDa in contrast are stable and have a similar behaviour for all set ups. Therefore, it can be assumed that the separation into the pellet was mainly achieved due to the centrifugation. The general behaviour of the main impurities was the same as the majority of the host proteins. In addition, fluorescence imaging revealed that GFP-β3GnT2 was at all NaCl concentrations mainly in the pellet (**Fig. 6B**). The best result was obtained with PEI 0.1 % and PEI 0.3 % both with a NaCl concentration of 0.1 mol/l, but this means that the GFP-β3GnT2 is together with most of the proteins precipitated and gives mainly a reduction of the main impurities at 20–30 kDa. If a loss of the GFP-β3GnT2 is acceptable, then the precipitation with a higher concentration of NaCl would be the methods of choice.

These PEI precipitations were promising and therefore, successfully repeated. Additionally, they were investigated in their DNA concentration regarding a possible benefit

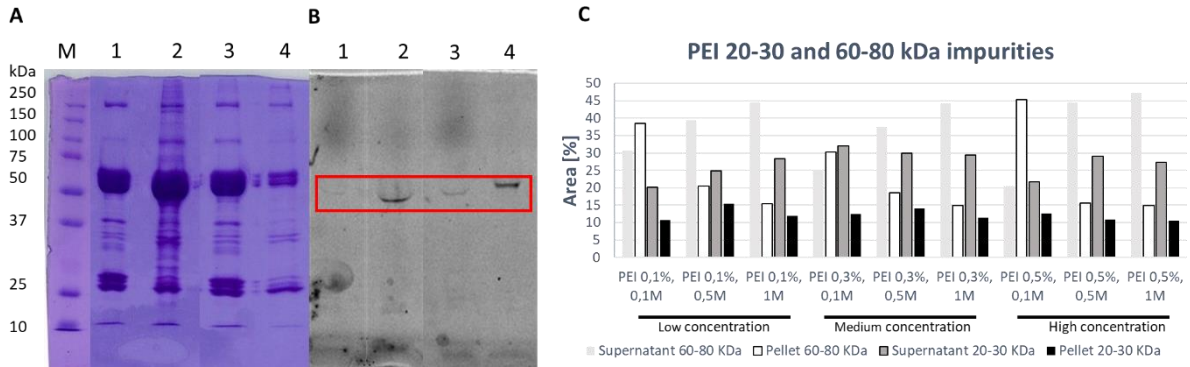


Fig. 6: Poly ethylene imine precipitation overview of GFP-β3GnT2 (A) Coomassie blue staining SDS-gel with example set ups for PEI in different concentrations and different NaCl concentrations compared with **(B)** fluorescence Image. On each line 20 μl was loaded. On the SDS-PAGE it was a 1.2 to 10 dilution and on the Fluorescence image it was a 1 to 2.5 dilution
Lane 1 and 2: supernatant and pellet PEI 0.1 % 0.1 mol/l NaCl ; Lane 3 and 4: supernatant and pellet PEI 0.1 % 1 mol/l NaCl ; M is Marker; Red box indicates GFP
(C) Distribution of the main impurities between the supernatant and pellet for the different concentrations of PEI with their respective NaCl concentrations; The concentration of the NaCl is denoted through the molarity.

for DNA separation (**Fig. 7**), but the result is the opposite what Burgess [64] stated. The main concentration of the DNA wasn't in the pellet, but in the supernatant. The higher concentration in the pellet was found for PEI 0.1 % and 0.3 % at a sodium chloride concentration from 0.1 mol/l. It can't be ruled out, that the assay was influenced by PEI or other compounds and that there is a stronger interaction between PEI and fluorescence dye. This wasn't further investigated.

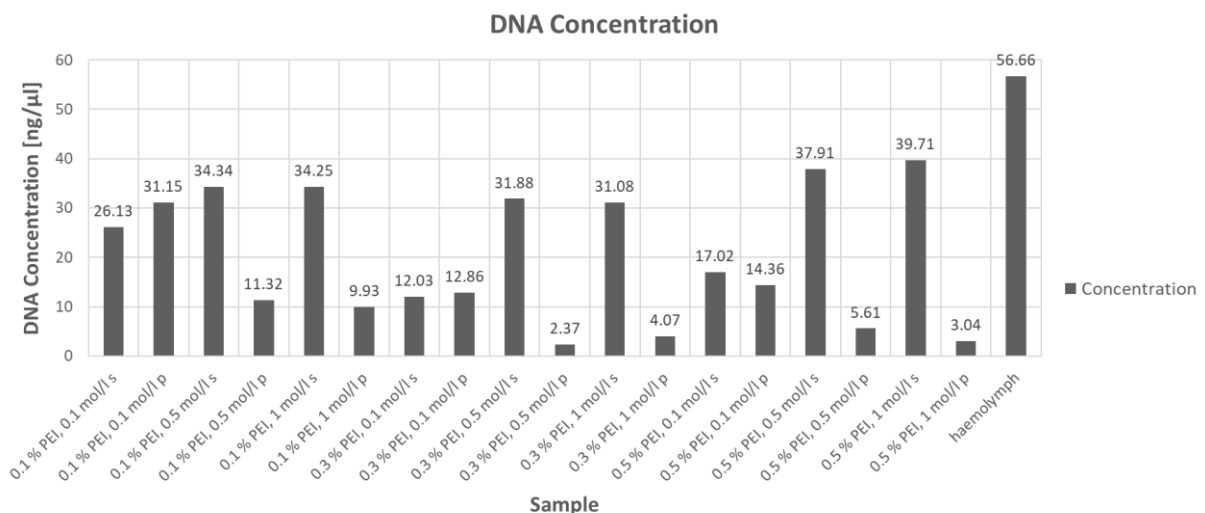


Fig. 7: A graphical overview of the DNA concentration of the precipitation with PEI and different concentrations of NaCl. s: supernatant; p: pellet

3.3.6. Precipitation in general

For all set ups protein assays were done (**Fig. 8**) and for PEI precipitation repeated (**Fig. 9**). These results support the former mentioned conclusions. All of the results, the SDS-PAGES, fluorescence images, protein concentration, DNA concentrations and relative Area Quantification were for internal use combined in one Standard Operation Procedure (SOP), which can be used as reference. Moreover, the areas of the main impurities at 20-30 and 60-80 kDa were also used to calculate a ratio as previously with the centrifugation (**Table 2**). If the value is smaller than 1, more of the impurities are in the pellet than in the supernatant.

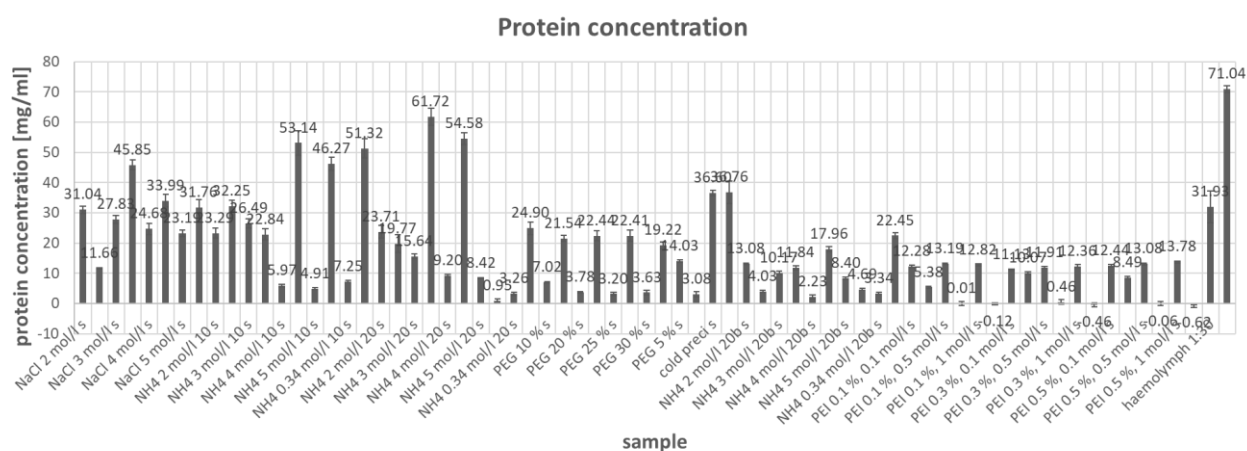


Fig. 8: A graphical overview of the protein concentration done with the BCA protein Assay Kit (Thermo Scientific). The error bars indicate the standard derivation of multiple repeats, at least 2, but in general 3 repeats; s: supernatant; p: pellet

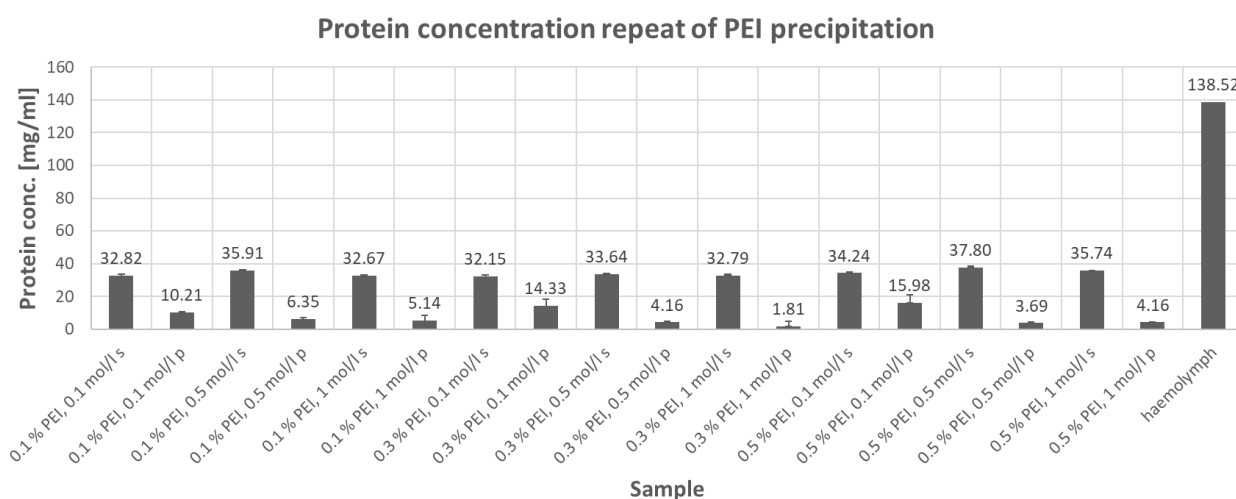


Fig. 9: A graphical overview of the repeated protein concentration of PEI done with the BCA protein Assay Kit (Thermo Scientific). The error bars indicate the standard derivation of 3 repeats; s: supernatant; p: pellet

The precipitation methods gave not a perfect result for the GFP- β 3GnT2 purification. 2.5 % PEG and 0.1 % PEI, 0.1 mol/l NaCl seemed to be usable if a small loss of GFP- β 3GnT2 is acceptable, but with just a small purification benefit. For PEI 0.3 % and 0.5 %, both with 0.1

mol/l NaCl, the loss of GFP-β3GnT2 was very low or even non detectable. However, these methods seemed promising enough to test if a combination of them provides a better purification without/less loss of GFP. If the focus is on the purity and a higher loss is acceptable, then the PEI precipitations with a higher NaCl concentration are the precipitations of choice. NaCl gave a similar impression, but had a bigger loss of the GFP-β3GnT2. (NH₄)₂SO₄ precipitated all proteins indiscriminately and was therefore, not usable for the pre-treatment of GFP-β3GnT2. These findings made a centrifugation at 500 x g 5 min, followed by 2.5 % PEG, 0.1 % PEI with 0.1 mol/l NaCl or 0.3 % and 0.5 % PEI, both with 0.1 mol/l NaCl, the best option as a pre-treatment for the purification of GFP-β3GnT2 from the silkworm haemolymph.

Table 2: Ratio of the impurities from supernatant and pellet of the precipitation methods

Set up	ratio 60–80 kDa	ratio 20–30 kDa
NaCl 2 mol/l	3.12	6.41
NaCl 3 mol/l	1.86	3.38
NaCl 4 mol/l	2.24	4.40
NaCl 5 mol/l	1.94	2.74
NH4 2 mol/l 10	0.95	2.86
NH4 3 mol/l 10	2.06	4.56
NH4 4 mol/l 10	0.03	0.00
NH4 5 mol/l 10	0.06	0.01
NH4 0.34 mol/l 10	0.03	0.02
NH4 1 mol/l 20	2.14	4.72
NH4 2 mol/l 20	0.88	3.67
NH4 3 mol/l 20	0.45	0.31
NH4 4 mol/l 20	0.06	0.02
NH4 5 mol/l 20	1.40	4.01
NH4 0.34 mol/l 20	0.35	0.14
NH4 1 mol/l 20b	2.00	4.02
NH4 2 mol/l 20b	1.50	20.46
NH4 3 mol/l 20b	0.56	1.17
NH4 4 mol/l 20b	0.03	0.00
NH4 5 mol/l 20b	0.64	1.51
NH4 0.34 mol/l 20b	0.05	0.02
PEG 2.5 %	1.70	3.11
PEG 5 %	2.22	6.10
PEG 10 %	0.43	0.33
PEG 20 %	0.00	0.00
PEG 25 %	0.29	0.00
PEG 30 %	0.10	0.00
Sedimentation	0.73	0.78
PEI 0.1 %, 0.1 mol/l	0.80	1.87
PEI 0.1 %, 0.5 mol/l	1.92	1.61
PEI 0.1 %, 1 mol/l	2.88	2.38
PEI 0.3 %, 0.1 mol/l	0.84	2.58
PEI 0.3 %, 0.5 mol/l	2.01	2.15
PEI 0.3 %, 1 mol/l	2.96	2.59
PEI 0.5 %, 0.1 mol/l	0.45	1.71
PEI 0.5 %, 0.5 mol/l	2.86	2.66
PEI 0.5 %, 1 mol/l	3.16	2.57

3.3.7. Anion exchange screening

The results of the AIEX screening showed always no binding of the GFP-β3GnT2 to the material (**data only party shown**). Only utile was the DEAE material with a 10 mol/l Tris, pH 8 buffer, because under this condition a major part of the impurities at 60–80 kDa and a small

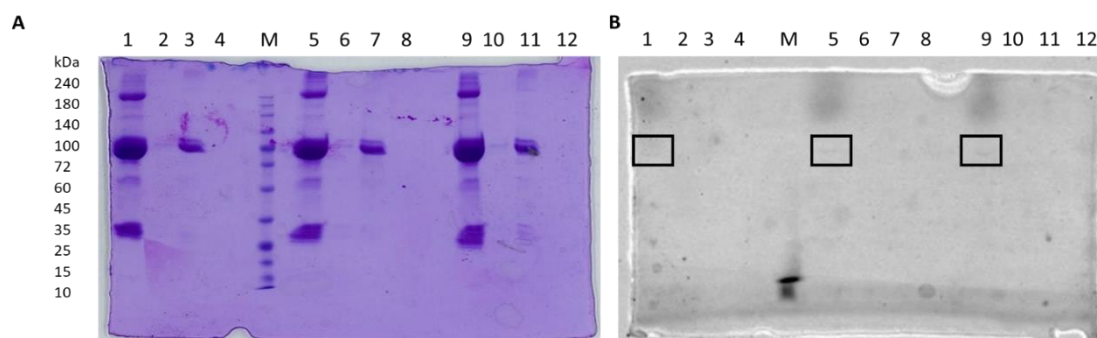


Fig. 10: GFP-β3GnT2 AIEX screening example 1 (A) Coomassie blue staining SDS-gel in comparison with **(B)** fluorescence Image. On each line 15 μl was loaded. On the SDS-PAGE it was 10 μl sample to 22 μl dilution and on the Fluorescence image it was 12 μl to 24 μl dilution. All samples were applied to DEAE material. Lane 1,2,3 and 4: Load, wash, elution and regeneration fraction of 25 mol/l MOPS, pH 7; Lane 5,6,7 and 8: Load, wash, elution and regeneration fraction of 0.1 mol/l NaH₂PO₄, pH 8; Lane 9,10,11 and 12: Load, wash, elution and regeneration fraction of 10 mol/l Tris, pH 8; M is Marker; The black boxes indicate the weak fluorescence response of the GFP-β3GnT2

part of the 20–30 kDa impurities did bind to the material. The GFP- β 3GnT2 was like always in the flow through (**Fig. 10B**). Because of this, a 10 mmol/l Tris buffer was used for the consecutive chromatography experiments. Furthermore, it became evident that even a small factor change can have an impact on the chromatography purification. In this case a small part of the impurities at 60-80 kDa could bind to the material with PBS buffer, pH 8, but not with PBS buffer, pH 7 (**Fig. 11A**).

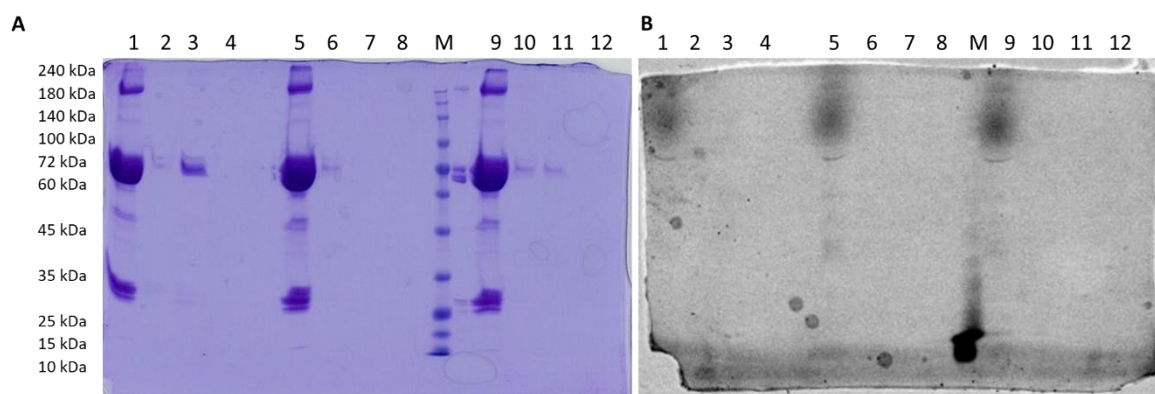


Fig. 11: GFP- β 3GnT2 AIEX screening example 2 (A) Coomassie blue staining SDS-gel of the GFP- β 3GnT2 AIEX screening in comparison with (B) fluorescence Image. On each line 15 μ l was loaded. On the SDS-PAGE it was 10 μ l sample to 22 μ l dilution and on the Fluorescence image it was 12 μ l to 24 μ l dilution. All samples were applied to Capto Q material. Lane 1,2,3 and 4: Load, wash, elution and regeneration fraction of 45 mol/l MOPS, pH 8; Lane 5,6,7 and 8: Load, wash, elution and regeneration fraction of PBS, pH 7; Lane 9,10,11 and 12: Load, wash, elution and regeneration fraction of PBS, pH 8; M is Marker

3.3.8. Chromatographic separation

During the AIEX screening GFP- β 3GnT2 didn't bind with 10 mmol/l Tris, pH 8 to the material, but this was in opposite to our data (internal note, Prof. assoc. Tatsuya Kato), as GFP- β 3GnT2 could bind to a DEAE column with a 50 mmol/l Tris, pH 8. Therefore, we confirmed this with success, but with low separation of impurities, because they also bound more or less completely to the column (**data not shown**). Moreover, the same conditions as in the AIEX screening were applied and GFP- β 3GnT2 bound now to the column (**data not shown**). For both buffer systems the chromatograms and SDS-PAGEs showed almost similar behaviour. Most likely an experiment mistake during the AIEX screening was the reason. The samples prior to the screening were maybe diluted with PBS buffer (pH 8) instead of MilliQ water. Therefore, NaCl was already in the buffer, hypothetically 0.0513 mol/l. It was tried to repeat the conditions of the AIEX screening with adding additional NaCl to the buffer, but due to a mistake the starting buffer contained 10 mmol/l Tris, pH 8 and even 0.06417 mol/l NaCl. This time the chromatogram was different and showed also a slightly different elution behaviour.

But the GFP- β 3GnT2 still did bind to the column (**Fig. 12**). Only a small part was still in the flow through fractions. Despite that the elution was done with a linear gradient, all proteins eluted at the same time. Therefore, no separation could be achieved with the gradient, but a high amount of impurities was in the flow through, especially the main impurities at 20–30 kDa. This result was successfully repeated (**data not shown**).

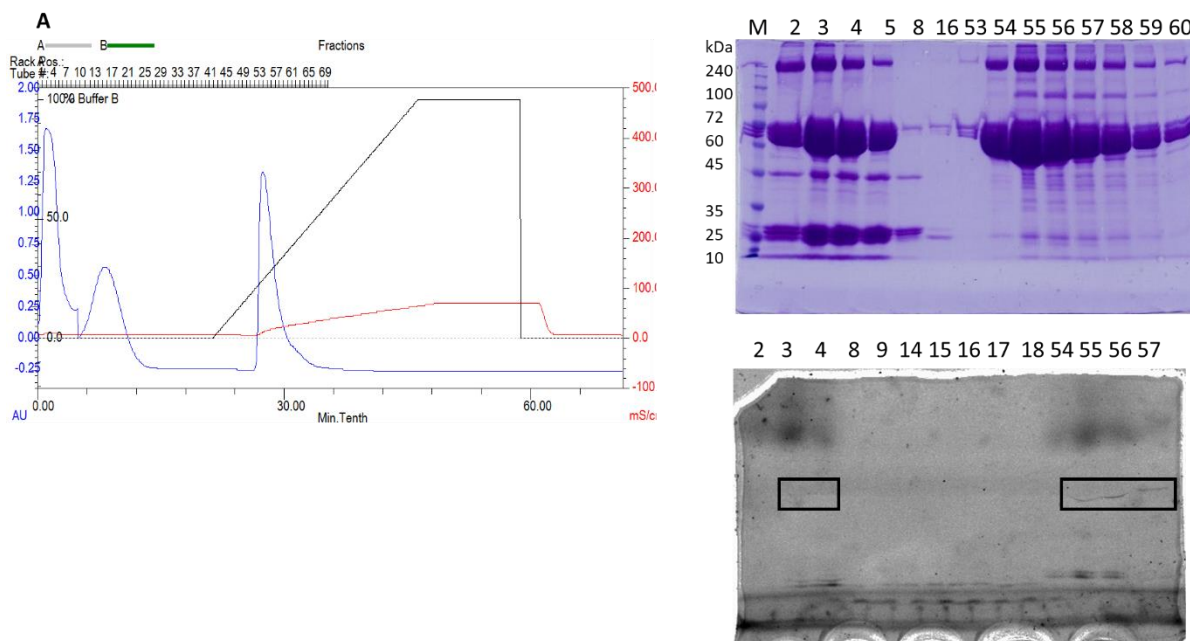


Fig. 12: AIEX of GFP- β 3GnT2 on DEAE with 10 mM Tris, pH 8 + 0.06417 mol/l NaCl. (A) Elution was done with up to 1 mol/l NaCl. **(B)** Coomassie blue staining SDS-gel of the fractions in comparison with **(C)** fluorescence Image. On each line 15 μ l was loaded. On the SDS-PAGE it was 10 μ l sample to 22 μ l dilution and on the Fluorescence image it was 12 μ l to 24 μ l dilution. The program was 10 CV binding buffer, 2 ml load, 6 CV binding buffer, 10 CV linear gradient up to 100 % elution buffer, 5 CV elution buffer and 5 CV binding buffer. Flow rate was 2 ml/min. The number indicates fraction number, which are up to 1 ml; M is Marker; Black boxes indicate GFP- β 3GnT2 fluorescence

Next hydrophobic interaction chromatography (HIC) based columns were investigated. The Butyl FF and Butyl FF were used in combination with a 10 mmol/l Tris buffer, pH 8 containing 1.2 mol/l $(\text{NH}_4)_2\text{SO}_4$ or 3 mol/l NaCl. Using the Phenyl FF column, it wasn't possible to separate the target protein with both buffers even after optimization with a step gradient elution (**data not shown**). Moreover, the general affinity of the proteins was so high, that a high amount of proteins was only from the column eluted during the cleaning step (**data not shown**). Because of this strong protein-column interactions, the Phenyl FF column was not further investigated.

The Butyl FF column didn't show such a strong protein adsorption behaviour like the Phenyl column, but with the 1.2 mol/l $(\text{NH}_4)_2\text{SO}_4$ buffer proteins separation was also not achieved (**Fig. 13A**). In addition, fluorescence couldn't be certain detected in the elution fraction (**Fig. 13B**). Opposite to this, using a 3 mol/l NaCl buffer showed a promising separation

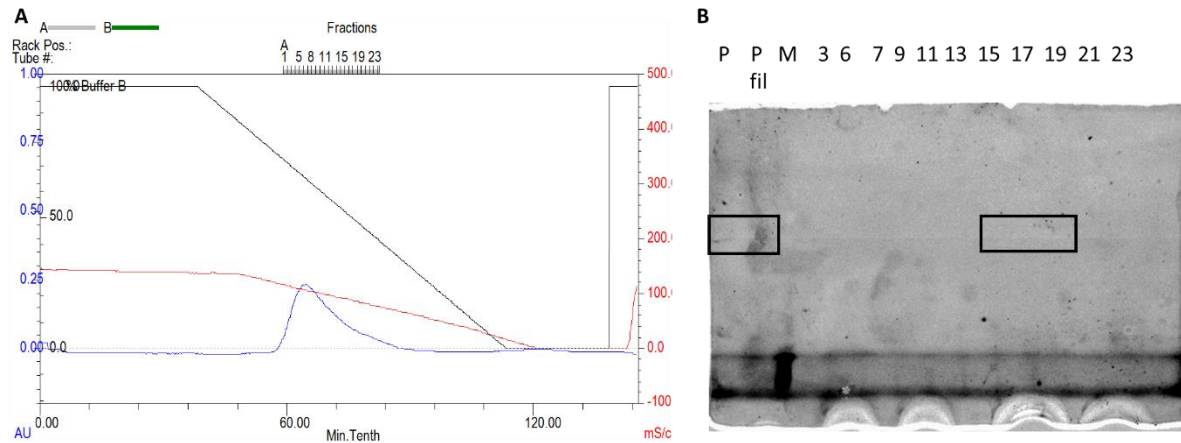


Fig. 13: HIC of GFP- β 3GnT2 on Butyl with 10 mM Tris, pH 8 + 1.2 mol/l $(\text{NH}_4)_2\text{SO}_4$. (A) Elution was done with down to 0 mol/l $(\text{NH}_4)_2\text{SO}_4$. (B) Fluorescence imaging on an SDS-gel of the fractions. On each line 15 μ l was loaded. For the Fluorescence image 12 μ l to 24 μ l dilution was used. The program was 2 ml binding buffer, 1.5 ml load, 7 CV binding buffer, 15 CV linear gradient, 5 CV elution buffer and 3 CV binding buffer. Flow rate was 1 ml/min. The number indicates fraction number, which are up to 1 ml and collected via threshold of 0.03 AU; P: pooled DEAE elution fraction; P fil: 0.45 μ m filtered DEAE elution fraction = load; M is Marker; Black boxes indicate (presumably) GFP- β 3GnT2 fluorescence

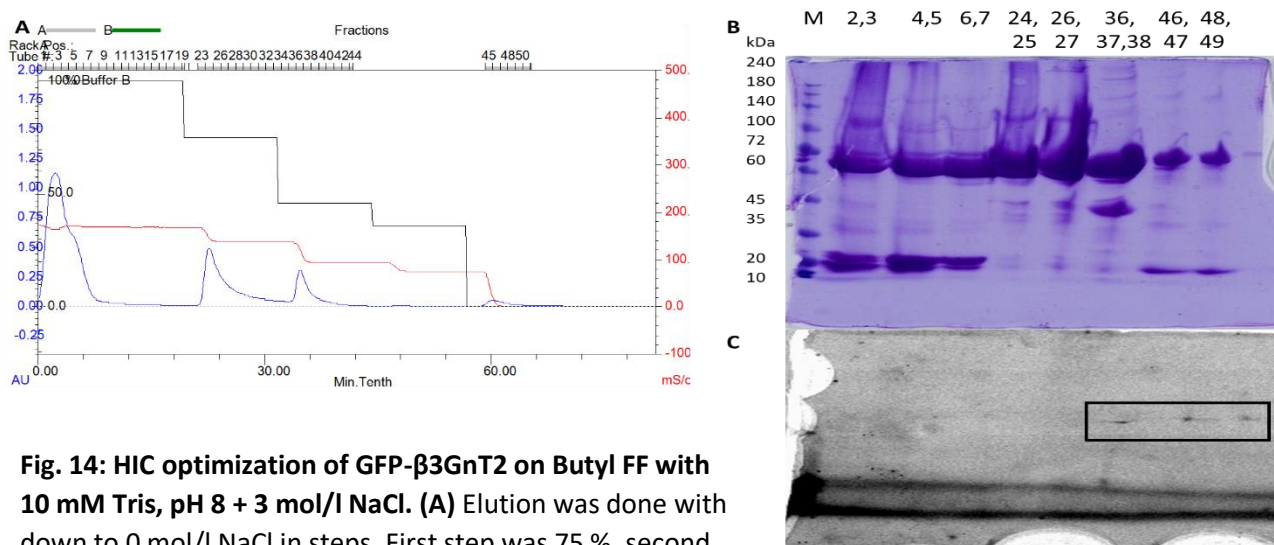


Fig. 14: HIC optimization of GFP- β 3GnT2 on Butyl FF with 10 mM Tris, pH 8 + 3 mol/l NaCl. (A) Elution was done with down to 0 mol/l NaCl in steps. First step was 75 %, second step 46 %, third step 36 % and the last step 0 % binding buffer. (B) Coomassie blue staining SDS-gel of the fractions in comparison with (C) fluorescence Image. On each line 15 μ l was loaded. On the SDS-PAGE it was 10 μ l sample to 22 μ l dilution and on the Fluorescence image it was 12 μ l to 24 μ l dilution. The program was 2 ml binding buffer, 1.5 ml load, 7 CV binding buffer, for each elution step 5 CV and 10 CV elution buffer. Flow rate was 2 ml/min. The numbers indicate pooled and concentrated fractions, which were up to 2 ml and collected via threshold of 0.015 AU; M is Marker; Black boxes indicate GFP- β 3GnT2 fluorescence

effect (**data not shown**). Therefore, instead of a linear gradient a four-step gradient was applied. With this step gradient the proteins could be further separated and the last two collectable fractions showed after concentration the GFP- β 3GnT2 fluorescence (**Fig. 14**). This step gradient was then further optimized to a two-step gradient protocol, which resulted in a lessened protein burden (**Fig 15**). Nevertheless, it was also impossible to separate the main impurities around 60–80 kDa completely, even if the major part couldn't bind to column.

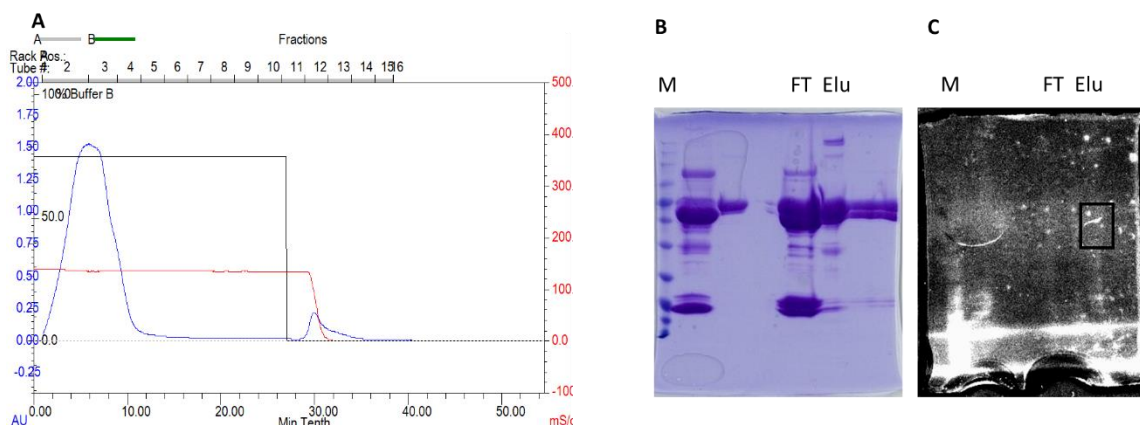


Fig. 15: HIC final optimization of GFP- β 3GnT2 on Butyl FF with 10 mM Tris, pH 8 + 3 mol/l NaCl. (A) Elution was done with down to 0 mol/l NaCl in steps. First step was 75 % and last step 0 % binding buffer. **(B)** Coomassie blue staining SDS-gel of the fractions in comparison with **(C)** fluorescence Image. On each line 15 μ l was loaded. On the SDS-PAGE it was 10 μ l sample to 22 μ l dilution and on the Fluorescence image it was 12 μ l to 24 μ l dilution. The program was 2 ml 75 % binding buffer, 6 ml load, 8 CV 75 % binding buffer, 11 CV elution buffer. Flow rate was 2 ml/min; 5 ml fractions were collected via threshold of 0.01 AU, pooled and concentrated; FT is the flow through; Elu indicates the elution fraction; M is Marker; Black boxes indicate GFP- β 3GnT2 fluorescence

Because Blue Sepharose has an affinity to human serum albumin, it was investigated if this principle could be used for the separation of the main impurities at 60–80 kDa, which also have a similar task as serum albumin. In contrary, regarding the UV signal it seemed that most of the proteins didn't bind to the column (**data not shown**), but actual most of the proteins bound to the column very strongly. Moreover, they bound so strongly that they were only eluted during a washing step with 1 mol/l NaOH. Therefore, this separation principle was not further investigated, because the target GFP- β 3GnT2 also bound too strongly to the column as it was not in the flow through fraction (**data not shown**).

At last a Ceramic hydroxyapatite (CHT) column was used, which combines a metal affinity and a cation exchange principle. One more time, this showed that it is again difficult to separate the impurities. The target protein bound to the column together with the

impurities (**Fig 16**), but as shown later with the mCherry purification, these results were turned over as the mCherry was together with the impurities in the flow through.

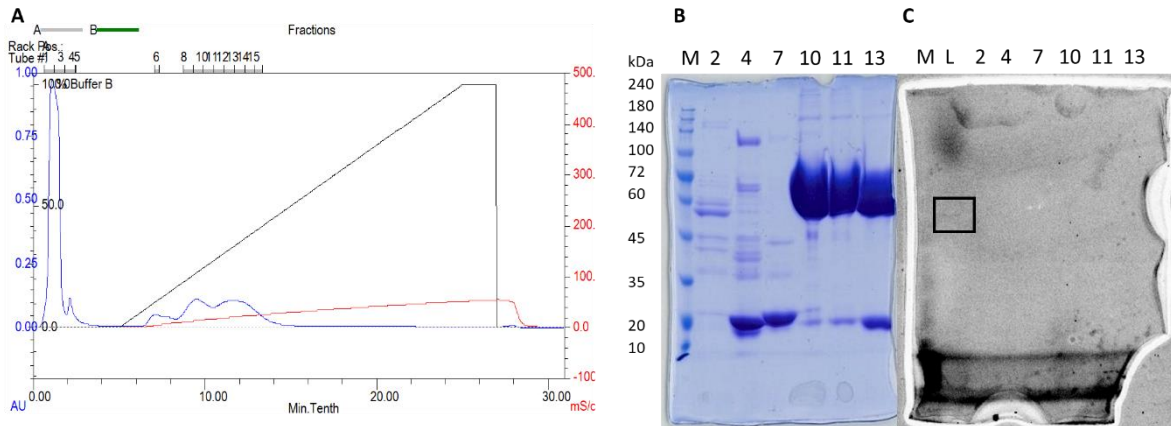
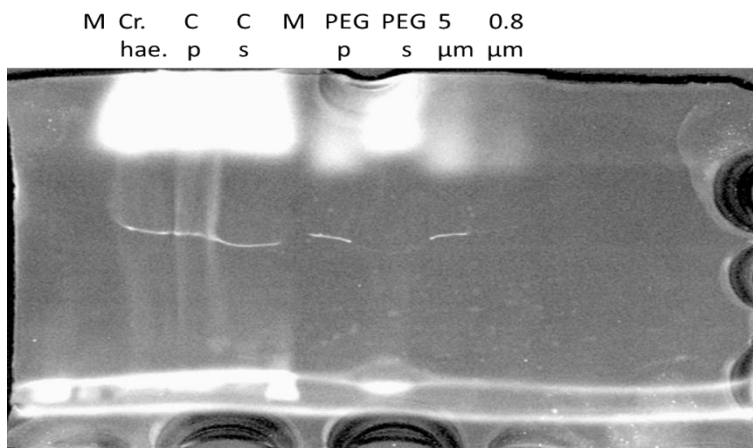


Fig. 16: CHT II chromatography of GFP-β3GnT2 with 8 mmol/l KH_2PO_4 , pH 8. (A) Elution was done with up to 600 mmol/l KH_2PO_4 , pH 8. (B) Coomassie blue staining SDS-gel of the with Amicon 30K around 32-fold concentrated fractions in comparison with (C) fluorescence Image. On each line 15 μl was loaded. On the SDS-PAGE it was 10 μl sample to 22 μl dilution and on the Fluorescence image it was 12 μl to 24 μl dilution. The program was 5 ml load, 4 CV binding buffer, 20 CV linear gradient, 2 CV elution buffer and 4 CV binding buffer. Flow rate was 5 ml/min. The number indicates fraction number, which were up to 3 ml and collected via threshold of 0.05 AU; M is Marker; Black boxes indicate GFP-β3GnT2 fluorescence

3.3.9. Additional aspects regarding filtration

Moreover, as seen in the fluorescence Image (**Fig. 16C**) the fluorescence of the load fraction was already weak and no fluorescence could be in the fractions detected. One known reason was that the during the infection cycle of the silkworms the expression rate of the GFP-β3GnT2 decreasing steadily, most likely because the reuse of the haemolymph as infectious agent resulted in a decreasing concentration of recombinant baculovirus in each infection cycle. Additionally, it was determined that the filtration also results in a high GFP-β3GnT2 loss



supernatant; PEG p: 2.5 % PEG 6000 precipitation pellet; PEG s: 2.5 % PEG 6000 precipitation supernatant; 5 μm : resuspended PEG pellet filtrated with 5 μm filter; 0.8 μm : 5 μm filtrate filtered with 0.8 μm filter; M is Marker

Fig. 17: Fluorescence Imaging of GFP-β3GnT2 to show the sudden loss of GFP-β3GnT2 in the later stage during filtration. On each line 15 μl was loaded. It was a 12 μl to 24 μl dilution used. Cr. Hae. : for crude haemolymph; C p: Centrifugation 500 g, 5min pellet; C s: Centrifugation

(Fig. 17). A 5 μm filtration is still fine, but a 0.8 μm resulted in more or less a total GFP- β3GnT2 loss.

3.4. Conclusion

The last filtration experiments indicated that during the previous experiments always high loss of GFP- β3GnT2 occurred during the filtration step, but the initial GFP- β3GnT2 concentration was so high, that it covered this loss and this effect was unnoticed. Because of the repeated infection cycles, the expression level was at the end so low, that now the critical concentration was reached and the effect noticeable. Therefore, and because of the difficulties to separate the around 70 kDa GFP- β3GnT2 from the main impurities around 60–80 kDa, it was decided to abandon this project and shift to the mCherry, because of its smaller size of 34.5 kDa and with the additional advantage that it should be easily separated from the main impurities around 60–80 kDa with a size exclusion chromatography.

4. A systematic and methodical approach for efficient purification from silkworm haemolymph

4.1. Introduction

The aim of this study was to establish an easy up-scalable purification protocol for industrial use. Again, high purity and recovery rate were targeted. Affinity Strep-tag purification was used as comparison method. The aforementioned pre-treatment and chromatography strategies, and some additional methods were investigated for this new model protein, a modified mCherry. With its strong red fluorescence (Ex. 540-590 nm Em. 550-650 nm) [106] and red colour, it is even easier traceable during the purification process. Moreover, the molecular mass was approximately 34.5 kDa, which should make the separation from the 60–80 kDa impurities via SEC easier.

This study reported the first industrial usable and up-scalable purification protocol for silkworm haemolymph. Centrifugation and polyethylene glycol precipitation as pre-treatments were followed by hydrophobic interaction, size exclusion and heparin affinity chromatography steps. The introduction of a thermal precipitation step further improved the purity and recovery of the protocol.

4.2. Specific Material and Methods

4.2.1. Recombinant *Bombyx mori* nucleopolyhedrovirus (BmNPV) bacmid preparation for mCherry

The DNA fragment of the mCherry was sub-cloned from a commercial plasmid pmCherry (Catalog # 632522, TakaraBio, Kusatsu, Japan) using specific primers (mCherryFw: 5'-GTGAGCAAGGGCGAGGAGGAT-3', mCherryRv: 5'-CTACTTGTACAGCTCGTCCATG-3'). A DNA sequence coding for secreted poly-tags (30K-Flag-Strep-SpyTag, 30K-FSS, MRLTLFAFVLAVCALASNADYKDDDDKGGGSAWSHPQFEKGGGSENLYFQGSQPVTIVMVDAYKRYK GSSGSGGSG) was designed and synthesized by GeneWiz (Suzhou, China). It consists of the signal peptides (SPs) from silkworm 30K proteins for secretion, followed by a Flag-, StrepTag II-, tobacco etch virus (TEV) protease cleavage site and a Spy-tag. The resulting plasmid was designated as pFastBac-30K-FSS-mCherry for expressing the secreted mCherry protein. It was constructed and then utilized for making of a recombinant BmNPV bacmid. Subsequently, the

recombination baculovirus was generated in the cultured silkworm Bm5 cells according to our previous reports [107]. The cell culture supernatant was collected and used for serial infections to obtain high titer virus stocks, which were employed to infect silkworm larvae.

4.2.2. Capillary electrophoresis sodium dodecyl sulfate (CE-SDS)

The CE-SDS experiments for the mCherry purification protocol were planned and done from Holger Zagst and Imke Oltmann-Norden from the research group of Professor Hermann Wätzig at the Technical University Braunschweig. The following equipment and reagents were used: ultrapure water (arium pro VF, Sartorius, Goettingen, Germany), HEPES (Carl Roth, Karlsruhe, Germany), β -mercaptoethanol (BME) (Carl Roth, Karlsruhe, Germany), Rotilabo CME syringe filter 0.22 μ m (Carl Roth, Karlsruhe, Germany), Amicon Ultracell 10k (Merck KGaA, Darmstadt, Germany), sodium hydroxide (Merck KGaA, Darmstadt, Germany), centrifuge 5417C (Eppendorf, Hamburg, Germany), vortex VV3 (VWR, Leuven, Belgium), Maurice (ProteinSimple, San Jose, USA), Maurice CE-SDS Application Kit (ProteinSimple, San Jose, USA) and Maurice CE-SDS Molecular Weight Markers (ProteinSimple, San Jose, USA).

The lyophilized samples were dissolved in ultrapure water leading to a final protein concentration of about 1 mg/ml. For desalting, the sample solutions were transferred to the Amicon Ultracell filter devices and centrifuged for 10 min at 14 000 \times g. Thereafter, 200 μ l HEPES buffer (10 mmol/l, pH 7.5) was added, carefully mixed (20 \times aspirating & dispensing with pipette) and the filter devices were centrifuged with the same parameters as before. In total the buffer addition and centrifugation were repeated four times. Deviating from the previous parameters, the last centrifugation step was performed at 14 000 \times g for 20 min. Afterwards the samples were weighed and buffer was added as previously described, until the starting weight was achieved. The filter devices were inverted and centrifuged for 2 min at 1020 \times g into collection tubes. To 25 μ l of each sample, 25 μ l of the 1 \times sample buffer, 2 μ l of the internal standard and 2.5 μ l BME were added. The mixes were vortexed thrice for 5s and subsequently centrifuged for 5 min at 1000 \times g. Next, they were heated at 70°C for 10 min and immediately thereafter cooled on ice for 5 min. Finally, the samples were vortexed and centrifuged as described in the preceding step and then transferred to a 96-well plate for measurements on the Maurice (ProteinSimple, San Jose, CA). The measurements were performed using the CE-SDS Size Application Kit, the Maurice CE-SDS IgG Standard and Maurice CE-SDS Molecular Weight Markers. The used CE-SDS cartridges contain a fused-silica

capillary of 15 cm effective length and 50 μm internal diameter. The sample tray was tempered at 10 °C, the samples were loaded electrokinetically at 4600 V for 20 s and separated at 5750 V for 35 min. For detection the UV absorption at 220 nm was measured, Compass for iCE version 2.0.10 was used for instrument control and integration.

4.3. Results and Discussion

4.3.1. Centrifugation

The behaviour of mCherry was at low, medium and high centrifugal forces investigated (**Fig. 18; data only partially shown**). Besides the easy-to-see red colour, mCherry has also a red fluorescence, which makes traceability and detection very simple. Even with high centrifugal forces mCherry was only in low concentrations present in the pellet and this low mCherry loss can be explained by a small amount of mCherry remaining in the cells. This mCherry was not secreted into the haemolymph and therefore, remained trapped inside and descending together with the cells during centrifugation. According to the CBB staining and fluorescence images there were no significant differences among the different centrifugation forces and therefore, 17800 \times g for 10 min was selected as the best option. The reason is the comparable short time and high centrifugal force to separate the cell host cell proteins and debris into the pellet. The effect for the former of them was hard to evaluate, because of the

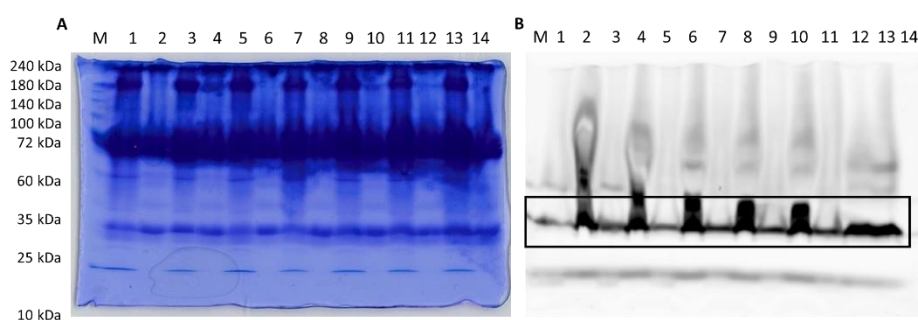


Fig. 18: Pre-treatment centrifugation. Coomassie blue staining SDS-gel (**A**) with set ups for high and medium centrifugation forces in comparison with fluorescence Image (**B**) for mCherry purification. On each line 15 μl was loaded. On the SDS-PAGE it was 10 μl sample to 22 μl dilution and on the Fluorescence image it was 12 μl to 24 μl dilution. Lane 1 and 2: pellet and supernatant 20400 g, 60 min; Lane 3 and 4: pellet and supernatant 17800 g, 10 min; Lane 5 and 6: pellet and supernatant 10000 g, 30 min; Lane 7 and 8: pellet and supernatant 6000g, 30 min; Lane 9 and 10: pellet and supernatant 5000 g, 15 min; Lane 11 and 12: pellet and supernatant 3000 g, 5 min; Lane 13 and 14: pellet and supernatant 2000, 10 min; M is Marker. This figure is from Minkner et al. (2020) under license by Elsevier B.V. (<https://doi.org/10.1016/j.jchromb.2019.121964>)

high protein quantity. Important is that there was no mCherry loss at this force, but most likely more host cells are precipitated at this force compared to lower forces.

4.3.2. Precipitation

On a small scale $(\text{NH}_4)_2\text{SO}_4$, PEG 6000 and polyethylene (PEI) precipitations were investigated. On a larger-scale only 2 mol/l $(\text{NH}_4)_2\text{SO}_4$ and 5 % PEG were investigated, because in these cases were no mCherry loss into the precipitate (**Fig. 19; data only partially shown**). However, 2 mol/l $(\text{NH}_4)_2\text{SO}_4$ 5 % PEG resulted in a higher loss of mCherry during this compared

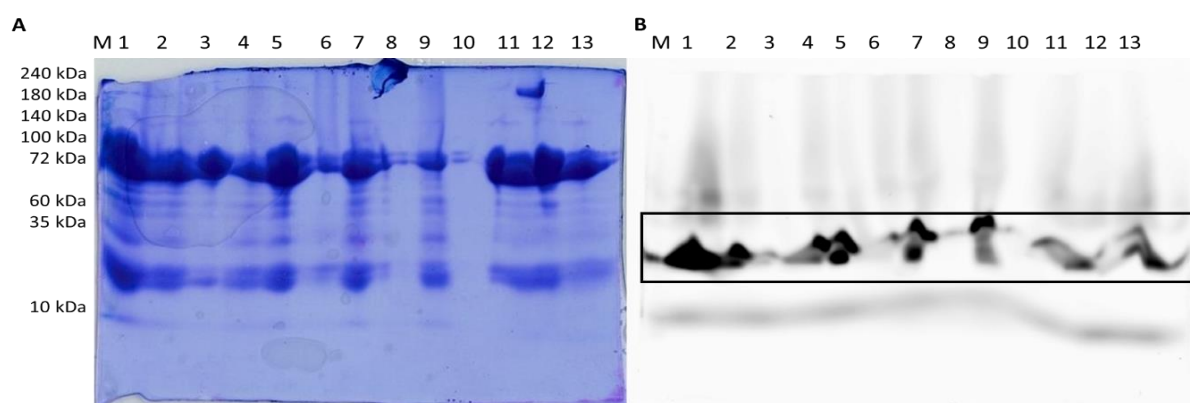


Fig. 19: Pre-treatment precipitations. Coomassie blue staining SDS-gel (**A**) with mCherry precipitations in comparison with fluorescence Image (**B**). On each line 15 μl was loaded. On the SDS-PAGE it was 10 μl sample to 22 μl dilution and on the Fluorescence image it was 12 μl to 24 μl dilution. Lane 1: centrifugation supernatant 17800 g, 10 min; Lane 2: failed precipitation 1 M $(\text{NH}_4)_2\text{SO}_4$; Lane 3 and 4: pellet and supernatant 2 mol/l $(\text{NH}_4)_2\text{SO}_4$; Lane 5 and 6: pellet and supernatant 3 mol/l $(\text{NH}_4)_2\text{SO}_4$; Lane 7 and 8: pellet and supernatant 4 mol/l $(\text{NH}_4)_2\text{SO}_4$; Lane 9 and 10: pellet and supernatant 5 mol/l $(\text{NH}_4)_2\text{SO}_4$; Lane 11: failed 2.5 % PEG precipitation; Lane 12 and 13: pellet and supernatant 5 % PEG; M is Marker; black box indicates mCherry fluorescence. This figure is from Minkner et al. (2020) under license by Elsevier B.V. (<https://doi.org/10.1016/j.jchromb.2019.121964>)

to the small-scale procedure (**data not shown**). Therefore, 2.5 % PEG was additionally investigated. The 2.5 % precipitation on a larger scale was comparable to those of the small-scale precipitation with 2 mol/l $(\text{NH}_4)_2\text{SO}_4$ (**data not shown**), and therefore, was chosen and the supernatant used for the next chromatography steps. These results revealed an issue; usually this kind of screening experiments are performed on a small scale with the expectation that there will be no major differences during upscaling aside from some minor ones due to the industrial scale. This problem during screening for the haemolymph purification method means that all screening experiments have to be repeated, if a more certain result for the larger scale is desired.

4.3.3. Chromatography matrixes as 1st or 2nd purification steps

Using the anion exchange (AIEX) principle with a DEAE column, most of the host cell proteins bound together with the mCherry to the column and could not be separated from it during the linear gradient (**Fig. 20**). Since a phenyl column showed high adsorption and low recovery in the GFP-β3GnT2 experiments (**data not shown**), only the Butyl FF column was again investigated for the HIC principle. With 1.2 mol/l (NH₄)₂SO₄ as binding buffer, most mCherry bound to the column and was mostly eluted in the middle of the linear gradient (**Fig. 21**) which reduced the overall protein amount. This was optimized to a two-step gradient protocol with 66 % and 0 % binding buffer (**Fig. 22**), but contrary the expectation, mCherry and most of the proteins were not able to bind to the column. This behaviour cannot be explained by the change in the pre-treatment, because the theoretically hydrophobic interaction of the proteins with the column matrix increased with the change from 2.5 % PEG to a 2 mol/l (NH₄)₂SO₄ precipitation. The most likely explanation is that the ionic strength of 66 % binding buffer is already insufficient for holding the protein on the column material. Therefore, it can be assumed that the previous elution of mCherry in the linear gradient protocol was delayed and that the elution had already started at a lower ionic strength.

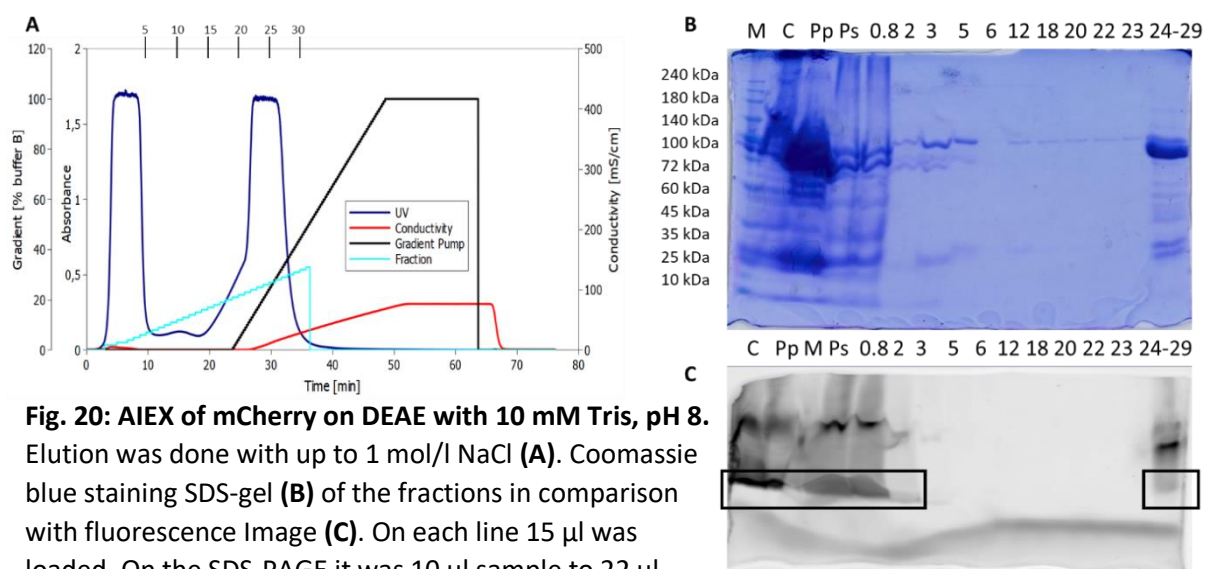


Fig. 20: AIEX of mCherry on DEAE with 10 mM Tris, pH 8.

Elution was done with up to 1 mol/l NaCl (**A**). Coomassie blue staining SDS-gel (**B**) of the fractions in comparison with fluorescence Image (**C**). On each line 15 µl was loaded. On the SDS-PAGE it was 10 µl sample to 22 µl dilution and on the Fluorescence image it was 12 µl to 24 µl dilution. The program was 2 ml binding buffer, 5.2 ml load, 7 CV binding buffer, 10 CV linear gradient up to 100 % elution buffer, 6 CV elution buffer and 5 CV binding buffer. Flow rate was 2 ml/min and for load 1 ml/min. The number indicates fraction number, which is up to 2 ml and collection threshold was 0.05 AU; M is Marker; C: supernatant of centrifugation; Pp: 5 % PEG precipitation; Ps: precipitation supernatant; 0.8: 0.8 µm filtration of supernatant; black boxes indicates mCherry fluorescence. This figure is from Minkner et al. (2020) under license by Elsevier B.V. (<https://doi.org/10.1016/j.jchromb.2019.121964>)

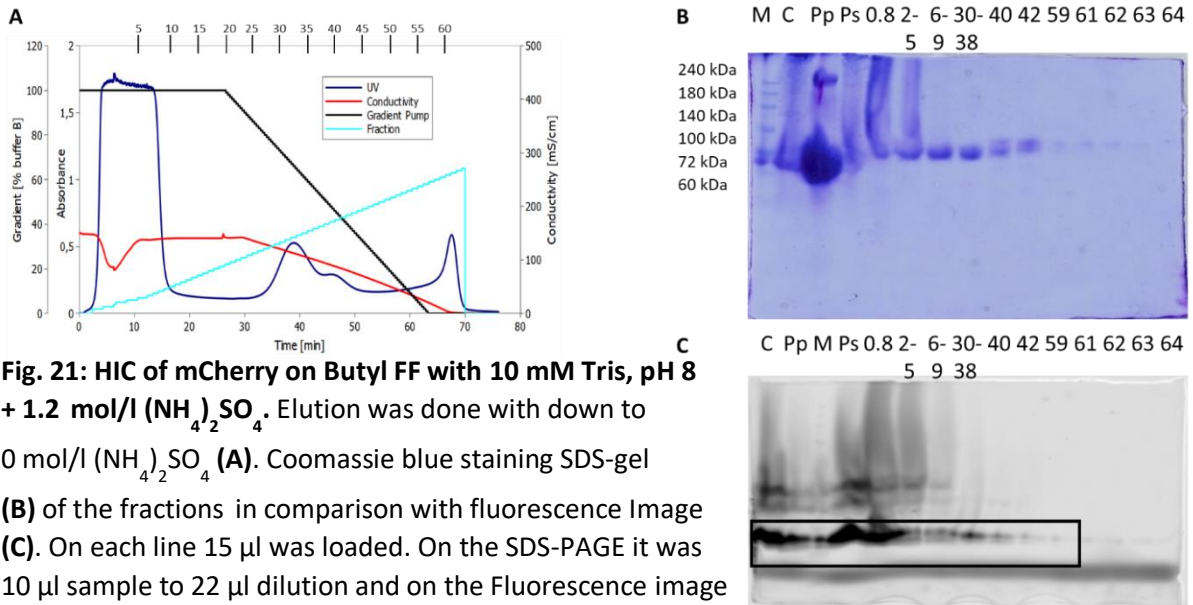


Fig. 21: HIC of mCherry on Butyl FF with 10 mM Tris, pH 8 + 1.2 mol/l (NH₄)₂SO₄. Elution was done with down to 0 mol/l (NH₄)₂SO₄ (A). Coomassie blue staining SDS-gel (B) of the fractions in comparison with fluorescence Image (C). On each line 15 µl was loaded. On the SDS-PAGE it was 10 µl sample to 22 µl dilution and on the Fluorescence image it was 12 µl to 24 µl dilution. The sample was adjusted with additional 1.2 mol/l (NH₄)₂SO₄. The program was 2 ml binding buffer, 5.2 ml load, 7 CV binding buffer, 15 CV linear gradient up to 100 % elution buffer, 5 CV elution buffer. Flow rate was 2 ml/min and for load 1 ml/min. The number indicates fraction number, which is up to 2 ml and collection threshold was 0.05 AU; M is Marker; C: supernatant of centrifugation; Pp: 2.5 % PEG precipitation; Ps: precipitation supernatant; 0.8: 0.8 µm filtration of supernatant; black box indicates mCherry fluorescence. This figure is from Minkner et al. (2020) under license by Elsevier B.V. (<https://doi.org/10.1016/j.ichromb.2019.121964>)

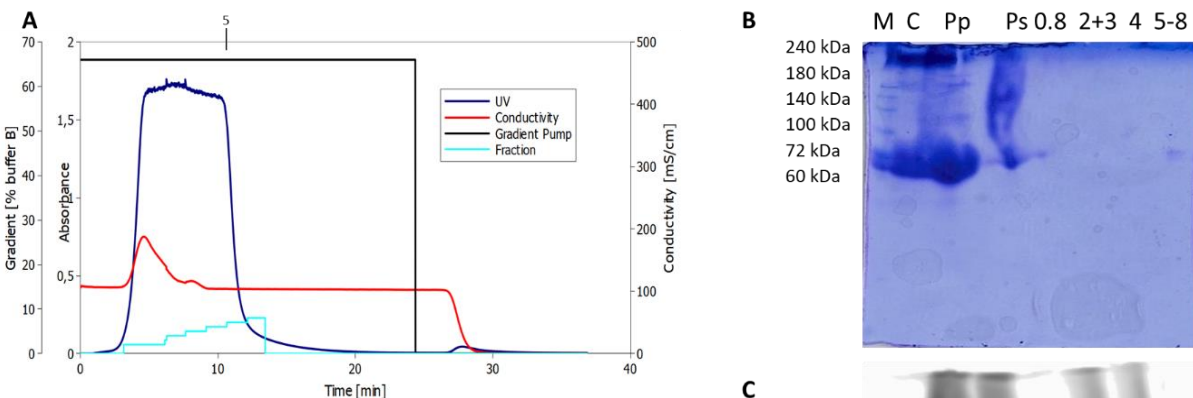


Fig. 22: HIC of mCherry on Butyl FF with 10 mM Tris, pH 8 + 1.2 mol/l (NH₄)₂SO₄. Elution was done with a two-step gradient, thereby the first step contained of 66 % and the second step 0% binding buffer (A). Coomassie blue staining SDS-gel (B) of the fractions in comparison with fluorescence Image (C). On each line 15 µl was loaded. On the SDS-PAGE it was 10 µl sample to 22 µl dilution and on the Fluorescence image it was 12 µl to 24 µl dilution. The sample was adjusted with additional 1.2 mol/l (NH₄)₂SO₄. The program was 2 ml 66 % binding buffer, 5.2 ml load, 7 CV 66 % binding buffer and 5 CV elution buffer. Flow rate was 2 ml/min and for load 1 ml/min. The number indicates fraction number, which is up to 3 ml and collection threshold was 0.1 AU; M is Marker; C: supernatant of centrifugation; Pp: 2 mol/l (NH₄)₂SO₄ precipitation; Ps: precipitation supernatant; 0.8: 0.8 µm filtration of supernatant; black box indicates mCherry fluorescence. This figure is from Minkner et al. (2020) under license by Elsevier B.V. (<https://doi.org/10.1016/j.jchromb.2019.121964>)

Furthermore, using also 3 mol/l NaCl to promote hydrophobic interactions, the Butyl FF column was reinvestigated (**Fig. 23**). This time, because most of the host proteins were in the flow-through fraction and most of the mCherry was in the elution fractions, the host protein burden could be strongly reduced.

CHT, the metal affinity combined with cation exchange, didn't achieve the desired separation (**Fig. 24**), because the main impurities were together with the mCherry in the same fractions. Moreover, this time the main impurities had different elution behaviour than with the GFP-β3GnT2 as previously described (**Fig. 16**). They were eluted during the linear gradient together with the GFP-β3GnT2 (**Fig. 16**), but now they were in the flow-through fraction with the mCherry (**Fig. 24**). For GFP fusion protein purification, the sample had a slightly higher ionic strength, but for elution on CHT columns, the phosphate concentration is the relevant

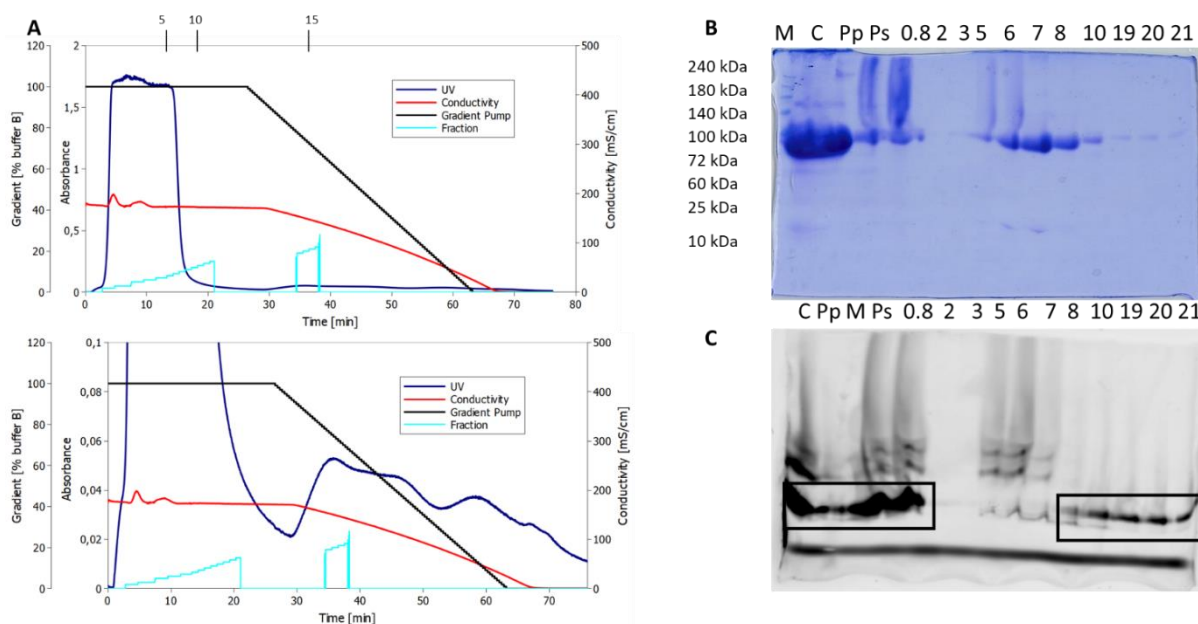


Fig. 23: HIC of mCherry on Butyl FF with 10 mM Tris, pH 8 + 3 mol/l NaCl. Elution was done with down to 0 mol/l NaCl. A zoomed in version for the elution fraction is also shown (**A**). Coomassie blue staining SDS-gel (**B**) of the fractions in comparison with fluorescence Image (**C**). On each line 15 µl was loaded. On the SDS-PAGE it was 10 µl sample to 22 µl dilution and on the Fluorescence image it was 12 µl to 24 µl dilution. The sample was adjusted with additional 3 mol/l NaCl. The program was 2 ml binding buffer, 5.2 ml load, 7 CV binding buffer, 15 CV linear gradient up to 100 % elution buffer, 5 CV elution buffer. Flow rate was 2 ml/min and for load 1 ml/min. The number indicates fraction number, which is up to 2 ml and collection threshold was 0.05 AU; M is Marker; C: supernatant of centrifugation; Pp: 2 mol/l $(\text{NH}_4)_2\text{SO}_4$ precipitation; Ps: precipitation supernatant; 0.8: 0.8 µm filtration of supernatant; black boxes indicates mCherry fluorescence. This figure is from Minkner et al. (2020) under license by Elsevier B.V. (<https://doi.org/10.1016/j.jchromb.2019.121964>)

factor. This issue is interesting for further investigation, because this effect could be also the cause for the joint elution of target protein and impurities.

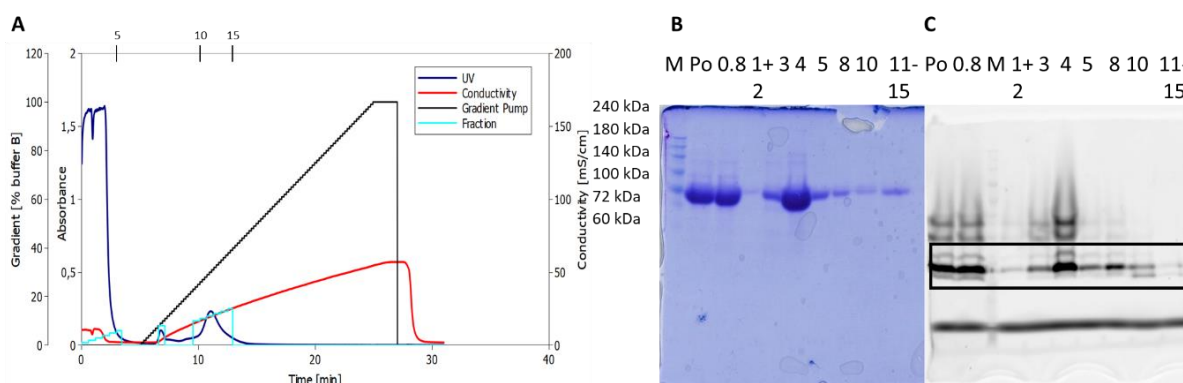


Fig. 24: CHT chromatography of mCherry with 8 mmol/l KH_2PO_4 , pH 8. Elution was done with up to 600 mmol/l KH_2PO_4 , pH 8 (A). Coomassie blue staining SDS-gel (B) of the fractions in comparison with fluorescence Image (C). On each line 15 μl was loaded. On the SDS-PAGE it was 10 μl sample to 22 μl dilution and on the Fluorescence image it was 12 μl to 24 μl dilution. The program was 5 ml load, 4 CV binding buffer, 20 CV linear gradient up to 100 % elution buffer, 2 CV elution buffer. Flow rate was 5 ml/min. The number indicates fraction number, which is up to 3 ml and collection threshold was 0.05 AU; M is Marker; Po: DEAE pool for load; 0.8: 0.8 μm filtration; black box indicates mCherry fluorescence. This figure is from Minkner et al. (2020) under license by Elsevier B.V. (<https://doi.org/10.1016/j.jchromb.2019.121964>)

As a further attempt, a HisTrap column was used as a negative chromatography principle. This was done to separate remaining storage proteins at approximately 70 kDa in haemolymph, because due the His-content, these proteins may have an affinity to the nickel column. However, these proteins were as the other proteins also present in the flow-through (**data not shown**). Therefore, this approach was not further employed.

The elution fraction from HIC NaCl purification (**Fig. 23**) was used to investigate the separation performance of SEC with a 60 cm Superdex Sephacryl S-200 column. Except for small traces, the main impurities at 60–80 kDa could be separated from mCherry (**Fig. 25**). Challenging is that proteins with similar sizes as the target protein remained and that the elution fractions were diluted due to the nature of SEC. A longer separation distance or a more suitable matrix might significantly improve the separation. It was from these preliminary investigations concluded, that an HIC with NaCl followed by an SEC step had the best outcome, and therefore, this protocol was repeated and further investigated.

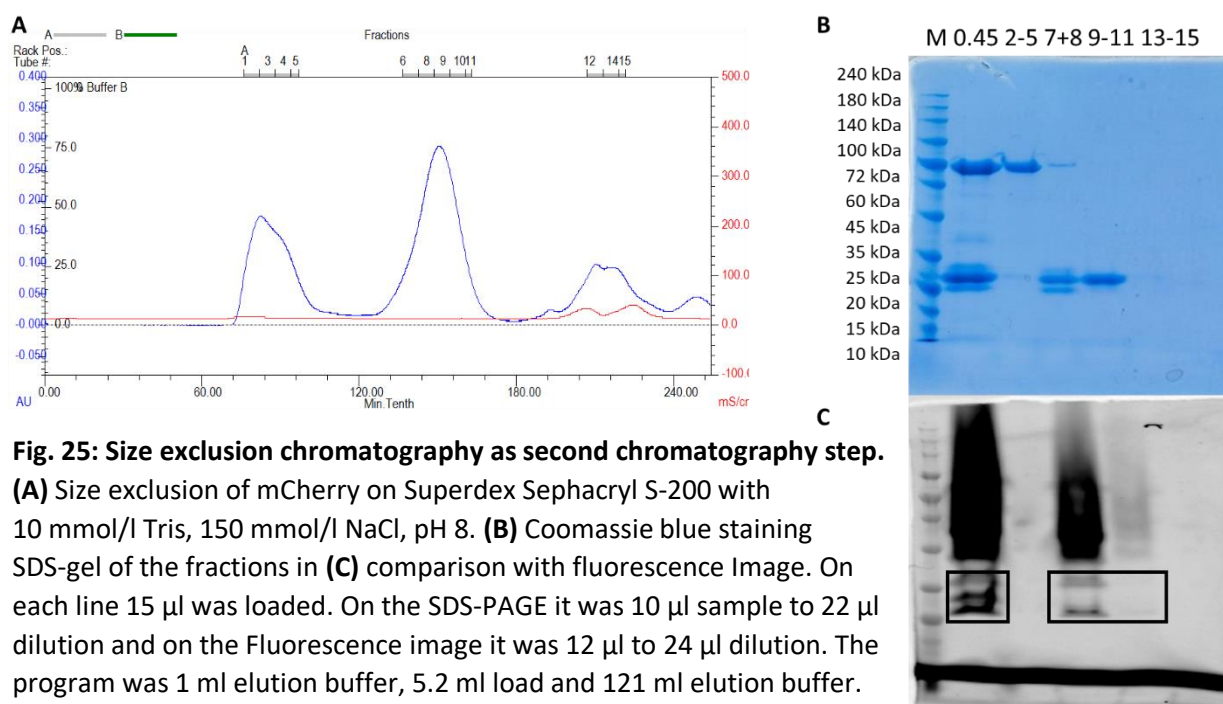


Fig. 25: Size exclusion chromatography as second chromatography step.

(A) Size exclusion of mCherry on Superdex Sephacryl S-200 with 10 mmol/l Tris, 150 mmol/l NaCl, pH 8. **(B)** Coomassie blue staining SDS-gel of the fractions in **(C)** comparison with fluorescence Image. On each line 15 μ l was loaded. On the SDS-PAGE it was 10 μ l sample to 22 μ l dilution and on the Fluorescence image it was 12 μ l to 24 μ l dilution. The program was 1 ml elution buffer, 5.2 ml load and 121 ml elution buffer. Flow rate was 0.5 ml/min. The number indicates fraction number, which are up to 3 ml and collection threshold was 0.075 AU; M is Marker; 0.45: 0.45 μ m filtration of pooled HisTrap flow through pool; 1–15 in A and B: fraction numbers; black boxes indicate mCherry fluorescence. This figure is from Minkner et al. (2020) under license by Elsevier B.V. (<https://doi.org/10.1016/j.jchromb.2019.121964>)

4.3.4. Further HIC and SEC investigations

This protocol was combined and in the order haemolymph centrifugation at 17800 \times g for 10 min, 2 mol/l $(\text{NH}_4)_2\text{SO}_4$ precipitation, HIC with NaCl and followed by SEC, was twice performed. NaCl was chosen for the ionic strength of HIC, and the linear gradient was changed to a two-step gradient in which the first step consisted of 100 % and the last step consisted of 0 % binding buffer. The purple and red fluorescence emitting elution fraction was combined with a red and purple fluorescence emitting part of the flow-through fraction. This was then loaded on the SEC column. The same elution behaviour was achieved in both runs (**Fig. 26**). Previously the DEAE chromatography had shown good results in binding mCherry, even if it was unable to separate impurities from mCherry, therefore, this method was used to concentrate one of the pooled SEC elution fractions and to remove further impurities. However, this attempt failed (**data not shown**). The interaction with the column matrix was most likely disturbed, because the ionic strength of the 150 mmol/l NaCl of the SEC elution

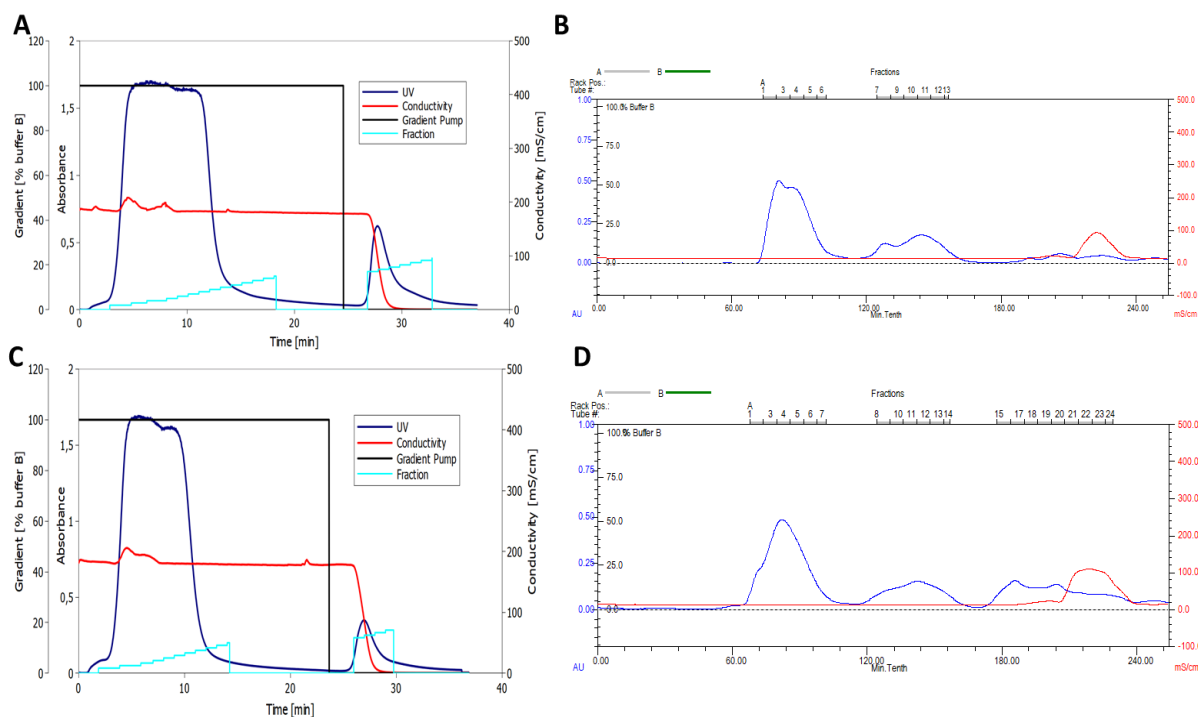


Fig. 26: Two step chromatography protocol for mCherry purification (A+C) HIC of mCherry on Butyl FF with 10 mM Tris, pH 8 + 3 mol/l NaCl. Elution was done with a two-step gradient, thereby the first step contained of 100 % and the second step 0% binding buffer. The sample was adjusted with additional 3 mol/l NaCl. The program was 2 ml binding buffer, 5.2 ml load, 7 CV binding buffer and 5 CV elution buffer. Flow rate was 2 ml/min and for load 1 ml/min. Fraction were collected up to 2 ml with a threshold of 0.075 AU **(B+D)** Size exclusion of mCherry on Superdex Sephacryl S-200 with 10 mmol/l Tris, 150 mmol/l NaCl, pH 8. The program was 1 ml elution buffer, 5.2 ml load and 121 ml elution buffer. Flow rate was 0.5 ml/min. Fraction were collected up to 3 ml with a threshold of 0.075 AU. Loaded was the elution fraction of the HIC chromatography pooled together with one flow through fraction which had a strong red colour. **(A+B)** are Run 1 and **(C+D)** are Run 2. This figure is from Minkner et al. (2020) under license by Elsevier B.V. (<https://doi.org/10.1016/j.jchromb.2019.121964>)

buffer was already great enough to weaken the binding. According to the fluorescence analysis, mCherry was distributed in all AIEC fractions. Nevertheless, the amount of host proteins was reduced because of the SEC, even if the protein concentration of the elution fraction was diluted due to the high volume (**data not shown**). The second SEC run repeated these results and was this time concentrated with an ultrafiltration system with a molecular cut-off of 30 kDa (**Fig. 27**). There was also a mCherry loss, most likely because of the higher molecular cut-off, even if mCherry should theoretically not be able to pass the filter with its 34.5 kDa. As it was shown, impure proteins with similar sizes (in a broad range) as mCherry were still present that in the elution fraction with mCherry (**Fig. 27**).

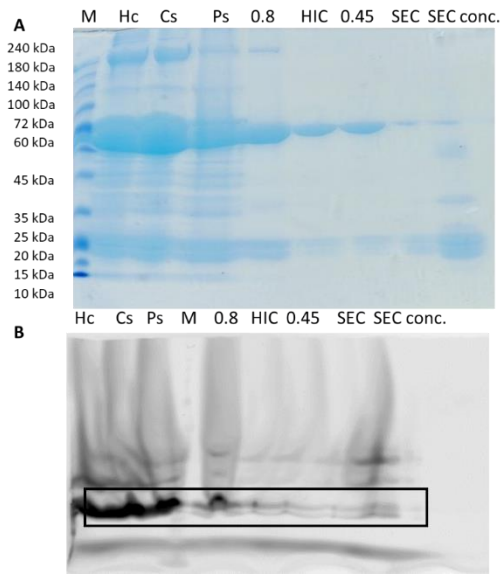


Fig. 27: Results of the two-step chromatography protocol for mCherry purification concentrated with ultracentrifugation.

Coomassie blue staining SDS-gel (A) of the fractions in comparison with fluorescence Image (B). On each line 15 μ l was loaded. On the SDS-PAGE it was up to "0.45" 2 μ l sample diluted to 22 μ l, after this 8 μ l to 22 μ l. On the Fluorescence image it was 12 μ l to 24 μ l dilution. Hc: crude haemolymph; Cs: 17800 g, 10 min centrifugation supernatant; Ps: 2 mol/l $(\text{NH}_4)_2\text{SO}_4$ precipitation supernatant; M is Marker; 0.8: 0.8 μ m filtration of supernatant; HIC: pooled HIC fraction; 0.45: 0.45 μ m filtration; SEC: SEC pool; SEC conc.: SEC pool concentrated with Amicon 30K; black box indicates mCherry fluorescence. This figure is from Minkner et al. (2020) under license by Elsevier B.V.

(<https://doi.org/10.1016/j.jchromb.2019.121964>)

4.3.5. Fine-tuning the first two chromatography steps and addition of a 3rd step

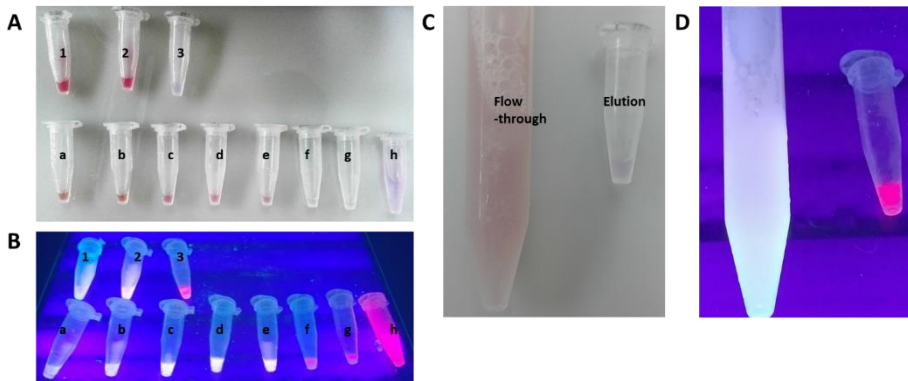


Fig. 28: Oversight about the colour and fluorescence changes during the Strep-ag purification and the heat treatment protocol. (A) shows the colour of each purification step and (B) the corresponding fluorescence. It's becomes clear that the red colour is associated with the purple fluorescence and the purple colour with the typical red mCherry fluorescence. 1: haemolymph; 2: Load; 3: Strep-tag affinity elution; a: haemolymph; b: centrifugation supernatant; c: 70°C supernatant; d: PEG precipitation supernatant; e: filtration; f: Butyl elution fraction; g: SEC elution fraction concentrated; h: Heparin elution fraction concentrated. (C) is the direct colour comparison the flow-through and the elution of the Strep-tag affinity purification, whereby (D) is the direct fluorescence comparison and this also shows that the purple colour is associated with the red fluorescence and the red colour with a weak purple fluorescence. This figure is from Minkner et al. (2020) under license by Elsevier B.V. (<https://doi.org/10.1016/j.jchromb.2019.121964>)

For protocol optimization from the HIC step only the elution fraction with the red fluorescence was used for the next step. It was concluded that the red part of the flow-through fraction with the purple fluorescence emission is most likely denatured protein. This reasoning was also

supported by the fact that the Strep-tag affinity purified reference mCherry (A-3 of Fig. 28) did not emit this fluorescence. Moreover, the purple fluorescence only appeared in the flow-through fraction during affinity chromatography (Fig. 28 C+D), which means it did not have a

Strep-tag. Furthermore, as already mentioned a 2.5 % PEG was performed instead of a 2 mol/l $(\text{NH}_4)_2\text{SO}_4$ precipitation. The protocol was performed with these changes and to see if the freeze/thaw cycle has as well an influence on the purification and recovery of the target protein, without freezing of the samples. The performed chromatograms were as expected and were the same as those obtained previously, despite the aforementioned changes and without freezing/thaw interruptions (**Fig. 29**). In addition, this time the SEC elution fraction was concentrated with ultrafiltration with a molecular cut-off of 3 kDa, which led to a smaller loss of small proteins and the it was shown by CBB staining that the purity also improved (**Fig. 30**). Moreover, it was shown that the HIC flow-through fraction with the purple fluorescence emission had more host proteins and a lower fluorescence response at the expected protein size than the elution fraction with the red fluorescence (**Fig. 30**; see HIC FT and HIC Elu). With two runs this result was also repeated, whereby the samples were frozen between the chromatography steps (**Figs. 31**). This was also clear in the CBB staining and fluorescence imaging analysis (**Fig. 32**).

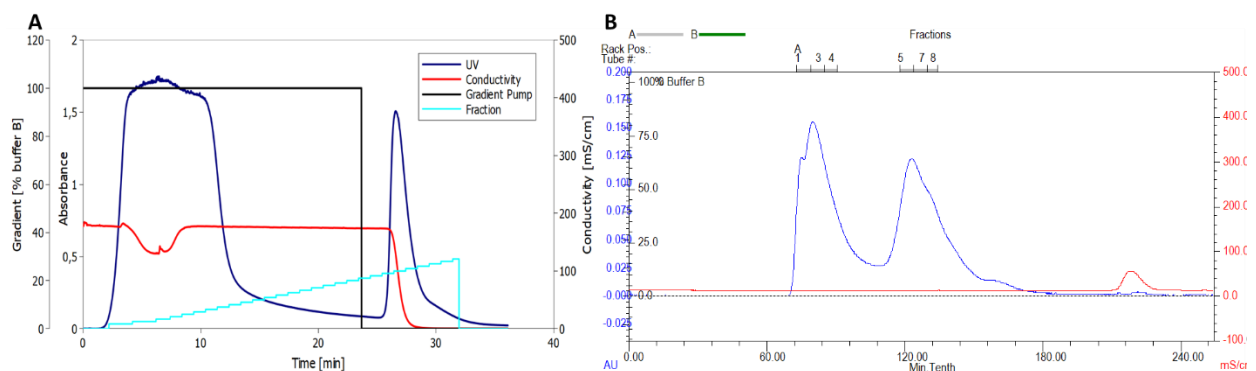


Fig. 29: Two-step chromatography protocol for mCherry purification continuous. (A) HIC of mCherry on Butyl FF with 10 mM Tris, pH 8 + 3 mol/l NaCl. Elution was done with a two-step gradient, thereby the first step contained of 100 % and the second step 0% binding buffer. The sample was adjusted with additional 3 mol/l NaCl. The program was 2 ml binding buffer, 5.2 ml load, 7 CV binding buffer and 5 CV elution buffer. Flow rate was 2 ml/min and for load 1 ml/min. Fraction were collected up to 2 ml with a threshold of 0.075 AU (B) Size exclusion of mCherry on Superdex Sephacryl S-200 with 10 mmol/l Tris, 150 mmol/l NaCl, pH 8. The program was 1 ml elution buffer, 5.2 ml load and 121 ml elution buffer. Flow rate was 0.5 ml/min. Fraction were collected up to 3 ml with a threshold of 0.075 AU. Loaded was the elution fraction of the HIC chromatography. This figure is from Minkner et al. (2020) under license by Elsevier B.V. (<https://doi.org/10.1016/j.jchromb.2019.121964>)

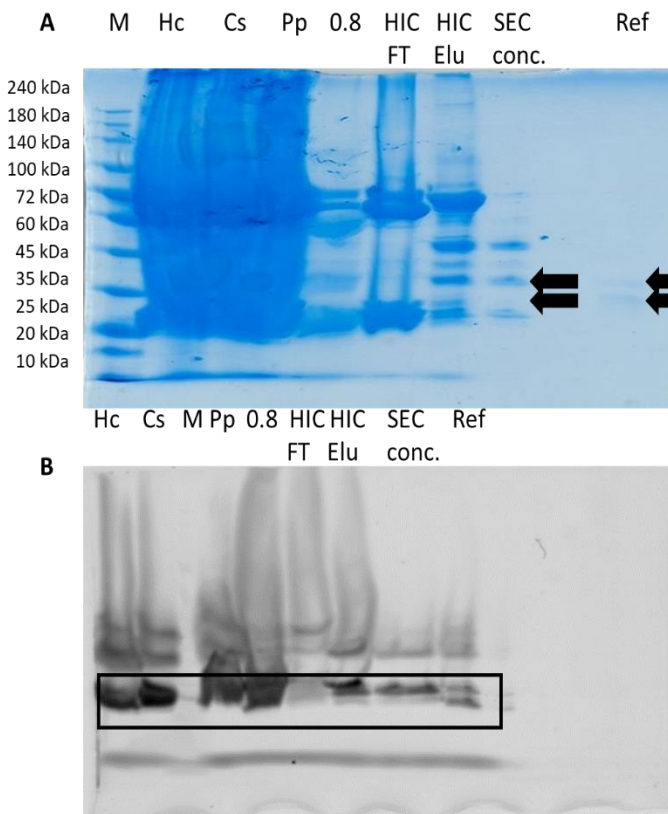


Fig. 30 (left): Results of the two-step chromatography protocol for mCherry purification continuous. (A) Coomassie blue staining SDS-gel of the fractions in (B) comparison with fluorescence image. On each line 10 μ l was loaded. On the SDS-PAGE it was 8 μ l sample to 22 μ l dilution and on the fluorescence image it was 10 μ l to 24 μ l dilution. Hc: crude haemolymph; Cs: 17800 g, 10 min centrifugation supernatant; Pp: 2.5 % PEG precipitation pellet; M is Marker; 0.8: 0.8 μ m filtration of precipitation supernatant; HIC FT: HIC red flow through fraction; HIC Elu: HIC elution fraction with red fluorescence; SEC conc.: SEC pool concentrated with Amicon 3K; Ref: reference mCherry which was purified with affinity chromatography and SEC; arrows indicates mCherry; black box indicates mCherry fluorescence. This figure is from Minkner et al. (2020) under license by Elsevier B.V. (<https://doi.org/10.1016/j.jchromb.2019.121964>)

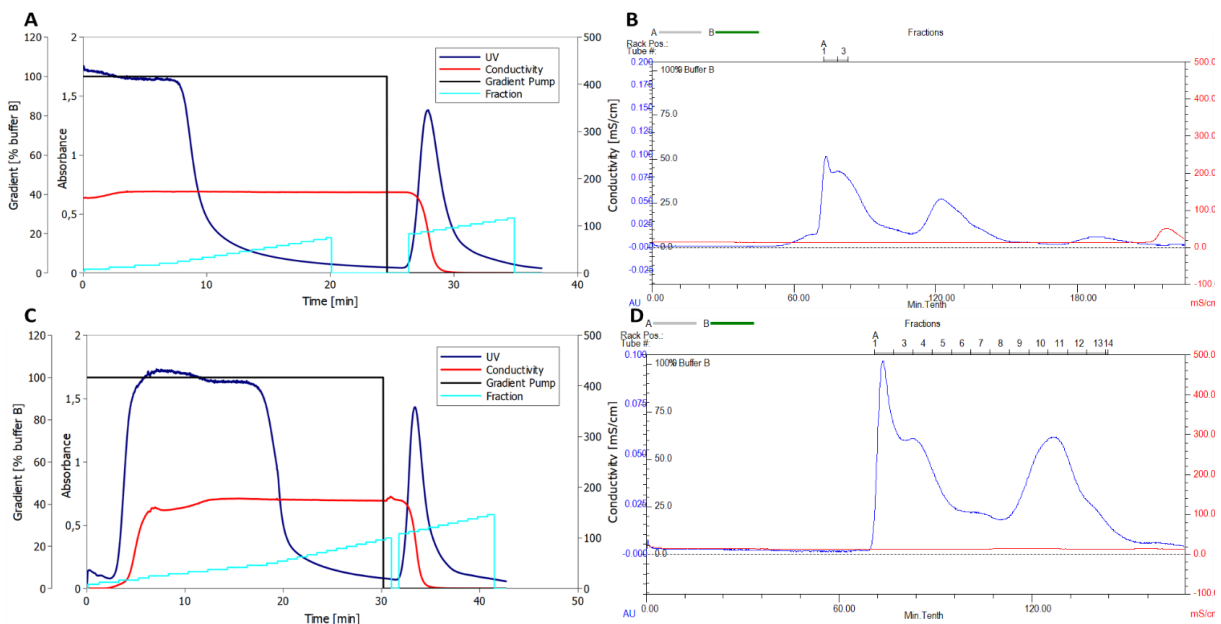


Fig. 31: Reproducibility of the two-step chromatography protocol for mCherry purification (A+C) HIC of mCherry on Butyl FF with 10 mM Tris, pH 8 + 3 mol/l NaCl. Elution was done with a two-step gradient, thereby the first step contained of 100 % and the second step 0% binding buffer. The sample was adjusted with additional 3.5 mol/l NaCl. The program was 2 ml binding buffer, 5.2 ml load, 7 CV binding buffer and 5 CV elution buffer. Flow rate was 2 ml/min and for load 1 ml/min. Fraction were collected up to 2 ml with a threshold of 0.075 AU (B+D) Size exclusion of mCherry on Superdex Sephacryl S-200 with 10 mmol/l Tris, 150 mmol/l NaCl, pH 8. The program was 1 ml elution buffer, 5.2 ml load and 121 ml elution buffer. Flow rate was 0.5 ml/min. Fraction were collected up to 3 ml with a threshold of 0.075 AU. Loaded was the elution fraction of the HIC chromatography. Divergent: (B) The threshold for the SEC was too low, therefore, the target elution fraction wasn't collected. (D) The SEC run was abridged after elution of the target fraction. This figure is from Minkner et al. (2020) under license by Elsevier B.V. (<https://doi.org/10.1016/j.jchromb.2019.121964>)

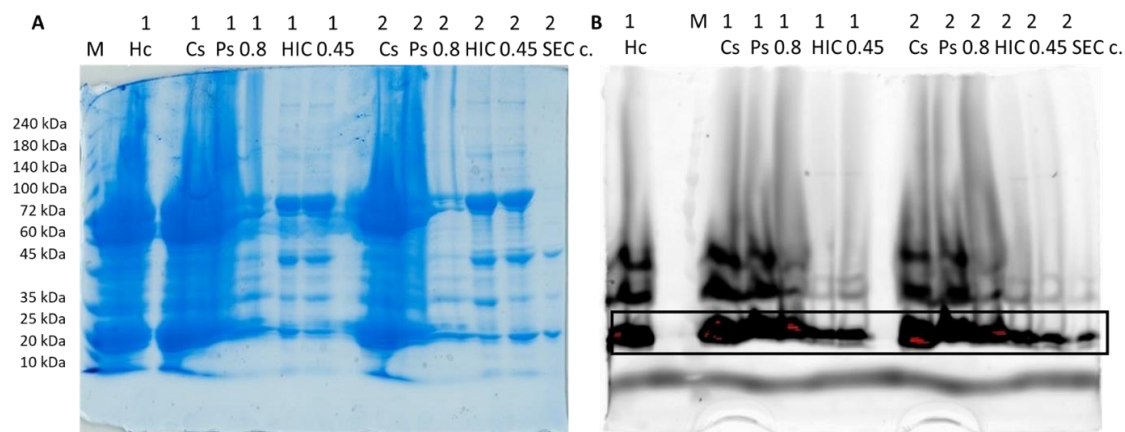


Fig. 32: Results of the two-step chromatography protocol for mCherry purification 2 run 1 and run 2 Coomassie blue staining SDS-gel (A) of the fractions in comparison with fluorescence Image (B). On each line 10 μ l was loaded. On the SDS-PAGE it was 8 μ l sample to 22 μ l dilution and on the Fluorescence image it was 10 μ l to 24 μ l dilution. Hc: crude haemolymph; Cs: 17800 g, 10 min centrifugation supernatant; Ps: 2.5 % PEG precipitation supernatant; M is Marker; 0.8: 0.8 μ m filtration of supernatant; HIC: HIC elution fraction with red fluorescence; SEC c.: SEC pool concentrated with Amicon 3K; The numbers 1 and 2 indicate if the sample belongs to run 1 or 2; black boxes indicate mCherry fluorescence. This figure is from Minkner et al. (2020) under license by Elsevier B.V. (<https://doi.org/10.1016/j.jchromb.2019.121964>)

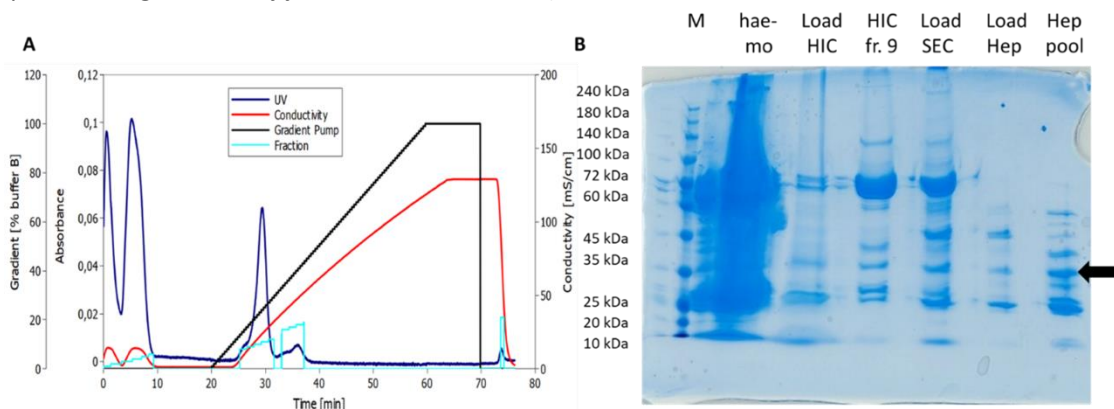


Fig. 33: Results of the heparin chromatography step (A) mCherry on HiTrap Heparin HP with 10 mM NaH_2PO_4 , pH 7. Elution was done with a linear gradient up to 2 mol/ NaCl. The program was 2 ml binding buffer, 5.2 ml load, 4 CV binding buffer and 12 CV linear gradient up to 100 % elution buffer. After this, 3 CV 100 % elution buffer, followed from 2 CV binding buffer. Flow rate was 1.5 ml/min and for load 1 ml/min. Fraction were collected up to 2 ml with a threshold of 0.003. (B) CBB staining of the purification protocol. On each line 15 μ l was loaded. On the SDS-PAGE it was 8 μ l sample to 22 μ l dilution. M is Marker; haemo: crude haemolymph; Load HIC: Sample after pre-treatment; HIC fr. 9: Flow through fraction 9 of the HIC; Load SEC: Pooled HIC pool; Load Hep: Pooled SEC elution pool; Hep pool: With Amicon 3K concentrated Heparin flow through pool; black arrow indicates mCherry. This figure is from Minkner et al. (2020) under license by Elsevier B.V. (<https://doi.org/10.1016/j.jchromb.2019.121964>)

To remove the large amounts of remaining impurities with sizes of approximately 45 kDa and 25 kDa (Fig. 30), CHT, strong AIEQ HP and heparin affinity columns were investigated, but as not only was no separation achieved by Q HP and CHT columns, but both had also a high loss of the target protein (data not shown). On the other hand, it was hypothesized that

the mCherry will most likely not bind on the heparin column, but that the host proteins will more likely bind to heparin. The reason is, that plasma proteins have usually a high affinity for heparin. As expected, mCherry was in the flow through, but unfortunately only one of the remaining impurities bound to the column (**Fig. 33**). For this 3-step chromatography protocol the heparin elution was changed from a linear to a one-step gradient and successfully repeated. Moreover, as mentioned a Strep-tag purification was used as a purity comparison purification method (**Fig. 34A and B**). In **Table 3** are the results for each step of the densitometry analysis and the protein and DNA assays. The protein and DNA reductions after the heparin step were 99.58 and 99.29 %, respectively, but the mCherry recovery was very low at 1.57%.

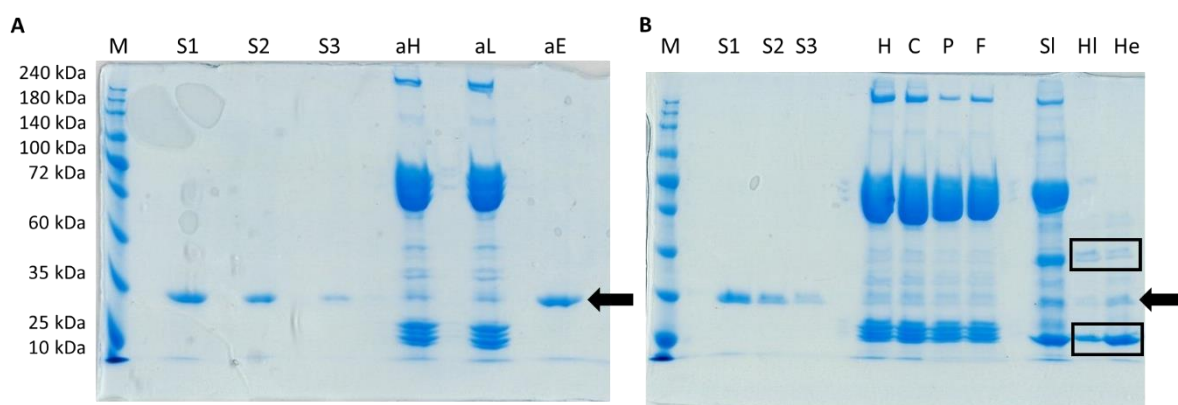


Fig. 34: Coomassie blue staining SDS-gel for mCherry purification protocol without thermal-treatment (A) with mCherry purified using Strep-Tactin affinity. **(B)** With mCherry purified using 3-step protocol. Both gels also contain three standards used for the recovery calculation via densitometry. It was 8 μ l sample to 22 μ l. On each line 15 μ l was loaded. Lane S1: Standard with no dilution (same as aE); Lane S2: Standard in a 1:1 dilution; S3: Standard in a 1:4 dilution; Lane aH: Haemolymph used for affinity purification 1:20; Lane aL: Load for affinity column after 17800 g, 5 min 1:20; Lane aE: Elution fraction of the Strep tag affinity purification; Lane H: haemolymph 1:20; Lane C: centrifugation supernatant 1:20; Lane P: supernatant PEG precipitation 1:20; Lane F: 0.8 μ m filtration 1:20, Load on HIC; Lane SI: Load on SEC; Lane HI: Load on Heparin column; He: With Amicon 3K concentrated Heparin elution pool; M is Marker; Black arrows indicate target protein; Black boxes indicate major remaining impurities or their reduction. This figure is from Minkner et al. (2020) under license by Elsevier B.V. (<https://doi.org/10.1016/j.jchromb.2019.121964>)

Table 3: Results of the mCherry protocol without the thermal treatment. This table is from Minkner et al. (2020) under license by Elsevier B.V. (<https://doi.org/10.1016/j.jchromb.2019.121964>)

Sample	Volume [ml]	mCherry conc [mg/ml]	mCherry amount [mg]	mCherry recovery [%]	Protein amount [mg]	Protein reduction [%]	DNA amount [mg]	DNA reduction [%]
Affinity chromatography								
Affinity Haemolymph	5	0.90	4.49	---	395.7	---	411.7	---
Affinity Load	4.67	0.86	4.02	89.62	313.0	20.91	304.8	25.96
Affinity Elution	1.5	0.12	0.18	4.09	0.2	99.95	2.0	99.52
Three-step protocol								
Haemolymph	5	0.88	4.42	---	329.9	---	463.6	---
Centrifugation supern.	4.25	0.77	3.27	74.09	283.5	14.06	325.1	29.88
PEG preci supernatant	4.82	0.49	2.38	53.88	260.5	21.03	250.7	45.93
Filtered (0.8 mm)	4	0.56	2.25	51.03	195.3	40.79	252.2	45.61
SEC load	3.2	0.10	0.32	7.25	9.0	97.28	20.3	95.63
Heparin load	9	0.02	0.14	3.10	2.8	99.16	11.2	97.58
Heparin elution (FT) conc.	1.7	0.04	0.07	1.57	1.4	99.58	3.3	99.29

4.3.6. Improved purification protocol with additional thermal treatment

This result so far was not satisfying, because the three-step protocol was not comparable to affinity chromatography. Therefore, to further reduce the protein amounts before the chromatography steps a thermal treatment was investigated. Small scale experiments for the parallel RSV-LP project had shown that 30 min treatment at 30°C or 40°C was not enough for haemolymph protein denaturation (**data not shown/see also 7.3.2.**), but with increasing temperature, more and more proteins were denatured and could be removed. During a small scaled screening with 1 ml haemolymph, no mCherry denatured visible even at 70°C, but at a bigger scale with 5 ml, the pellet showed a weak pink colour (**data not shown**); but the mCherry denaturation was significantly decreased by decreasing the incubation time to 20

min at 70°C. The previous protocol was with this thermal treatment upgraded (**Fig. 35**) and showed a significant improvement in purity. Furthermore, during the PEG precipitation step there was only a very weak pellet and the CBB staining also showed no visible differences, so that this step can be omitted (**Fig. 36**). Similar unnecessary was the heparin column chromatography step considered, because the final purity was only slightly improved after SEC purification (**Fig. 36**). Most proteins were removed by the butyl column and remaining ones were removed during the polishing step with the SEC. The mCherry recovery for each step was roughly calculated using densitometry (**Table 4**). As standards three different dilutions of affinity Strep-tag purified mCherry were used for mCherry quantification. The improved 3-step protocol achieved an overall recovery of 5.78 %, compared to 4.09 % with Strep-tag affinity purification. Both were calculated using the CBB band intensity at 35 kDa from the crude and following samples, but as already mentioned, we hypothesise that in the crude sample at the size of 35 kDa (**Lane H of Fig. 36**) were still other host cell proteins or denatured/miss-

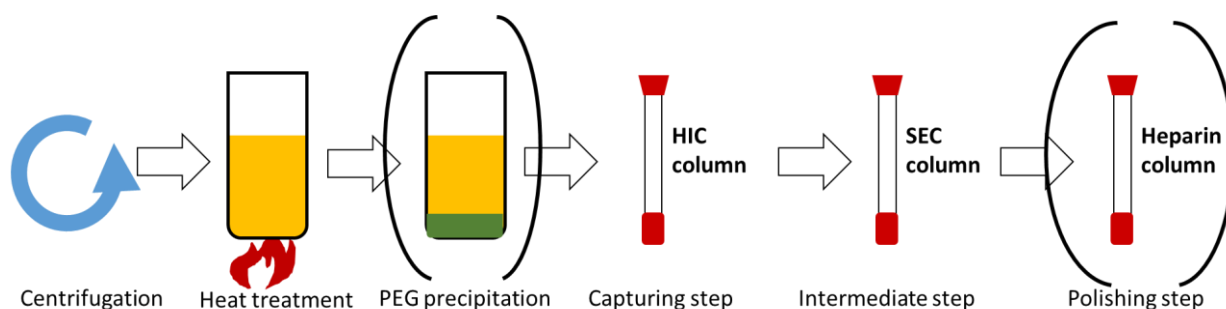
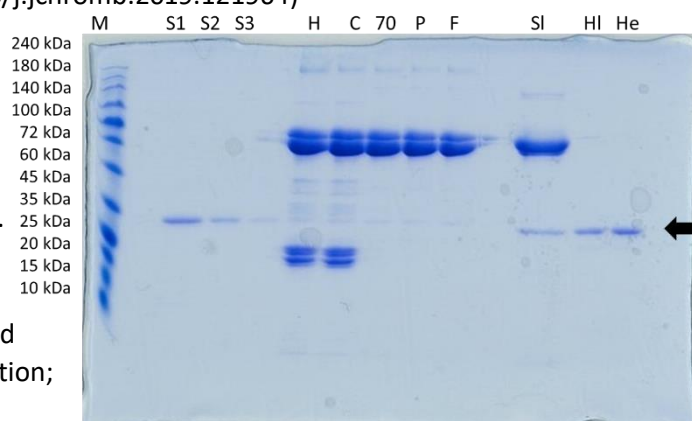


Fig. 35: A short summary of the final 3-step chromatography purification protocol including the pre-treatment. Whereby the PEG 6000 precipitation step can be omitted and if not necessary, the polishing step with the Heparin column also. This figure is from Minkner et al. (2020) under license by Elsevier B.V. (<https://doi.org/10.1016/j.jchromb.2019.121964>)

Fig. 36 (right): Coomassie blue staining SDS-gel with mCherry purified using 3-step protocol with thermal-treatment.

It also contains three standards used for the recovery calculation via densitometry. It was 8 µl sample to 22 µl. On each line 15 µl was loaded. Lane S1: Standard with no dilution (same as aE); Lane S2: Standard in a 1:1 dilution; S3: Standard in a 1:4 dilution; Lane H: haemolymph 1:20;

Lane C: centrifugation supernatant 1:20; Lane 70: supernatant after 70°C treatment with followed centrifugation 1:20; Lane P: supernatant PEG precipitation 1:20; Lane F: 0.8 µm filtration 1:20, Load on HIC; Lane SI: Load on SEC; Lane HI: Load on Heparin column; He: With Amicon 3K concentrated Heparin elution pool; M is Marker; Black arrows indicate target protein. This figure is from Minkner et al. (2020) under license by Elsevier B.V. (<https://doi.org/10.1016/j.jchromb.2019.121964>)



expressed mCherry which were removed from the final purified sample. This is the reason for the theoretical recovery calculation problem. Therefore, the recovery of the functional mCherry from the Strep-tag method and our 3-step protocol should be actually significantly higher than theoretically calculated. Another point is that this recovery is paradoxically quite high compared to the other methods. The protocol without thermal treatment had one step less, but only 1.57 % recovery, and the even shorter affinity purification protocol had 4.09 %. In **Table 4**, purification results were all summarized. Furthermore, further improvement can be done for the HIC step in regards to the final recovery and the sample loading amount. The loading for the column was overloaded, because mCherry was still partly in the flow-through fraction. To ensure a sufficient concentration in the elution fraction for the following steps, the loading amount was not reduced. To sum it up, the 3-step protocol achieved a DNA reduction of over 99 %, similar to the comparison method and protein reduction was over 99.98 % and 99.95 % for them, respectively (**Table 4**).

Table 4: Results of the mCherry purification with and without thermal treatment compared to affinity tag purification. This figure is from Minkner et al. (2020) under license by Elsevier B.V. (<https://doi.org/10.1016/j.jchromb.2019.121964>)

Sample	Volume [ml]	mCherry conc [mg/ml]	mCherry amount [mg]	mCherry recovery [%]	Protein amount [mg]	Protein reduction [%]	DNA amount [mg]	DNA reduction [%]
Affinity chromatography								
Hemolymph	5	0.90	4.5	---	395.7	---	411.7	---
Loading	4.67	0.86	4.0	89.62	313.0	20.91	304.8	25.96
Elution	1.5	0.12	0.2	4.09	0.2	99.95	2.0	99.52
Three-step purification								
Hemolymph	6	0.54	3.3	---	434.8	---	147.8	---
Centrifugation supernatant	5.77	0.44	2.5	78.04	375.2	13.69	127.9	13.46
70°C supernatant	5	0.39	2.0	60.26	225.5	48.13	88.2	31.04
PEG precipitation supernatant	5.41	0.35	1.9	58.59	223.4	48.63	97.6	23.69
0.45 µm Filtered	4.8	0.35	1.7	52.20	166.4	61.74	105.6	17.49
Butyl elution	6.1	0.06	0.4	11.46	13.7	96.86	10.4	91.85
SEC elution conc.	2.75	0.08	0.2	6.75	1.1	99.75	3.8	97.02
Heparin Flow-through conc.	1.5	0.13	0.2	5.78	0.7	99.84	2.0	98.41
Heparin elution fr. 7 conc.	0.98	Not possible	Not possible	Not possible	0.1	99.98	1.2	99.03
Three-step purification without heat treatment								
Heparin flow-through conc.	1.7	0.04	0.07	1.57	1.4	99.58	3.3	99.29

4.3.7. Purity comparison using capillary electrophoresis

The purity of the purified samples was analysed with capillary electrophoresis sodium dodecyl sulphate (CE-SDS) (**Fig. 37 and 38**). The protocol without thermal treatment achieved a very low purity of 11 % by densitometry and 14.86 % by CE (**Fig 39, Table 5**). However, the protocol with thermal treatment achieved 85.45 % and 43.60 % purity by densitometry and

CE, respectively (**Fig. 37B; Table 6**). In opposite, a purity of 100 % by densitometry and 63.69 % by CE was achieved for affinity tag purification (**Fig. 37A, Table 7**). With these results the thermal treatment proved itself as beneficial for the purification and the CE as superior for purity analysis. The molecular weight of the CE analysis was indicated with an internal standard (**Fig. 38**), and this led to a different molecular mass for the mCherry than the theoretical mass of approximately 34.5 kDa, which itself was already confirmed by SDS-PAGE. Therefore, affinity purification resulted in a (apparent) molecular weight of 40.8 kDa, and for thermal treatment protocol 43 kDa. This size difference is curious and therefore, subjected to further investigations.

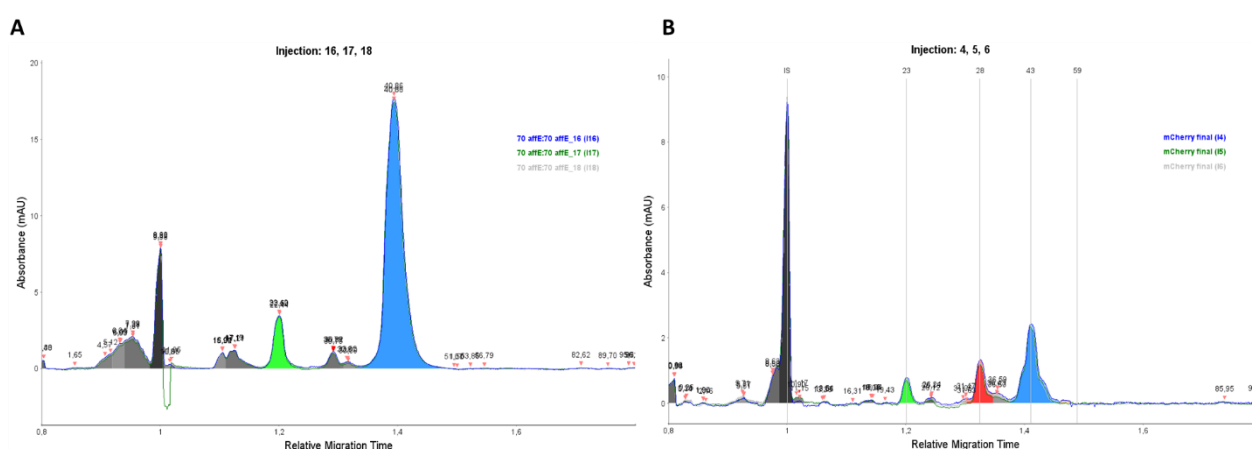


Fig. 37: This is the overlay of three electropherograms respectively from the purification protocols. (A) shows the purification with the Strep tag affinity column. (B) shows the purification using our proposed protocol in full length. The target protein mCherry is located at 40.8 or 43 relative migration time respectively. Each different colour indicates the area under the curve for the peaks. This figure is from Minkner et al. (2020) under license by Elsevier B.V. (<https://doi.org/10.1016/j.jchromb.2019.121964>)

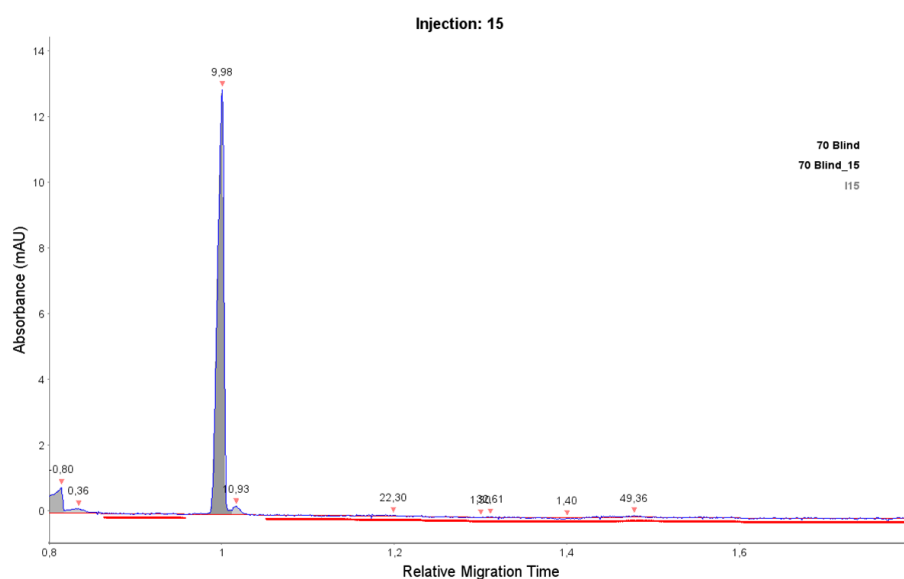


Fig. 38 (left): CE-SDS for internal standard. This is the blind electropherograms for the purification protocol with the Strep tag affinity column. The run only contains the internal standard (IS) at 9.98 relative migration time. This blind run stands representative for all blind runs. This figure is from Minkner et al. (2020) under license by Elsevier B.V. (<https://doi.org/10.1016/j.jchromb.2019.121964>)

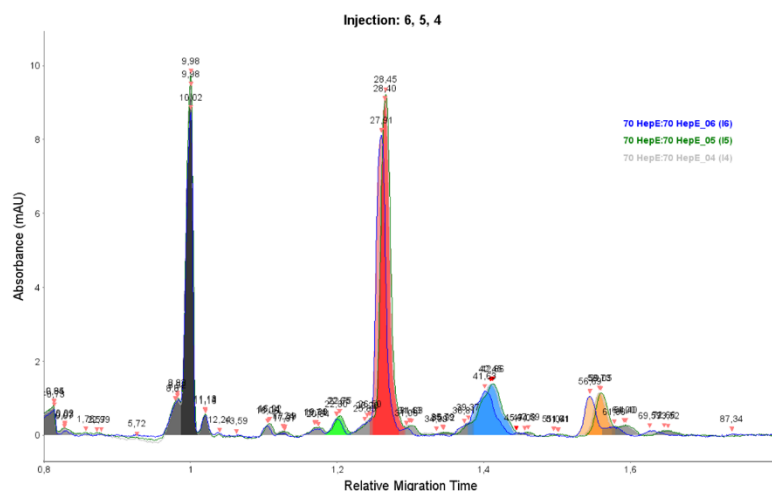


Fig. 39: CED-SDS of the proposed purification protocol without heat-treatment. This is the overlay of the three electropherograms from the purification protocol without heat treatment. Here the molecular weight of the mCherry is around 42 kDa. Each different colour indicates the area under the curve for the peaks. This figure is from Minkner et al. (2020) under license by Elsevier B.V. (<https://doi.org/10.1016/j.jchromb.2019.121964>)

Table 5: CE-SDS mean values, their standard deviation (SDV) and their relative standard (RSD) deviation calculated from the three injections of the purification protocol without heat treatment. This table is from Minkner et al. (2020) under license by Elsevier B.V.

MW	SDV	RSD	%Area	SDV	RSD
8.886	0.052	0.589	7.605	0.924	12.155
12.237			0.027		
13.588			0.000		
16.139	0.066	0.410	1.507	0.126	8.333
17.335	0.069	0.398	0.474	0.177	37.286
19.888	0.120	0.604	1.614	0.124	7.666
22.567	0.195	0.863	3.473	0.129	3.700
26.176	0.272	1.039	2.815	0.118	4.199
28.255	0.243	0.861	53.554	0.554	1.034
31.372	0.236	0.754	1.483	0.271	18.247
35.567	0.411	1.156	1.115	1.229	110.291
39.089	0.281	0.720	1.813	0.252	13.902
42.248	0.446	1.055	14.858	0.149	1.002
46.872	0.688	1.469	0.402	0.054	13.513
51.456	0.294	0.571	0.124	0.038	30.628
58.156	1.046	1.798	6.655	0.071	1.066
63.425	1.105	1.742	2.093	0.145	6.933
71.921	1.687	2.345	0.974	0.070	7.214
87.342	0.000	0.000	0.113		

Table 6: CE-SDS mean values, their standard deviation (SDV) and their relative standard (RSD) deviation calculated from the three injections of the purification protocol with heat treatment.

This table is from Minkner et al. (2020) under license by Elsevier B.V. (<https://doi.org/10.1016/j.jchromb.2019.121964>)

MW	SDV	RSD	%Area	SDV	RSD
1.866	0.042	2.274	0.127	0.101	80.183
5.765	0.047	0.812	3.700	1.572	42.495
8.613	0.027	0.310	18.169	2.260	12.442
13.496	0.098	0.727	0.566	0.283	50.062
18.157	0.079	0.436	1.456	0.233	15.969
19.434			0.054		
22.379	0.071	0.319	8.806	0.221	2.511
26.184	0.076	0.292	1.927	0.484	25.120
29.550	2.975	10.066	0.730	0.475	65.064
33.725	0.080	0.238	17.077	0.587	3.440
36.550	0.103	0.282	3.548	0.971	27.369
42.214	0.107	0.253	43.597	2.077	4.765
47.676			0.914		
85.951			0.407		
97.020	1.845	1.902	0.523	0.075	14.307

Table 7: CE-SDS mean values, their standard deviation (SDV) and their relative standard (RSD) deviation calculated from the three injections of the affinity tag purification. This table is from Minkner et al. (2020) under license by Elsevier B.V. (<https://doi.org/10.1016/j.jchromb.2019.121964>)

MW	SDV	RSD	%Area	SDV	RSD
4.849	0.276	5.692	3.128	0.209	6.678
6.053	0.028	0.469	5.815	1.482	25.491
7.292	0.015	0.203	9.509	0.360	3.781
16.007	0.031	0.192	2.014	0.056	2.789
17.187	0.016	0.095	4.292	0.113	2.621
22.455	0.032	0.144	9.083	0.370	4.073
30.784	0.030	0.096	2.352	0.230	9.762
32.974	0.122	0.369	0.992	0.157	15.785
40.842	0.027	0.065	63.685	1.449	2.275
56.791			0.031		
86.160	3.542	4.111	0.065	0.063	96.706
96.327	0.717	0.744	0.118	0.026	21.860

4.4. Conclusion

The host protein burden during purification was significantly lessened and mCherry was successfully purified with an up-scalable protocol. Moreover, this protocol was successful repeated. Strong centrifugal forces were applied to achieve a good separation from cell debris and high-molecular weight proteins, because of the low molecular mass of mCherry. Most host cell proteins were removed with the 70°C thermal treatment without noticeable mCherry loss. Followed by HIC and SEC the mCherry was purified to a high degree, but some minor traces of proteins still remained. By heparin column in a flow-through mode one of those remaining proteins was removed. Separation of the host proteins was difficult which was obvious during the chromatography experiments. Especially the elution behaviours of the main impurities at 60–80 kDa are ambivalent. During HIC there present in the flow-through, but also in the elution fractions. Moreover, binding behaviour could be reversed compared to the GFP-β3GnT2 purification project (**Fig. 16; Fig. 24**). Moreover, the haemolymph batch and especially the amount of used preservative played also a crucial role in the purification process. With increasing preservative concentration, the recovery was negatively affected, because not were only more host proteins denatured, but also the target protein.

For this mCherry project were several different pre-treatments and chromatography principles investigated based on the experience from the GFP-β3GnT2 project and again, for purification of the target protein only some were useful (**Fig. 40**). Only with a later introduced heat treatment the amount of host protein was significantly reduced. But in addition, this protocol has further optimization possibilities. 2–3 SEC columns in a row or a better performing SEC column as the 2nd chromatography step should be able to significantly improve

the separation resolution of the target protein and therefore, the 3rd step would be not necessary, which would also increase the recovery. The heat-treatment was introduced because the former protocol did not achieve a sufficient reduction of the unwanted proteins and we had to lessen the protein amount already before the chromatography steps. The different chromatography principles at our disposal were after all not able to further separate the proteins. Nevertheless, a significant protein reduction was obtained, but the thermal treatment limited the process to only partially heat stable proteins. However, it was as later described also shown that it already sufficient to use 50°C to denature high amount of silkworm proteins. In the end the possibility to purify thermal stable proteins from the silkworm larval haemolymph with a high purity was demonstrated. Moreover, these methods can be easily be up-scaled for industrial use.



Fig. 40 (left): Investigated chromatography methods. Here are all used chromatography methods listed with were investigated for the purification of mCherry. The left row names the used principle, the middle row for what purpose and the last row summarize very shortly the outcome. ALEX: Anion exchange chromatography; HIC: Hydrophobic interaction chromatography; CHT: Ceramic Hydroxyapatite; SEC: Size exclusion chromatography. This figure is from Minkner et al. (2020) under license by Elsevier B.V. (<https://doi.org/10.1016/j.jchromb.2019.121964>)

5. Purification of non-enveloped VLPs from silkworm fat body

5.1. Introduction

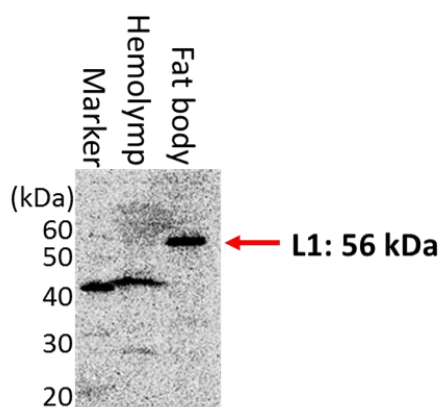


Fig. 41: Confirmation of expression of HPV 6b L1 protein by western blotting. The size of the HPV 6b L1 protein was 56 kDa, and the expression of HPV 6b L1 protein was confirmed in the fat body sample. Primary antibody was a monoclonal anti-DYKDDDDK antibody and the secondary antibody was an anti-mouse IgG-HRP antibody. Red arrow indicates L1 protein. This figure is from Minkner et al. (2018) under license by Elsevier B.V. (<https://doi.org/10.1016/j.jchromb.2018.08.007>).

To establish a new purification protocol for VLPs expressed in silkworms, only by chromatographic methods, self-assembled human papillomavirus (HPV) L1 VLPs, non-enveloped VLPs, were expressed in silkworm. HPV 6b L1 protein expression was confirmed in the silkworm fat body, but not in the haemolymph (Fig. 41) and the molecular mass of the protein was determined by western blotting as 56 kDa. Therefore, the haemolymph was discarded, only the fat body collected and the HPV 6b L1 protein VLP purified from it.

Three different chromatography stages in series were the base of this protocol. AIEC served as capturing and for the DNA separation. For baculovirus separation, a CHT column was used as intermediate step, because of its metal affinity and cation exchange

dual principle. Polishing was done by heparin affinity and this concentrated the sample after the volume rich 2nd stage-elution. As comparison HPV-VLPs were also purified by sucrose gradient centrifugation and Flag-tag affinity chromatography.

5.2. Specific Material and Methods

5.2.1. Sucrose gradient centrifugation

For concentration and purification of viruses or VLPs. The used ultracentrifuge tubes have a capacity of 4.9 ml. 0.8 ml sucrose (20 % or 30 %) solution was laid as a cushion, 4 ml sample solution was carefully added and centrifuged at 4°C, 122000 × g for 60 min. After washing the pellet with 1 ml PBS, it was resuspended in 1 ml PBS. Starting from the ground the gradient was carefully made with 800 µl 60 % sucrose solution, 700 µl 50 % Sucrose, 700 µl 40 % Sucrose, 700 µl 30 % Sucrose and 700 µl 20 % Sucrose solution. The suspended pellet

was carefully applied at the top and centrifuged at 4°C, 122000 × g for 3 h. The whole gradient was then collected in 500 µl fractions.

5.2.2. FLAG tag affinity purification

For the FLAG-tag purification the affinity gel and elution peptide from Medical & Biological Laboratories was used.

Column procedure:

Protocol was according to company. Briefly, mostly 1 ml affinity gel was used to prepare the column. These was washed with 10 column volume (CV) wash buffer and the sample was applied. The loading flow through could be loaded again on the column. The column is then flushed with washing buffer until the OD280 < 0.01. The elution is done at 4°C with 8 CV of elution buffer, but the first CV had 5 min. time to equilibrate. The flow through was collected in fractions. After this, the column was regenerated with 10 CV of regeneration buffer. The column was stored at 2-8°C with 2 CV of storage buffer.

Batch procedure:

Protocol was similar to the column version. 100 µg affinity gel was placed in a micro tube and incubated with the 7 CV sample. This was shortly vortexed and for at least 1 h incubated at 4°C under steadily mixing. After centrifugation 2 min at 4°C, 1500 rpm the supernatant was separately as loading flow through collected and the pellet with washing buffer washed until OD280 < 0.01. The first washing step lasted at least 1 h steadily mixed at 4°C. After every (following) incubation the sample was centrifuged 2 min at 4°C, 1500. The elution was done 2 times at 4 °C with 5 CV elution buffer each 1 h incubated steadily mixed. Regeneration was done steadily mixed for 1 h with 10 CV at 4°C. The batch was stored at 4°C with 3 CV storage buffer.

5.2.3. Agarose gel electrophoresis for DNA analysis

For the gel electrophoresis were agarose gels, in most cases 1 % in TAE (Tris acetate EDTA) with 0.2 µl/20 ml Ethidium bromide, used. The samples were directly put on the gel. Detection was done with ultra-violet light. Determination of the size was done through an also carried standard (1 Kb DNA Ladder, Smobio, Tokyo, Japan).

5.3. Results and Discussion

5.3.1. Screening of Ion-exchange chromatography and reproducibility test

HPV-L1 DNA and proteins were found in the flow through of the cation-exchange GigaCap S-650M column (**Fig. 42A**). On the GigaCap Q-650M with the anion exchange principle, negatively charged DNA bound to the column and was later eluted than the bound VLPs (**Fig. 42B**). Compared to GigaCap Q-650M, UNOsphere Q (BioRad, Hercules, CA, USA) separated DNA and proteins poorly (**Fig. 43A and B**). For this reason, the anion exchanger GigaCap Q-650M was designated as the 1st stage column for the purification protocol.

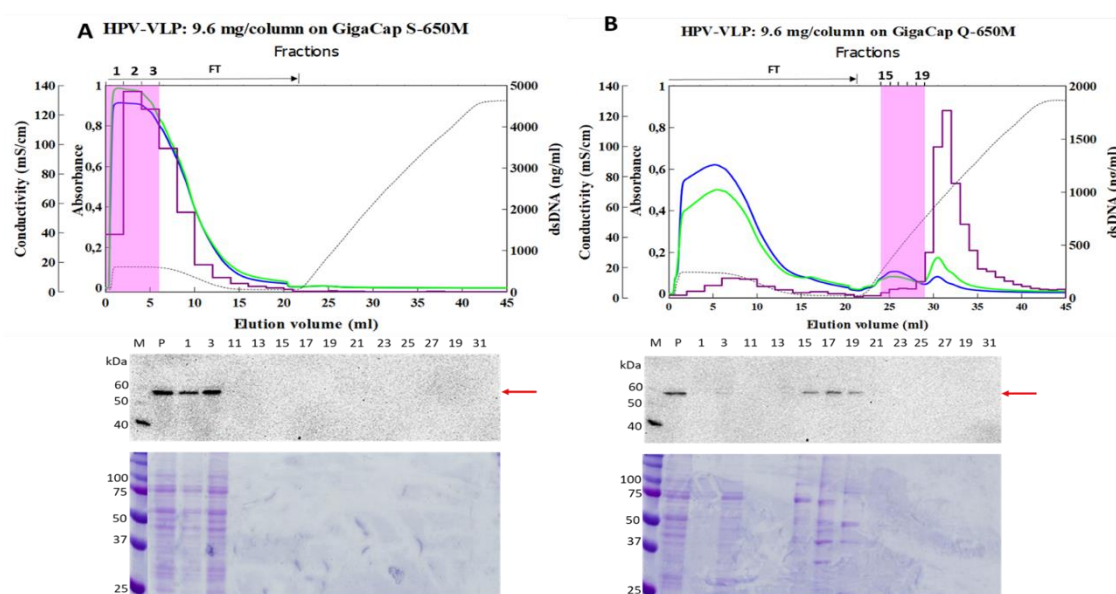


Fig. 42: Chromatogram, the SDS-PAGE and Western blot results of the (A) cation exchange column GigaCap S-650M and (B) the anion exchange column GigaCap Q-650M. Flow rate was 1 ml/min and in both cases 9.6 ml sample was loaded. The linear gradient was done within 20 ml up to 1.5 mol/l NaCl in 10 mmol/l sodium phosphate buffer (pH 7.2). Upper panels show of the chromatogram and lower panels shows the SDS-PAGE and Western blot.

Blue line: absorbance at 280 nm; Green lines: absorbance at 260 nm; Dotted lines: conductivity (mS/cm); Purple lines: DNA concentration (ng/ml); Pink areas: elution position of HPV L1 confirmed by western blotting; M: molecular marker; P: load. Numbers indicate fractions. Flow through and elution fractions are 1–12 and 13–35, respectively. Red arrows indicate L1 protein.

This figure is from Minkner et al. (2018) under license by Elsevier B.V. (<https://doi.org/10.1016/j.jchromb.2018.08.007>).

Reproducibility of GigaCap Q-650M column chromatography was confirmed by purification of five different batches of HPV6b L1. In each case similar elution behaviour of DNA and protein was observed (**Fig. 44**). Reproducibility was confirmed on a 12-fold up-scaled GigaCap Q-650M (35 mm × φ 16 mm) column by 6 runs with the same conditions (**Fig. 45**). The elution behaviour of DNA and HPV L1 on this larger column was almost identical as shown in **Figure 44**.

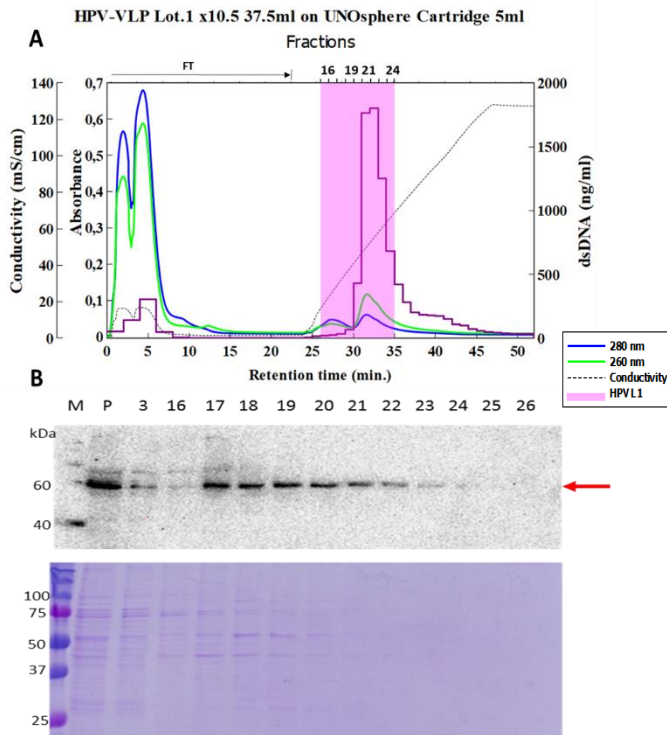


Fig. 43 (left): (A) Chromatogram of the anion exchange column and (B) SDS-PAGE and Western blot of UNOsphere Q column. Flow rate was 7.5 ml/min. The linear gradient was done within 172.5 ml up to 1.5 mol/l NaCl in 10 mmol/l sodium phosphate buffer (pH 7.2). Blue lines: absorbance at 280 nm; Green lines: absorbance at 260 nm; Dotted lines: conductivity (mS/cm); Purple lines: DNA concentration (ng/ml); Pink areas: elution position of HPV L1 confirmed by western blotting. Flow through and elution fractions are 1–12 and 13–41, respectively. Whereupon the flow through fractions consist of 15 ml and the elution fractions of 7.5 ml. This figure is from Minkner et al. (2018) under license by Elsevier B.V. (<https://doi.org/10.1016/j.jchromb.2018.08.007>).

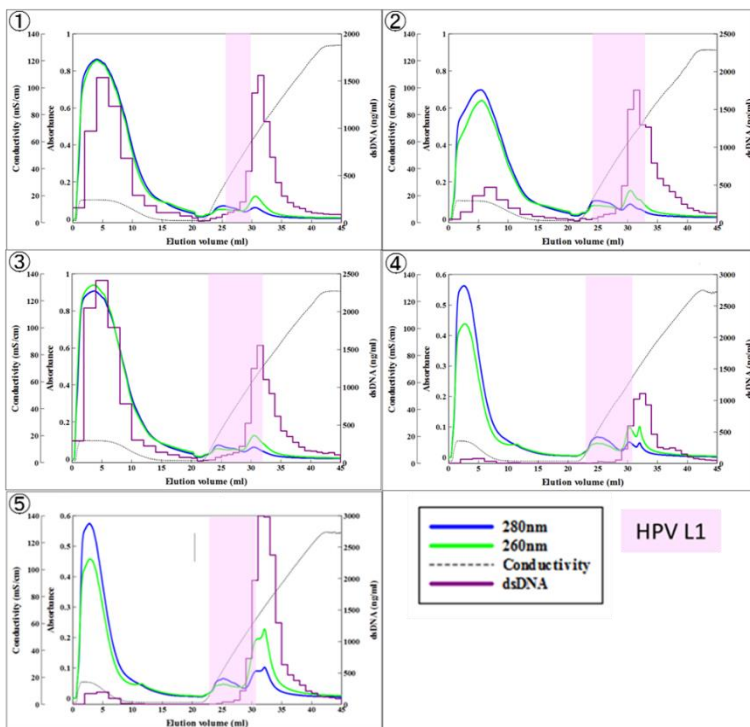


Fig. 44 (left): GigaCap Q-650M Column Elution Check 1 (f 4.6 x 35 mm). A different batch HPV6b L1 expressed in silkworm fat body was carried out five times. DNA and protein show in each case similar elution behavior. (1) Sample was diluted in saline and loaded 2 times (9.6 ml sample); (2) was diluted in PBS and loaded once (9 ml sample); (3) was diluted in PBS and loaded 2 times (9 ml sample); (4) was diluted in saline and loaded once (4.9 ml sample); (5) was diluted in saline and loaded 2 times (4.9 ml sample). Flow rate was 1 ml/min and the linear gradient was done within 20 ml up to 1.5 mol/l NaCl in 10 mmol/l sodium phosphate buffer (pH 7.2). Lines and pink areas are the same as those of Figure 23. This figure is from Minkner et al. (2018) under license by Elsevier B.V. (<https://doi.org/10.1016/j.jchromb.2018.08.007>).

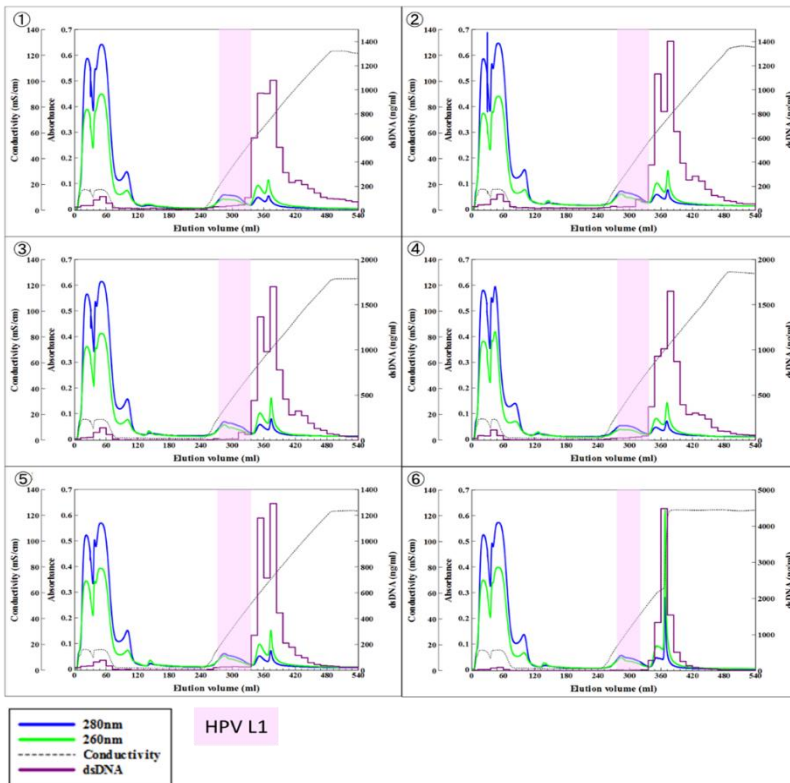


Fig. 45 (left): Confirmation of reproducibility of GigaCap Q-650M using large column (\varnothing 16 x 35 mm). The GigaCap Q-650M column chromatography was up scaled, and the experiment was 6 times repeated. Flow rate was 10 ml/min and the linear gradient was done within 20 ml. For No. (4) 46 ml was loaded, for the other experiments 60 ml. The linear gradient was done within 240 ml up to 1.5 mol/l NaCl in 10 mmol/l sodium phosphate buffer (pH 7.2). The chromatograms 1 to 6 show the same elution behavior. Lines and pink areas are the same as those of Figure 23. This figure is from Minkner et al. (2018) under license by Elsevier B.V. (<https://doi.org/10.1016/j.jchromb.2018.08.007>).

5.3.2. Conditions for the CHT chromatography buffer and gradient analysis

The AIEX purification was followed by CHT chromatography investigations as the 2nd stage. Buffer screening with different buffer pH's showed no changes in the elution position of HPV L1; however, with increasing pH the baculovirus protein BmGP64 eluted earlier (**Fig. 46**). It is already reported, that for viruses such as influenza virus and dengue virus during CHT

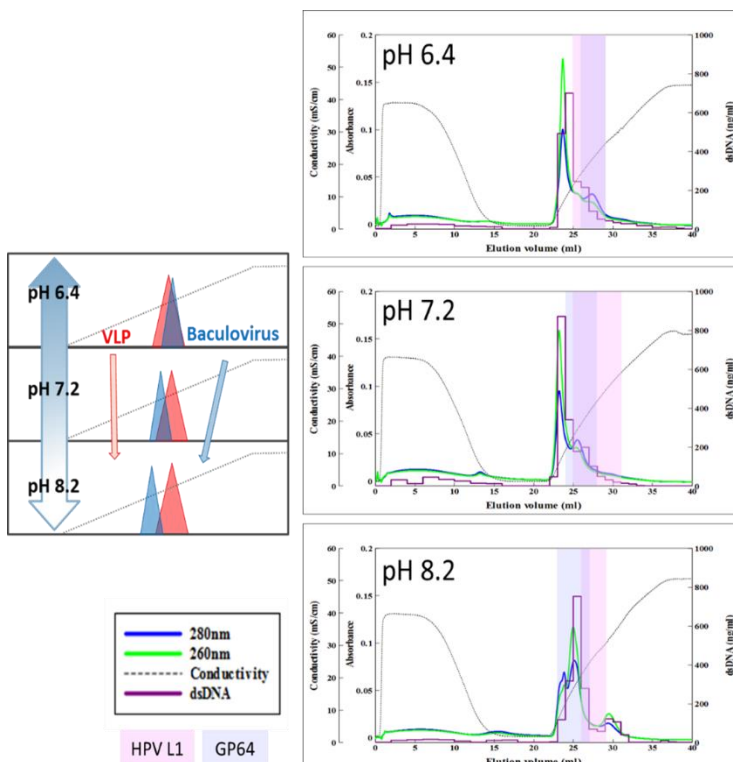


Fig. 46 (left): Effect on pH on the elution behavior of VLP and baculovirus in the CHT column chromatography. These figures show the different elution behavior of VLP and baculovirus with changing pH. Flow rate was 1 ml/min and the linear gradient was done within 15 ml of sodium phosphate gradient (10 mmol/l to 600 mmol/l) at pH 6.4, 7.2 or 8.2. Samples were 10 ml from the AIEX eluate. Blue line: absorbance at 280 nm; Green lines: absorbance at 260 nm; Dotted lines: conductivity (mS/cm); Purple lines: DNA concentration (ng/ml); Pink areas: elution position of HPV L1 confirmed by western blotting; Purple areas: elution position of BmGP64 confirmed by western blotting. **Left side figure:** The shift of VLP and baculovirus corresponded by pH of the elution buffer in CHT column chromatography. This figure is from Minkner et al. (2018) under license by Elsevier B.V. (<https://doi.org/10.1016/j.jchromb.2018.08.007>).

chromatography similar changes in the elution positions can happen [84,111]. After adding NaCl (0.5, 1 and 1.5 mol/l) to the elution buffer, HPV L1, DNA and BmGP64 were eluted together (**Fig. 47**), as shown by SDS-PAGE and western blotting (**data not shown**). Therefore, no NaCl was added in the improved protocol. HPV L1 eluted later and BmGP64 eluted earlier in the linear gradient when the pH was increased; therefore, the increasing of the pH improved the separation efficiency. In most cases DNA elution is delayed by increasing the salt concentration of the buffer. Here was no significant change of the DNA elution position, and the DNA was together eluted with HPV L1 and BmGP64. For improving the purification efficiency five different sodium phosphate gradients (pH 7.2) were tested by changing the starting sodium phosphate concentration of the wash and elution buffer (**Fig. 48**). The contaminants have been removed from the target protein and were eluted in the flow-through fraction at higher sodium phosphate concentrations. However, sodium phosphate gradients of 200 to 600 mmol/l and 250 to 600 mmol/l were deemed as not useful, because HPV 6b L1 was also detected in the flow-through fraction. Therefore, the elution set up using a 150-600 mmol/l sodium phosphate gradient was chosen.

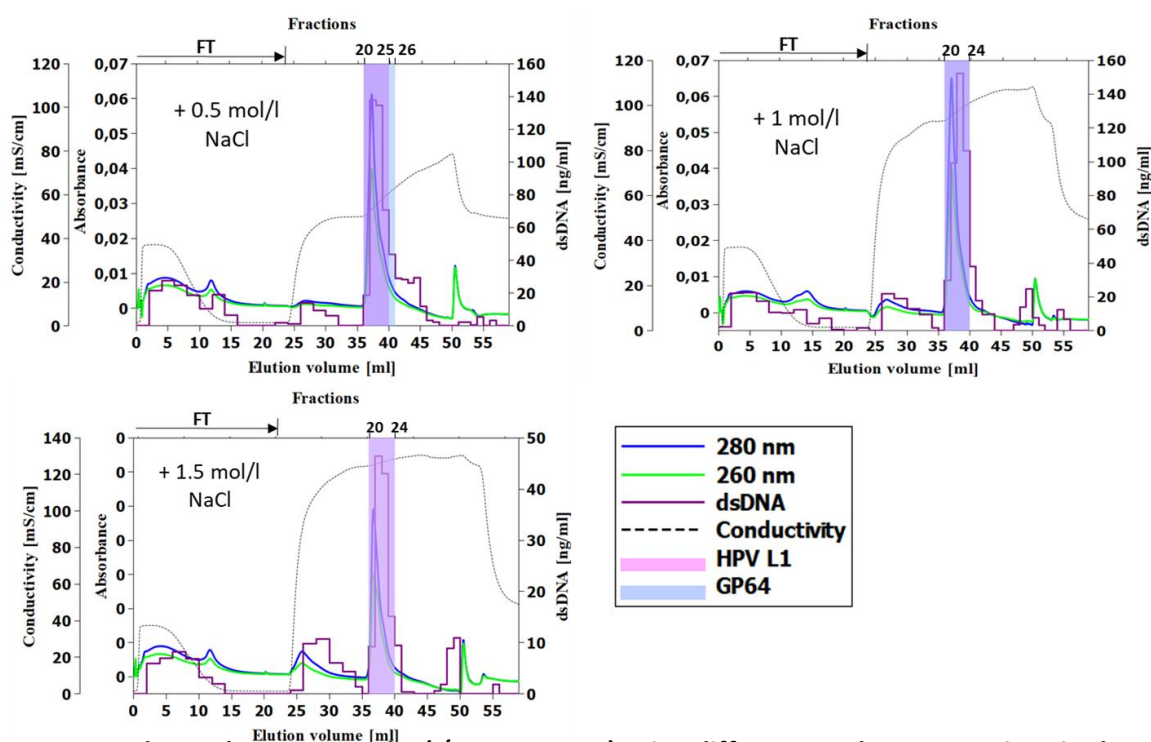


Fig. 47: CHT column chromatography (\varnothing 4.6 x 35 mm) using different NaCl concentrations in the elution buffer. This figure shows the different behavior of the proteins during the purification when the NaCl concentration in the elution buffer was changed. Flow rate was 1 ml/min and the linear gradient was done within 15 ml (10 mmol/l to 600 mmol/l sodium phosphate). Samples were 10 ml from the AIXE eluate. Blue lines: Absorbance at 280 nm; Green lines: absorbance at 260 nm; Dotted lines: conductivity (mS/cm); Purple lines: DNA amount (ng/ml); Pink areas and blue areas indicate elution positions of HPV L1 and BmGP64 confirmed by western blotting, respectively. This figure is from Minkner et al. (2018) under license by Elsevier B.V. (<https://doi.org/10.1016/j.jchromb.2018.08.007>).

Confirmation of the reproducibility of CHT column chromatography could be achieved. Pooled AIEX purification fractions were loaded and CHT chromatography was conducted three times by elution with the 150-600 mmol/l sodium phosphate gradient (pH 7.2). UV peaks and elution position of the HPV L1 were in all chromatograms similar (**Fig. 49**).

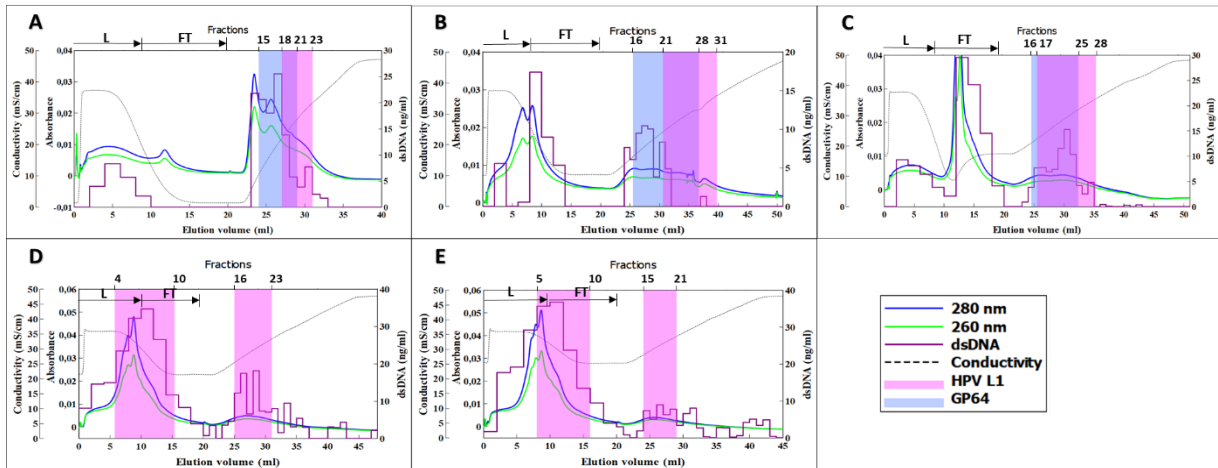


Fig. 48: Investigation of the use of various sodium phosphate gradients to elute proteins in CHT column chromatography. Flow rate was always 1 ml/min. Sodium phosphate (pH 7.2) gradient elution was performed **(A)** from 10 to 600 mmol/l (linear gradient 15 ml), **(B)** from 80 to 600 mmol/l (linear gradient 30 ml), **(C)** from 150 to 600 mmol/l (linear gradient 26 ml), **(D)** from 200 to 600 mmol/l (linear gradient 23 ml) and **(E)** from 250 to 600 mmol/l (linear gradient 20 ml). Loaded sample volume was for (A) to (C) 8 ml and for (D) and (E) 10 ml, because of a batch change. Blue lines: absorbance at 280 nm; green lines: absorbance at 260 nm; dotted lines: conductivity (mS/cm); purple lines: DNA concentration (ng/ml). The pink and purple areas indicate the elution positions of HPV L1 and BmGP64, respectively, as confirmed by western blotting. This figure is from Minkner et al. (2018) under license by Elsevier B.V. (<https://doi.org/10.1016/j.jchromb.2018.08.007>).

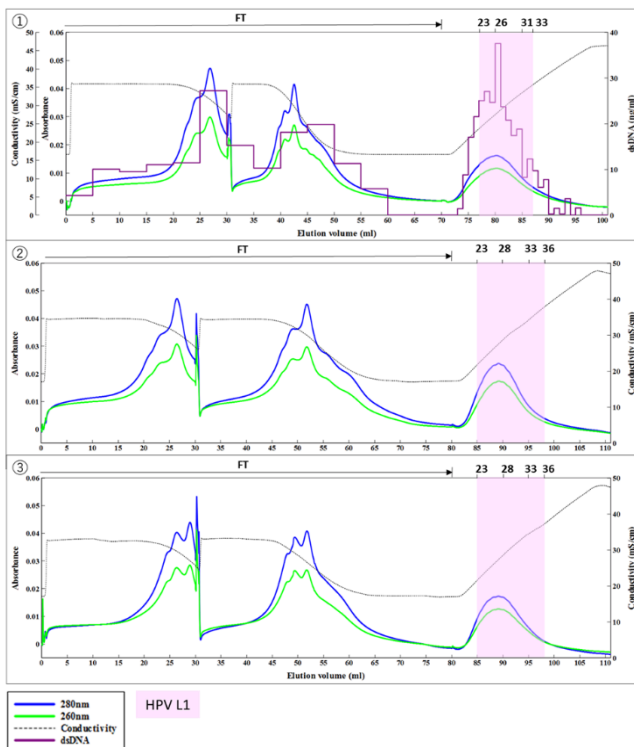


Fig. 49 (left): Reproducibility of CHT column chromatography using standard column (\varnothing 4.6 x 35 mm). Elution gradient was 150 to 600 mmol/l sodium phosphate (pH 7.2) and the experiment was 3 times repeated with loading amounts of 5 (42 ml), 6 (53 ml), and 5.8 (51 ml) mg/column. Flow rate was 1 ml/min and the linear gradient was done within 26 ml. Blue lines: absorbance at 280 nm; Green lines: absorbance at 260 nm; Dotted lines: conductivity (mS/cm); Purple lines: DNA concentration (ng/ml); Pink areas: elution position of HPV L1 confirmed by western blotting. Flow through and elution fractions are 1–15 or 16 and 16 or 17–45 or 47, respectively. Whereupon the flow through fractions consist of 5 ml and the elution fractions of 1 ml. This figure is from Minkner et al. (2018) under license by Elsevier B.V. (<https://doi.org/10.1016/j.jchromb.2018.08.007>).

5.3.3. Three-stage column chromatography

The AIEX chromatography procedure was examined, the CHT chromatography buffers carefully chosen, and an optimized 3-stage column chromatography purification protocol for in silkworm fat body expressed HPV 6b L1 was attempted as described in the following.

5.3.3.1. AIEX GigaCap Q-650M column chromatography

In the first stage AIEX chromatography was used for removing the main amount of DNA, which was also on a large column of GigaCap Q-650M (ϕ 32 × 35 mm) successful (**Fig. 50**). Chromatography on the AIEX column GigaCap Q-650M was performed twice with same

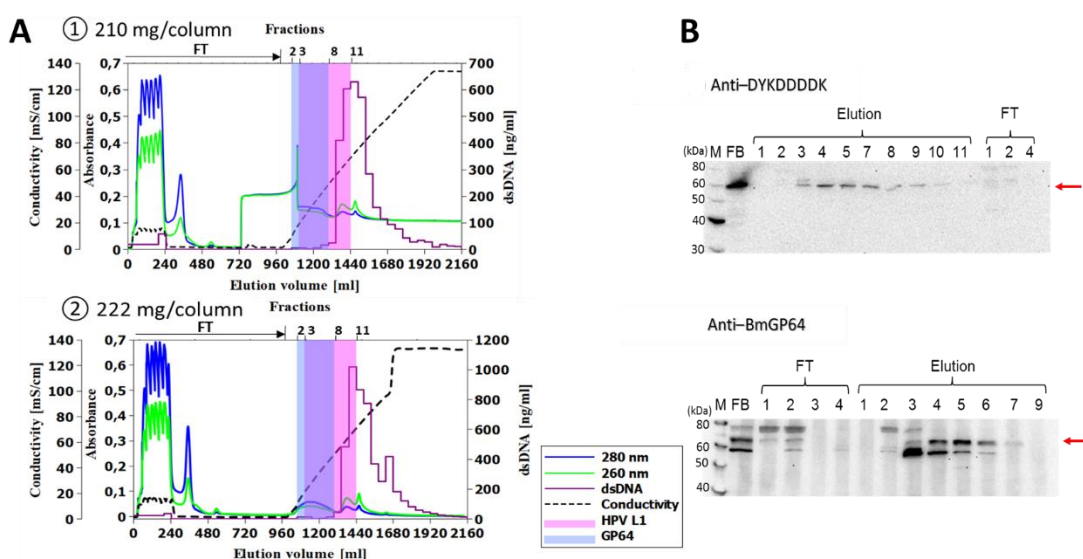


Fig. 50: Purification of HPV 6b L1 by GigaCAP Q-650M column chromatography using a large column (ϕ 32 mm × 35 mm) with a flow rate of 1 ml/min. (A) GigaCap Q-650M column chromatography. Sample was loaded 7 times, each time 30 ml. The linear gradient was performed within 960 ml of 0 – 1.5 mol/l NaCl in a 150 mmol/l sodium phosphate (pH 7.2) buffer. FT: flow-through; other lines and symbols are the same as those used in Figure 1. **(B)** Western blot analysis of the GigaCap Q-650M-column chromatography. The HPV L1 and BmGP64 proteins in each fraction were detected by western blotting using as primary antibody anti-DYKDDDDK tag monoclonal antibody and anti-BmGP64 antibody, respectively. M: Magic Mark XP; FB: HPV 6b L1-expressing fat bodies (9.2 dil + 0.45- μ m filter). The red arrows in (A) and (B) indicate the positions of HPV L1 and BmGP64, respectively. This figure is from Minkner et al. (2018) under license by Elsevier B.V. (<https://doi.org/10.1016/j.jchromb.2018.08.007>).

conditions and compared to the small column (ϕ 16 × 35 mm), almost identical elution behaviour of VLPs and DNA was observed (**Fig. 45**). VLPs were eluted prior to DNA, and therefore, DNA was effectively removed (**Fig. 50A**). Associated western blot results for this purification step are shown in **Figure 50B**. Approximately 31.4 % HPV 6b L1 recovery was achieved in this stage, based on densitometry calculations by comparing the amount of the loading fraction with the amount of the elution fraction.

5.3.3.2. CHT column chromatography

For the separation of baculovirus CHT chromatography was performed as an intermediate stage now on a larger column (ϕ 16 × 35 mm) (Fig. 51). Again, UV pattern and HPV 6b L1 protein elution positions were similar as for the smaller column (ϕ 4.6 × 35 mm) (Fig. 47), which is supported by the western blot analysis (Fig. 52A). A major part of the BmGP64 was in the flow-through fraction and did not bind to the stationary phase (Fig. 52B).

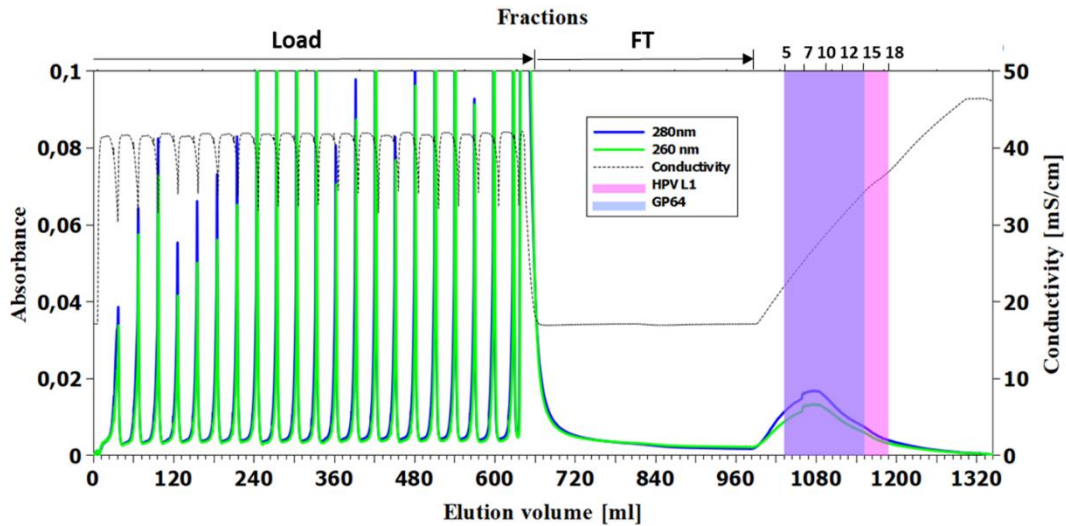


Fig. 51: CHT column chromatography purification using a large column (ϕ 16 × 35 mm) (stage 2). Example chromatogram of the process of the purification on the CHT column. Flow rate was 1 ml/min and the sample were loaded 21 times, each time 30 ml volume. The linear gradient was performed within 312 ml of 150 to 600 mmol/l sodium phosphate (pH 7.2). FT: flow-through; other lines and symbols are the same as those used in Figure 1. This figure is from Minkner et al. (2018) under license by Elsevier B.V. (<https://doi.org/10.1016/j.jchromb.2018.08.007>).

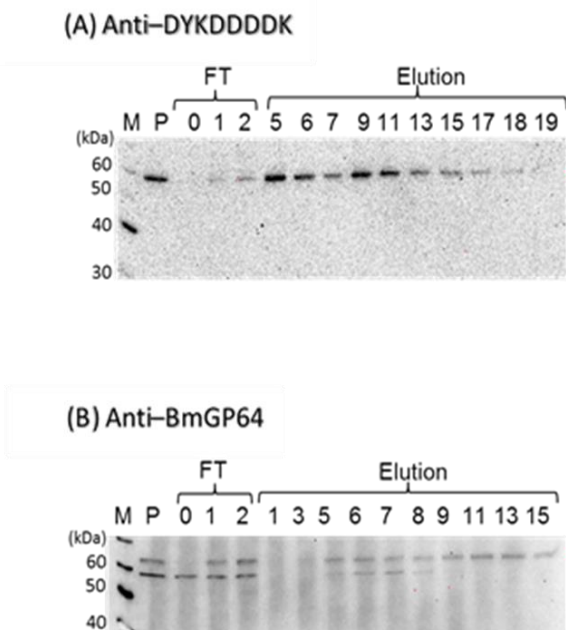


Fig. 52 (left): Western blot analysis of each fraction in the large-scale CHT column chromatography. (A) Detection of HPV L1 protein by western blot. The L1 protein was detected using an anti-DYKDDDDK tag monoclonal antibody as a primary antibody. **(B)** Detection of BmGP64 in each fraction by western blot. BmGP64 was detected using anti-BmGP64 antibody as the primary antibody. M: Magic Mark XP; P: Q sample after column purification pool sample. Red arrows in (A) and (B) indicate position of the HPV L1 and BmGP64, respectively. This figure is from Minkner et al. (2018) under license by Elsevier B.V. (<https://doi.org/10.1016/j.jchromb.2018.08.007>).

HPV 6b L1 recovery was approximately 22.7 % at this stage, based on quantification of band intensity by densitometry.

5.3.3.3. Heparin column chromatography

As 3rd stage of purification, HPV 6b L1 was concentrated by heparin affinity chromatography. Without desalting the pooled CHT elution fraction was loaded on HiTrap Heparin HP. The western blot indicated that HPV 6b L1 was present at around 200 ml of the overall volume, which is slightly behind the main UV absorption peak (Fig. 53B). HPV 6b L1

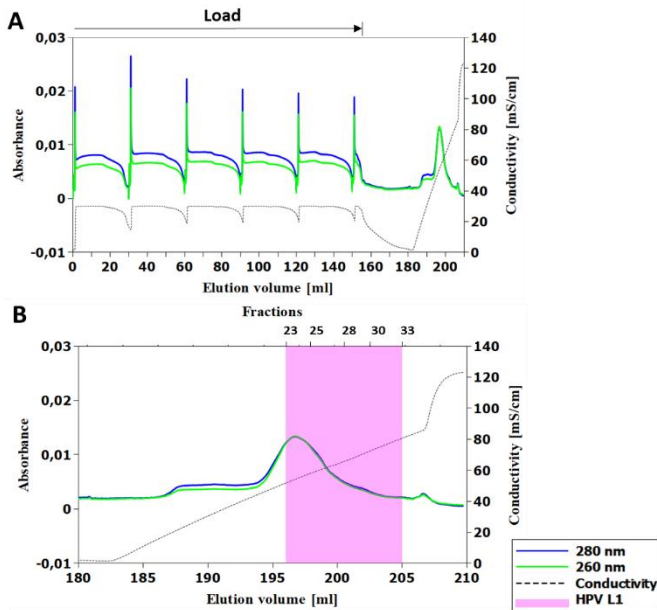


Fig. 53 (left): Chromatogram showing the results of heparin column chromatography (Ø 7 × 25 mm) (stage 3). Both chromatograms show an example of the process of purification on the heparin column. (A) shows the whole process; (B) presents a more detailed and enlarged version. Flow rate was 1 ml/min and 155 ml sample was loaded in 6 steps. The elution was performed within 25 ml of a 0 to 1 mol/l NaCl gradient in a 10 mmol/l sodium phosphate buffer (pH 7.2). Lines and symbols are the same as those used in Figure 1. This figure is from Minkner et al. (2018) under license by Elsevier B.V. (<https://doi.org/10.1016/j.jchromb.2018.08.007>).

(A) Anti-DYKDDDDK

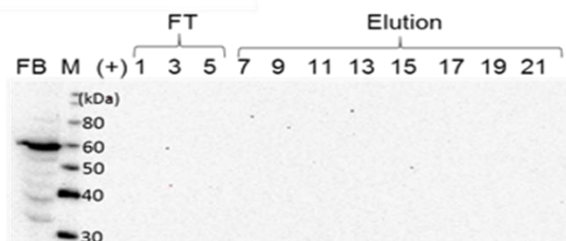
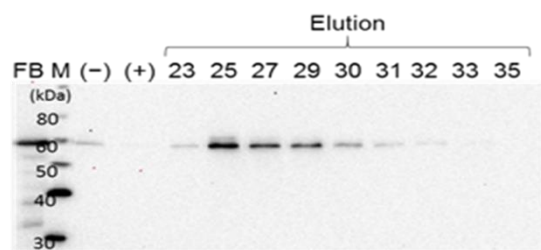
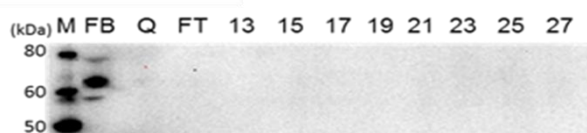


Fig. 54 (left): Fraction analysis in heparin column chromatography. (A) Detection of HPV L1 protein by western blot. Anti-DYKDDDDK tag monoclonal antibody was used as the primary antibody. (B) Detection of BmGP64 by western blot. Anti-BmGP64 antibody was used as the primary antibody. M: Magic Mark XP; FB: HPV 6b L1 expressing fat body (× 10); Q: Large Q pool; (+): CHT Fr.4-17 pool + 0.45 µm filter; (-): CHT Fr.4-17 pool; FT: Flow through; 1 to 35: Fr. No. Red arrows in (A) and (B) indicate position of the HPV L1 and BmGP64, respectively. This figure is from Minkner et al. (2018) under license by Elsevier B.V. (<https://doi.org/10.1016/j.jchromb.2018.08.007>).



(B) Anti-BmGP64



was detected in fractions 23-32 (**Fig. 54A**), but no BmGP64 protein was present in those fractions (**Fig. 54B**). This indicates that BmGP64 and further host cell proteins were removed. Calculated HPV 6b L1 recovery was in this stage approximately 86.9 %, based on densitometry.

5.3.4. Analysis of purified HPV L1

For baculovirus removal investigation during the purification process, samples from HPV 6b L1 fat body, pooled GigaCap Q-650M elution fractions, CHT elution fractions and heparin elution fractions were examined using quantitative PCR (qPCR) for baculovirus DNA and virus titration by TCID₅₀ method (**Table 8**). TCID₅₀ virus measurement revealed that infectious baculovirus was present with 1.07×10^4 pfu/ml in the fat body samples, expressing HPV 6 b L1; however, no infectious baculovirus was detected after AIEX GigaCap Q-650M chromatography (**Table 8**). In the fat body sample baculovirus DNA was present at levels equivalent to 4.00×10^6 pfu/ml, but baculovirus DNA was after the 1st purification stage reduced to 8.85×10^3 pfu/ml, a more than two-fold reduction. Using CHT column as 2nd purification stage of purification didn't remove significantly more baculovirus DNA. To

Table 8: Separation and purification results (each value besides the TCID₅₀ was measured at least twice) This table is from Minkner et al. (2018) under license by Elsevier B.V. (<https://doi.org/10.1016/j.jchromb.2018.08.007>).

Sample	Volume	Densitometry		TCID ₅₀	qPCR	dsDNA (Pico Green)	
	Volume	Gp64	Gp64 Removal	Virus titer	Virus DNA	DNA	Removal
	ml		%	Pfu/ml	Pfu/ml	µg	%
3-Stage purification							
Fat body × 9.2 dil.	380	25.89	---	1.07×10^4	4.00×10^6	670	---
Stage 1: Q pool	672	17.41	48.06	N.D.	8.85×10^3	83	86.4
Stage 2: CHT pool	168	1.46	94.33	N.D.	8.75×10^3	2.9	99.5
Stage 3: Heparin pool	6	0.02	99.92	N.D.	5.82×10^3	0.02	99.997
Sucrose gradient ultracentrifugation							
Fat body 0.45 µm filtered	4				6.17×10^7	125.23	---
Fraction 7	0.5				9.66×10^7	2.95	97.64
Anti-FLAG-tag affinity purification							
Fat body 0.45 µm filtered	10				6.17×10^7	313.07	---
Elution fraction 3	1				1.53×10^4	0.05	99.98
Elution fraction 4	1				1.49×10^4	0.33	99.89

determine whether the qPCR results is because of the presence of baculovirus DNA, the qPCR products were investigated with agarose gel electrophoresis. Whereby only one band with the expected baculovirus DNA size (200 bp) could be confirmed (**data not shown**). This result leads to the conclusion that baculovirus DNA may bind to HPV L1, because removing of the rest baculovirus DNA after the third purification stage was not possible.

DNA assays were performed to investigate the DNA removal rate at each purification stage. More than 80 % of the DNA was removed after the first purification stage with AIEX GigaCap Q-650M (**Table 8**). After the 2nd stage with the CHT column, the majority of the DNA was removed. Followed by the 3rd stage with the heparin column, more than 99 % DNA removal was achieved. The DNA assay results for DDDDK-tag-based affinity chromatography and sucrose density gradient centrifugation purification are also shown in **Table 8**.

Based on densitometry analysis the individual HPV L1 recovery at each purification stage was 31.4 %, 22.7 % and 86.9 %, and the overall recovery 5.5 %. However, using the individual recoveries of each stage the theoretical calculated recovery is 6.19 %. There are two hypotheses for this low yield, even if the reason could not be determined certainty. First, the samples were several times frozen and thawed during the development of the method. Therefore, the possibility of protein denaturation increased. The mentioned second possible reason for the low yield is also associated with the freeze/thaw cycle. After thawing a part of the sample precipitated and completely resuspending the precipitate was not possible. Therefore, before applying to the next column the samples had to be filtered. During this procedure, further loss of HPV L1 may happened. Both effects were shown with an unprocessed fat body sample, which was frozen, thawed, filtered and then this cycle was again was several times repeated (**Fig. 55; Table 9**). The trend of HPV L1 loss during the freezing/thawing cycle was shown with a high variance because of the low number of repeats. During the initial filtration with a specific pore size the main loss of VLP occurred. This was for 0.8 μm filter 64.4 % loss and for the 0.45 μm filter additional 27.6 % loss. Because of the variability, the steadily filtration and the filter change is the effect of the freezing not definitely, but the effect of the filtration is distinct. During the last filtration alone a loss of 57.79 %. To

optimise the protocol and the overall yield of the VLP, this aspect of the method requires further investigation.

Table 9 Influence of freezing/thawing and filtration on the stability/amount of HPV L1 VLP as shown in Fig. 36. This table is from Minkner et al. (2018) under license by Elsevier B.V. (<https://doi.org/10.1016/j.jchromb.2018.08.007>).

	0.8 µm filtered								0.45 µm filtered					
	1 day		2 day		3 day		4 day		5 day		6 day		7 day	
	W/O	Filtered	W/O	Filtered	W/O	Filtered	W/O	Filtered	W/O	Filtered	W/O	Filtered	W/O	Filtered
Average area	286.5	102	117.5	111.5	87.5	87	84.5	100	125	90.5	69	57	77	32.5
Average area [%]	20.07	7.15	8.23	7.81	6.13	6.09	5.92	7.01	8.76	6.34	4.83	3.99	5.39	2.28
Intensity Order of Area	1	5	3	4	8	9	10	6	2	7	12	13	11	14
Degradation [%] (1 is 100 %)	0.00	64.40	58.99	61.08	69.46	69.63	70.51	65.10	56.37	68.41	75.92	80.10	73.12	88.66
Degradation because of freezing [%]	0.00	///	-15.20	///	21.52	///	2.87	///	-25.00	///	23.76	///	-35.09	///
Degradation because of filtering [%]	///	64.40	///	5.11	///	0.57	///	-18.34	///	27.60	///	17.39	///	57.79

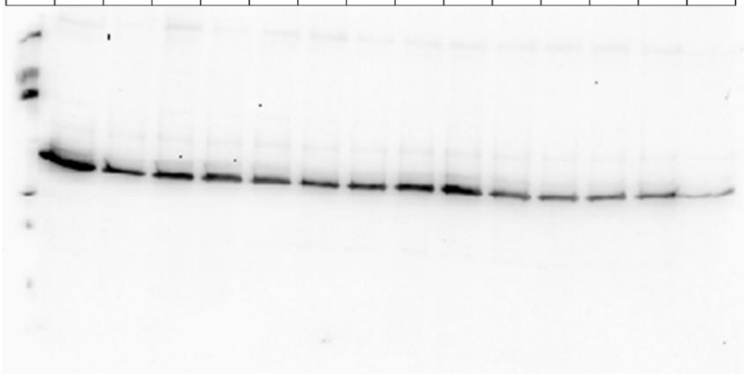
This table shows the degradation of HPV L1 VLPs. The data was obtained using densitometry. The program ImageJ was used to calculate the area of the HPV L1 bands obtained from the Western Blot. The densitometry was done twice with the same base membrane and the Table shows the average values. The trend of HPV L1 loss is clear, even if there is a high variability in the degradation through freezing. On the other hand, the degradation because of filtration is clearly shown. The intensity order shows the descending order of the calculated area size. W/O: sample after thawing/without filtration.

Fig. 55: Influence of freezing/thawing and filtration on the stability/amount of HPV L1 VLP shown with Western Blot.

An original unprocessed fat body sample was several days in a row thawed, filtered and frozen again. Each time two samples were taken for analysis, one after thawing and one after filtration before freezing again. The first four days a 0.8 µm filter was used and for the last three days a 0.45 µm filter was used. Both filters show the reduction of the HPV L1 protein. The decreasing is with the 0.45 µm filter even stronger with the 0.8 µm filter.

For the gel 1:10 dilution of the samples were mixed 1:1 with SDS-buffer and 15 µl was loaded on each lane. M: YesBlot Western Marker I; W/O: sample after thawing/without filtration; Fil: filtrated sample. This figure is from Minkner et al. (2018) under license by Elsevier B.V. (<https://doi.org/10.1016/j.jchromb.2018.08.007>).

M	0.8 µm filtered								0.45 µm filtered					
	1 day		2 day		3 day		4 day		5 day		6 day		7 day	
	W/O	Fil	W/O	Fil	W/O	Fil	W/O	Fil	W/O	Fil	W/O	Fil	W/O	Fil



5.3.5. Comparison with other purification methods

To compare the purification of HPV 6b L1 two other methods were also applied to purify from silkworm fat bodies. After the 3rd stage heparin purification HPV 6b L1 was found in elution fractions 23–26 (**Fig. 56A**). With affinity Flag-tag purification most of the target protein was found in the fourth elution fraction, but more impurities compared to the 3-stage protocol were present (**Fig. 56B**). Of these elution fractions, the third and fourth were used as reference for the purification. It was possible to obtain an overall yield of 350 µg of L1 protein eluted in a volume of 2 ml from originally 10 ml fat body sample.

HPV 6b L1 protein was found in fractions 5-10 together with many impurities, when purified using sucrose density gradient centrifugation (**Fig. 56C**). The DNA assay supported these findings, because of the higher rest DNA concentration by sucrose density gradient purification compared to the affinity-tag purification. Moreover, the latter method had still a higher amount of impurities than those from using the 3-stage protocol. On the one hand,

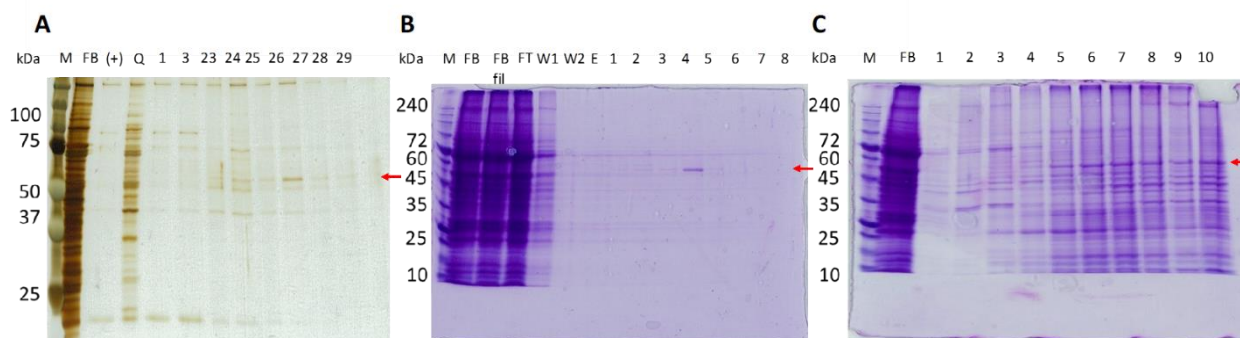


Fig. 56: Comparison of purification methods. (A) Silver stain analysis of SDS-PAGE of fractions from the heparin column chromatography. M: Magic Mark XP; FB: HPV 6b L1 expressing fat body ($\times 10$); (+): CHT Fr. 4-17 pool + 0.45-µm filter; Q: Large Q pool; 1 – 29: Fr. No. (B) CBB staining of anti-DDDDK-tag gel purification results obtained for HPV6b L1. M: Protein Marker; FB: fat body extract expressing HPV 6 b L1 VLP; FB fil: filtered fat body sample; FT: flow-through fraction; W1-2: washing fraction; E: equilibration fraction; 1-8: elution fractions. (C) CBB staining showing the results of sucrose density gradient centrifugation purification of HPV6b L1. M: Protein Marker; FB: fat body extract expressing HPV 6 b L1 VLP; 1-10: fraction numbers. The volume of each fraction was 500 µl. The red arrows indicate HPV 6 L1. This figure is from Minkner et al. (2018) under license by Elsevier B.V. (<https://doi.org/10.1016/j.jchromb.2018.08.007>).

these methods achieved a higher yield than the 3-stage chromatography protocol, but on the other hand the final product contained more host cell proteins. Therefore, at the expense of the overall yield the 3-stage chromatographic protocol removed more effective DNA than the affinity-tag-based purification (**Table 8**), despite that originally a comparable or higher yield was intended.

HPV L1 morphology after the 3-stage chromatography purification was with TEM investigated (**Fig. 57**). Spherical particles with diameters of approximately 10-50 nm were observed and this suggest that VLPs were formed from HPV L1 in silkworms and survived the

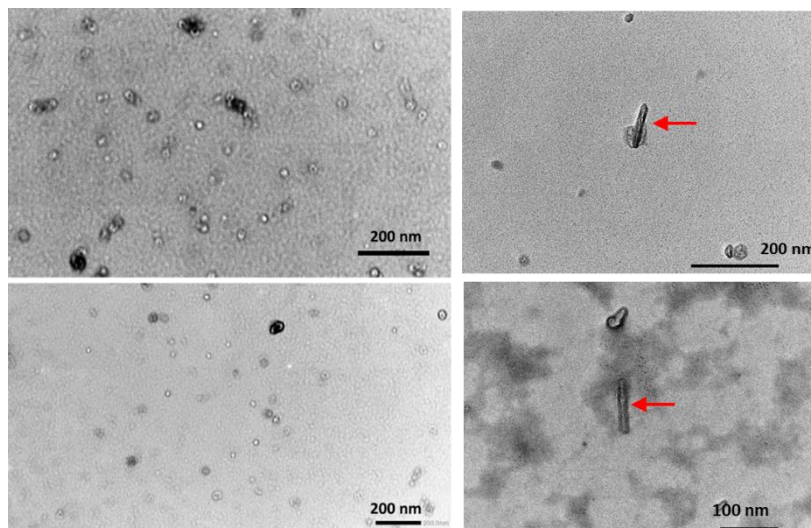


Fig. 57 (left): Morphological observation by TEM. (A-1 and A-2)

Purified VLP sample after 3-stage column chromatography purification. **(B)** Purified VLP sample after DDDDK-tag purification. **(C)** Purified VLP sample after sucrose density gradient purification. The bars in (A-1), (A-2) and (B) indicate 200 nm; those in (C) indicate 100 nm. The red arrows indicate baculovirus particles. This figure is from Minkner et al. (2018) under license by Elsevier B.V.

(<https://doi.org/10.1016/j.jchromb.2018.08.007>).

purification process. Moreover, no baculovirus particles could be observed (**Fig. 57A-1 and A-2**). In opposite, the anti-Flag-tag affinity purification resulted in a good purification, but parts of baculovirus were still visible in the elution fractions (**Fig. 57B**). The sucrose density gradient centrifugation purification showed not only with the qPCR method less baculovirus, removal, but also baculovirus was detected in the elution fraction (**Fig. 57C**). Moreover, the TEM images show easily that many sucrose crystals and impurities are present in the sample (**Fig. 57C**). This conclude that these purification methods are therefore only semi-usable for the separation of the HPV L1. This VLP is based on pentamers, whereby the L1 protein forms one pentamer and one virus particle is formed by the assembly of 72 pentamers. One pentamer has approximately a size of 10 nm and a full particle is around 50 nm. However, it is known that L1 VLPs expressed in *E. coli*, yeast or mammalian cells forms besides large 50 nm particles also 20-40 nm particles [112,113]. Because of this, it was suggested that L1 expressed in silkworm larvae doesn't have a uniform particle size, but forms instead VLPs of various sizes [6].

5.4. Conclusion

A purification method for non-enveloped VLPs from HPV L1 protein from silkworm fat bodies was established which is the first reported study without using affinity chromatography

or sucrose gradient ultracentrifugation aiming for high purity and recovery. This 3-stage chromatography protocol was optimized for the purification of HPV L1 VLP expressed into the silkworm fat body. A complete removal of the DNA and the infectious baculovirus from the silkworm fat body was achieved. All infectious baculovirus was removed using AEX GigaCap Q-650M with a 150 mmol/l sodium phosphate (pH 7.2) buffer and elution with a gradient up to 1.5 mol/l NaCl. The second step with CHT using a 10 mmol/l sodium phosphate buffer (pH 7.2), and an elution up to 600 mmol/l sodium phosphate, removed 99.5 % of the remaining baculovirus DNA. Concentration of the sample at the end of the process was achieved with a heparin column. Impurities removal of this 3-stage chromatography protocol outmatched those of the widely used sucrose density gradient ultracentrifugation purification and affinity tag-purification and a high reproducibility was confirmed. As the only serious drawback of this method, the yield of the target VLP is disappointing. Especially considering that repeating freezing and filtering had partially affected the actual HPV L1 recovery of 5.5 %. Due to this instability of the protein the VLP purification definitely needs more research. However, only as a proof of concept this project aimed to show the possibility of purification of VLPs from the silkworm fat body using chromatographic methods.

6. Standard purification investigations of modified non-enveloped norovirus VLPs from the silkworm fat body

6.1. Introduction

As another non-enveloped VLP, a norovirus VLP based on the VP1 protein was designated to be purified from the silkworm fat body. This purification project was designed for three associated proteins. The complete VLP consists of SpCaVP1 and EDIII, whereby SpCaVP1 is a SpyCatcher (SpCa) norovirus VP1 construct and EDIII is the envelope domain 3 from the dengue virus 1 which contains additional a Spytag. The SpCaVP1 will self-assembly into a non-enveloped VLP and the EDIII can bind covalent to the VLP via the Spy-tag/-Catcher system. These constructs could be used as antigens for single-unit vaccination, but also a multiunit vaccination would be possible. Because of the modularity of the Spy-tag/-Catcher system this system could be used after purification to display several different antigenic proteins on the VLP surface, single or multi proteins, which would be beneficial for vaccination production. Therefore, the purification was investigated for the single expressed particles, as also for the coexpressed VLP construct.

6.2. Results and Discussion

6.2.1. Pre-treatment of SpCaVP1, EDIII and their complex

SpCaVP1, EDIII and their coexpression complex were successfully expressed in the

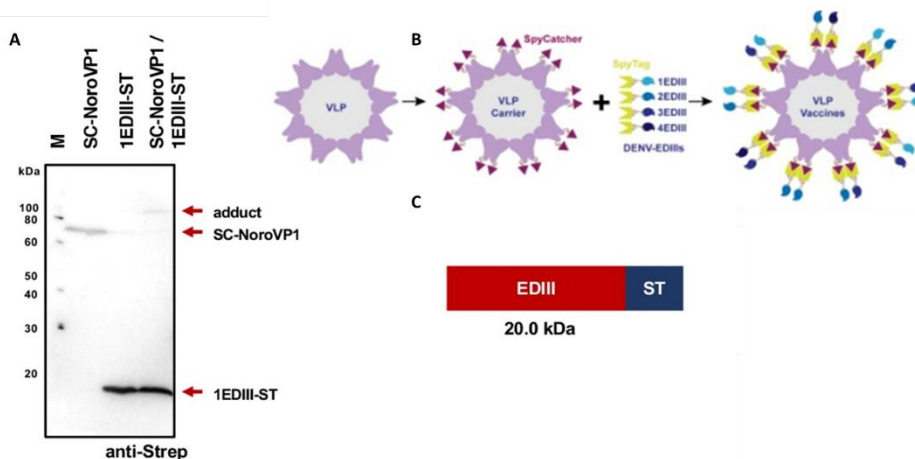


Fig. 58: SpCaVP1 + EDIII (A) Western Blot of SpCaVP1, ED III and the coexpression adduct. (B) Schematic illustration of the intended VLP Spy-tag/-Catcher system. (C) Illustration from the ED III construct with the Spytag. This graphic was provided from Dr. Jian Xu (internal note) and modified.

silkworm fat body as previously shown (Fig.58).

Centrifugation force of 20400 x g at 60 min, 17800 x g at 10 min and 10000 x g at 30 min were investigated, but pellets were insignificantly (data not shown), so that 17800 x g at 10 min was used for

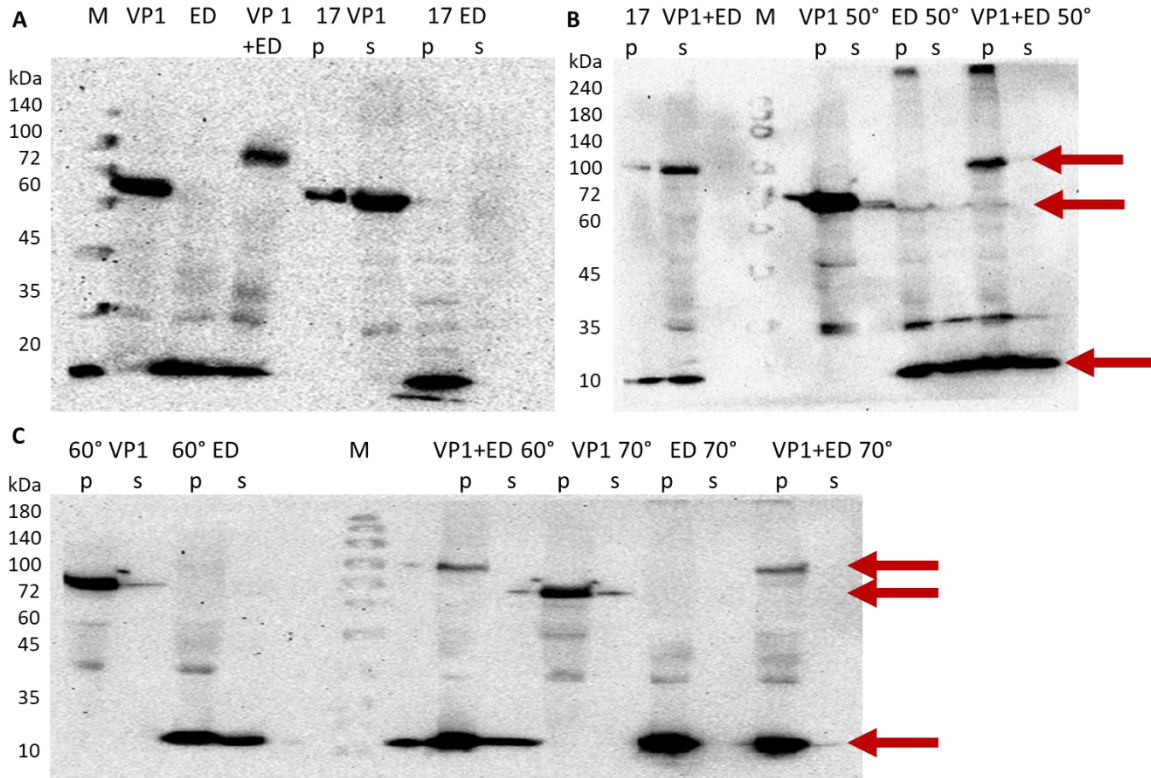


Fig. 59: Western Blot of SpCaVP1, EDIII and their complex for centrifugation (A) and thermal treatment (B+C). On each line 15 μ l was loaded. It was a 8 μ l sample to 22 μ l dilution.
s: supernatant; p: pellet VP1: SpCaVP1; ED: EDIII; VP1+ED: SpCaVP1 + EDIII coexpression; 17: 17800 x g, 10 min; 50°: 50°C thermal treatment, 20 min; 60°: 60°C thermal treatment, 20 min; 70°: 70°C thermal treatment, 20 min; M is Marker; red arrows indicate target proteins

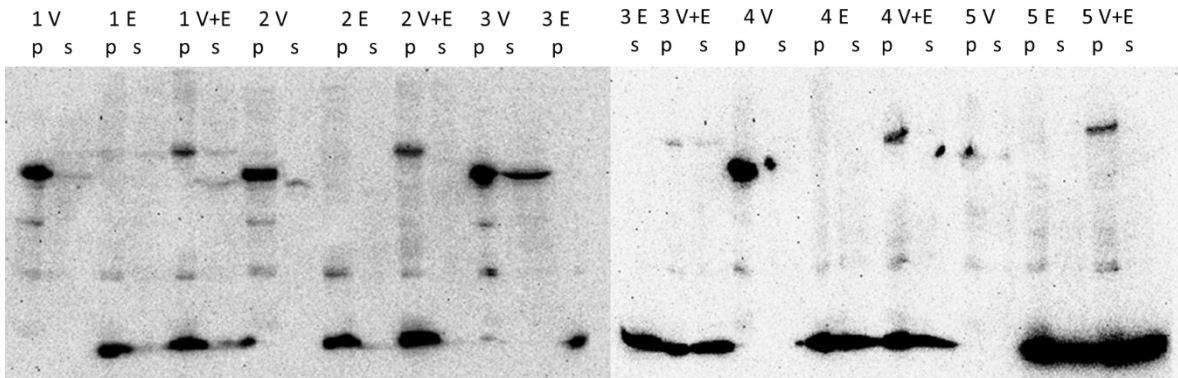
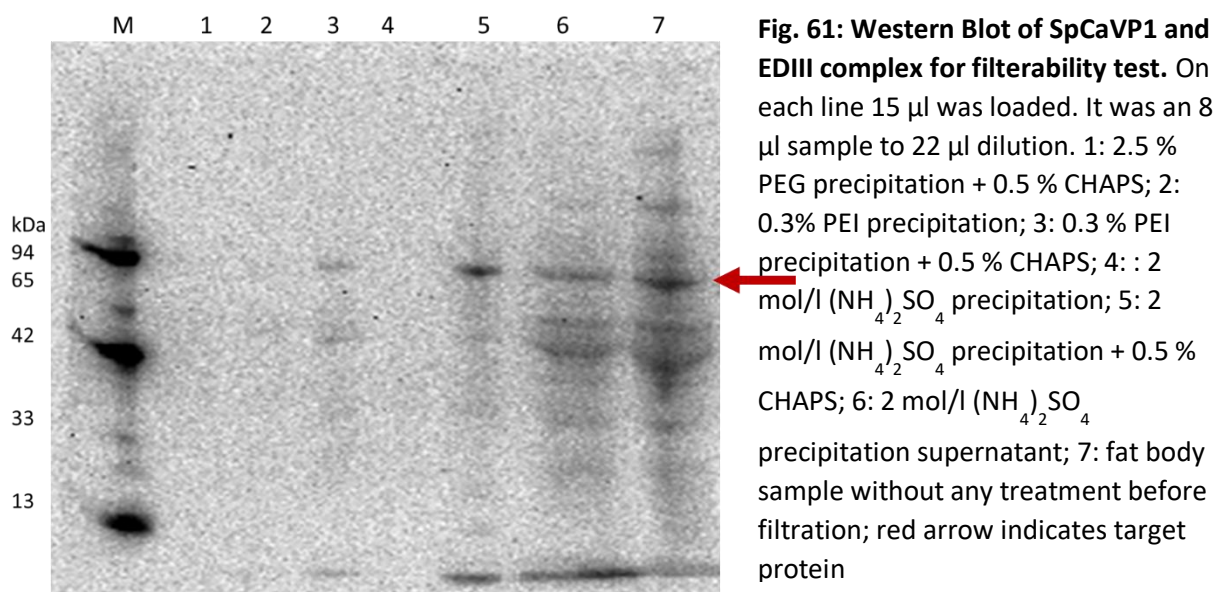


Fig. 60: Western Blot of SpCaVP1, EDIII and their coexpression for precipitation. On each line 15 μ l was loaded. It was a 8 μ l sample to 22 μ l dilution.
s: supernatant; p: pellet; V: SpCaVP1; E: EDIII; V+E: SpCaVP1 + EDIII coexpression; 1: 2.5 % PEG precipitation; 2: 5 % PEG precipitation; 3: 1 mol/l $(\text{NH}_4)_2\text{SO}_4$ precipitation; 4: 2 mol/l $(\text{NH}_4)_2\text{SO}_4$ precipitation; 5: 0.3 % PEI precipitation; same target bands as in Fig. 59

removing aggregated proteins and lipids. Additionally, the thermal treatment was applied. However, all proteins are already denatured at 50°C and precipitated (Fig. 59), so that this treatment was not included. The investigation of precipitation methods revealed that for all three proteins only 2.5 % or 5 % PEG are able to separate them completely, into the pellet (Fig.

60). Therefore, 2.5 % PEG 6000 was chosen as precipitation, because of the lower PEG concentration means also less precipitation of other host proteins. However, following experiments showed that the target protein in the resuspended pellet solution is not fully dissolved. SpCaVP1+EDIII was lost during filtration. To change this, additional 0.5 % CHAPS, a zwitterionic surfactant, was added to the pellet solution. This helped to resolve the target protein and to let it pass the filter, but only for 2 mol/l ammonium sulphate precipitate. For the other precipitations it failed (**Fig. 61**). During later experiments, it became evident that the CHAPS is destroying the filters of the ultrafiltration devices (Amicon 3K; **data not shown**). To solve this, the final CHAPS concentration was several times reduced (**data not shown**). Finally, a CHAPS concentration of 0.5 % is used to resuspend the pellet and this solution is diluted until a final concentration of 0.05 % CHAPS. In the end, the pre-treatment is based on 17800 x g at 10 min centrifugation, a 2 mol/l ammonium sulphate precipitation and this pellet is resolved with CHAPS, but with final concentration of lower than 0.05 %.



6.2.2. Chromatography purification of the SpCaVP1 and EDIII complex

After the pre-treatment several different principles for the FPLC were used. Because of a previous study with the HIC columns, only the Butyl FF column was investigated. These experiments showed that the column is not suited to be used. A linear gradient showed no or very weak UV signals in the elution fractions (**data not shown**), but the target protein was already lost during filtration. A one step gradient revealed that most proteins and the SpCaVP1+EDIII complex bound to the column, even if they gave a comparable weak UV signal (**Fig. 62**). Moreover, the target protein could not be completely eluted, because it bound too strong to the column.

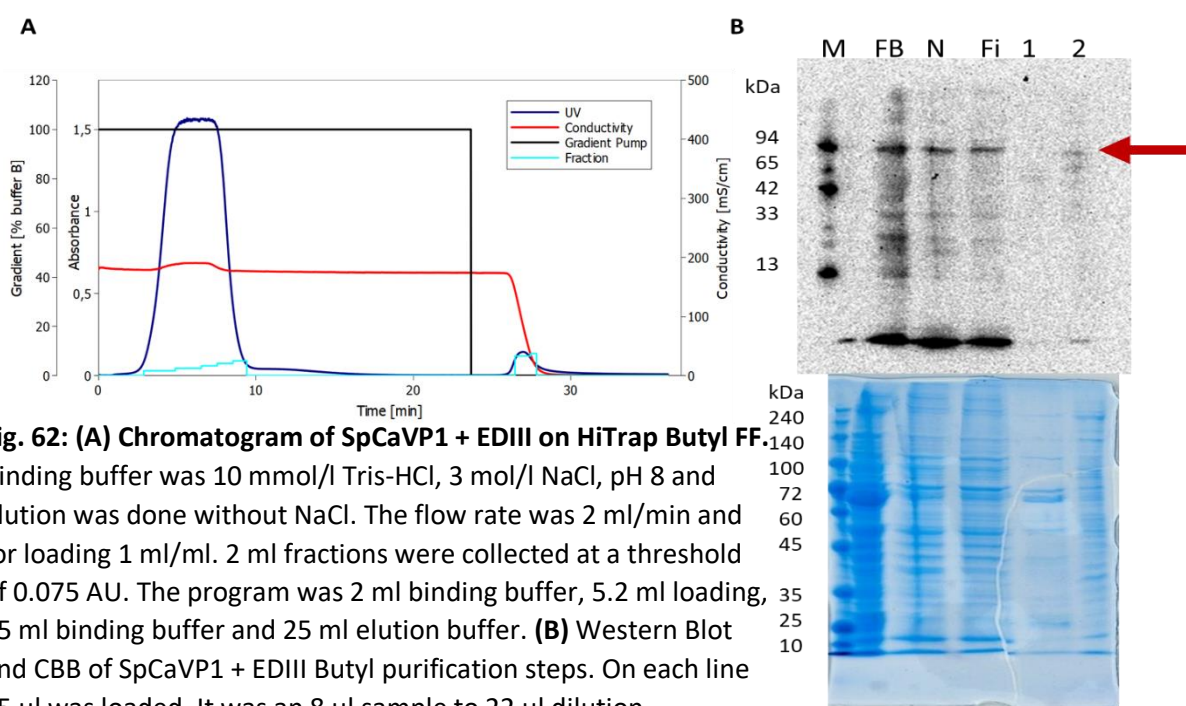


Fig. 62: (A) Chromatogram of SpCaVP1 + EDIII on HiTrap Butyl FF.

Binding buffer was 10 mmol/l Tris-HCl, 3 mol/l NaCl, pH 8 and elution was done without NaCl. The flow rate was 2 ml/min and for loading 1 ml/ml. 2 ml fractions were collected at a threshold of 0.075 AU. The program was 2 ml binding buffer, 5.2 ml loading, 35 ml binding buffer and 25 ml elution buffer. **(B)** Western Blot and CBB of SpCaVP1 + EDIII Butyl purification steps. On each line 15 µl was loaded. It was an 8 µl sample to 22 µl dilution.

FB: fat body; N: 2 mol/l ammonium sulphate precipitation pellet; Fi: filtered load; 1: concentrated pooled flow through fractions 2-6; 2: concentrated pooled elution fraction 8 and 9; M: marker; red arrow indicates target protein

The CaptoCore 700 with its size exclusion cut-off principle was also studied. Theoretically, proteins with a size smaller than 70 kDa should be trapped inside the hollow particles and bigger proteins should be in the flow through, because they cannot pass the pores. In opposite, in our case all proteins were indiscriminately of size reduced and the target complex completely removed, despite of a size of around 100 kDa (**Fig. 63**). The reason for this cannot be explained.

Next, the CHT type II column with its cation exchange and metal affinity was used for the separation. This principle was with a linear gradient able to separate the proteins in one flow through and two elution fractions. But on one side the target protein was in very low

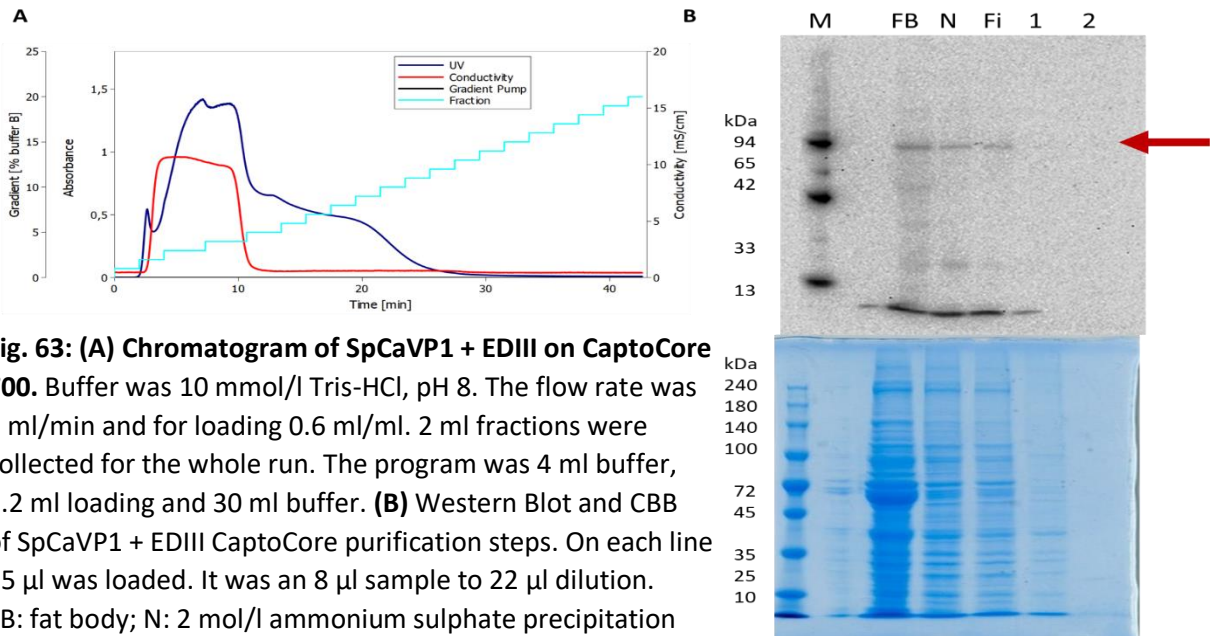


Fig. 63: (A) Chromatogram of SpCaVP1 + EDIII on CaptoCore 700. Buffer was 10 mmol/l Tris-HCl, pH 8. The flow rate was 1 ml/min and for loading 0.6 ml/ml. 2 ml fractions were collected for the whole run. The program was 4 ml buffer, 5.2 ml loading and 30 ml buffer. **(B) Western Blot and CBB of SpCaVP1 + EDIII CaptoCore purification steps.** On each line 15 μ l was loaded. It was an 8 μ l sample to 22 μ l dilution. FB: fat body; N: 2 mol/l ammonium sulphate precipitation pellet; Fi: filtered load; 1: concentrated pooled flow through fractions 1-5; 2: concentrated pooled flow through fraction 6-14; M: marker; red arrow indicates target protein

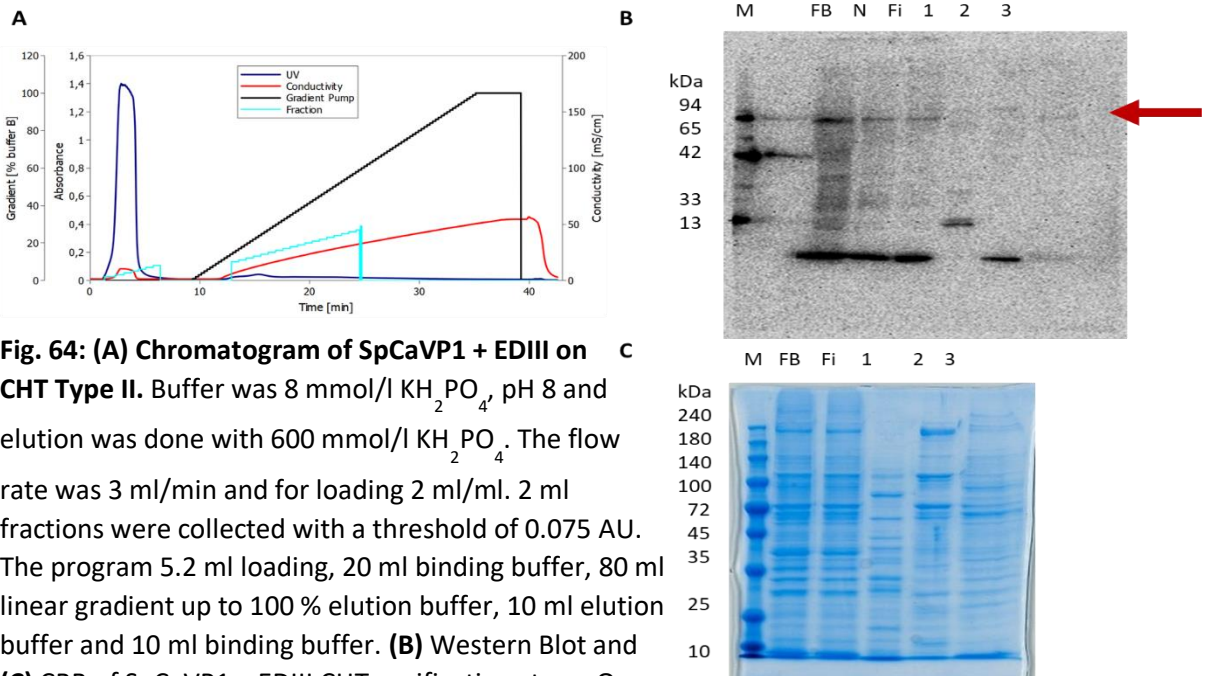


Fig. 64: (A) Chromatogram of SpCaVP1 + EDIII on CHT Type II. Buffer was 8 mmol/l KH_2PO_4 , pH 8 and elution was done with 600 mmol/l KH_2PO_4 . The flow rate was 3 ml/min and for loading 2 ml/ml. 2 ml fractions were collected with a threshold of 0.075 AU. The program 5.2 ml loading, 20 ml binding buffer, 80 ml linear gradient up to 100 % elution buffer, 10 ml elution buffer and 10 ml binding buffer. **(B) Western Blot and (C) CBB of SpCaVP1 + EDIII CHT purification steps.** On each line 15 μ l was loaded. It was an 8 μ l sample to 22 μ l dilution. FB: fat body; N: 2 mol/l ammonium sulphate precipitation pellet; Fi: filtered load; 1: concentrated pooled flow through fractions 2-8; 2: concentrated pooled elution fraction 10-16; 3: concentrated elution fraction 16-29; M: marker; red arrow indicates target protein

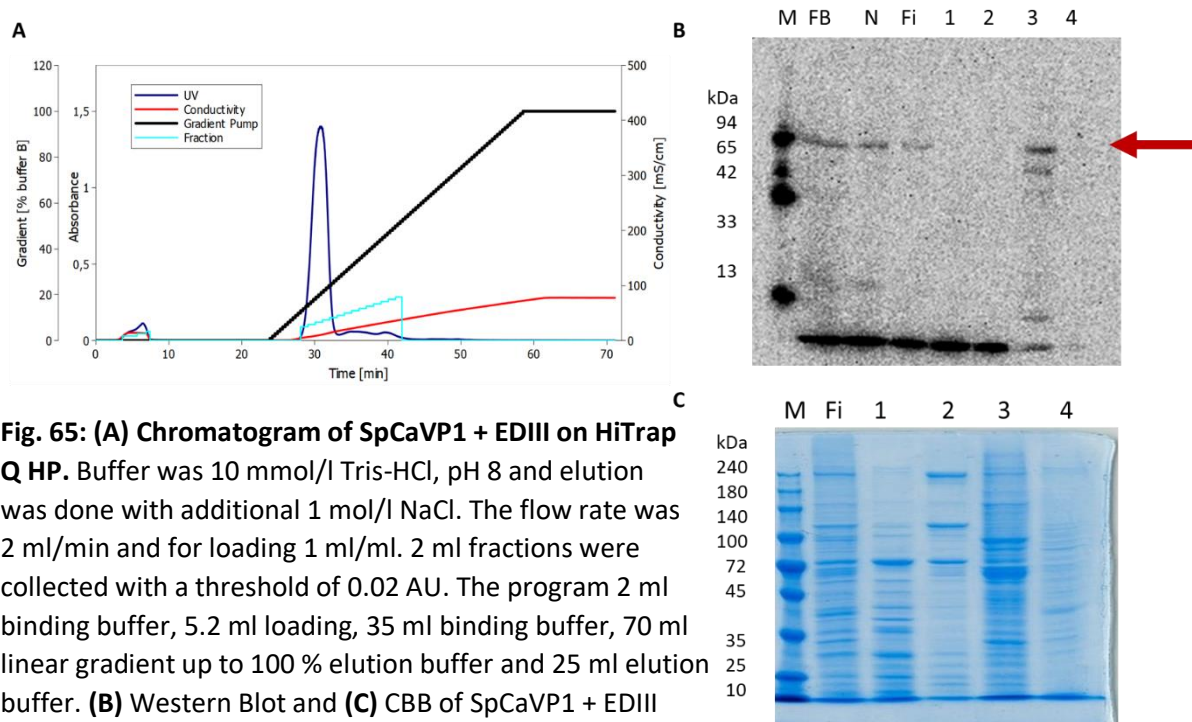


Fig. 65: (A) Chromatogram of SpCaVP1 + EDIII on HiTrap Q HP. Buffer was 10 mmol/l Tris-HCl, pH 8 and elution was done with additional 1 mol/l NaCl. The flow rate was 2 ml/min and for loading 1 ml/ml. 2 ml fractions were collected with a threshold of 0.02 AU. The program 2 ml binding buffer, 5.2 ml loading, 35 ml binding buffer, 70 ml linear gradient up to 100 % elution buffer and 25 ml elution buffer. **(B) Western Blot and (C) CBB** of SpCaVP1 + EDIII Q HP AIEX steps. On each line 15 μ l was loaded. It was a 8 μ l sample to 22 μ l dilution. FB: fat body; N: 2 mol/l ammonium sulphate precipitation pellet; Fi: filtered load; 1: concentrated pooled flow through fractions 2-4; 2: concentrated pooled elution fraction 6-10; 3: concentrated elution fraction 11-15; 4: concentrated pooled elution fraction 16-19; M: marker; red arrow indicates target protein

amount in the elution fractions and on the other side for unknown reasons some kind of degraded target protein was found in the flow through fraction (**Fig. 64**). The reason for this kind of degradation happened is unclear. The binding buffer is an 8 mmol/l potassium phosphate buffer (pH 8) which doesn't provide the conditions for degradation. Because this result was repeated, further optimization of this principle was deemed not necessary.

Using the anion exchange principle (AIEX) with the Q HP, a slightly separation of the proteins could be achieved, but the target protein complex still remains with the majority of the host proteins (**Fig. 65**). Using this as a base, because this is the best separation and recovery which could be achieved so far, the protocol was optimized to a step gradient and the elution fraction with 31 % elution buffer was then concentrated and loaded on a size exclusion chromatography (SEC) column to separate bigger and smaller proteins from the target protein. Unfortunately, the chosen start concentration with 15 % elution buffer was already too high, so that the target protein did not bind to the column at all. Moreover, during the later SEC only one UV peak with a big tailing could be observed (**Fig. 66**). Therefore, the step gradient protocol was updated to 10 % elution buffer at first, so that the target protein

could bound to the column completely (**Fig. 67**). On a side note, the remaining overexpressed EDIII could be removed from the SpCaVP1+EDIII complex, because it remained mainly in the first flow through fraction. The Q HP (AIEX) elution fraction was then concentrated and loaded to the SEC, but the SEC failed to separate any proteins. No size separation could be achieved and only one UV peak with a strong tailing was obtained (**Fig. 68A**). The peak and the tail contain the target protein as well as all loaded proteins (**Fig. 68B+C**). The reason for the failed SEC is still unknown.

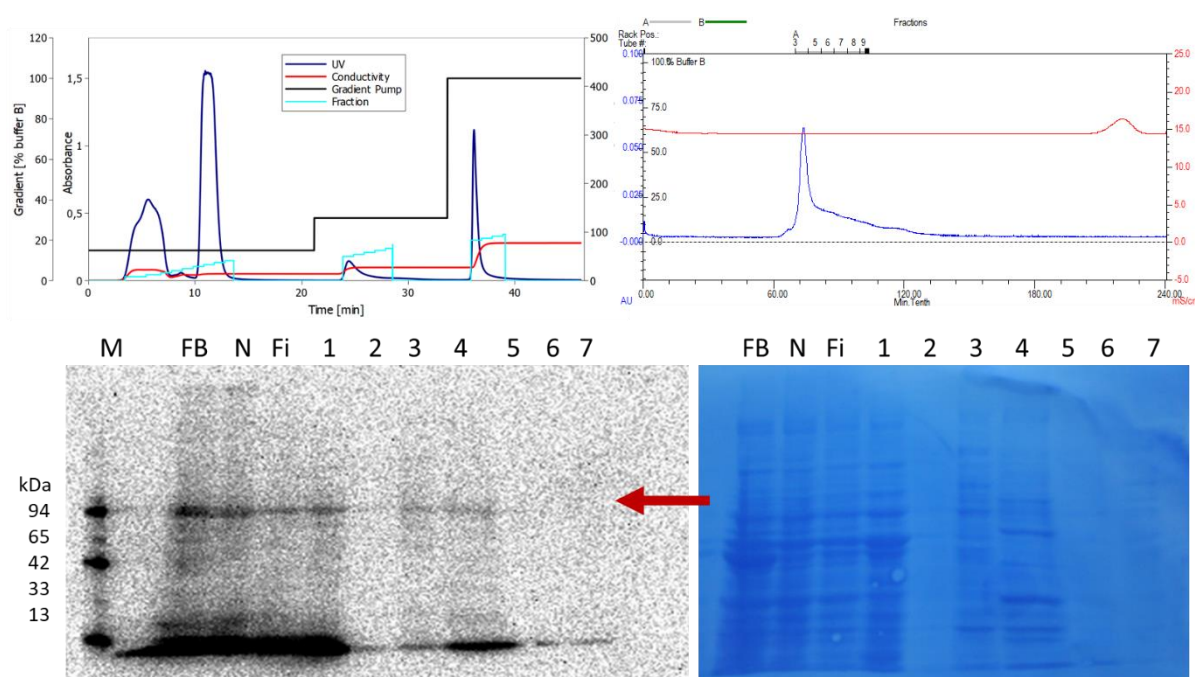


Fig. 66: HIC and SEC chromatography in a row (A) Chromatogram of SpCaVP1 + EDIII on HiTrap Q HP. Buffer was 10 mmol/l Tris-HCl, pH 8 and elution was done with additional 1 mol/l NaCl in step gradients. The flow rate was 2 ml/min and for loading 1 ml/ml. 2 ml fractions were collected with a threshold of 0.02 AU. The program 2 ml 15 % elution buffer, 5.2 ml loading, 30 ml 15 % elution buffer, 25 ml 31 % elution buffer and 25 ml 100 % elution buffer. **(B)** Chromatogram of SpCaVP1 + EDIII on Superdex Sephacryl S-200 with 10 mmol/l Tris, 150 mmol/l NaCl, pH 8. The program was 1 ml elution buffer, 5.2 ml load, and 121 ml elution buffer. The flow rate was 0.5 ml/min. Fractions were collected up to 3 ml with a threshold of 0.01 AU. Loaded was the elution fraction of the Q HP purification. **(C)** Western Blot and **(D)** CBB of SpCaVP1 + EDIII for the purification steps. On each line 15 μ l was loaded. It was an 8 μ l sample to 22 μ l dilution. FB: fat body; N: 2 mol/l ammonium sulphate precipitation pellet; Fi: filtered load; 1: concentrated pooled Q HP flow through fractions 2-6; 2: concentrated pooled Q HP flow through fractions 7-10; 3: concentrated Q HP elution fraction 12-16; 4: concentrated pooled Q HP elution fractions 18-23; 5: concentrated pooled SEC fractions 4+5; 6: concentrated pooled SEC fractions 6+7; 7: concentrated pooled SEC fractions 8-10; M: marker; red arrow indicates target protein

Fig. 67 (right): (A) Chromatogram of SpCaVP1 + EDIII on HiTrap Q HP. Buffer was 10 mmol/l Tris-HCl, pH 8 and elution was done with additional 1 mol/l NaCl in step gradients. The flow rate was 2 ml/min and for loading 1 ml/ml. 2 ml fractions were collected with a threshold of 0.02 AU. The program 2 ml 10 % elution buffer, 5.2 ml m loading, 30 ml 10 % elution buffer, 25 ml 31 % elution buffer and 25 ml 100 % elution buffer. **(B) Western Blot of SpCaVP1 + EDIII of the purification steps.** On each line 15 μ l was loaded. It was an 8 μ l sample to 22 μ l dilution. FB: fat body; N: 2 mol/l ammonium sulphate precipitation pellet; Fi: filtered load; 1: concentrated pooled Q HP flow through fractions 2-6; 2: concentrated pooled flow through fractions 7-12; 3: concentrated elution fraction 14-17; 4: concentrated pooled elution fractions 19-22; M: marker; red arrow indicates target protein

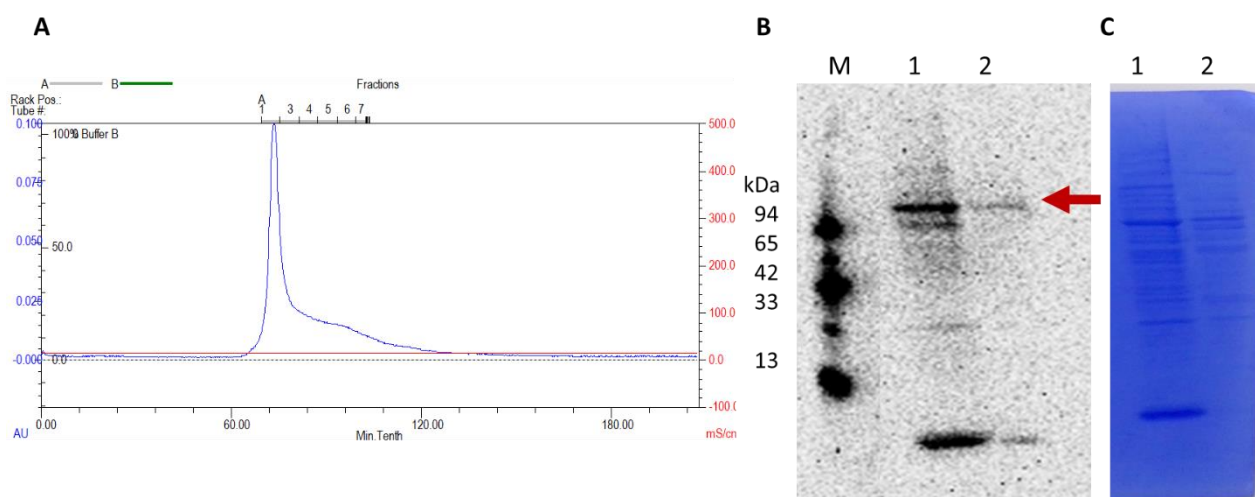
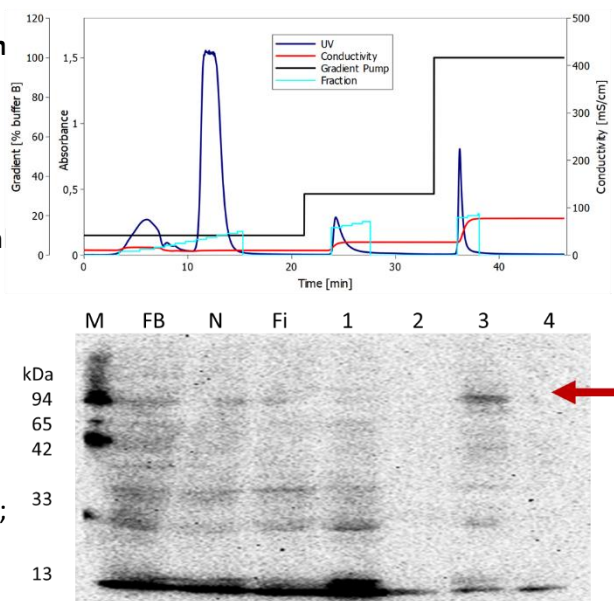


Fig. 68: (A) Chromatogram of SpCaVP1 + EDIII on Superdex Sephacryl S-200 with 10 mmol/l Tris, 150 mmol/l NaCl, pH 8. The program was 1 ml elution buffer, 5.2 ml load, and 121 ml elution buffer. The flow rate was 0.5 ml/min. Fractions were collected up to 3 ml with a threshold of 0.01 AU. Loaded was the elution fraction of the Q HP purification. **(B) Western Blot and (C) CBB** of SpCaVP1 + EDIII for the pooled fractions. On each line 15 μ l was loaded. It was an 8 μ l sample to 22 μ l dilution. 1: concentrated pooled fractions 2-4; 2: concentrated pooled fractions 5-9; M: marker; red arrow indicates target protein

6.2.3. Additional precipitation investigation before chromatography

To reduce the protein amount before the chromatography steps to tackle the arising problems, a 3 % (w/v) polyvinyl pyrrolidone precipitation was done, as this method is commonly used for lipid protein precipitation. This approach also failed, because the complex was also with the majority of the proteins in the pellet, which is not easily resuspend able (**Fig. 69**).

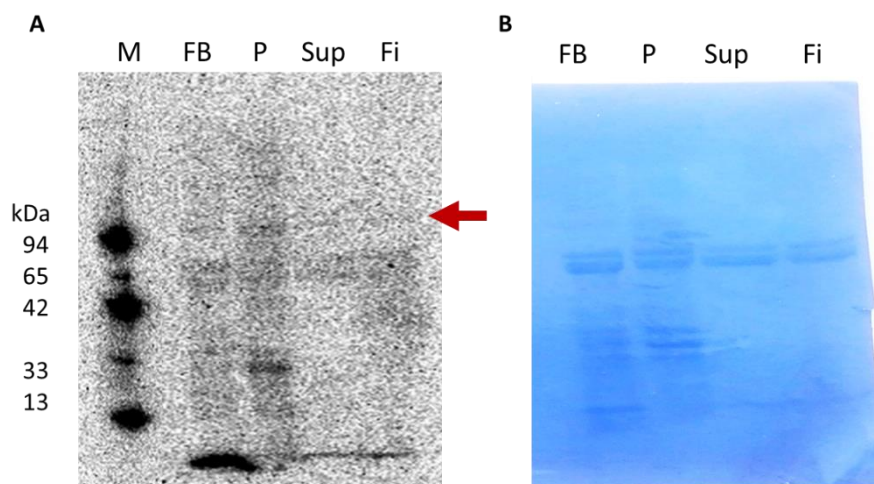


Fig. 69 (right): Further precipitation test (A) Western Blot and (B) CBB of SpCaVP1 + EDIII of the 3 % (w/v) polyvinylpyrrolidone precipitation test. On each line 15 μ l was loaded. It was an 8 μ l sample to 22 μ l dilution.

FB: fat body; P: 3 % (w/v) polyvinylpyrrolidone precipitation pellet; Sup: 3 % (w/v) polyvinylpyrrolidone precipitation supernatant; Fi: filtered supernatant M: marker; red arrow indicates target protein

6.3. Conclusion

The SpCaVP1, EDIII and their, because of the Spy-tag/-Catcher system, covalent bound complex were successfully expressed. However, using only the standard purification approach reached on one side a bottleneck situation and on the other side unexplainable problems with the SEC during the purification of the complex. The latter problem needs to be investigated and addressed, before further experiments on this study can be done. It has to be determined if this is a sample problem, or in worst case a sudden column problem, even if the column otherwise seems in perfect shape. These further investigations were not done yet.

7. Purification investigations of enveloped VLPs from silkworm haemolymph

7.1. Introduction

Rous sarcoma virus (RSV) is an enveloped virus and the VLP from the group-specific antigen (Gag) has as well an envelope. The purification intended for two RSV-LPs constructs, consisting of RSV-gag protein, using only standard purification methods. These RSV-LPs displayed antigens of *Neospora caninum*, a single-celled parasite. This parasite is causing worldwide abortions in cattle, which is causing economic damages. Therefore, these VLPs were intended to function as a vaccine candidate for cattle.

7.2. Specific Material and Methods

7.2.1. RSV-LP construction

The constructs were kindly provided by Mr. Rikito Hiramatsu and a flag tagged version by Mr. Yuuki Machida (Laboratory of Biotechnology; both VLP group) and were expressed into the haemolymph. The VLP construction is based on a recombinant BmNPV containing *Rous sarcoma* virus Gag protein expression cassette (BmNPV/Gag) which was previously constructed [55]. To express surface antigen 1 of *Neospora caninum* (NcSAG1) fused with C-terminal domain of GP64 from BmNPV (BmGP64), the previously constructed BmNPV/SAG1-GP64TM was used [21]. To express the SAG1-related sequence 2 of *N. caninum* (NcSRS2) fused with C-terminal domain of GP64 from BmNPV (BmGP64), the also previously constructed BmNPV/SRS2-GP64TM was used [114].

For the construction of a single polycistronic BmNPV containing Gag, NcSAG1 and NcSRS2 expression cassettes, these expression cassettes were amplified by PCR using three primer sets; set 1 (α -1-F and β -1-R), set 2 (β -2-F and γ -2-R) and set 3 (γ -3-F and ω -4-R) (**Table 10**). A linear pFastbac1 vector (Thermo Fisher Scientific K. K., Tokyo, Japan) was also prepared by PCR using the primer set 4 (ω -pFB-F and α -pFB-R, **Table 10**). These DNA fragments were assembled by Gibson assembly technology [115] to construct pFB/SAG1-SRS2-Gag. These

plasmids were transformed into *Escherichia coli* BmDH10Bac individually, and BmNPV/SAG1-SRS2-Gag bacmid DNA were extracted from a white colony.

These recombinant BmNPV bacmids were injected into silkworm larvae using chitosan, respectively [116]. After 6–7 days, haemolymph was collected from recombinant BmNPV bacmid-injected silkworm larvae. Virus titers in haemolymph were determined according to the protocol reported previously [83] using Bm-ie1 F and Bm-ie1 R as primers (**Table 10**). By the co-infection strategy, three recombinant BmNPVs (BmNPV/Gag, BmNPV/SAG1 and BmNPV/SRS2) were injected into silkworm larvae at the same titre. By the single infection

Table 10: Primers used for the Rous sarcoma VLP construction

Name	5'-3'
α -1-F	AACGCTCTATGGTCTAAAGATTTACTCCGGAATATTAATAG
β -1-R	AAACGTGCAATAGTATCCAGTTTTAGATTTCACTTATCTGG
β -2-F	AAACTGGATACTATTGCACGTTTACTCCGGAATATTAATAG
γ -2-R	AAACATCAGGCATCATTAGGTTTTAGATTTCACTTATCTGG
γ -3-F	AAACCTAATGATGCCTGATGTTTACTCCGGAATATTAATAG
ω -3-R	AAACTAAGCTATGTGAACCGTTTTAGATTTCACTTATCTGG
ω -pFB-F	AAACACTGACATTGACTTGGTTTCCCGGTCCGAAGCGCGCG
α -pFB-R	AAATCTTTAGACCATAGAGCGTTCTATTAATATTCCGGAGT
Bm-ie1 F	CCCGTAACGGACCTTGTGCTT
Bm-ie1 R	TTATCGAGATTATTTACATACAACAAG

strategy, the BmNPV only containing Rous sarcoma virus Gag protein expression cassette BmNPV/Gag was injected into silkworm larvae. By the single polycistronic strategy, BmNPV/SAG-SRS-Gag was injected into silkworm larvae. After 4 days, haemolymph and fat body were collected. 1-phenyl-2-thiourea was added into the haemolymph at 2 mmol/l. The collected haemolymph was used to infect further silkworms for this study.

7.2.2. Bare iron MNPs as protein depletion method

Bare negatively and positively charged FeO₃ MNPs were provided by Mr. Kenshin Takemura (Laboratory of Biotechnology; Shizuoka University). Generally, it was as a liquid chromatography in batch method style. The MNPs were mixed with the sample and after an

incubation time, they were separated using a magnet. For protein depletion, the supernatant was further used and the MNP pellet with the adsorbed proteins discarded.

A 1.7 mg MNP/1.2 ml MilliQ water solution was 1 h sonicated and after 20 min rest, only the upper layer was used in the experiments. Because of bound target protein, it was tried to elute these with 400 μ l Citrate buffered saline (CBS; 50 mmol/l citrate, 137 mmol/l NaCl, 2.7 mmol/l KCl, pH 7) and 30 min after magnetic separation of the MNPs and removing of the supernatant, as this was successful done for other recombinant proteins on bare iron MNPs [104].

7.3. Results and Discussion

7.3.1. RSV-LP construct 1

The first investigated VLP construct was provided by Mr. Rikito Hiramatsu (Laboratory of Biotechnology; Shizuoka University) and was expressed into the haemolymph. This project was stopped because of two reasons. This VLP construct was not separable from cell debris using low centrifugation forces and with high centrifugation forces the VLPs were most likely destroyed in the pellets (**Fig. 70**). Moreover, it seemed that the stability of this VLP seemed insufficient (**data not shown**). The other reason was that for an intended MNP purification project (see Chapter 10.2) a flag tagged protein was required, so that the VLP was switched to the second RSV-LP which contains a flag-tag. However, this VLP was still used to investigate if positively or negatively charged FeO_3 MNPs are able to deplete the abundant host proteins in the silkworm haemolymph. The results showed that both particles had a very strong unspecific

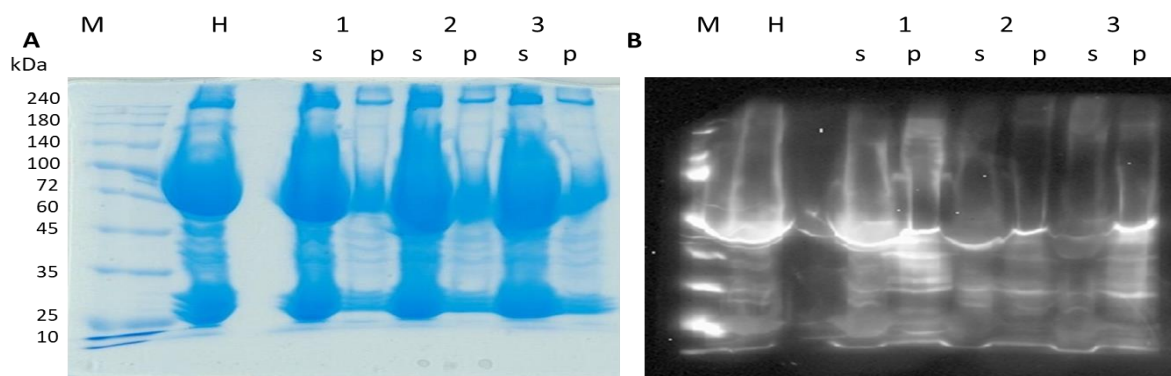


Fig. 70:RSV-LP precipitation (A) Coomassie blue staining SDS-gel with set ups for centrifugation forces and precipitation **(B)** in comparison with Western Blot for RSV-LP construct 1 pre-treatment. On each line 15 μ l was loaded. It was an 8 μ l sample to 24 μ l dilution. s: supernatant; p: pellet
 Lane 1: pellet and supernatant 10000 x g, 30 min; Lane 2: pellet and supernatant 3000 x g, 5 min;
 Lane 3: pellet and supernatant 17800 x g, 10 min; M is Marker

binding of the MNPs, which could not be eluted, even with Citrate based saline (**Fig. 71**) which was shown to disturb FeO₃ binding mechanism [104].

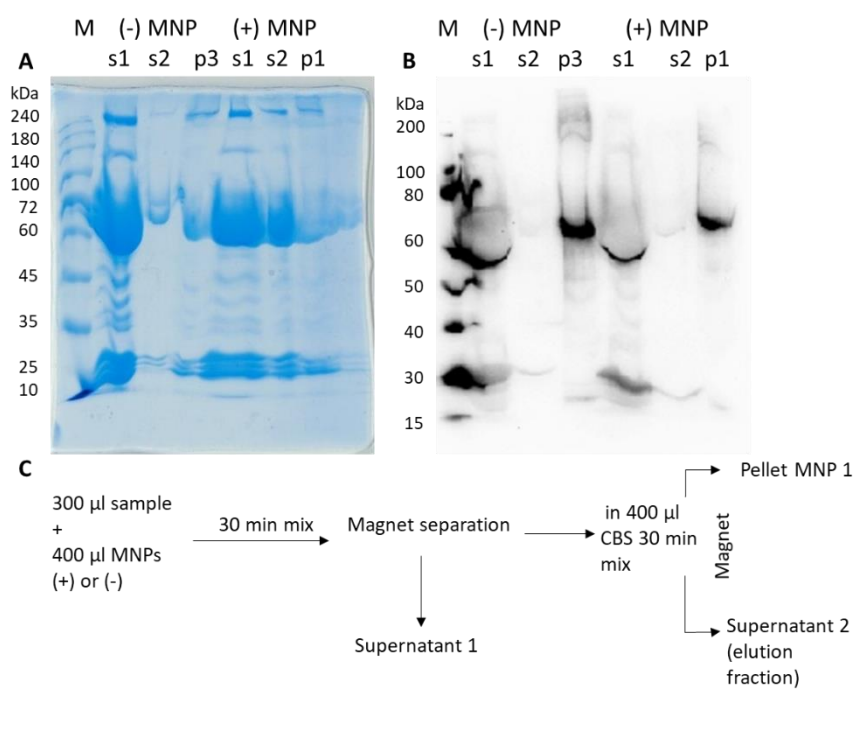


Fig. 71: MNP depletion (A) Coomassie blue staining SDS-gel for the magnetic nanoparticle depletion of host proteins from the haemolymph (**B**) in comparison with Western Blot. Used was RSV-LP construct 1 with a size of around 70 kDa. On each line 15 µl was loaded. It was an 8 µl sample to 24 µl dilution.

(C) MNP experimental set up. s: supernatant; p: pellet; +: positively charged MNP; -: negatively charged MNP s1: Supernatant 1; s2: Supernatant 2; p1: pellet MNP 1; M is Marker

7.3.2. RSV-LP construct 2

A second try for purification was in the same way investigated as previously reported proteins with the RSV-LP construct from Mr. Yuuki Machida (Laboratory of Biotechnology; Shizuoka University). The centrifugation revealed that no set up was able to separate the target protein in a satisfying way. From the Western Blot was no difference distinguishable (**Fig. 72**). Followed up precipitation experiments showed that a centrifugation force of a least

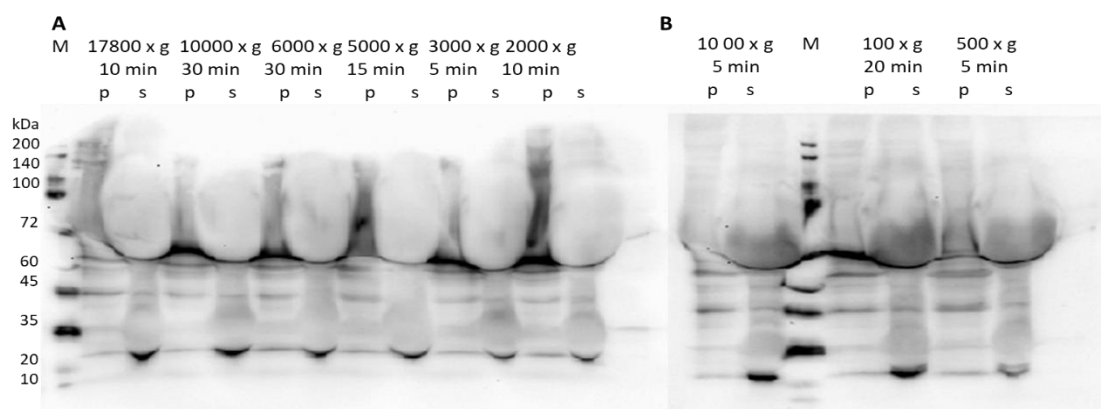


Fig. 72: (A) + (B) Western Blot of RS-VLP centrifugation pre-treatment. Used was RS-VLP construct 2. On each line 15 µl was loaded. It was a 6 µl sample to 22 µl dilution. s: supernatant; p: pellet; The numbers give the centrifugation forces and spinning time; M is Marker

6000 x g is preferable to separate most of the cell debris from the supernatant (**data not shown**). For precipitation 2.5 % PEG 6000 and 0.5% PEI were determined as best option to separate the RSV-LP into the pellet, because DTT and ammonium sulphate precipitated higher amount of proteins, and therefore, the pellet was significantly bigger (**Fig. 73**). Additionally, a multi-stage heat treatment was investigated. This showed that no haemolymph protein is denatured up to 40°C, but starting from 50°C to 70°C more and more proteins are denatured. Unfortunately, the RSV-LP was also already at 50°C denatured, and in the pellet (**data not shown**). Therefore, for the following chromatography experiments the 2.5 % PEG precipitation was used. Using the size exclusion cut off column CptoCore 700 the VLP was not detectable

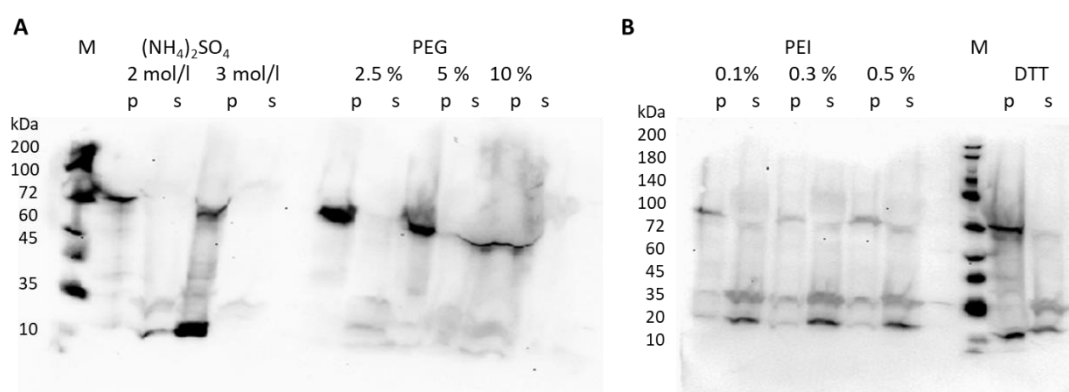


Fig. 73: (A) + (B) Western Blot of RSV-LP precipitation pre-treatment. Used was RSV-LP construct 2. On each line 15 µl was loaded. It was a 3 µl sample to 22 µl dilution. s: supernatant; p: pellet; M is Marker

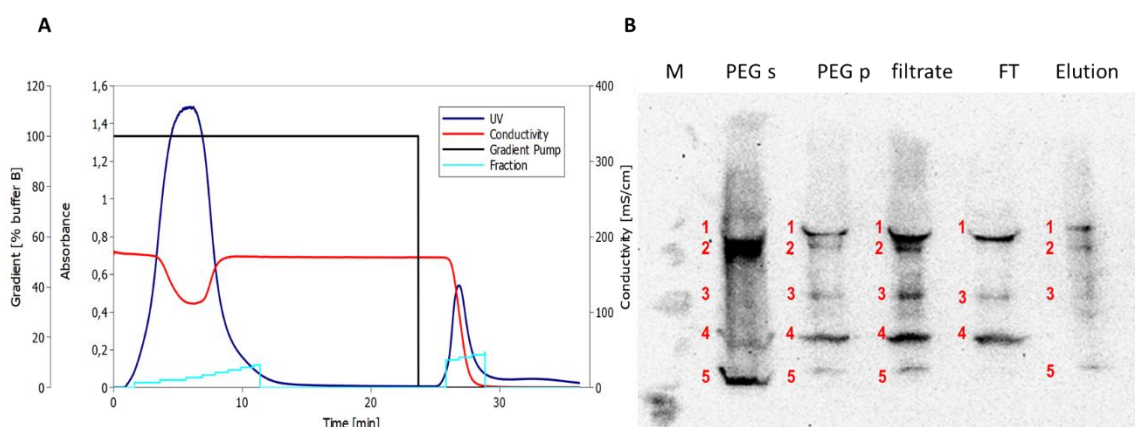


Fig. 74: (A) Chromatogram of RSV-LP construct 2 on HiTrap Butyl FF. Binding buffer was 10 mmol/l Tris-HCl, 3 mol/l NaCl, pH 8 and elution was done without NaCl. The flow rate was 2 ml/min and for loading 1 ml/ml. 2 ml fractions were collected at a threshold of 0.075 AU. The program was 2 ml binding buffer, 5.2 ml loading, 35 ml binding buffer and 25 ml elution buffer. **(B) Western Blot of RSV-LP Butyl purification steps.** On each line 15 µl was loaded. It was a 8 µl sample to 22 µl dilution. PEG s: supernatant of 2.5 % PEG precipitation; PEG p: pellet of 2.5 % PEG precipitation; filtrate: filtrate of pellet from the 2.5 % PEG precipitation; FT: Flow through of HIC; elution: Elution fraction of HIC; M: marker; Red number indicate the structure proteins necessary for the VLP

in any fraction (**data not shown**). This implied, that the VLPs broke down into their single compounds and were trapped inside the beads. Using HiTrap Butyl FF column for hydrophobic interaction chromatography (HIC) it was shown that the VLP is not stable, can't withstand the chromatography process, and is maybe already after the precipitation step damaged. This is visible because of the missing structure proteins in the different fractions as seen in the western blot (**Fig. 74**). Even if the most important one is band No. 1 at 61 kDa, most of it was not in the elution fraction and VLP formation detection was not attempted because of still abundant impurities.

7.4. Conclusion

Due to the instability of the RSV-LPs both projects were stopped. The instability raises questions about the production efficiency of these two VLPs. Of course, because they were supposedly enveloped VLPs there is also the possibility that the envelope was not stable enough to withstand the used purification methods. This was not further investigated, but there were signs that made it very likely. For the first RSV-LP was already an incoherence in the experimental data between the designer Mr. Hiramatsu and this study in the very beginning. So were in his experimental data even with high centrifugation forces the RSV-LP still in high amount in the supernatant, but not in this study (**data not shown**). This raised questions, because the infection agent for this study was provided from him and there were no known relevant differences in the silkworm caring and protein expression process.

For the second RSV-LP it could be theoretically possible that the PEG precipitation already damaged the VLPs, but normally the PEG precipitation is considered as mild and the used centrifugation force was weaker than for the prior step. Because the sample were still too dirty, VLPs could not be distinguished in TEM images (**data not shown**). If the VLP were able to withstand the pre-treatment, then they definitely were too unstable to withstand the following chromatography procedure as already discussed. This is also interesting, because regarding Mr. Machida these RSV-LPs are purifiable using an open anti flag-tag affinity column. As conclusion, it is also possible that the envelope is not able withstand the pressure in an FPLC system. Therefore, the RSV-LP purification project was paused until the RSV-LP expression and stability could be without doubt confirmed.

8. Magnetic nano particles for the affinity purification of His-tagged proteins from complicated matrixes as a pre-treatment step

8.1. Introduction

The former mentioned purification protocols showed that standard purification from silkworm is not easy. Therefore, a study was initiated to develop magnetic nano particles (MNPs) for the purification. As first trial for His-tagged proteins, because it easier to modify MNPs in a way that they bind to affinity-tagged proteins. Of course, commercial magnetic particles for the purification of affinity-tagged proteins are already available, but they are expensive and often not yet were efficient, especially for an up-scaled purification. The MNPs for this study were designed with the intention of improved efficiency, and moreover, a high purity is not intended, but a high target protein recovery. Of course, a high purity is beneficial, but these particles are foremost intended as a mild pre-treatment before further purification steps such as FPLC. These MNPs were tested for His-tagged recombinant proteins, this includes also VLPs, and even for the complex and hard to purify silkworm fat body matrix. For purification investigations the proteins the previous mCherry, SpCaVP1+EDIII and SpCaVP1 were used as model proteins.

8.2. Specific Material and Methods

8.2.1. Nickel²⁺ MNPs preparation

All nickel magnetic nanoparticles are based on a FeO₃ core, had multiple layer and were silica and then nickel coated. These MNPs were provided by Mr. Kenshin Takemura (Laboratory of Biotechnology; Shizuoka University). The characterisation is still ongoing. Four different MNPs were prepared, whereby MNP 1 and MNP 2 did not received a special name. On the other hand, MNP 3 can be referred as “Ni rich MNPs” and MNP 4 to “highly dispersible MNPs”. The MNPs were usually used with a 2 mg/ml solution in MilliQ water if not mentioned otherwise.

The highly dispersible MNPs (MNPs 4) were prepared as following. Using Massart’s method the superparamagnetic iron oxide nanoparticles (SPIONs) were synthesized[117], wherby 5 ml ammonium hydroxide was added to 5 mmol FeCl₂ and 10 mmol FeCl₃ in 40 ml of

ultrapure water. This mix was strongly stirred (30 min, room temperature) and the synthesized MNP magnetically then separated.

For functionalization and stabilization, these MNPs were coated with SiO₂ [118]. The SPIONs were sonicated in 120 ml ethanol for 30 min at RT and 150 μl tetraethyl orthosilicate (TEOS) was added. The MNP@SiO₂ were magnetically separated and 6 hours washed stirring at RT.

MNP Amino group functionalisation modification was performed as a previous study reported [119]. Washed MNP@SiO₂ were dissolved in 100 ml toluene anhydrous and sonicated over 30 min and then loaded into a three-neck round bottom flask. (3-Aminopropyl) trimethoxysilane (APTMS) was added slowly and heated at 40 °C with vigorous stirring for 24 hours. The product MNP@SiO₂@NH₂ was separated magnetically and several times washed by ethanol.

After this, the 2-amino benzamide (2-AB) and Nickel coating have been prepared by following a reported process [120]. 0.32 g of isatoic anhydride was added to 0.5 g MNP@SiO₂@NH₂ dissolved in 100 ml ethanol and refluxed for 12 h. The modified MNP@SiO₂@NH₂@2-AB were separated by magnetic decantation and several times washed with ethanol. 0.5 g MNP@SiO₂@NH₂@2-AB were suspended in 100 ml of ethanol and ultrasonically dispersed to form a homogeneous dispersion. After this, the solution was mixed with 2mmol of Ni(OAc)₂ · 4H₂O and refluxed for 12 h. Finally, MNP@SiO₂@NH₂@Ni were separated via magnet and washed with ethanol to remove unreacted reagents and dried overnight.

8.2.2. Nickel²⁺ MNPs and commercial magnetic beads for purification of His-tagged proteins

Generally, the purification using MNPs was as a liquid chromatography in batch method style. The MNPs were mixed with the sample and after an incubation time, they were separated using a magnet. The supernatant was discarded and the pellet washed and again separated with a magnet. The elution was done with specific buffers and after the incubation time, the MNPs were separated with a magnet, thereby the target protein remained in the elution buffer.

For the nickel MNPs the used volume of sample/buffers/MNPs varied in the protocols. Mainly only two elution steps were done, but it could be also a third one. The basic structure of the protocols was the following. The MNPs were 30 min in water bath sonicated and 350 μl

2 mg/ml MNPs were added to 250 μ l sample and 200 μ l wash buffer (20 mmol/l Tris-HCl, 0.5 mol/l NaCl, 20 mmol/l imidazole, pH 7.5). This was mixed and then 30 min on ice incubated with occasional additional mixing. After magnetic separation the supernatant was removed, 200 μ l wash buffer was added and 10 min on ice incubated. After magnetic separation the wash step was once repeated. After magnetic separation a weak elution buffer (20 mmol/l Tris-HCl, 0.5 mol/l NaCl, 300 mmol/l imidazole, pH 7.5) or strong elution buffer (20 mmol/l Tris-HCl, 0.5 mol/l NaCl, 1 mol/l imidazole, pH 7.5) was used. Incubation time was 30 min on ice with occasionally additional mixing. After magnetic separation the previous step was repeated with the strong elution buffer.

For the purification with the MagneHis[®] (Promega, Tokyo, Japan) the protocol was according to the manufacturer's manual, but the used amounts varied depending on the scale. Usually, the Ni²⁺-particles were vortexed before usage, and then 100 μ l particles were added to 1 ml sample. Incubation was 10 min after mixing, but for the big scale it was 2 h rotating a 4°C. A magnet was used for the magnetic separation. The supernatant was removed and 500 μ l wash buffer (100 mmol/l HEPES, 10 mmol/l imidazole) was added and mixed. After magnetic separation, the previous step was two times repeated. For elution, 200 μ l elution buffer (100 mmol/l HEPES, 500 mmol/l imidazole) was used. For the strong elution was a different buffer (20 mmol/l Tris-HCl, 0.5 mol/l NaCl, 1 mol/l imidazole, pH 7.5) applied.

8.2.3. Lysis of *E. coli* cells

A thawed cell pellet containing *E. coli* with expressed mCherry was resuspended in 3 ml ice-cold PBS per 50 ml culture. To a 15 ml solution 15 μ l lysozyme and 15 μ l 1x cOmplete Mini[®] EDTA free Version protease inhibitor (from a 100X stock solution) were added and incubated on ice for 30 min. Sonication was done with an amplitude of 70 in a cycle with 30 sec sonication and 30 sec on ice for 20 min. This solution was then centrifuged at 12000 \times g, 10 min, 4°C. The supernatant was filtered with a 0.2 μ m filter before further use.

8.3. Results and Discussion

8.3.1. Preliminary and purification comparison tests

To compare the MNPs with the MagneHis magnetic beads from Promega, MNP 1 and the commercial MNP were used to purify the SpCaVP1+EDIII VLP from silkworm fat body. To avoid high amount of unspecific binding of proteins to the magnetic particles, a low concentration of imidazole was in the washing buffer, 10 mmol/l for MagneHis as recommended from the company and 20 mmol/l for MNPs. The 1st elution buffer contained 300 mmol/l for commercial magnetic beads and 500 mmol/l imidazole for the MNPs, the 2nd elution buffer contained in all cases 1 mol/l imidazole. As in the shown in chapter 10.1 the Spy-tag/-Catcher linked coexpression construct has a size from around 95 kDa and it was clear that MNP 1 was not able to bind this His-tagged VLP. The commercial magnetic beads in contrast were able to bind the target protein and to separate them from all other unspecific bound proteins in the

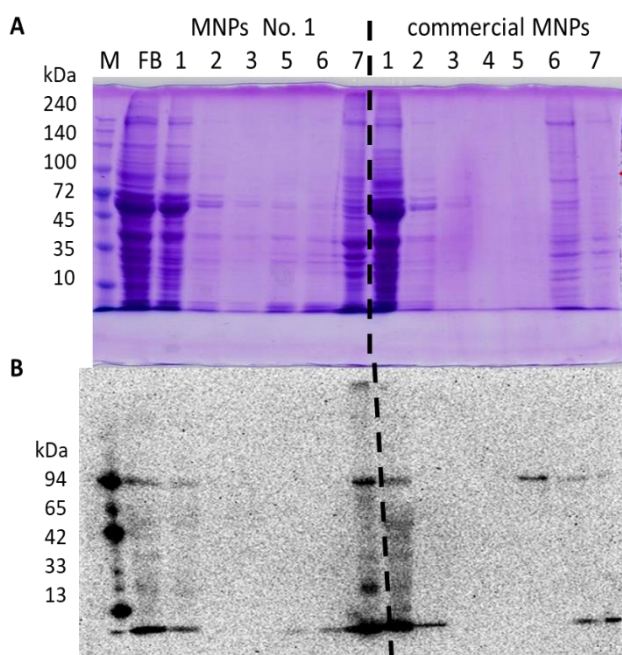


Fig. 75 (right): MNP purification comparison between MNP 1 and commercial MNP using complex sample matrix (A) CBB and (B) Western Blot of SpCaVP1 + EDIII purification using Ni-MNPs No. 1 and commercially available Ni-MNPs. On each line 15 μ l was loaded. It was an 8 μ l sample to 22 μ l dilution. FB: fat body; 1: Flow through; 2: 1. Wash fraction; 3: 2. Wash fraction; 4: 3. Wash fraction; 5: 1. Elution fraction; 6: 2. Elution fraction; 7: MNPs after elution of target protein; M: marker; red arrow indicates target protein. From Minkner R., Takemura K., Xu J. et al (unpublished results)

first elution fraction (**Fig. 75**). One mol/l imidazole removed most unspecific bound proteins from the magnetic beads. However, the magnetic beads were not able to bind all the target protein and to elute them in such a high concentration that a protein band is visible with Coomassie staining (**Fig. 75**). The process was scaled up to get a protein band for the target protein with the commercial magnet beads after Coomassie staining. Former it was 1 ml fat body and 100 μ l magnetic beads, this time 3.4 ml fat body and 400 μ l magnetic beads were used. Moreover, the flow through was again loaded with the regenerated magnetic beads and all elution fractions pooled. Despite that, the western blot signal for the non-concentrated

elution fraction was very weak compared to previously (**Fig. 76 B**). Only the western blot signal for the around threefold concentrated elution fraction was strong as before (**Fig. 76 B**), but the protein band was still not visible with a Coomassie staining (**Fig. 76 A**).

Because of the binding inability of MNP 1; MNP 2 and MNP 3 abilities to separate the his tagged VLP were investigated. These MNPs were also not able to bind the VLP (**Fig. 77**). This result raised the issue if the silkworm fat body as a sample matrix for the proof of concept is too difficult. Therefore, the His-tagged protein mCherry was as a model sample purified from *E. coli* cell lysate. As already described one additional benefit is the strong red fluorescence (Ex. 540-590 nm Em. 550-650 nm) and the red colour of mCherry which makes the tracing of the protein during the purification process easy. Using this sample matrix and model protein, MNP 2 and MNP 3 were able to bind and separate the mCherry from the host cell proteins (**Fig. 78 A**). MNP 3 is more advantageous than MNP 2, because more target protein could be eluted from it and was not strongly bound to the MNP (**Fig. 78 A**). Moreover, the protein amount in the elution fraction is higher, compared to MNP 2 (**Fig. 78 A**), this is also observable

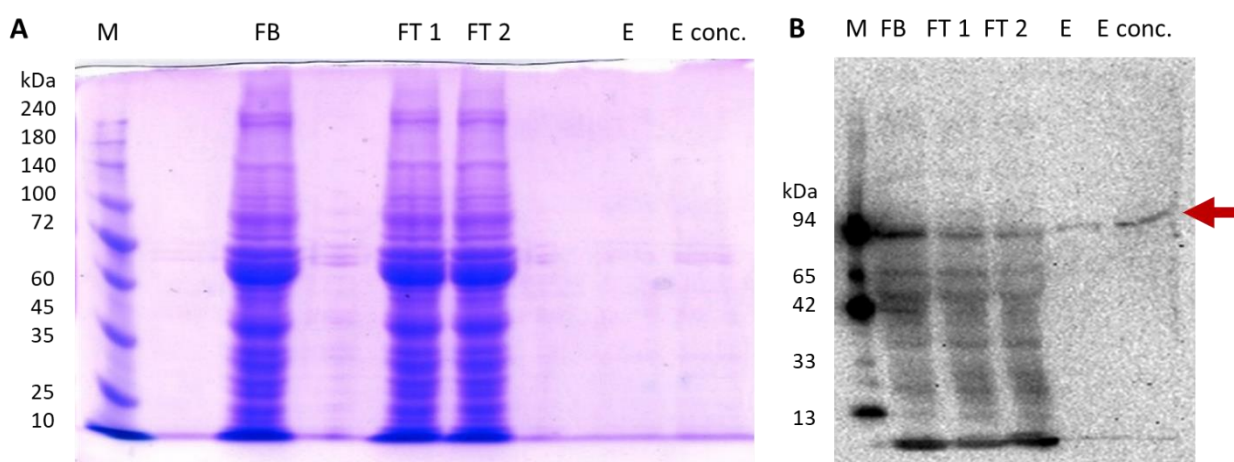


Fig. 76: Scaled up purification of SpCaVP1+EDIII with commercial beads (A) CBB and (B) Western Blot of a upscaled purification test of SpCaVP1 + EDIII using commercially available Ni-MNPs. On each line 15 μ l was loaded. It was an 8 μ l sample to 22 μ l dilution. FB: fat body; FT1: Flow through 1; FT2: Flow through after the repeated loading with regenerated MNPs; E: All elution fractions pooled; E conc.: Concentrated elution pool; red arrow indicates target protein; From Minkner R., Takemura K., Xu J. et al (unpublished results)

by the fluorescence, as the red fluorescence of the elution fraction 1 from MNP 3 is already stronger than from MNP 2 (Fig. 78 B).

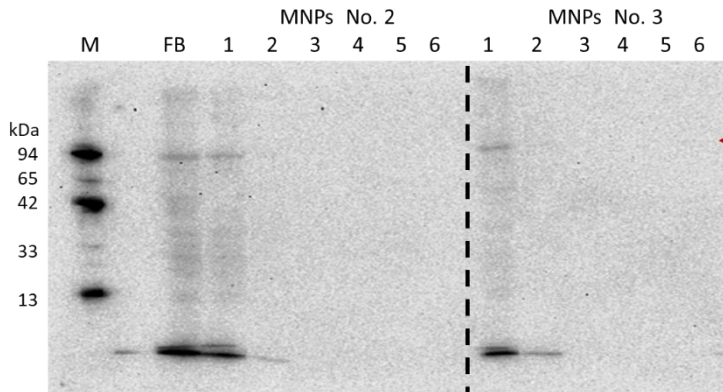


Fig. 77 (left): Western Blot of SpCaVP1 + EDIII purification using Ni-MNPs No. 2 and No. 3. On each line 15 μ l was loaded. It was an 8 μ l sample to 22 μ l dilution.

FB: fat body; 1: Flow through ; 2: 1. Wash fraction; 3: 2. Wash fraction; 4: 1. Elution fraction; 5: 2. Elution fraction; 6: MNPs after elution of target protein; M: marker; red arrow indicates target protein. From Minkner R., Takemura K., Xu J. et al (unpublished results)

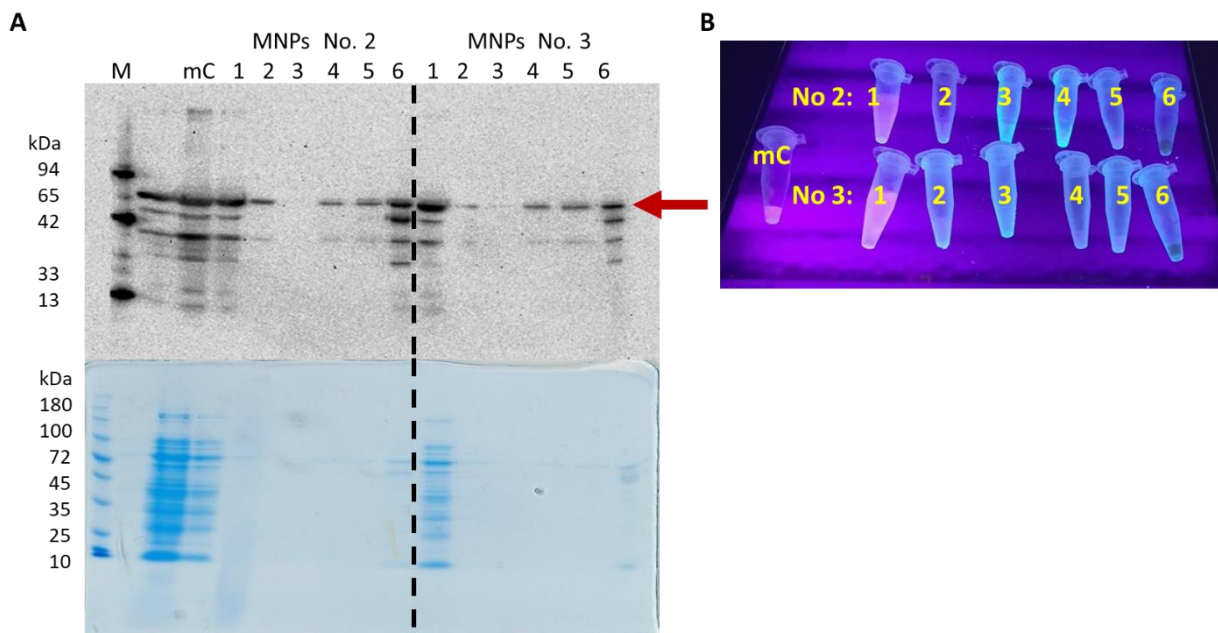


Fig. 78: (A) Western Blot and CBB of mCherry *E. coli* cell lysate purification using Ni-MNPs No. 2 and No. 3. (B) The red fluorescence shows directly the behaviour of the mCherry during the purification steps. On each line 15 μ l was loaded. It was a 8 μ l sample to 22 μ l dilution.

mC: mCherry *E. coli* cell lysate ; 1: Flow through ; 2: 1. Wash fraction; 3: 2. Wash fraction; 4: 1. Elution fraction with 300 mmol/l imidazole; 5: 2. Elution fraction with 1 mol/l imidazole; 6: MNPs after elution of target protein; M: marker; red arrow indicates target protein. From Minkner R., Takemura K., Xu J. et al (unpublished results)

8.3.2. Highly dispersible magnetic nano particles

The previous MNPs easily aggregated and stuck to the tube walls during the purification. Besides complicating the whole purification process, the loss increased and therefore, the recovery of the target proteins was also reduced. To overcome these problems, the MNPs were further improved to be easier dispersible in aqueous solutions. The resulting particles were named “highly dispersible MNPs” (MNPs 4) and successfully tested for purification. The previous mCherry purification was repeated with MNP 3 as comparison, whereby the sample amount was slightly increased (250 μ l versus 300 μ l) and the MNP amount slightly reduced (350 μ l versus 300 μ l of a 2 mg/ml MNP solution). The purification results of MNPs 4 clearly outmatched that from MNPs 3. Both the unspecific binding decreased significantly, compared to MNPs 3 the amount of eluted target protein was as well increased and by western blot the specificity of the eluted proteins improved (**Fig. 79 A**). Decreased unspecific binding and better elution ability were also visible on the western membrane stained by CBB, thereby even a strong band of the target mCherry was visible (**Fig. 79 A**). The fluorescence emission of the samples from the different purification steps supported this conclusion (**Fig. 79 B**). On the

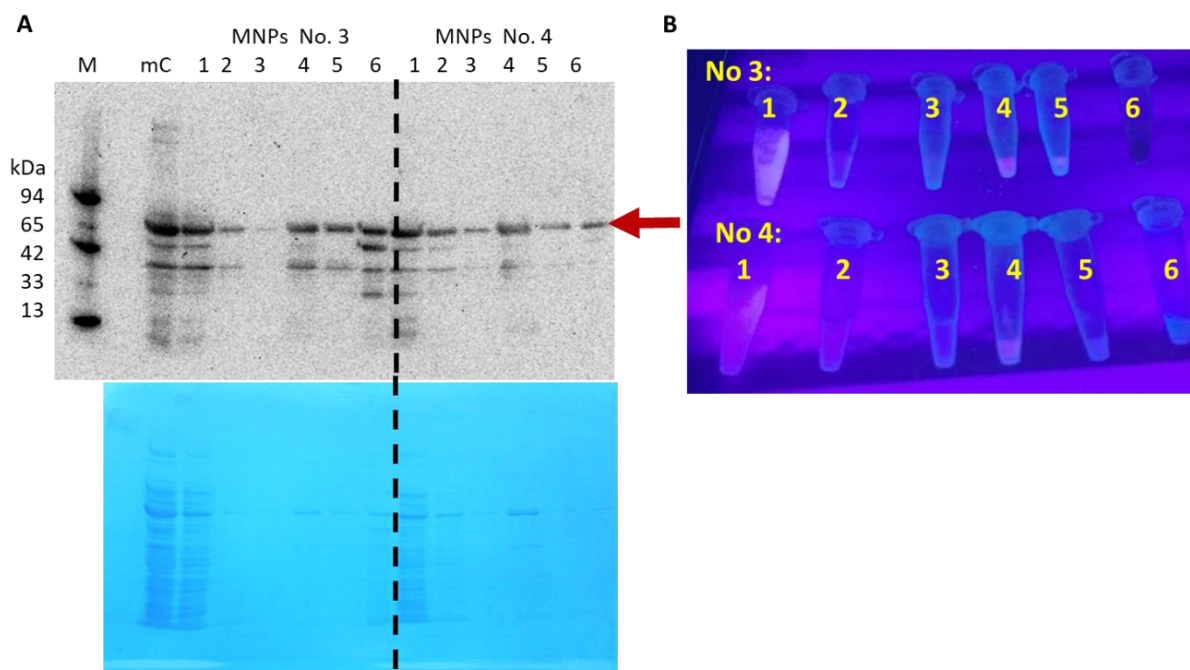


Fig. 79: (A) Western Blot and CBB from blot membrane of mCherry *E. coli* cell lysate purification using Ni-MNPs No. 3 and No. 4. (B) The red fluorescence shows directly the behaviour of the mCherry during the purification steps. On each line 15 μ l was loaded. It was an 8 μ l sample to 22 μ l dilution. mC: mCherry *E. coli* cell lysate; 1: Flow through; 2: 1. Wash fraction; 3: 2. Wash fraction; 4: 1. Elution fraction with 1 mol/l imidazole; 5: 2. Elution fraction with 1 mol/l imidazole; 6: MNPs after elution of target protein; M: marker; red arrow indicates target protein. From Minkner R., Takemura K., Xu J. et al (unpublished results)

other hand, the fluorescence shows that compared to MNPs 3 a high amount of target protein could not bind strongly enough and was in the wash fractions and this was supported by western blot (**Fig. 79 A and B**).

8.3.3. Proof of concept for purification from a complex sample matrix using highly dispersible MNPs

After the functionality of the MNPs 4 was proved, the purification of the His-tagged

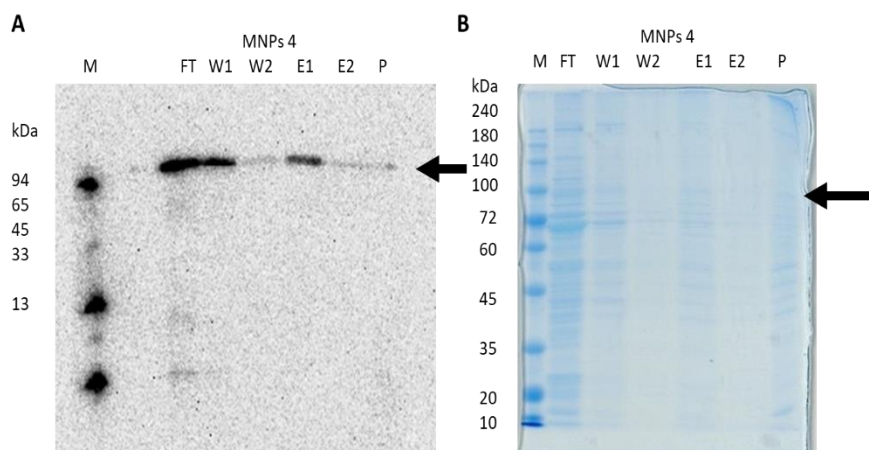


Fig. 80: Purification of SpCaVP1 + ED III fat body with MNPs 4. (A)

Western blot and **(B)** Coomassie blue stained SDS-PAGE of the purification with MNPs No.4. Wash buffer contained 20 mmol/l imidazole. The elution for was done with 1 mol/l imidazole, each 50 μ l. It was 8 μ l sample to 22 μ l dilution and on each line 15 μ l was loaded. No load was shown. FT: Flow through; W1: 1st Wash fraction; W2: 2nd Wash fraction; E1: 1st Elution fraction; E2: 2nd Elution fraction; P: MNPs; M is Marker; Black arrow indicates target protein. From Minkner R., Takemura K., Xu J. et al (unpublished results)

SpCaVP1+EDIII VLPs from the silkworm fat body was again challenged. The protocol was similar as for the MNPs 1, MNPs 2 and MNPs 3. Major changes were the increase in MNP quantity (from 100 μ l to 500 μ l 2 mg/ml solution) and that the first elution was already done with 1 mol/l instead of only 300 mmol/l imidazole. This

time the VLP were successfully separated with the MNPs and only a small loss occurred due to strong binding to the MNPs, because most VLPs were already in the first step eluted (**Fig. 80 A**), also compared to the results using the mCherry as sample. In opposite, directly using 1 mol/l imidazole as first elution buffer proved to be disadvantageous. The band cannot be clearly distinguished from the also eluted unspecific bound host cell proteins, even if the western blot band of the target protein was strong (**Fig. 80 B**). This is different from the previous result in which mainly the target protein was detectable and only some other impurities were remaining (**Fig. 79 A**). Nevertheless, highly dispersible MNPs were proven to be efficient for purification of recombinant proteins/VLPs from a complex matrix.

A scaling up using only SpCaVp1 VLPs showed that the recovery of the is still insufficient (**Fig. 81**), but total elution is successful. For recovery improvement the scaling up was repeated, but the MNP amount was increased (from 4.6 mg to 5.7 mg) and the buffer for washing did not contained any imidazole. However, even if all SpCaVP1 bound to the MNPs and could be eluted, the purity of the elution fraction decreased because of unspecific binding (**data not shown**). For further improving the protocol imidazole was once again in the washing buffer,

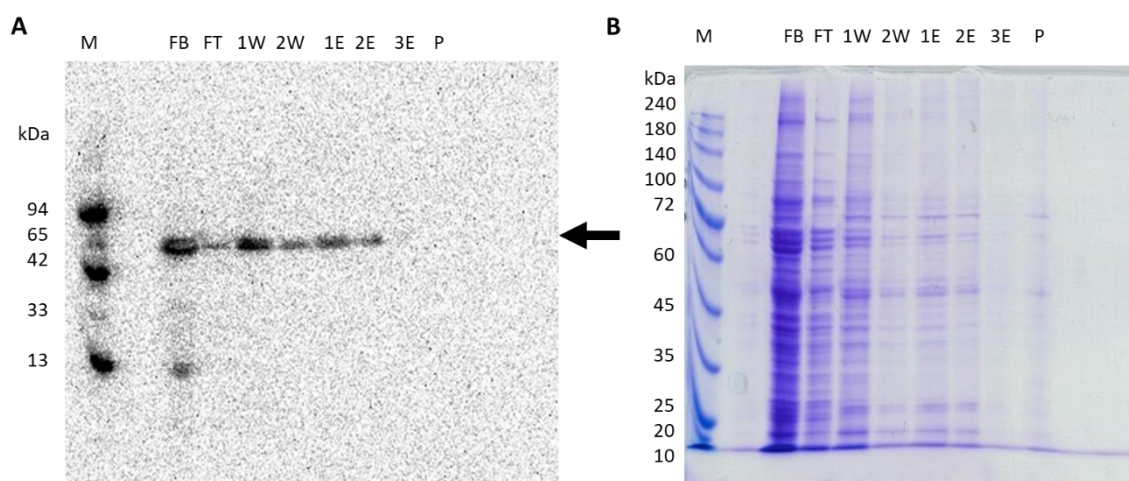


Fig. 81: Up-scaled purification of 1 ml SpCaVP1 fat body with self-made MNPs 4. (A) Western blot and **(B)** Coomassie blue stained SDS-PAGE of the purification with self-made MNPs No.4. Wash buffer contained 20 mmol/l imidazole. 1 ml fat body and 4.6 mg MNPs. First elution for was done with 300 mmol/l, the second and third with 1 mol/l imidazole, each 500 μ l. It was 8 μ l sample to 22 μ l dilution and on each line 15 μ l was loaded. FT: Flow through; W1: 1st Wash fraction; W2: 2nd Wash fraction; E1: 1st Elution fraction; E2: 2nd Elution fraction; E3: 3rd Elution fraction; P: MNPs; M is Marker; Black arrow indicates target protein
 From Minkner R., Takemura K., Xu J. et al (unpublished results)

but the MNP amount was now increased to 7.5 mg. This resulted also in total binding of the SpCaVP1, but in a small loss during the washing phase (**Fig. 82 A**). However, surprisingly much more proteins still bound to the MNPs and were eluted together with the SpCaVP1 (**Fig. 82 B**). Even if this amount is slightly lower than without imidazole in the washing buffer, the high amount is unusual, as the imidazole prevents this unspecific binding as already shown (**Fig. 81**). Hypotheses are that the MNPs also trapped non-His-tagged proteins, this effect because of the higher amount of MNPs increased and that they can maybe be released with improved washing, or that the unspecific binding of to the MNPs is too strong. The latter one could be improved with a slightly increased concentration of imidazole in the washing buffer, but it's most likely that also the recovery of the SpCaVP1 would decrease. Please note, that the flow through consisted of 2.6 ml, washing fractions of 1 ml and the elution fractions only of 500 μ l. For the last purification protocol (**Fig. 82**), a Bradford assay revealed that elution fractions 1

and 2 are only containing 22.26 % of the total protein amount (compared to the sum of FT, 1W, 2W, 1E, 3E and MNP fraction). That means a protein reduction of around 77.74 %.

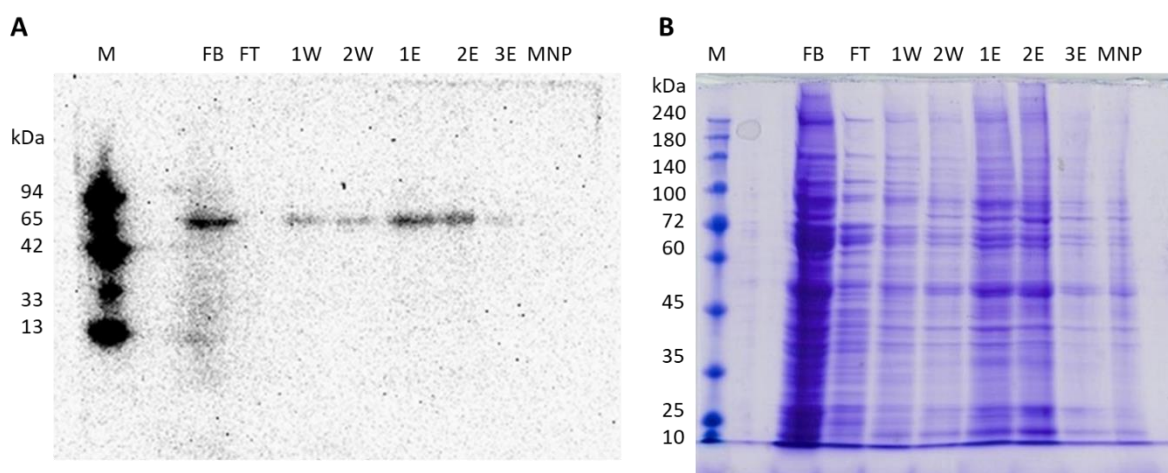


Fig. 82: Up-scaled purification of 1 ml SpCaVP1 fat body with self-made MNPs 4 in higher amount.

(A) Western blot and **(B)** Coomassie blue stained SDS-PAGE of the purification with self-made MNPs No.4. Wash buffer contained 20 mmol/l imidazole. 1 ml fat body and 7.5 mg MNPs. First elution for was done with 300 mmol/l, the second and third with 1 mol/l imidazole, each 500 μ l. It was 8 μ l sample to 22 μ l dilution and on each line 15 μ l was loaded. FT: Flow through; W1: 1st Wash fraction; W2: 2nd Wash fraction; E1: 1st Elution fraction; E2: 2nd Elution fraction; E3: 3rd Elution fraction; P: MNPs; M is Marker; Black arrow indicates target protein

From Minkner R., Takemura K., Xu J. et al (unpublished results)

8.3.4. Binding study of the highly dispersible MNPs

Using pure mCherry and as negative control bovine serum albumin (BSA), the binding to the MNPs was visualized using TEM (**Fig. 83**). **(A)** and **(C)** shows the MNP after incubation and **(B)** and **(D)** shows the MNP after washing and elution. It was shown that that the MNPs bound

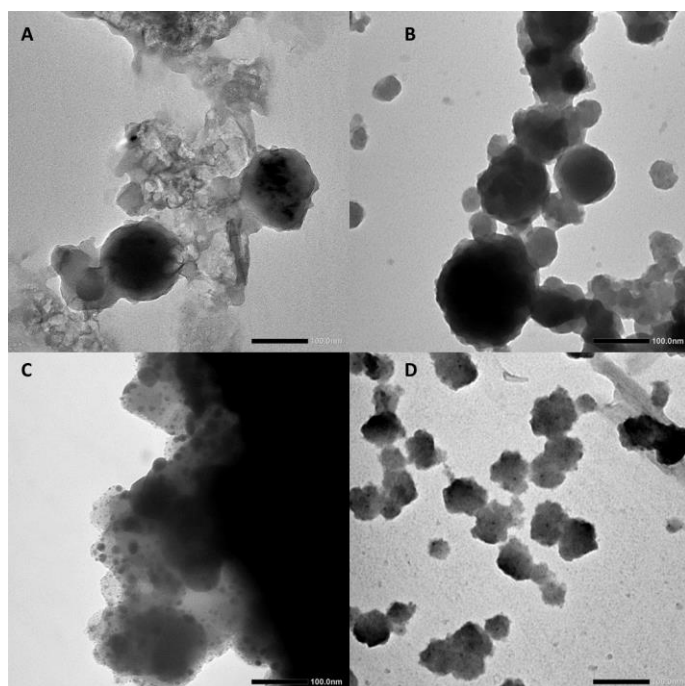


Fig. 83: Binding behaviour of MNPs No. 4 **(A)** mCherry + MNP (20 mM imidazole) **(B)** mCherry + MNP + 1 mol/l Imidazole (elution, after 2-times washing) **(C)** BSA + MNP (20 mM imidazole) **(D)** BSA + MNP + 1 mol/l Imidazole (elution, after 2-times washing); In all cases the MNP pellet was used and the supernatant discarded. **(C)** and **(D)** should theoretically not contain BSA, because of the washing; Scale bar is 100 nm; From Minkner R., Takemura K., Xu J. et al (unpublished results)

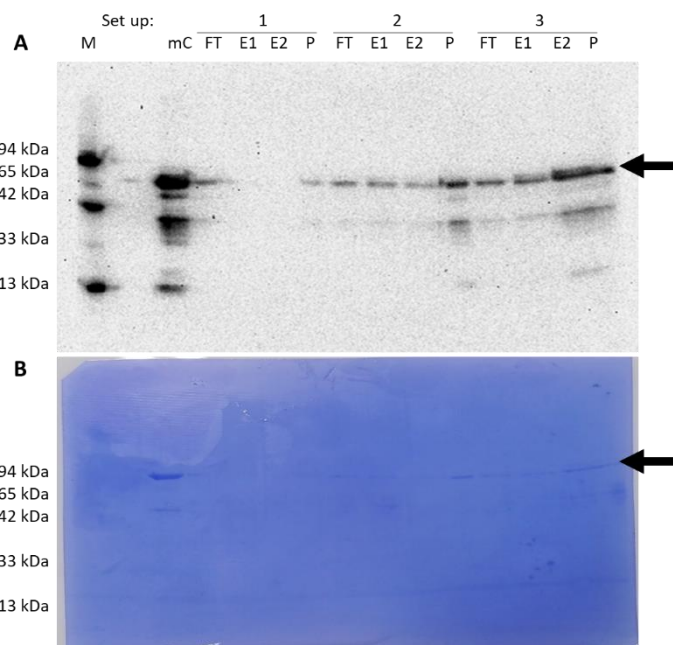
to mCherry and released it after elution (**Fig. 83 A+B**). However, it seems that BSA has a high affinity to the MNPs as it is visible in high amount around the MNPs, but it is also removed after the washing and elution steps (**Fig. 83 C+D**).

Using via Streptag affinity column pre-purified mCherry, it was intended to do a binding study with the highly dispersible MNPs. For this purified mCherry sample (120 $\mu\text{g/ml}$ protein) was added with three different volumes (100 μl = 12 μg ; 250 μl = 30 μg ; 400 μl = 48 μg) to 300 μl MNP solution (2 mg/ml) and buffer volume each time adjusted up to 950 μl . Besides the pre-purified mCherry with 120 μg protein/ml, no other protein concentration could be determined via Kit Pierce™ BCA Protein Assay Kit (Thermo Scientific, Waltham, USA) or BioRad Protein-Assay (BioRad, Hercules, CA, USA), because of the interaction with imidazole and the too low protein concentration (**data not shown**). Moreover, the low sample amount made it also impossible to do a buffer dialysis. Therefore, it was tried to solve this issue by using the intensity of Western Blot as reference (**Fig. 84**). Unfortunately, the western blot bands are too unstable and inconsistent to be analysed and calculated with image software (**data not shown**). This includes that the flow through signal is more or less stable and the elution fraction signal is only slightly increasing even if the loaded protein was increased. Moreover, the amount of protein which gives a signal during western blot is likewise increasing despite the strong elution buffer with 1 mol/l imidazole (**Fig. 84 A**). Nevertheless, several things are already indicated by these results. With the lowest protein amount, the target protein bound mainly to the MNPs and could not be eluted, but the target protein was also found in the flow through. On the other hand, with increased loaded protein amount, the loss in the flow through fractions remains mainly the same, but the amount eluted and still bound to the MNPs increased significantly (**Fig. 84 A**). The protein is still bound to the MNPs, despite the strong elution buffer with 1 mol/l imidazole. The failed plotting of the band intensities via image software also indicted this (**data not shown**). This rises two possibilities. One is that the elution from the nickel MNPs is not only imidazole dependent, but also at the same time concentration dependent on the already eluted amount in the surrounding buffer, compared to the amount which is still bound to the MNPs. The other option is that the amount of target protein, which is bound to the MNPs, is very high and the relative amount of the imidazole in the used buffer is too low to compete with all binding sites, despite the concentration of 1 mol/l, because in all elution's only 50 μl buffer were used. Moreover, with the highest amount of loaded protein the second elution fraction contained also high amount of target proteins,

which was not the case with the lower load amount (**Fig. 84**). As summary it has to be said that the binding study is not yet finished and has to be redone.

Fig. 84: Binding study of MNPs 4.

(A) Western blot and **(B)** Coomassie blue stained SDS-PAGE of small binding study with MNPs No.4. Wash buffer contained 20 mmol/l imidazole. The elution for was done with 1 mol/l imidazole, each 50 μ l. It was 8 μ l sample to 22 μ l dilution and on each line 15 μ l was loaded. Different set ups were used by the same amount of MNPs (300 μ l; 2 mg/ml): 1) 100 μ l sample + 550 μ l buffer = 12 μ g mCherry (protein); 2) 250 μ l sample + 400 μ l buffer = 30 μ g mCherry; 3) 400 μ l sample + 250 μ l buffer = 48 μ g mCherry; FT: Flow through; W1: 1st Wash fraction; W2: 2nd Wash fraction; E1: 1st Elution fraction; E2: 2nd Elution fraction; P: MNPs; M is Marker; Black arrow indicates target protein



8.4. Conclusion

As progress summary for the study of “Magnetic nano particles for the affinity purification of His-tagged proteins from complicated matrixes as pre-treatment” it can be said that these MNPs were successfully synthesized and the functionality proven. Even if the characterization is still not finished, the proof of concept and the feasibility of up-scaled purifications from complex sample matrixes such as the silkworm fat body were shown.

Unfortunately another study reported a quite similar project while this project was still ongoing [121]. In opposite to our work, bare iron oxide nano particles were used and a His-tagged GFP was as model protein purified. However, the most complex sample matrix was only a *E. coli* cell lysate which is comparable much easier than the silkworm fat body sample. Moreover, this reported particles seems to have the tendency to loosely agglomerate in opposite to the MNPs No. 4. Furthermore, their desorption time seems comparable longer, but no experiments for this were yet done to underlay this assumption with facts. Nevertheless, the published study has another advantage, as they were able to use High-Gradient Magnetic Fishing and proof this concept also on a larger scale.

9. Conclusion and Outlook

As described, many projects (some only mentioned in the appendix) were done not only with the intention to purify a specific recombinant protein, but to establish a wider general purification protocol. This purification protocol should have been easy, cheap, fast, industrial up-scalable and resulting in a high yield and purity. Of course, this ideal protocol was never achievable. Moreover, the majority of the projects were stopped. The GFP- β 3GnT2 project was stopped because of the decrease of the protein expression level, the RSV-LPs proved to be too unstable for purification, the MERS-VLPs were not express-able and three small MNPs studies were also paused because of failed binding ability which was not further investigated. However, the non-enveloped norovirus VP1 + EDIII VLP standard purification is rather ambivalent. So far, the purification hit a dead end, but this dead end is maybe still solvable, but with the addition that the SEC problem can be solved. Regrettably, this work could not be further investigated before finishing this dissertation. Nevertheless, much progress for the silkworm purification could be made with the remaining projects. It was possible to report the first study about VLP purification aiming for industrial usability. This purification protocol avoids the cost intensive affinity tag purification and the insufficient sucrose gradient centrifugation, which gives neither a good purity nor is easily up-scalable. The purity excelled the from affinity purification and besides removed all infective baculovirus compared to the aforementioned methods. However, the recovery left a lot to be desired with 5.5 %, even if it could be shown, that this low recovery was partly due to the VLP instability. This study was the motive for further investigations and trials to improve the purity and recovery of recombinant proteins from silkworm compounds. This led to the successful purification of the red fluorescence protein mCherry from the haemolymph, which was designated as an easy traceable model recombinant protein. The purification protocol lacked purity and therefore, a thermal treatment was investigated and included prior the chromatography steps. This treatment proved to be so successful, that theoretically the precipitation step and the 3rd chromatography step could be omitted. Moreover, the purity and recovery should be even better, if a more suitable SEC column can be utilized. However, this protocol has one big flaw and this is the thermal treatment itself. The thermal treatment was 70°C for 20 min and even if it can be lowered to 50°C for the silkworm host cell proteins, it remains unchanged that this protocol is only applicable for (partly) heat stable proteins. Yet, this drawback may not be as great as it seems at the moment. There seems to be the trend in

biotechnology to design recombinant proteins more stable, this includes also heat stability. It still has to be seen, if this protocol can benefit from this trend. As last project, which is currently in its final stages, is the purification of His-tagged proteins from silkworm compounds. Well, purification of His-tagged proteins is itself nothing new, not even with using MNPs, but the commercially available MNPs are still far from sufficient for purification, especially for larger scale. The aim is to develop sufficiently efficient and easy self-makeable MNPs by low cost. Up to now, the project is well underway and the functionality of the MNPs could not only be proved with a pure sample, but also from crude *E. coli* cell lysate and even from the more complex silkworm fat body as sample matrix. This project still needs some more refinement, but this is scheduled to be finished after this dissertation.

To discuss another aspect, in the introduction chapter the different structures and stabilities of VLPs were mentioned. This stability was also evident in these studies, as there were rarely problems with the stability of the non-enveloped VLPs (HPV-LPs and NoV-LPs), but with the enveloped VLPs, the RSV-LPs. The latter one degraded faster and were significantly more sensitive regarding the purification process, as they could be easily destroyed. Moreover, in the early purification stages the destroyed VLPs could not be visually confirmed via TEM, as the sample matrix still contained high amount of other proteins. It could be only assumed or as shown via western blot detected, when not all respective protein bands were in the same fraction. However, because it was not further investigated it cannot be said that the instability and destruction is because of the purification process, the instability of the constructs or even if the VLPs did not form properly right from the beginning.

Finally, as in this dissertation shown, a lot of progress was made, but there is still a long way to go, before a satisfying purification protocol will be achieved. What could be the next steps for this? First and foremost, it would be advisable to determine the proteome of this silkworm strain, especially for the purification relevant proteins. That refers to the host cell proteins which are abundant and proved to be hard to remove from the sample by the former purification attempts. At minimum the identity of the proteins at 20–30 kDa and 60–80 kDa have to be undoubtedly determined, so that hopefully purification strategies can be devised for them. So that these proteins can be removed, or maybe it will be even possible to genetically modify the silkworms to express these proteins less. If these proteins are mainly storage proteins as suspected, this approach seems reasonable as these storage proteins

should be mainly relevant for the pupae stage, before which the silkworms die. Another approach is to improve the MNPs for the purification, at first the purification using affinity tags, but also later to a more general purification principle to avoid affinity tags. Furthermore, a very intriguing idea of this laboratory is to produce stable, non-toxic MNPs and to use them in a one-step harvesting and purification strategy. In this strategy the infected silkworms will be injected with the MNPs, which then will bind to the into the haemolymph secreted proteins. After haemolymph collection the recombinant protein can be then directly magnetically separated. Of course, this idea brings other issues such as toxicity, stability, point of time and biopharmaceutical effects. Nevertheless, this fascinating idea is something to look forward to.

10. Acknowledgment

Research is nowadays not a one man show; therefore, I did not work on each project every time alone, but was also part of one team or worked based on the work of someone else.

Provided research projects: Prof. Enoch Y. Park, Prof. Tatsuya Kato, Dr. Jian Xu and Prof. Vipin Kumar Deo

Cooperation work on projects: Rina Baba, Yae Kurosawa, Shinichiro Suzuki, Shintaro Kobayashi, Holger Zagst, Dr. Imke Oltmann-Norden, Prof. Hermann Wätzig, Kenshin Takemura, Dr. Jaewook Lee and Dr. Jian Xu

CE-SDS: Holger Zagst, Dr. Imke Oltmann-Norden and Prof. Hermann Wätzig

Provided material: Yuki Machida, Rikito Hiramatsu, Hirono Ichikawa, Jirayu Boonyakida, Takafumi Nakanishi, Prof. Vipin Kumar Deo, Yoshihiro Takami, Kenshin Takemura, Dr. Jaewook Lee, Dr. Jian Xu and Dr. Ankan Dutta Chowdhury

Specifically, the HPV purification project was done in cooperation with Ms. Yae Kurosawa and Mr. Shintaro Kobayashi (R&D Department, Hoya Technosurgical Co.), Prof. Tatsuya Kato, Mr. Shinichiro Suzuki and was taken over from the former Master student Ms. Rina Baba.

11. References

- [1] V.K. Deo, T. Kato, E.Y. Park, Chimeric virus-like particles made using GAG and M1 capsid proteins providing dual drug delivery and vaccination platform, *Molecular pharmaceutics* 12 (2015) 839–845.
- [2] Y.E. Khudyakov, H.A. Fields, *Artificial DNA: Methods and applications*, CRC Press, Boca Raton Fla., 2003.
- [3] L.H.L. Lua, N.K. Connors, F. Sainsbury, Y.P. Chuan, N. Wibowo, A.P.J. Middelberg, Bioengineering virus-like particles as vaccines, *Biotechnology and bioengineering* 111 (2014) 425–440.
- [4] M.P. Rudolf, S.C. Fausch, D.M. Da Silva, W.M. Kast, Human Dendritic Cells Are Activated by Chimeric Human Papillomavirus Type-16 Virus-Like Particles and Induce Epitope-Specific Human T Cell Responses In Vitro, *The Journal of Immunology* 166 (2001) 5917–5924.
- [5] M. Peacey, S. Wilson, M.A. Baird, V.K. Ward, Versatile RHDV virus-like particles: Incorporation of antigens by genetic modification and chemical conjugation, *Biotechnology and bioengineering* 98 (2007) 968–977.
- [6] M. Palaniyandi, T. Kato, E.Y. Park, Expression of human papillomavirus 6b L1 protein in silkworm larvae and enhanced green fluorescent protein displaying on its virus-like particles, *SpringerPlus* 1 (2012) 29.
- [7] H.L. Greenstone, J.D. Nieland, K.E. de Visser, M.L.H. de Bruijn, R. Kirnbauer, R.B.S. Roden et al., Chimeric papillomavirus virus-like particles elicit antitumor immunity against the E7 oncoprotein in an HPV16 tumor model, *Proceedings of the National Academy of Sciences* 95 (1998) 1800–1805.
- [8] R. Wagner, L. Deml, R. Schirmbeck, M. Niedrig, J. Reimann, H. Wolf, Construction, expression, and immunogenicity of chimeric HIV-1 virus-like particles, *Virology* 220 (1996) 128–140.
- [9] T. Latham, J.M. Galarza, Formation of wild-type and chimeric influenza virus-like particles following simultaneous expression of only four structural proteins, *Journal of virology* 75 (2001) 6154–6165.
- [10] S.L. Young, M. Wilson, S. Wilson, K.W. Beagley, V. Ward, M.A. Baird, Transcutaneous vaccination with virus-like particles, *Vaccine* 24 (2006) 5406–5412.

- [11] V.K. Deo, K. Yoshimatsu, T. Otsuki, J. Dong, T. Kato, E.Y. Park, Display of Neospora caninum surface protein related sequence 2 on Rous sarcoma virus-derived gag protein virus-like particles, *Journal of biotechnology* 165 (2013) 69–75.
- [12] L.L. Villa, K.A. Ault, A.R. Giuliano, R.L.R. Costa, C.A. Petta, R.P. Andrade et al., Immunologic responses following administration of a vaccine targeting human papillomavirus Types 6, 11, 16, and 18, *Vaccine* 24 (2006) 5571–5583.
- [13] R. Wagner, V.J. Teeuwesen, L. Deml, F. Notka, A.G. Haaksma, S.S. Jhagjhoorsingh et al., Cytotoxic T cells and neutralizing antibodies induced in rhesus monkeys by virus-like particle HIV vaccines in the absence of protection from SHIV infection, *Virology* 245 (1998) 65–74.
- [14] G.T. LAYTON, S.J. HARRIS, J. MYHAN, D. WEST, F. GOTCH, M. HILL-PERKINS et al., Induction of single and dual cytotoxic T-lymphocyte responses to viral proteins in mice using recombinant hybrid Ty-virus-like particles, *Immunology* 87 (1996) 171–178.
- [15] T. Kato, M. Kajikawa, K. Maenaka, E.Y. Park, Silkworm expression system as a platform technology in life science, *Applied microbiology and biotechnology* 85 (2010) 459–470.
- [16] M. Tan, W. Zhong, D. Song, S. Thornton, X. Jiang, E. coli-expressed recombinant norovirus capsid proteins maintain authentic antigenicity and receptor binding capability, *Journal of medical virology* 74 (2004) 641–649.
- [17] S. Brumfield, D. Willits, L. Tang, J.E. Johnson, T. Douglas, M. Young, Heterologous expression of the modified coat protein of Cowpea chlorotic mottle bromovirus results in the assembly of protein cages with altered architectures and function, *The Journal of general virology* 85 (2004) 1049–1053.
- [18] N.M. Molino, S.-W. Wang, Caged protein nanoparticles for drug delivery, *Current opinion in biotechnology* 28 (2014) 75–82.
- [19] P. Singh, G. Destito, A. Schneemann, M. Manchester, Canine parvovirus-like particles, a novel nanomaterial for tumor targeting, *Journal of nanobiotechnology* 4 (2006) 2.
- [20] R.L. Garcea, L. Gissmann, Virus-like particles as vaccines and vessels for the delivery of small molecules, *Current opinion in biotechnology* 15 (2004) 513–517.
- [21] T. Kato, M. Yui, V.K. Deo, E.Y. Park, Development of Rous sarcoma Virus-like Particles Displaying hCC49 scFv for Specific Targeted Drug Delivery to Human Colon Carcinoma Cells, *Pharmaceutical research* 32 (2015) 3699–3707.

- [22] T. Yamada, Y. Iwasaki, H. Tada, H. Iwabuki, M.K.L. Chuah, T. VandenDriessche et al., Nanoparticles for the delivery of genes and drugs to human hepatocytes, *Nature Biotechnology* 21 (2003) 885–890.
- [23] A. Zeltins, Construction and characterization of virus-like particles: A review, *Molecular biotechnology* 53 (2013) 92–107.
- [24] C. Goldmann, N. Stolte, T. Nisslein, G. Hunsmann, W. Lüke, H. Petry, Packaging of small molecules into VP1-virus-like particles of the human polyomavirus JC virus, *Journal of virological methods* 90 (2000) 85–90.
- [25] F.A. Galaway, P.G. Stockley, MS2 viruslike particles: A robust, semisynthetic targeted drug delivery platform, *Molecular pharmaceuticals* 10 (2013) 59–68.
- [26] V.K. Deo, T. Kato, E.Y. Park, Virus-Like Particles Displaying Recombinant Short-Chain Fragment Region and Interleukin 2 for Targeting Colon Cancer Tumors and Attracting Macrophages, *Journal of pharmaceutical sciences* 105 (2016) 1614–1622.
- [27] S. Peretti, I. Schiavoni, K. Pugliese, M. Federico, Selective elimination of HIV-1-infected cells by Env-directed, HIV-1-based virus-like particles, *Virology* 345 (2006) 115–126.
- [28] X. Geng, G. Doitsh, Z. Yang, N.L.K. Galloway, W.C. Greene, Efficient delivery of lentiviral vectors into resting human CD4 T cells, *Gene therapy* 21 (2014) 444–449.
- [29] C. Ludwig, R. Wagner, Virus-like particles-universal molecular toolboxes, *Current opinion in biotechnology* 18 (2007) 537–545.
- [30] A. Strods, V. Ose, J. Bogans, I. Cielens, G. Kalnins, I. Radovica et al., Preparation by alkaline treatment and detailed characterisation of empty hepatitis B virus core particles for vaccine and gene therapy applications, *Scientific reports* 5 (2015) 11639.
- [31] Y. Morikawa, T. Goto, D. Yasuoka, F. Momose, T. Matano, Defect of human immunodeficiency virus type 2 Gag assembly in *Saccharomyces cerevisiae*, *Journal of virology* 81 (2007) 9911–9921.
- [32] F. Krammer, T. Schinko, D. Palmberger, C. Tauer, P. Messner, R. Grabherr, *Trichoplusia ni* cells (High Five) are highly efficient for the production of influenza A virus-like particles: A comparison of two insect cell lines as production platforms for influenza vaccines, *Molecular biotechnology* 45 (2010) 226–234.
- [33] E.V.B. Catrice, F. Sainsbury, Assembly and Purification of Polyomavirus-Like Particles from Plants, *Molecular biotechnology* 57 (2015) 904–913.

- [34] A.J. Pietrzyk, A. Bujacz, M. Lochynska, M. Jaskolski, G. Bujacz, Isolation, purification, crystallization and preliminary X-ray studies of two 30 kDa proteins from silkworm haemolymph, *Acta crystallographica. Section F, Structural biology and crystallization communications* 67 (2011) 372–376.
- [35] P. Molinari, A. Peralta, O. Taboga, Production of rotavirus-like particles in *Spodoptera frugiperda* larvae, *Journal of virological methods* 147 (2008) 364–367.
- [36] A.L. Demain, P. Vaishnav, Production of recombinant proteins by microbes and higher organisms, *Biotechnology advances* 27 (2009) 297–306.
- [37] A. Miyajima, J. Schreurs, K. Otsu, A. Kondo, K.-i. Aral, S. Maeda, Use of the silkworm, *Bombyx mori*, and an insect baculovirus vector for high-level expression and secretion of biologically active mouse interleukin-3, *Gene* 58 (1987) 273–281.
- [38] T. Mitsudome, J. Xu, Y. Nagata, A. Masuda, K. Iiyama, D. Morokuma et al., Expression, purification, and characterization of endo-beta-N-acetylglucosaminidase H using baculovirus-mediated silkworm protein expression system, *Applied biochemistry and biotechnology* 172 (2014) 3978–3988.
- [39] S. Hervas-Stubbs, P. Rueda, L. Lopez, C. Leclerc, Insect Baculoviruses Strongly Potentiate Adaptive Immune Responses by Inducing Type I IFN, *The Journal of Immunology* 178 (2007) 2361–2369.
- [40] T. Abe, H. Takahashi, H. Hamazaki, N. Miyano-Kurosaki, Y. Matsuura, H. Takaku, Baculovirus Induces an Innate Immune Response and Confers Protection from Lethal Influenza Virus Infection in Mice, *The Journal of Immunology* 171 (2003) 1133–1139.
- [41] K. Nerome, S. Matsuda, K. Maegawa, S. Sugita, K. Kuroda, K. Kawasaki et al., Quantitative analysis of the yield of avian H7 influenza virus haemagglutinin protein produced in silkworm pupae with the use of the codon-optimized DNA: A possible oral vaccine, *Vaccine* 35 (2017) 738–746.
- [42] X. Zheng, S. Wang, W. Zhang, X. Liu, Y. Yi, S. Yang et al., Development of a VLP-based vaccine in silkworm pupae against rabbit hemorrhagic disease virus, *International immunopharmacology* 40 (2016) 164–169.
- [43] S. Matsuda, R. Nerome, K. Maegawa, A. Kotaki, S. Sugita, K. Kawasaki et al., Development of a Japanese encephalitis virus-like particle vaccine in silkworms using codon-optimised prM and envelope genes, *Heliyon* 3 (2017) e00286.

- [44] G. Mallikarjun, N.K. Neetha, B. Manjunatha, V. Sivaprasad, V. Shyam Kumar, A Mini Review of Functional Proteins in Silkworm *Bombyx mori* L Haemolymph, *Indian Journal of Science and Technology* 9 (2016).
- [45] Hideyuki Kajiwara, Yoko Itou, Atsue Imamaki, Masatoshi Nakamura, Kazuei Mita, Masumi Ishizaka, Proteomic Analysis of Silkworm Fat Body, *Journal of Insect Biotechnology and Sericology* 75 (2006) 47–56.
- [46] Y. Hou, Y. Zou, F. Wang, J. Gong, X. Zhong, Q. Xia et al., Comparative analysis of proteome maps of silkworm hemolymph during different developmental stages, *Proteome science* 8 (2010) 45.
- [47] C. Lamberti, F. Gai, S. Cirrincione, M. Giribaldi, M. Purrotti, M. Manfredi et al., Investigation of the protein profile of silkworm (*Bombyx mori*) pupae reared on a well-calibrated artificial diet compared to mulberry leaf diet, *PeerJ* 7 (2019) e6723.
- [48] R. Li, C. Hu, T. Geng, D. Lv, K. Gao, X. Guo et al., Expressional analysis of the silkworm storage protein 1 and identification of its interacting proteins, *Insect molecular biology* (2019).
- [49] Jae Man Lee, Hiroaki Mon, Masateru Takahashi, Naoya Kawakami, Hitoshi Mitsunobu, Yutaka Banno, Katsumi Koga, Keiro Uchino, Yutaka Kawaguchi, Takahiro Kusakabe, Screening of high-permissive silkworm strains for efficient recombinant protein production in *Autographia californica* Nuclear Polyhedrovirus (AcNPV), *Journal of Insect Biotechnology and Sericology* 76 (2007) 101–105.
- [50] J. Xu, P. Zhang, T. Kusakabe, H. Mon, Z. Li, L. Zhu et al., Comparative proteomic analysis of hemolymph proteins from *Autographa californica* multiple nucleopolyhedrovirus (AcMNPV)-sensitive or -resistant silkworm strains during infections, *Comparative biochemistry and physiology. Part D, Genomics & proteomics* 16 (2015) 36–47.
- [51] H.B. Manjunatha, R.K. Rajesh, H.S. Aparna, Silkworm thermal biology: A review of heat shock response, heat shock proteins and heat acclimation in the domesticated silkworm, *Bombyx mori*, *Journal of Insect Science* 1 (2010).
- [52] F. Sun, C.J. Ye, B. Li, T. Wang, T. Fan, Application of mass spectrometry in silkworm research-Review, *Biomedical chromatography BMC* 33 (2019) e4476.
- [53] A. Morio, J. Xu, A. Masuda, Y. Kinoshita, M. Hino, D. Morokuma et al., Expression, purification, and characterization of highly active endo- α -N-acetylgalactosaminidases

expressed by silkworm-baculovirus expression system, *Journal of Asia-Pacific Entomology* 22 (2019) 404–408.

[54] D. Morokuma, J. Xu, M. Hino, H. Mon, J.S. Merzaban, M. Takahashi et al., Expression and Characterization of Human beta-1, 4-Galactosyltransferase 1 (beta4GalT1) Using Silkworm-Baculovirus Expression System, *Molecular biotechnology* 59 (2017) 151–158.

[55] V.K. Deo, Y. Tsuji, T. Yasuda, T. Kato, N. Sakamoto, H. Suzuki et al., Expression of an RSV-gag virus-like particle in insect cell lines and silkworm larvae, *Journal of virological methods* 177 (2011) 147–152.

[56] J. Dong, M. Harada, S. Yoshida, Y. Kato, A. Murakawa, M. Ogata et al., Expression and purification of bioactive hemagglutinin protein of highly pathogenic avian influenza A (H5N1) in silkworm larvae, *Journal of virological methods* 194 (2013) 271–276.

[57] M. Ogata, M. Nakajima, T. Kato, T. Obara, H. Yagi, K. Kato et al., Synthesis of sialoglycopolypeptide for potentially blocking influenza virus infection using a rat alpha2,6-sialyltransferase expressed in BmNPV bacmid-injected silkworm larvae, *BMC biotechnology* 9 (2009) 54.

[58] P. Steppert, D. Burgstaller, M. Klausberger, E. Berger, P.P. Aguilar, T.A. Schneider et al., Purification of HIV-1 gag virus-like particles and separation of other extracellular particles, *Journal of chromatography. A* 1455 (2016) 93–101.

[59] T. Vicente, J.P.B. Mota, C. Peixoto, P.M. Alves, M.J.T. Carrondo, Rational design and optimization of downstream processes of virus particles for biopharmaceutical applications: Current advances, *Biotechnology advances* 29 (2011) 869–878.

[60] P. Nestola, C. Peixoto, R.R.J.S. Silva, P.M. Alves, J.P.B. Mota, M.J.T. Carrondo, Improved virus purification processes for vaccines and gene therapy, *Biotechnology and bioengineering* 112 (2015) 843–857.

[61] T. Vicente, M.F.Q. Sousa, C. Peixoto, J.P.B. Mota, P.M. Alves, M.J.T. Carrondo, Anion-exchange membrane chromatography for purification of rotavirus-like particles, *Journal of Membrane Science* 311 (2008) 270–283.

[62] S. Tsoka, O.C. Ciniawskyj, O.R. Thomas, N.J. Titchener-Hooker, M. Hoare, Selective flocculation and precipitation for the improvement of virus-like particle recovery from yeast homogenate, *Biotechnology progress* 16 (2000) 661–667.

- [63] L. Maranga, P. Rueda, A.F.G. Antonis, C. Vela, J.P.M. Langeveld, J.I. Casal et al., Large scale production and downstream processing of a recombinant porcine parvovirus vaccine, *Applied microbiology and biotechnology* 59 (2002) 45–50.
- [64] R.R. Burgess, Chapter 20 Protein Precipitation Techniques, in: *Guide to Protein Purification*, 2nd Edition, Elsevier, 2009, pp. 331–342.
- [65] S. Englard, S. Seifter, [22] Precipitation techniques, in: M.P. Deutscher (Ed.), *Guide to protein purification*, Academic Press, San Diego, Calif., 1990, pp. 285–300.
- [66] K.C. Ingham, [23] Precipitation of proteins with polyethylene glycol, in: M.P. Deutscher (Ed.), *Guide to protein purification*, Academic Press, San Diego, Calif., 1990, pp. 301–306.
- [67] T. Kröber, A. Knöchlein, K. Eisold, B. Kalbfuß-Zimmermann, U. Reichl, DNA Depletion by Precipitation in the Purification of Cell Culture-Derived Influenza Vaccines, *Chem. Eng. Technol.* 33 (2010) 941–959.
- [68] Z. Li, J. Wei, Y. Yang, L. Liu, G. Ma, S. Zhang et al., A two-step heat treatment of cell disruption supernatant enables efficient removal of host cell proteins before chromatographic purification of HBc particles, *Journal of chromatography. A* 1581-1582 (2018) 71–79.
- [69] M.F.X. Lee, E.S. Chan, W.S. Tan, K.C. Tam, B.T. Tey, Negative chromatography purification of hepatitis B virus-like particles using poly(oligo(ethylene glycol) methacrylate) grafted cationic adsorbent, *Journal of chromatography. A* 1415 (2015) 161–165.
- [70] M. Zaveckas, S. Snipaitis, H. Pesliakas, J. Nainys, A. Gedvilaite, Purification of recombinant virus-like particles of porcine circovirus type 2 capsid protein using ion-exchange monolith chromatography, *Journal of chromatography. B, Analytical technologies in the biomedical and life sciences* 991 (2015) 21–28.
- [71] L. Xue, J. Liu, Q. Wang, C. Zhang, L. Xu, J. Luo et al., Purification and assembling a fused capsid protein as an enterovirus 71 vaccine candidate from inclusion bodies to pentamer-based nanoparticles, *Biochemical Engineering Journal* 117 (2017) 139–146.
- [72] C. Gurramkonda, M. Zahid, S.K. Nemani, A. Adnan, S.K. Gudi, N. Khanna et al., Purification of hepatitis B surface antigen virus-like particles from recombinant *Pichia pastoris* and in vivo analysis of their immunogenic properties, *Journal of chromatography. B, Analytical technologies in the biomedical and life sciences* 940 (2013) 104–111.

- [73] B. Leuchs, V. Frehtman, M. Riese, M. Muller, J. Rommelaere, A novel scalable, robust downstream process for oncolytic rat parvovirus: Isoelectric point-based elimination of empty particles, *Applied microbiology and biotechnology* 101 (2017) 3143–3152.
- [74] P. Nestola, C. Peixoto, L. Villain, P.M. Alves, M.J.T. Carrondo, J.P.B. Mota, Rational development of two flowthrough purification strategies for adenovirus type 5 and retro virus-like particles, *Journal of chromatography. A* 1426 (2015) 91–101.
- [75] P. Du, S. Sun, J. Dong, X. Zhi, Y. Chang, Z. Teng et al., Purification of foot-and-mouth disease virus by heparin as ligand for certain strains, *Journal of chromatography. B, Analytical technologies in the biomedical and life sciences* 1049-1050 (2017) 16–23.
- [76] S.T. Mundle, M. Kishko, R. Groppo, J. DiNapoli, J. Hamberger, B. McNeil et al., Core bead chromatography for preparation of highly pure, infectious respiratory syncytial virus in the negative purification mode, *Vaccine* 34 (2016) 3690–3696.
- [77] D. Sviben, D. Forcic, J. Ivancic-Jelecki, B. Halassy, M. Brgles, Recovery of infective virus particles in ion-exchange and hydrophobic interaction monolith chromatography is influenced by particle charge and total-to-infective particle ratio, *Journal of chromatography. B, Analytical technologies in the biomedical and life sciences* 1054 (2017) 10–19.
- [78] M.F.X. Lee, E.S. Chan, W.S. Tan, K.C. Tam, B.T. Tey, Negative chromatography of hepatitis B virus-like particle: Comparative study of different adsorbent designs, *Journal of chromatography. A* 1445 (2016) 1–9.
- [79] J. Freivalds, A. Dislers, V. Ose, P. Pumpens, K. Tars, A. Kazaks, Highly efficient production of phosphorylated hepatitis B core particles in yeast *Pichia pastoris*, *Protein expression and purification* 75 (2011) 218–224.
- [80] M.F.X. Lee, E.S. Chan, B.T. Tey, Negative chromatography: Progress, applications and future perspectives, *Process Biochemistry* 49 (2014) 1005–1011.
- [81] P. Marichal-Gallardo, M.M. Pieler, M.W. Wolff, U. Reichl, Steric exclusion chromatography for purification of cell culture-derived influenza A virus using regenerated cellulose membranes and polyethylene glycol, *Journal of Chromatography A* 1483 (2017) 110–119.
- [82] S.-Y. Lin, H.-Y. Chiu, B.-L. Chiang, Y.-C. Hu, Development of EV71 virus-like particle purification processes, *Vaccine* 33 (2015) 5966–5973.

- [83] T. Kato, S.L. Manoha, S. Tanaka, E.Y. Park, High-titer preparation of Bombyx mori nucleopolyhedrovirus (BmNPV) displaying recombinant protein in silkworm larvae by size exclusion chromatography and its characterization, *BMC biotechnology* 9 (2009) 55.
- [84] Y. Kurosawa, M. Saito, S. Kobayashi, T. Okuyama, Purification of Dengue Virus Particles by One-Step Ceramic Hydroxyapatite Chromatography, *WJV* 02 (2012) 155–160.
- [85] C.S. Burden, J. Jin, A. Podgornik, D.G. Bracewell, A monolith purification process for virus-like particles from yeast homogenate, *Journal of chromatography. B, Analytical technologies in the biomedical and life sciences* 880 (2012) 82–89.
- [86] P. Steppert, D. Burgstaller, M. Klausberger, P. Kramberger, A. Tover, E. Berger et al., Separation of HIV-1 gag virus-like particles from vesicular particles impurities by hydroxyl-functionalized monoliths, *Journal of separation science* 40 (2017) 979–990.
- [87] L. Hu, J.M. Trefethen, Y. Zeng, L. Yee, S. Ohtake, D. Lechuga-Ballesteros et al., Biophysical characterization and conformational stability of Ebola and Marburg virus-like particles, *Journal of pharmaceutical sciences* 100 (2011) 5156–5173.
- [88] A.K. Dalton, P.S. Murray, D. Murray, V.M. Vogt, Biochemical characterization of rous sarcoma virus MA protein interaction with membranes, *Journal of virology* 79 (2005) 6227–6238.
- [89] G.D. Lewis, T.G. Metcalf, Polyethylene Glycol Precipitation for Recovery of Pathogenic Viruses, Including Hepatitis A Virus and Human Rotavirus, from Oyster, Water, and Sediment Samples, *Applied and Environmental Microbiology* 8 (1988) 1983–1988.
- [90] D.I. Lipin, Y.P. Chuan, L.H.L. Lua, A.P.J. Middelberg, Encapsulation of DNA and non-viral protein changes the structure of murine polyomavirus virus-like particles, *Archives of virology* 153 (2008) 2027–2039.
- [91] H. Mach, D.B. Volkin, R.D. Troutman, B. Wang, Z. Luo, K.U. Jansen et al., Disassembly and reassembly of yeast-derived recombinant human papillomavirus virus-like particles (HPV VLPs), *Journal of pharmaceutical sciences* 95 (2006) 2195–2206.
- [92] Q. Zhao, Y. Modis, K. High, V. Towne, Y. Meng, Y. Wang et al., Disassembly and reassembly of human papillomavirus virus-like particles produces more virion-like antibody reactivity, *Virology journal* 9 (2012) 52.
- [93] V.K. Deo, M. Yui, J. Alam, M. Yamazaki, T. Kato, E.Y. Park, A model for targeting colon carcinoma cells using single-chain variable fragments anchored on virus-like particles via glycosyl phosphatidylinositol anchor, *Pharmaceutical research* 31 (2014) 2166–2177.

- [94] M. Zochowska, A. Paca, G. Schoehn, J.-P. Andrieu, J. Chroboczek, B. Dublet et al., Adenovirus dodecahedron, as a drug delivery vector, *PloS one* 4 (2009) e5569.
- [95] T. Hahne, M. Palaniyandi, T. Kato, P. Fleischmann, H. Wätzig, E.Y. Park, Characterization of human papillomavirus 6b L1 virus-like particles isolated from silkworms using capillary zone electrophoresis, *Journal of bioscience and bioengineering* 118 (2014) 311–314.
- [96] Hamed Nosrati, Marziyeh Salehiabar, Soodabeh Davaran, Ali Ramazani, Hamidreza Kheiri Manjili, Hossein Danafar, New advances strategies for surface functionalization of iron oxide magnetic nano particles (IONPs).
- [97] I. Safarik, M. Safarikova, Magnetic nano- and microparticles in biotechnology, *Chemical Papers* 63 (2009) 301.
- [98] N. Singh, G.J.S. Jenkins, R. Asadi, S.H. Doak, Potential toxicity of superparamagnetic iron oxide nanoparticles (SPION), *Nano reviews* 1 (2010).
- [99] R.V. Mehta, Synthesis of magnetic nanoparticles and their dispersions with special reference to applications in biomedicine and biotechnology, *Materials science & engineering. C, Materials for biological applications* 79 (2017) 901–916.
- [100] Y. Wang, M. Zhang, L. Wang, W. Li, J. Zheng, J. Xu, Synthesis of hierarchical nickel anchored on Fe₃O₄@SiO₂ and its successful utilization to remove the abundant proteins (Bhb) in bovine blood, *New J. Chem.* 39 (2015) 4876–4881.
- [101] A. Mierczynska-Vasilev, P. Mierczynski, W. Maniukiewicz, R.M. Visalakshan, K. Vasilev, P.A. Smith, Magnetic separation technology: Functional group efficiency in the removal of haze-forming proteins from wines, *Food Chemistry* 275 (2019) 154–160.
- [102] Y. Oz, Y. Abdouni, G. Yilmaz, C.R. Becer, A. Sanyal, Magnetic glyconanoparticles for selective lectin separation and purification, *Polym. Chem.* 10 (2019) 3351–3361.
- [103] D.T. Ta, R. Vanella, M.A. Nash, Magnetic Separation of Elastin-like Polypeptide Receptors for Enrichment of Cellular and Molecular Targets, *Nano Lett.* 17 (2017) 7932–7939.
- [104] S.P. Schwaminger, S.A. Blank-Shim, I. Scheifele, V. Pipich, P. Fraga-García, S. Berensmeier, Design of Interactions Between Nanomaterials and Proteins: A Highly Affine Peptide Tag to Bare Iron Oxide Nanoparticles for Magnetic Protein Separation, *Biotechnology journal* 14 (2019) e1800055.

- [105] L. Jose, C. Lee, A. Hwang, J.H. Park, J.K. Song, H.-j. Paik, Magnetically steerable Fe₃O₄@Ni²⁺-NTA-polystyrene nanoparticles for the immobilization and separation of his6-protein, *European Polymer Journal* 112 (2019) 524–529.
- [106] X. Shu, N.C. Shaner, C.A. Yarbrough, R.Y. Tsien, S.J. Remington, Novel chromophores and buried charges control color in mFruits, *Biochemistry* 45 (2006) 9639–9647.
- [107] H. Suhaimi, R. Hiramatsu, J. Xu, T. Kato, E.Y. Park, Secretory Nanoparticles of *Neospora caninum* Profilin-Fused with the Transmembrane Domain of GP64 from Silkworm Hemolymph, *Nanomaterials (Basel, Switzerland)* 9 (2019).
- [108] J.R. de Jesus, R. da Silva Fernandes, G. de Souza Pessôa, I.M. Raimundo, M.A.Z. Arruda, Depleting high-abundant and enriching low-abundant proteins in human serum: An evaluation of sample preparation methods using magnetic nanoparticle, chemical depletion and immunoaffinity techniques, *Talanta* 170 (2017) 199–209.
- [109] T. Kato, S. Arai, H. Ichikawa, E.Y. Park, Versatility of chitosan/BmNPV bacmid DNA nanocomplex as transfection reagent of recombinant protein expression in silkworm larvae, *Biotechnology letters* 38 (2016) 1449–1457.
- [110] T. Kato, T. Murata, T. Usui, E.Y. Park, Efficient production of human β -1,3-N-acetylglucosaminyltransferase-2 fused with green fluorescence protein in insect cell, *Biochemical Engineering Journal* 19 (2004) 15–23.
- [111] Kurosawa Y., Saito M., Okuyama T., 26th International Symposium, Exhibit and Workshops on Preparative and Process Chromatography, Boston, USA, 2013.
- [112] S. Matić, V. Masenga, A. Poli, R. Rinaldi, R.G. Milne, M. Vecchiati et al., Comparative analysis of recombinant Human Papillomavirus 8 L1 production in plants by a variety of expression systems and purification methods, *Plant biotechnology journal* 10 (2012) 410–421.
- [113] Q. Zhao, M.J. Allen, Y. Wang, B. Wang, N. Wang, L. Shi et al., Disassembly and reassembly improves morphology and thermal stability of human papillomavirus type 16 virus-like particles, *Nanomedicine nanotechnology, biology, and medicine* 8 (2012) 1182–1189.
- [114] T. Kato, T. Otsuki, M. Yoshimoto, K. Itagaki, T. Kohsaka, Y. Matsumoto et al., *Bombyx mori* nucleopolyhedrovirus displaying neospora caninum antigens as a vaccine candidate against *N. caninum* infection in mice, *Molecular biotechnology* 57 (2015) 145–154.

- [115] D.G. Gibson, L. Young, R.-Y. Chuang, J.C. Venter, C.A. Hutchison, H.O. Smith, Enzymatic assembly of DNA molecules up to several hundred kilobases, *Nature methods* 6 (2009) 343–345.
- [116] T. Kato, S. Arai, H. Ichikawa, E.Y. Park, Versatility of chitosan/BmNPV bacmid DNA nanocomplex as transfection reagent of recombinant protein expression in silkworm larvae, *Biotechnology letters* 38 (2016) 1449–1457.
- [117] R. Massart, Preparation of aqueous magnetic liquids in alkaline and acidic media, *IEEE Trans. Magn.* 17 (1981) 1247–1248.
- [118] S. Kralj, D. Makovec, S. Čampelj, M. Drofenik, Producing ultra-thin silica coatings on iron-oxide nanoparticles to improve their surface reactivity, *Journal of Magnetism and Magnetic Materials* 322 (2010) 1847–1853.
- [119] M. Keshtkar, D. Shahbazi-Gahrouei, M.A. Mehrgardi, M. Aghaei, S.M. Khoshfetrat, Synthesis and Cytotoxicity Assessment of Gold-coated Magnetic Iron Oxide Nanoparticles, *Journal of Biomedical Physics & Engineering* 2018 // 8 (2018) 357–364.
- [120] Z. Rashid, H. Naeimi, A.-H. Zarnani, M. Nazari, M.-R. Nejadmoghaddam, R. Ghahremanzadeh, Fast and highly efficient purification of 6×histidine-tagged recombinant proteins by Ni-decorated MnFe₂O₄@SiO₂@NH₂@2AB as novel and efficient affinity adsorbent magnetic nanoparticles, *RSC Adv.* 6 (2016) 36840–36848.
- [121] S.P. Schwaminger, P. Fraga-García, S.A. Blank-Shim, T. Straub, M. Haslbeck, F. Muraca et al., Magnetic One-Step Purification of His-Tagged Protein by Bare Iron Oxide Nanoparticles, *ACS omega* 4 (2019) 3790–3799.
- [122] Y. Tsuji, V.K. Deo, T. Kato, E.Y. Park, Production of Rous sarcoma virus-like particles displaying human transmembrane protein in silkworm larvae and its application to ligand-receptor binding assay, *Journal of biotechnology* 155 (2011) 185–192.
- [123] T. Kato, Y. Takami, V. Kumar Deo, E.Y. Park, Preparation of virus-like particle mimetic nanovesicles displaying the S protein of Middle East respiratory syndrome coronavirus using insect cells, *Journal of biotechnology* 306 (2019) 177–184.
- [124] A. Dutta Chowdhury, N. Agnihotri, R.-A. Doong, A. De, Label-Free and Nondestructive Separation Technique for Isolation of Targeted DNA from DNA-Protein Mixture Using Magnetic Au-Fe₃O₄ Nanoprobes, *Analytical chemistry* 89 (2017) 12244–12251.

12. Appendix

12.1. Coexpression of MERS-S protein and *Rous sarcoma* virus GAG protein as self-assembling VLP in silkworm haemolymph

12.1.1. Introduction

This study intended to produce RSV-Gag VLPs displaying the spike (S) protein from the Middle East respiratory syndrome coronavirus (MERS-CoV). This approach could have led to an enveloped VLP, which is displaying the S-protein and be therefore, a vaccine against MERS. The S protein is processed into the two subunits S1 and S2. Both subunits are required for viral infection of the cells, whereby S1 is required for cell binding as it has the receptor binding domain, and the membrane fusion is done by the S2 subunit. Therefore, the S protein would be one target for a possible MERS-CoV vaccine. The intention was, after a successful coexpression of these particles, their self-assembling to VLPs and the secretion into the haemolymph, to purify the VLPs only using up-scale able purification methods. This project was supposed to be a cooperation with Dr. Vipin Kumar Deo.

12.1.2. Specific Material and Methods

12.1.2.1. Bacmids

12.1.2.1.1. RSV-GAG protein bacmid

The RSV-GAG protein has its origin from pRep(A) from ATCC (ATCC number: 87702) and was produced previously reported [122]. The RSV GAG Protein is a modified version with just the amino acid 1-577 and has an estimated weight of 61 kDa. Received BmDH10Bac *E. coli* strain with the plasmid pFastBac (Thermo Scientific, Waltham, USA) coding for the bacmid was used for the first infection.

12.1.2.1.2. MERS-S protein bacmid

The cDNA encoding for the pcMV3-Spike from the betacoronavirus 2c EMC-2012 strain were ordered from Sino Biological Inc. (catalog no. VG0069-ACG). This was used for the production of a bacmid and the production of a Bacmid expression system (Deo V. K. intern, not published yet) [123]. Received BmDH10Bac *E. coli* strain with the plasmid pFastBac (Thermo Scientific, Waltham, USA) coding for the bacmid was used for the first infection.

12.1.2.2. Bacteria

12.1.2.2.1. BmDH 10 Bac *E. coli* containing the bacmid for the *Rous sarcoma virus-Gag* protein

This strain of *E. coli* contains a baculovirus-shuttle-vector (bMON14272) which can be combined with the plasmid pFastBac to produce an expression-bacmid. It has also a helper plasmid (pMON7142). For selection it has a resistance against Kanamycin and Tetracyclin. As modification this strain contains already an expression bacmid for RSV-GAG and a Gentamycin resistance.

12.1.2.2.2. BmDH 10 Bac *E. coli* containing the bacmid for the modified *Rous sarcoma virus-Gag* protein

This strain of *E. coli* contains a baculovirus-shuttle-vector (bMON14272) which can be combined with the plasmid pFastBac to produce an expression-bacmid. It has also a helper plasmid (pMON7142). This RSV-GAG protein has its origin from pRep(A) from ATCC (ATCC number: 87702). The RSV GAG Protein was modified and has just the amino acids 1-577 and an estimated weight of 61 KDa. For selection it has a resistance against Kanamycin and Tetracyclin.

12.1.2.2.3. BmDH 10 Bac *E. coli* containing the bacmid for the MERS-S protein

This strain of *E. coli* contains a baculovirus-shuttle-vector (bMON14272) which can be combined with the plasmid pFastBac to produce an expression-bacmid. It has also a helper plasmid (pMON7142). The cDNA encoding for the pcMV3-Spike from the betacoronavirus 2c EMC-2012 strain were ordered from Sino Biological Inc. (catalog no. VG0069-ACG). This was used for the production of a bacmid and the production of a Bacmid expression system (Deo V. K. intern, not published yet). This BmDH10Bac *E. coli* strain had for selection a Kanamycin, Tetracycline and Gentamycin resistance and was used for an overnight culture.

12.1.2.2.4. Viral nucleic acid Isolation

The isolation of viral DNA was done according the kit High Pure Viral Nucleic Acid Kit from Roche Applied Science. The principle is lysis of the sample and then binding of nucleic acids to the surface of glass fibres in presence of chaotropic salts.

Briefly the protocol is like follow.

200 µl sample was mixed with 200 µl binding buffer with poly(A) and 50 µl proteinase K. This

was incubated at 72°C for 10 min. before additional 100 µl binding buffer was added.

The solution was placed in the filter tube which was itself in a collection tube. In the next step the flow through was every time discard if not stated otherwise.

Centrifugation for 1 min. at 8000 × g. Added 500 µl inhibitor removal buffer.

Centrifugation for 1 min. at 8000 × g. Added 450 µl wash buffer.

Centrifugation for 1 min. at 8000 × g. Added 450 µl wash buffer.

Centrifugation for 1 min. at 8000 × g. Centrifugation for 1 min. at 13000 × g for total buffer removal. The filter tube was placed in a micro tube and 50 µl elution buffer was added. After centrifugation for 1 min. at 8000 × g the flow through was the isolated viral nucleic acid.

Before further usage it was stored at -30°C.

12.1.2.2.5. Bacmid Isolation

The bacmid isolation of the overnight culture was done with the following protocol which is used up to 200 ml. 25 to 50 ml of the culture solution was put in a falcon tube and centrifuged at 4°C, 8000 rpm for 10 min. The supernatant was discharged. This step could be repeated with more culture solution to archive a higher concentration. To the pellet were 3 ml of solution I given. This was vortexed and 6 ml of solution II added, this was then slowly mixed without vortexing. After 5 ml of solution III was added and slowly mixed, the solution was centrifuged at 4°C, 8000 rpm for 15 min. The white pellet was discharged and the supernatant put in a new falcon tube. The supernatant (around 14 ml) were mixed with 14 ml isopropanol and speedily mixed without vortexing. The solution was put on ice for 15 min. After that centrifuged at 4°C, 8000 rpm for 20 min. The supernatant was thrown away and the pellet dried. The pellet was then dissolved with 400 µl TE buffer using pipetting method. This solution was put in an Eppendorf tube and additional 100 µl TE buffer were added. Also 2 µl of RNase (25 mg/ml). This was incubated at 37°C for 1 h.

After the incubation 500 µl of Phenol/Chloroform/Isoamyl alcohol (25:24:1) was added, vortexed and then centrifuged at 4°C, 15000 rpm for 5 min. The upper layer (aqueous phase) was put in a new Eppendorf tube and the down layer discharged. To remove the phenol 500 µl chloroform was added and the steps beginning with the centrifugation repeated. After repeating 3 M sodium acetate were added in proportion 1:10 (for 450 µl → 45 µl). After mixing an equal volume of isopropanol was added and speedily mixed without vortexing. The sample were then 15 min on ice. After centrifugation at 4°C, 15000 rpm for 5 min, the supernatant

was discharged and the pellet melted with 300 μ l of 70 % ethanol and slowly mixed. After centrifugation the supernatant was discharged and the pellet dried. The dried pellet was dissolved with 200 μ l MES buffer. The concentration of the bacmid in μ g/ μ l was checked using the NanoDrop (Thermo Scientific, Waltham, USA) and also the purity using the ratio 260/280 nm. A ratio under 2.00 was considered as a good purity.

12.1.3. Results and Discussion

For purification of enveloped VLPs, coexpression of MERS-S protein and the *Rous sarcoma* virus Gag was conducted, which should together self-assemble and form a VLP. Haemolymph already containing the respective baculoviruses was received and used for silkworm infection. After several failures, the expression of the GAG protein was confirmed in the fat body, but not in the haemolymph (**data not shown**). Moreover, the expression of the S protein (around 160 kDa) could not be confirmed and only some artefact at 55 kDa was displayed in the fat body by the western blot (**data not shown**). Therefore, stored BmDH10Bac *E. coli* strains were investigated if they still contain the respective Bacmid expression systems. However, for both constructs no inserts detectable with agarose gel electrophoresis after the PCR (**data not shown**). This was also true after a colony PCR for BmDH10Bac *E. coli* containing a bacmid for RSV-Gag (**data not shown**).

12.1.4. Conclusion

The easy expression of the RSV-LP displaying the S-protein failed. Only the RSV gag protein was expressed and this only in the fat body, not into the targeted haemolymph. The S-protein was not expressible. Moreover, prepared stocked bacmids were not viable anymore. Even if the S-protein expression would have been a success, the original target to express it into the haemolymph would have been not easily achieved. Because the project focus shifted to expression optimization, it was paused until the complete expression, ideally into the silkworm haemolymph, would be successful. Unfortunately, this was not successfully done until now, therefore, the purification part could not be restarted.

12.2. MNPs for His-, Flag-and Strep-tag-affinity purification

12.2.1. Introduction

These two studies were initiated with a similar purpose as the already mentioned one in Chapter 7, but in opposite this study was initiated to test if the development of MNPs for

the purification purpose is possible in our laboratory. For the same reason as the other study, affinity tagged proteins were targeted. MNPs were modified to be able to bind to His-tagged and Flag- or Strep-tagged proteins.

12.2.2. Specific Methods

12.2.2.1. MNP for purification of Flag-tagged proteins

Ag-MNPs modified with monoclonal anti-His antibody were provided by Dr. Lee (Laboratory of Biotechnology, NanoBio group; Shizuoka University).

12.2.2.2. Preparation of MNPs for purification of Flag-tagged proteins

The Fe_3O_4 MNP were provided by Dr. Ankan (Laboratory of Biotechnology, NanoBio group; Shizuoka University) and were synthesized via sol-gel method in ammonia solution as previously reported [124]. 20 μl 1 mg/ μl anti-Flag monoclonal M185-3L antibodies were in a ratio to 1:1 with 20 μl 0.1 mol/l 1-Ethyl-3(3-dimethylaminopropyl) carbodiimide (EDC) solution 30 min at RT under stirring incubated. After this 20 μl 0.11 mol/l N-Hydroxy succinimide (NHS) solution was added to this for a ratio of 1:1.1 and at RT for 60 min under stirring. After Incubation 400 μl of MNPs were added and again for 60 min at RT under stirring incubated. Final the solution was centrifuged at 12000 x g, 10 min at RT and the supernatant was discarded. The MNPs were washed with 600 μl MilliQ, separated via magnet and resuspended in 200 μl MilliQ.

12.2.2.3. Preparation of MNPs for purification of Strep-tagged protein

Biotin displaying MNPs were provided by Dr. Ankan (Laboratory of Biotechnology, NanoBio group; Shizuoka University) and were synthesized via sol-gel method in ammonia solution as previously reported [124]. Biotin conjugation was done in two steps, whereby at first APTES conjugation was done and then biotin addition via EDC/NHS chemistry. The Biotin displaying MNPs were coupled with Streptavidin as followed. Because of the high affinity of streptavidin to biotin, it was sufficient only to mix them. 200 μl of a 1 mg/ml streptavidin solution was incubated with 400 μl MNP solution. After incubation the streptavidin-MNP complex was separated via magnet, washed with 600 μl MilliQ, again separated via magnet and resuspended in 200 μl MilliQ.

12.2.2.4. Purification using MNPs

For the anti-His-tag Ag-MNPs the protocol was the following. 50 or 60 μl MNPs were added to 20 or 40 μl sample. This was mixed and then 6 min under shaking at RT incubated. After magnetic separation the supernatant was removed, 150 μl PBS was added and 5 min under shaking at RT incubated. Washing was done twice. After magnetic separation the first elution buffer was 150 μl 20 mmol/l NaPO_4 , 0.5 mol/l NaCl, 500 mmol/l imidazole, pH 8.4 and for the second elution 150 μl 0.17 mol/l glycine HCl, pH 2.3 was used. Incubation time was 7 min at RT with shaking.

For the anti-Flag- and Strep-tag MNPs the protocol was the following. 200 μl MNPs were added to 300 μl sample. This was mixed and then 30 min under shaking at RT incubated. After magnetic separation the supernatant was removed, 300 μl wash buffer (Streptavidin-MNP: StrepTactin Wash buffer; Anti-Flag MNP: PBS) was added and 10 min under shaking at RT incubated. After magnetic separation an elution buffer (Streptavidin-MNP: StrepTactin elution buffer; Anti-Flag MNP: Glycine-HCl, pH 2.3) was used. Incubation time was 30 min at RT with shaking.

12.2.2.5. Enzyme-linked immunosorbent assay (ELISA)

Enzyme-linked Immunosorbent Assay (ELISA) is an analysis method which is based on antibody detection. Standard is the sandwich principle, whereby an antibody against a specific target protein is immobilized in a well. After binding of the target protein and washing, another antibody is added. This antibody will also bind to the target protein. It is a direct method if this antibody itself is already linked with an enzyme or another signal inducer. It is an indirect method if this antibody will be again bound from another antibody with a signal inducer. It is also possible that no antibody is immobilized in the well and that the target protein will be adsorbed to the surface.

In this case the direct ELISA was performed. 100 μl sample was overnight at 4°C in a microplate incubated. The micro plate was 2-3 with PBS-T washed and 2 h blocked with 5 % skimmed milk at RT. Again 2-3 washed and 100 μl antibody 2 % BSA solution (e.g. 1:999) was added and 1 h incubated. Again 2-3 washing. Adding 100 μl working solution. Stopping reaction with 100 μl 10 % sulfuric acid. The colour changed from blue to yellow. The absorbance is measured; 450 nm for yellow and 655 nm for blue.

12.2.3. Results and Discussion

For all projects the data about the MNPs affinity purification is not shown. For the anti-his antibody displaying MNP it was not possible to detect the model protein GFP on Western Blot and maximal only unspecific band with different sizes could be seen (**data not shown**).

The Biotin displaying MNP was coupled with Streptavidin, but the subsequent purification of a Strep tagged mCherry construct failed (**data not shown**). Regarding the ELISA the -other MNP was successfully coupled with an anti-flag antibody, but also here the subsequent purification of an RSV-LP with a flag-tag failed (**data not shown**).

12.2.4. Conclusion

The MNP for the His-tagged protein purification failed, paused and was intended that it will be continued after the production of new MNPs to investigate if the failing is because of the nature of the MNPs. However, the collaborator left the laboratory, so that the experiments were not continued. Furthermore, in the light of new findings after this project, it could be that in this case the concentration of the target protein was simply too low for detection and that this experiment should be repeated on a bigger scale. Another option would be also to switch the target protein.

Both other affinity purification also failed. Moreover, theoretically it should have function, as the ELISA showed that the anti-flag antibody bound to one MNP and that the coupling of streptavidin to the biotin modified MNPs should be also no problem, as biotin has a high affinity to Streptavidin. Maximal could the latter binding disrupted during the elution, but it seems to be failed already prior. Therefore, both projects were paused until the MNPs are investigated and reason for the failed binding was known. Until now, no investigations of the MNPs were done.

12.3. Standard purification of VP26 and VP28

12.3.1. Introduction

VP26 and VP28 are both transmembrane proteins of the White spot syndrome virus (WSSV). VP26 (23.1 kDa) orientation is inside, but it is one of the mayor virion proteins. VP28 (22.1 kDa) orientation is to the outside and therefore antigenic. Both proteins were expressed as vaccine candidates. This small side study aimed to purify these two

recombinant proteins without any affinity tag purification method and was done with low priority.

12.3.2. Specific Methods

12.3.2.1. Cell lysate containing VP26 or VP28

Fat body lysate containing VP26 and the pupae lysate containing VP28 were provided from Takafumi Nakanishi and Dr. Xu (Laboratory of Biotechnology, VLP group; Shizuoka University). The fat body lysate was processed as for the mentioned NoV-VLP project (see 2.11.4. Harvesting of the fat body; second part).

12.3.2.2. Glycoprotein staining in SDS-PAGE gels

This was done using the Pierce Glycoprotein Staining Kit from Thermo Scientific according to the manual for polyacrylamide gels. The principle is the oxidization of the present glycols to aldehydes, and then the colourless fuchsin dye reacts with the aldehydes and develops the magenta colour. This reaction is known as the periodic acid-Schiff stain (PAS).

In short, after the electrophoresis the gel was fixed in 100 ml 50 % methanol for 30 min. It was two times washed in 100 ml of 3 % acetic acid for 10 min. Then the gel was put in 25 ml oxidizing solution and incubated under gently agitation for 15 min, followed by 3 times the washing step for 5 min. The staining was done for 15 min in the Glycoprotein staining reagent under gently agitation. Then the gel was placed in 25 ml Reducing Solution for 5 min. At the end the gel was washed intensively in 3 % acetic acid, which was followed with ultrapure water. Glycoproteins appeared as magenta bands on the gel.

12.3.3. Results and Discussion

Centrifugation investigations showed that the effect of the high centrifugation forces is irrelevant for the separation and that only a small amount of proteins could be further removed, but this also included in lesser amount the target protein (**data not shown**).

For both proteins the results of the precipitation experiments were ambivalent on a small scale and hard to evaluate on the stained SDS-gel (**data not shown**). The precipitation was redone for 0.1 % PEI with 0.1 mol/l NaCl, 0.1 % PEI with 0.5 mol/l NaCl and 2.5 % PEG, because the quality of the gel was not satisfying and these set-ups were the only promising ones. However, the scaling up showed that these set-ups are not able to separate impurities

from the target protein and that all proteins were distributed equal between supernatant and pellet if a precipitation occurred (**data not shown**).

Furthermore, the samples were investigated if glycoproteins are present. Especially the VP28 sample showed many very weak background bands on the SDS-gel, but for both samples it could be also only artefacts (**data not shown**). Another possibility would be that, the proteins have only very few glycosylation's.

12.3.4. Conclusion

The pre-treatment investigations for these two recombinant proteins, from fat body or pupae lysate, showed that the standard pre-treatment methods seem to be in vain for them. However, it still seems worth to retry this precipitation pre-treatments and to investigate some more, such as the thermal treatment. But this project had only a low priority and was abandoned in favour of the RSV-LP purification project.